

Ghent University
Faculty of Pharmaceutical Sciences

**Development of a sensitive diagnostic
multiplex platform based on digitally
encoded microcarriers**

**Ontwikkeling van een gevoelig diagnostisch multiplex
platform gebaseerd op digitaal gecodeerde
micropartikels**

Stefaan Derveaux

Bio-engineer

Thesis submitted to obtain the degree of
Doctor in Pharmaceutical Sciences

Proefschrift voorgedragen tot het bekomen van de graad van
Doctor in de Farmaceutische Wetenschappen

2008

Dean:

Prof. dr. apr. Jean Paul Remon

Promoters:

Prof. dr. apr. Jo Demeester
Prof. dr. apr. Stefaan De Smedt

*Laboratory of General Biochemistry
and Physical Pharmacy*

The author and the promoters give the authorization to consult and to copy parts of this thesis for personal use only. Any other use is limited by the Laws of Copyright, especially the obligation to refer to the source whenever results from this thesis are cited.

De auteur en de promotoren geven de toelating dit proefschrift voor consultering beschikbaar te stellen en delen ervan te kopiëren voor persoonlijk gebruik. Elk ander gebruik valt onder de beperkingen van het auteursrecht, in het bijzonder met betrekking tot de verplichting uitdrukkelijk de bron te vermelden bij het aanhalen van resultaten uit dit proefschrift.

Gent, 13 januari 2009

De promotoren:

Prof. dr. apr. Jo Demeester

De auteur:

Ir. Stefaan Derveaux

Prof. dr. apr. Stefaan De Smedt

To Lien & Stan

To my parents

DANKWOORD

“Een doctoraat.....wie haalt het nu in godsnaam in zijn hoofd om eraan te beginnen?” Die vraag heb ik me de voorbije vijf jaar ettelijke keren gesteld. En ik niet alleen, daar ben ik zeker van. Het antwoord was al die tijd vrij evident voor mij: “je moet er goed zot voor zijn”. Maar nu de finale versie van mijn doctoraatsthesis hier uitgeprint naast mij ligt, en ik al een pak verstandiger ben geworden, zou ik dit even willen bijschaven: “je moet er goed zot voor zijn....maar ook omringd zijn door fantastische mensen! Hoogtijd dus om mijn *bedankings-lijstje* eens te overlopen....

Eerst en vooral zou ik mijn twee promotoren willen bedanken, Prof. dr. apr. Jo Demeester & Prof. dr. apr. Stefaan De Smedt, voor de kans die ik gekregen heb om dit doctoraatsonderzoek binnen hun fantastische onderzoeksgroep te mogen uitvoeren. **Jo**, je mag fier zijn op de enorme uitbreiding die het labo de afgelopen jaren heeft meegemaakt, zowel op het vlak van medewerkers, als wat de uitrusting betreft. **Stefaan** was diegene die het vijf jaar geleden waagde om een *totaal vreemd individu* (volgens hem dan toch) binnen te halen op zijn labo. Zo'n individu dat er feitelijk zelfs nog niet aan dacht om überhaupt te gaan doctoreren....Stefaan, bedankt voor het Memobead-voorstel, ik hou er een geweldige ervaring aan over! Ik ben me ervan bewust dat ik niet je gemakkelijkste doctoraatstudent ben geweest, maar hoop van harte dat je goede herinneringen koestert aan de voorbije periode en aan deze thesis. Beiden heel veel succes nog met het labo.

Zoals de meesten onder jullie weten, heb ik een groot deel van mijn doctoraatsperiode parttime doorgebracht in het *verre* Boom, bij *The M-Team*. Ik herinner me nog hoe ik daar als groentje, net van de unief en (dus) heel onwennig, terecht kwam tussen de afvaardiging van Tibotec, collega's met net dat ietsje meer ervaring....werken, lachen, zweten, roepen & tieren, pintjes, boterhammekes opeten tussen 'T Ruimerken en de schoorsteen,...we hebben het daar allemaal meegemaakt. Het Memobead-tijdperk heeft me wetenschappelijk & technologisch veel bijgeleerd, maar heeft me bovenal een groep fantastische vrienden opgeleverd. **Chris**, jij hebt me van in het begin gegidst, bedankt voor de boeiende gesprekken! Zoals je kan zien, heb ik je raad strikt opgevolgd: “Wie SCHRIJFT, die BLIJFT”. Het vervolg van dit boek ga ik wel ergens anders schrijven...**Philip**, mijn 'senior' collega met 'junior' karakter...vriestemperaturen trotserend om *nanuscuul* werk tot laat in de nacht uit te voeren...de Zwitsers kunnen nog wat van je leren! **Marc**, 'fysica-informatica-en ga zo maar verder top-specialist', jouw gedrevenheid en jouw oog voor detail zou iedere wetenschapper moeten hebben, je mag er zeker fier op zijn! **Walter**, jij bent pas op het einde in de picture gekomen, maar het is alsof we elkaar al jaren kennen. Bedankt om de serieuze momenten af te lossen met een goeie mop of uw gelach, en voor de toffe gocart- en cafémomenten. **Guy**, bedankt om het laden en lossen (bijna) volledig te automatiseren...ik heb er veel tijd mee gewonnen! Hopelijk vind je er nog iets op om ook je verbouwingen thuis te automatiseren... **Lies**, als vreemde eend in de bijt, stond je wel best je mannetje, moet ik toegeven... Jij zal ongetwijfeld gekende zaken tegenkomen in deze thesis...bedankt voor alle hulp! Memobead Technologies is ondertussen jammer genoeg opgedoekt, maar het doet goed om dit M-team zo nu en dan nog eens terug te zien...ik kijk al uit naar ons volgend cafébezoekje....

En na het Memobead-tijdperk kwam ik fulltime hier in Gent terecht. Heel kort heb ik eraan getwijfeld om te stoppen met dit project, maar gelukkig heb ik dat niet gedaan en ligt die thesis er nu. Bepaalde mensen hebben me bij deze beslissing enorm geholpen... bedankt hiervoor, zonder jullie had ik dit dankwoord nooit kunnen schrijven :-)

Ik heb de voorbije jaren 5 verschillende *bureaus* bemand op het 2^o verdiep van het FFW (weliswaar sequentieel, niet parallel, zo ijverig ben ik nu ook weer niet), niet zo'n slecht gemiddelde, nietwaar? Sommige collega's hebben een deel van dat bureautraject met mij gevolgd, anderen ben ik onderweg kwijtgeraakt, en met nog anderen ben ik uiteindelijk de laatste maanden van mijn doctoraat beland in onze *make-over* bureau, daar helemaal achteraan op de gang...Bij Bart en Farzaneh ben ik gestart. **Bart**, onze lab-manager van het jaar, jij verricht bergen werk in (en ver buiten) het labo....bedankt voor de vele bestellingen, verhuizingen,..., maar niet in het minst voor de toffe momenten! **Farzaneh**, I really enjoyed our collaboration during the past years. Although you have recently left your second home, you will always be in my mind. Good luck to you and your family! Vervolgens heb ik de 2 K's in mijn bureau binnengehaald, 2 zeer serieuze top-wetenschappers (beiden op weg naar een top-doctoraat), maar buiten de science nét ietsje minder serieus....**Koen** en **Kevin**, bedankt voor de geestige bureaumomenten, ik heb het trouwens ook enorm geapprecieerd dat jullie de 'huishoudelijke' gesprekken tijdens de middagpauze af en toe eens in een andere richting hebben geduwd :-)
Nathalie, jij hebt nog enkele jaren voor de boeg, maar met jouw inzet zal dat ongetwijfeld ook goed aflopen. Als er iemand is, die (bijna) altijd straalt, ben jij het wel. Bedankt daarvoor, en het ga je daar nog heel goed!

Met andere collega's heb ik niet de eer gehad om mijn bureau te kunnen delen. **Ine**, voor jou komt de eindstreep nu wel echt heel dichtbij, nog even doorzetten, en dan...verder genieten van de welverdiende rust! Veel geluk met je verdere plannen, thuis en in het labo! **Broes, Chaobo & Bart**, de jonge mannen van den overkant, die volgens mij allemaal het talent hebben om het nuttige aan het aangename te koppelen, veel succes nog met jullie ambtstermijn hier! **Marie-Luce**, jij bent nu echt wel vertrokken met je project, maak er iets moois van. Bedankt voor de leuke babbels tussendoor! En dan is er nog duracell-Dries, de vent van alle emoties.....hij zou naar het schijnt voor 3 doctoraten gaan, heb ik in de wandelgangen gehoord...**Dries**, ik weet niet hoe je het doet, maar het is fantastisch om je zo tegen 300 per uur bezig te zien! Bedankt om af en toe wat leven in het labo te brengen, maar ook voor de serieuzere momenten tussendoor. **Kevin**, jij bent nu echt vertrokken met je academische carrière, veel succes ermee. **Katrien, Joanna & Zanna**, de (*ehh*) vrouwen van de overkant, veel geluk in al jullie ondernemingen. **Hendrik, Oliwia** en **Geertrui**, jullie zijn net gestart en moeten jullie weg nog wat vinden....hopelijk hebben jullie binnen 4 à 5 jaar hetzelfde gevoel als ik nu!

Administratie, het is nooit mijn ding geweest. Gelukkig werd ik bijgestaan door twee fantastische krachten! **Katharine** en **Bruno**, jullie verdienen een speciale plaats...ik heb jullie de voorbije jaren de zwaarste beproevingen zien doorstaan. Zonder jullie zou het er heel wat chaotischer aan toegaan op het tweede en derde verdiep van het FFW. Bedankt voor het verzorgen van al mijn paparassen-werk!

Ondertussen hebben al een aantal andere collega's me het voorbeeld getoond en inmiddels andere oorden opgezocht: **Tinneke, Niek, Bruno & Barbara**, het ga jullie allemaal heel goed. **Lies**, de voorbije maanden hebben we je lach op het labo gemist. Hopelijk zet je er daar in Brussel ook af en toe de boel mee op stellen. Veel geluk met je (klein)mannen! **Roos**, met jouw gedrevenheid was je dé referentie van het labo. Ook jij bent niet ver gelopen. Ik wens je alle succes toe in je verdere onderzoek (maar dat zal zeker geen probleem zijn), en bovenal veel geluk met je gezin. **Sofie**, onze outsider, bedankt dat we jouw gang mochten inpalmen, hopelijk heb ik je niet al te veel gestoord met het heen en weer lopen naar de printer. Jouw relativeringsvermogen, je gelukkig zijn, en je

inspanningen voor je gezin, familie en vrienden...zijn fijn om te zien. Ook voor jou eindigt het doc-verhaal bijna, heel veel succes nog de komende tijd.

Enkele mensen hebben mijn doctoraat vanuit een andere hoek gevolgd...

Mama & papa, jullie hebben de voorbije 30 jaar enorm veel betekend voor mij. Dit doctoraat had er zonder jullie nooit geweest. Ik vind het fantastisch om jullie trots te zien op hun zoon....wie had dat verwacht hé?! Maar weet dat ik minstens even trots op jullie ben. Bedankt voor de fantastische kindertijd en jeugdijaren die ik bij jullie heb mogen doorbrengen...en bedankt dat Stan daar nu ook eens van mag proeven!

En dan zijn er nog die **2 grote zussen** en **die ene kleine zus**...ook jullie bedankt voor de leuke tijd die we meegemaakt hebben. Door jullie werd ik meerdere malen in de watten gelegd, dankzij jullie mocht ik, als enige jongen, altijd veel meer, en mede dankzij jullie **wederhelften** mag ik mezelf al ettelijke malen nonkel noemen. Hoewel we ondertussen allemaal onze eigen weg gevonden hebben, is het fijn jullie nog zo vaak te kunnen zien. **Emilyn, Sybelle, Xander, Hannelore, Kobe, Cato en Mattis**: bedankt voor jullie speelse inbreng. **Lybellia**, ook jij moet nog een eindje afleggen, je peter zal er altijd voor je zijn...

Verder zou ik ook heel graag mijn **bebonne, bompa, oma en nonkel Luc** willen bedanken voor de fantastische jaren, ook al kunnen ze dit niet meer meemaken. **Opa**, bedankt om mij het voorbeeld te geven! Ook al hebben we nu hetzelfde diploma, ik denk niet dat ik kan tippen aan je farmaceutische kennis. **Tante**, ook jij bedankt voor alle fijne herinneringen en de hechte vriendschap. Het is onmogelijk om hier iedereen een staande ovatie te geven, maar ter attentie van onze **beide families, onze fantastische vriendenkring, en het op-en-top Bolas-team**: vanaf nu mis ik geen enkel feestje, bijeenkomst, en training meer. Oei, misschien iets te voorbarig om dat zo te zeggen...

Lien, jij weet als geen ander welke weg ik de voorbije 5 jaar doorwandeld hebt. Bedankt om mijn klaagzangen af en toe aan te horen, bedankt voor de klusjes thuis, en bedankt voor je geduld bij het uitblijven van de renovatie van de gang, de afwerkingen van de ramen, de ontbrekende spotjes – en de rest ga ik hier niet aan iedereen zijn neus hangen -, de voorbije maanden waren ook voor jou niet altijd even evident. En nog maar eens merk ik hoe graag ik je wel zie! Lieve **Stan**, hoewel je op dit moment totaal niet beseft wat je mama en papa zo allemaal uitspoken, wil ik ook jou enorm bedanken. Niet alleen omdat je me de tijd geeft dit dankwoord af te werken, nu je hier zo stil, dromend, naast me ligt, maar vooral omdat je aanwezigheid, je glimlach, je gebrabbel, je knijpjes, je traantjes me wel eens stil & blij maken. De voorbije maanden waren niet altijd even simpel voor ons gezinnetje, ik hoop dat ik de goede middenweg gekozen heb tussen jou, je mama en het werk, en weet dat we er steeds voor je zullen zijn. Dikke kus, papa.

Bedankt !

Stefaan

Dendermonde, 8 januari 2009

TABLE OF CONTENTS

Table of Contents	1
List of Abbreviations and Symbols	3
General Introduction: Aim and Outline of this Thesis	5
Chapter 1: Introduction	9
Chapter 2: Multifunctional layer-by-layer coating of microcarriers	69
Chapter 3: Layer-by-layer coated digitally encoded microcarriers allow sensitive quantification of proteins in serum and plasma	101
Chapter 4: Faster and more sensitive bead based multiplexing by tyramide signal amplification	127
Chapter 5: Multiplexed SNP genotyping with layer-by-layer coated digitally encoded microcarriers	157
Chapter 6: Synergism between particle-based multiplexing and microfluidics technologies may bring diagnostics closer to the patient	187
Chapter 7: Integration of layer-by-layer coated digitally encoded microcarriers in microfluidic devices	217
Summary & General Conclusions	243
Samenvatting & Algemene Besluiten	251
Curriculum Vitae	261

LIST OF ABBREVIATIONS

A.U.	- Arbitrary units	MAPH	- Multiplex Amplifiable Probe Hybridization
Ab	- Antibody	MES	- 2-[N-morpholino]ethanesulfonic acid
AF647	- Alexa Fluor® 647	MFI	- Median Fluorescence Intensity
Ag	- Antigen	μTAS	- Micro total analysis systems
AIDS	- Acquired Immune Deficiency Syndrome	MLPA	- Multiplex Ligation-dependent Probe Amplification
ApoE	- Apolipoprotein E	mu APD	- Microavalanche photodiode
Arg	- Arginine	NA	- Numeric Aperture
bdDNA	- Branched Deoxyribonucleic acid	NaCl	- Sodium chloride
BSA	- Bovine serum albumine	NAT	- Nucleic Acid Test
C	- Cytosine	NFMP	- Non-Fluorescent Multiplex PCR
CAD	- Coronary artery diseases	nm	- Nanometer
CARD	- Catalyzed Reporter Deposition Technology	NP	- Nanoparticle
CCD	- Charge coupled device	OFM	- Optofluidic microscope
cdNA	- Complementary DNA	OLA	- Oligo ligation assay
CLSM	- Confocal Laser Scanning Microscopy	OT	- Optical tweezing
CP	- Capture probe	PAA	- Poly (acrylic acid)
CrO₂	- Chromium dioxide	PAGE	- Poly acrylamide gel electrophoresis
CRP	- C-reactive protein	PAH	- Poly (allylamine hydrochloride)
CV	- Coefficient of variation	PBS	- Phosphate Buffered Saline
Cy	- Cyanine	PCR	- Polymerase Chain Reaction
Cys	- Cysteine	PDMS	- Polydimethylsiloxane
DEP	- Dielectrophoresis	PE	- Phycoerythrin
DNA	- Deoxyribonucleic acid	PL	- Parameter logistic
dNTP	- Deoxynucleoside triphosphate	PP	- PCR primer
EDC	- 1-ethyl-3-(3-dimethyl aminopropyl) carbodiimide (HCl)	PS	- Polystyrene
EDTA	- Ethylenediaminetetraacetic acid	PSS	- Sodium poly (styrene sulfonate)
ELISA	- Enzyme-linked immunosorbent assay	QD	- Quantum Dot
EOF	- Electroosmotic flow	QMPSF	- Quantitative Multiplex PCR of Short fluorescent Fragments
FFF	- Field-flow fractionation	RCA	- Rolling Circle Amplification
FMAT	- Fluorometric Microvolume Assay Technology	RIA	- Radio-immunoassay
FRET	- Fluorescence Resonance Energy Transfer	RNA	- Ribonucleic acid
FSH	- Follicle Stimulating Hormone	ROI	- Region of interest
GMO	- Genetic Modified Organisms	Rpm	- Rotations per minute
HCV	- Hepatitis C Virus	RT-qPCR	- Reverse Transcriptase quantitative Polymerase Chain Reaction
HDL	- High Density Lipoprotein	S/N	- Signal-to-Noise
HIV	- Human immunodeficiency virus	SBE	- Single base extension
HPLC	- High Performance Liquid Chromatography	SD	- Standard deviation
HRP	- Horseradish Peroxidase	SDS	- Sodium dodecyl sulphate
HTS	- High-throughput screening	SE	- Standard error
Ig	- Immunoglobulin	SEM	- Scanning Electron Microscopy
IL	- Interleukin	SERS	- Surface-Enhanced Raman Spectroscopy
LAT	- Latex Agglutination Test	SNP	- Single Nucleotide Polymorphism
LbL	- Layer-by-Layer	SSC	- Saline-sodium citrate
LDL	- Low Density Lipoprotein	T	- Thymine
LED	- Light-emitting diodes	TNF	- Tumor Necrosis Factor
LIA	- Linear Immunoblot Assay	TP	- Target probe
LOC	- Lab-on-a-chip	TR	- Texas red
LOCI	- Luminescent Oxygen Channeling Assay	TSA	- Tyramide Signal Amplification
LOD	- Lower limit of detection	U	- Units
LP	- Long pass	UV	- Ultraviolet
LP	- Ligation primer	w/v	- Weight/ Volume
MAA	- Methyl acrylic acid		
MALDI	- Matrix-Assisted Laser Desorption		

LIST OF SYMBOLS

λ_{em}	- Emission Wavelength
λ_{ex}	- Excitation Wavelength
Å	- Angström

General Introduction

Aim and Outline of this Thesis

General Introduction

Aim and Outline of this Thesis

In answer to the ever-increasing need in biomolecular research and clinical diagnostics to carry out many assays simultaneously in one tube, several microcarrier-based multiplex technologies (suspension arrays) have arisen in the past few years. Simultaneous detection of different target molecules that are present in one sample, is possible by incubating the sample with a mixture of differently encoded microcarriers, each carrying another probe which can specifically interact with one of the targets. This means that each target will bind to a differently encoded microcarrier. When the targets are caught, several methods exist to label those 'positive' microcarriers. By means of this label, and by means of the code, it becomes possible to verify whether a target was caught at its surface, and which target was caught, respectively. Those multiplex measurements work quantitatively, because the more a certain target is present in the sample, the more targets will bind to their corresponding microcarrier. Five years ago, our research group proposed the use of spatial selective photobleaching, as an alternative method for the development of digitally encoded microcarriers, which were called 'memobeads'. It was suggested that this method could overcome the multiplexing limitations of existing technologies. The present study aimed to optimize the surface characteristics of those memobeads, and to verify whether they could then be applied to multiplex protein tests and nucleic acid tests. Furthermore, it was investigated in which way these memobead assays (and in general the assays performed with every kind of suspension arrays) could be improved to make them more efficient and sensitive.

Chapter 1 explains the pro's and contra's of multiplexing in molecular research and clinical diagnostics, and overviews the current available technologies thereto, with a detailed focus on suspension arrays. Because memobeads are basically composed of simple polystyrene (PS) microcarriers, a special emphasis is applied to overview the several methods that are used to allocate multiple functions to this kind of microcarriers. Besides the development of optimal encoding methods for generating suspension arrays, a major challenge of this field is the labeling of targets that are caught at the surface of the microcarriers. Because no effort has yet been done in literature to summarize the present methods, chapter 1 is closed with a short overview of labeling

technologies that were already applied and those that could be applied to suspension arrays. Because present commercial methods for the production of magnetic PS microcarriers impede their encoding by means of spatial selective photobleaching, we proposed a novel magnetic coating strategy that was based on the Layer-by-Layer (LbL) technology (**Chapter 2**), and proved that those LbL coated microcarriers could be efficiently encoded and decoded. Furthermore, their stability was investigated, and they were used for quantitative multiplex protein detection in complex samples, such as serum and plasma (**Chapter 3**), and in order to demonstrate their applicability to nucleic acid tests, we developed a proof-of-concept of SNP genotyping by combining this platform with the oligo ligation assay in **Chapter 5**. So far, little research has been done to improve the sensitivity of suspension arrays. One way to obtain a more sensitive platform, is by increasing the signal-to-noise ratio (S/N), which can be done by using signal amplification methods. To this end we explored in **Chapter 4** whether the enzymatic Tyramide Signal Amplification method (TSA) could be applied to the memobead platform, and suggested its applicability to any other kind of suspension array. Another way is by improving the interaction between capture probes and targets. Recent progress in microfluidics technologies is expected to strongly support the development of miniaturized analytical devices, where suspension arrays (with bound probes) can come in close contact with the sample (with targets), which will shorten the analysis time of those (bio)analytical assays. In **Chapter 6**, we launched the debate on the 'added value' that could be expected by (bio)analysis with multiplex suspension arrays in microfluidic devices, and focus on the challenges that exist to integrate the present detection platforms for suspension arrays in microfluidic devices, and on promising micro-technologies for down-scaling the detection units, in order to obtain compact miniaturized suspension arrays. We started some preliminary tests to support this idea by studying the kinetics of protein-interaction at the surface of memobeads that were integrated in a microchip, and compared those results with the conventional assay in a micro-centrifuge tube (**Chapter 7**).

CHAPTER One

INTRODUCTION

Parts of this chapter were published in:

Derveaux S.,¹ Stubbe, B.G.,¹ Braeckmans, K.,¹ Roelant, C.,² Sato, K.,³ Demeester, J.,¹ De Smedt, S.C.¹
Analytical and Bioanalytical Chemistry **2008**, 391 (7), 2453-2467.

¹ Laboratory of General Biochemistry and Physical Pharmacy, Department of Pharmaceutics, Ghent University, 9000 Ghent, Belgium.

² Memobead Technologies NV, Rupelweg 10, 2850 Boom, Belgium.

³ Department of Applied Chemistry, School of Engineering, The University of Tokyo, 7-3-1 Hongo, Bunkyo-Ku, Tokyo 113-8656, Japan

ABSTRACT

Already some decades, microparticles have played an important role as solid support in biological molecular research, drug discovery, and *in vitro* molecular diagnostics because of their important properties such as a high surface-to-volume, flexible handling, and easy fabrication. Advanced fabrication & coating technologies have meanwhile been developed that produce microparticles at high rate with a lot of functionalities, which has opened new applications, such as in multiplexing assays. Multiplexing, which aims to measure several analytes at once, have been introduced in those fields because they lower the expenditures by reducing the amount of material and reagents needed, they offer an alternative for existing labor-intensive procedures, and they often provide results with higher quality. This chapter introduces the fabrication of highly multi-functional microparticles, and overviews the state-of-the-art of multiplexing methods and the role of microparticles therein. A special emphasis is made on the microparticle encoding methods, and on target labeling methods in microparticle-based multiplex assays.

CHAPTER 1

INTRODUCTION

MICROPARTICLES

An old tool in molecular diagnostics.

Microparticles (beads, microspheres) are micron-sized, mostly spherical objects that are produced from a wide variety of materials (such as glass, silica, gold, silver, latex, polystyrene, polyacrylamide, dextran, etc.), and are available in a wide range of sizes (from a few nanometers to hundreds of micrometers). Microparticles have been used for decades in molecular research and clinical diagnostics. More than fifty years ago, the first immunoassays based on microparticles were developed, starting with the latex agglutination test (LAT), aimed to detect antibodies and high-molecular-weight antigens, which is still widely used due to its simplicity and cost-effectiveness^{1,2}. For the detection of antigens, antibody coated beads are used that are able to capture the antigens. Because multivalent antibodies are used, which recognize different epitopes on the antigens, antibodies that are bound to different microparticles can bind via another epitope the same antigen. In this way, aggregates are formed between multiple antigens and multiple antibody-attached microparticles, which are clearly visible to the eye without any sophisticated or expensive device (Figure 1). Since the discovery of the LAT, more and more microparticles were used in biomolecular tests, where they act as carriers or solid supports, such as in immunoassays and cell separation, in site-specific drug delivery systems, and in affinity separation of biological entities, or as (chemical, scattering, magnetic, or fluorescent) labels, such as in nuclear medicine for diagnostic imaging, in studying the phagocytic process, etc.^{3,4}. Microparticles became so important, because their benefits are several: the large binding capacity due to the high surface-to-volume ratio (inversely proportional to the diameter) of particle suspensions enables larger binding capacity compared to traditional test tubes or micro well-plates; the mobility of microparticles increases the speed of assays and makes

separation and/or enrichment possible ⁵; but the most important benefit is that they can have different surface properties for specific applications (see next paragraph).

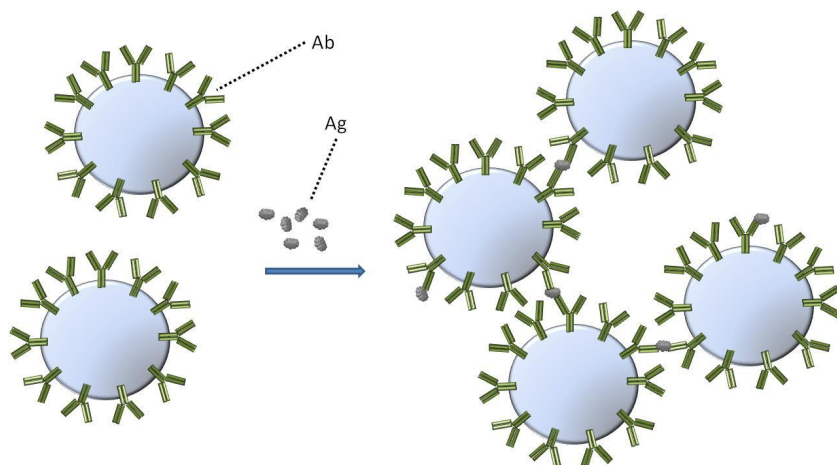


Figure 1: Principle of the Latex Agglutination Test, the first application of microparticles for immunoassays. Latex microparticles are coated with polyvalent antibodies (Ab) and mixed with a sample. If antigens of interest (Ag) are present in the sample, they will be captured by the antibodies, and as a result clumps of aggregated microparticles are formed.

Depending on their nature, microparticles have good chemical, physical and light stability properties, and the capacity to absorb and retain fluorescent dyes. They often can be made magnetic and their surface can be easily chemically modified to carry functional groups, such as carboxylic acids, amines, hydroxyl groups and others. Those functional groups can be used for covalent binding of biomolecules (proteins, oligonucleotides, drugs, enzymes...). It is therefore not surprising that a whole set of different microparticles is available for research and diagnostic applications, which is reflected in the high number of microparticle manufacturers (Table 1).

Table 1: List of notably microparticle manufacturers.

Company	Website	Particle core business
Seradyn products (Thermo Fisher Scientific Inc.)	www.seradyn.com	No
Gerlinde Kisker GbR	www.kisker-biotech.com	No
MagnaMedics GmbH	www.magnamedics.com	Yes
Bangs Laboratories, Inc.	www.bangslabs.com	Yes
Duke Scientific Corp. (Thermo Fisher Scientific Inc.)	www.dukescientific.com	Yes
Spherotech, Inc.	www.spherotech.com	Yes

Polymer Laboratories (part of Varian, Inc.)	www.polymerlabs.com	No
R&D Systems	www.rndsystems.com	No
Dynal Biotech (part of Invitrogen, Inc.)	www.invitrogen.com	No
Polysciences, Inc.	www.polysciences.com	No
Bioclone, Inc.	www.bioclon.com	No
Microparticles GmbH	www.microparticles.de	Yes
PolyMicrospheres (part of Vasmo, Inc.)	www.polymicrospheres.com	Yes
Promega, Corp.	www.promega.com	No
Ademtech	www.ademtech.com	Yes
Corpuscular Inc.	www.microspheres-nanospheres.com	Yes
Chemicell GmbH	www.chemicell.com	Yes

Polystyrene (PS) microparticles.

Production of (PS) microparticles

The particles most commonly used in biomolecular research and in medical applications are made of polystyrene (PS). This material plays a critical role in pharmaceutical and biomedical research since years (for instance as basic material of Petri dishes, test tubes,...), because it is an inert material with a low relative density (~ 1.05) that can be easily manufactured, modified and sterilized. PS microparticles are mainly produced in batch-mode, uniformly and at high amounts, by a so-called *emulsion polymerization process* with styrene as monomer, which occurs as follows (Figure 2) ⁶. The addition of an emulsifier, such as sodium dodecyl sulphate or kalium laurate, to a water solution of the monomer stabilizes the monomer droplets by the formation of micelles: the emulgator surrounds the droplets with the polar head oriented to the water, and the apolar tail to the inner of the droplet. In the next step a polymerization initiator such as benzoyl peroxide is added. Benzoyl peroxide produces benzoyl radicals at high temperatures. Those free radicals are very reactive and attack the double binding of styrene, to form another radical species, which on its turn can react with a styrene molecule, to begin chain propagation. The result is the polymerization of the styrene molecules in the droplet. Chain termination results from the collision of the growing chain species with another one, or with a primary free radical. In this way, very uniform particles of about 0.5-3 μm are formed.

After removing the detergent, larger particles are made by *seed emulsion polymerization*, which is the stepwise growing of smaller core microparticles by polymerization of monostyrene

molecules on their surface in the presence of the initiator, but without any additional detergent. Although this is the most conventional fabrication procedure, a lot of alternatives/variations exist ⁵; as an example, cross-linked polystyrene can be used instead of the linear state in order to make the microparticles more resistant to organic solvents.

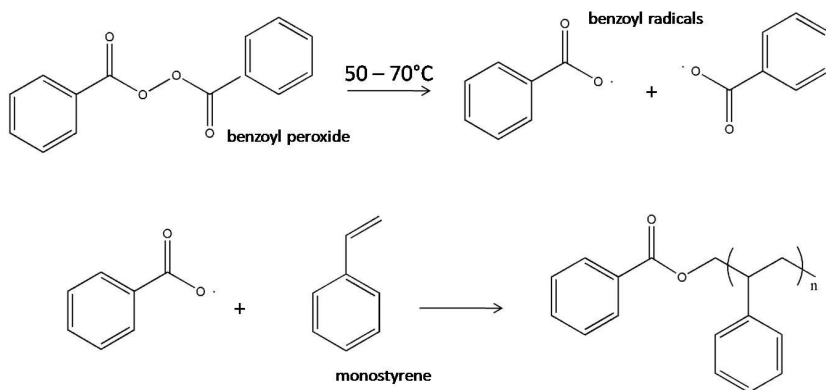


Figure 2: Conventional emulsion polymerization process of monostyrene in the production of PS microparticles. Micelles are formed by the addition of an emulsifier to a aqueous solution of monostyrene. Benzoyl peroxide produces benzoyl radicals at high temperatures that attack the double binding of monostyrene to form another radical species which on its turn react with a monostyrene molecule, to begin chain propagation.

Functionalization of PS microparticles

PS microparticles are often produced with a functionalized surface coating of active chemical groups in order to make them more hydrophilic (because the hydrophobicity of PS often favors microparticle clumping) or for covalent attachment of biomolecules. Several approaches can be used for the functionalization of microparticles, which can be categorized as ‘during particle synthesis’ and ‘after particle synthesis’ methods (Table 2):

- If potassium persulphate ($K_2S_2O_8$) is used as initiator, the surface will consist of sulphate groups. In a similar way, other functionalized surfaces can be obtained by using other functionalized initiators.
- Second, a functionalized surface can be obtained by using a functionalized monomer in the emulsion polymerization process. Co-polymerization with methyl acrylic acid (MAA) for instance results in a carboxylated surface.
- Third, functionalization is also possible via the ‘swelling procedure’: PS microparticles of a few micrometer are suspended during 24 hours in an hydrophobic chlorodecane solution, which forces the particles to swell and pores are formed. Subsequently,

monostyrene and a functionalized monomer, such as MAA, are added at the same time, which enter the pores, but because MAA is hydrophilic, it will appear mostly at the outer side of the microparticles. In the final step, polymerization takes place at a temperature of 70 °C in the presence of the initiator benzoylperoxide ⁷.

- Another way to obtain functionalized microparticles, is to modify the surface of the microparticles chemically by final coating with a functionalized monomer. A carboxylated surface can be obtained for instance with a coating of a carboxyl functionalized monomer via its alkyl chains, which consist of two to eight carbons in length depending on the type of the monomer used. The density of the functional groups can be adjusted by varying the amount of monomer used for coating.
- Finally, the *Layer-by-Layer* modification can be used to coat charged functionalized polymers on the surface of oppositely charged microparticles. A detailed overview of this approach, which is based on electrostatic interactions, is given in Chapter 2.

Table 2: Functionalization of polystyrene microparticles.

<i>During particle synthesis</i>	<i>After particle synthesis</i>
Use of functionalized initiator	Coating with functionalized monomer
Co-polymerization with functionalized monomer	Swelling method
	Layer-by-Layer coating

Fluorescent PS microparticles

Fluorescent PS microparticles can be applied as standards for flow cytometry and microscopy, as tracers in flow measurements, for the detection and analysis of biomolecules, etc. ^{5,8}. They can be created by incorporation of fluorescent molecules or nanoparticles during or after the synthesis of the microparticles. The first one occurs by co-precipitation of the fluorophores and the monomers during the polymerization process. The latter one can be categorized in internal and external fluorescent encoding. Internal fluorescent encoding is usually accomplished by swelling the microparticles into a solution of (lipophilic) fluorophores in organic solvents (*'swelling procedure'*, as previously described). This leads to the diffusion of the fluorophores into the inside of the microparticles. The microparticles are then transferred to a aqueous solution, where they shrink so that the fluorophores are entrapped. Fluorescent microparticles can also be created by adsorbing fluorescent semiconductor nanocrystals (quantum dots) into the porous structure of mesoporous

microparticles (internal encoding)^{9, 7,10}, and on the surface of dense magnetic polystyrene microparticles (external encoding)¹¹. External fluorescent encoding of microparticles is also achieved by covalently linking fluorescent dyes to the functionalized surface of microparticles, or by layer-by-layer (LbL) assembly of core-shell type microparticles with shell-embedded dyes or nanoparticles¹².

Biomolecule coupling to PS microparticles

Biomolecules can be bound via passive adsorption, via covalent coupling to functional groups or via intermediary coated binding proteins at the surface of PS microparticles.

Passive adsorption

Passive adsorption is based primarily on hydrophobic interactions (Van der Waals) between the polymer surface and hydrophobic parts of the ligands, or on electrostatic interactions between charged parts of the ligands and the charged surface of the particles (e.g. epoxy, hydroxyl, sulphate, or dimethylamino microparticles), or on both. Ligands, whose attachment is due in part to ionic interactions, are affected by the conditions of the environment in which they are suspended, and pH changes are more likely to result in desorption than if the attachment was made solely via hydrophobic interactions. Low molecular weight proteins (such as haptens) that might not adsorb well on their own, can be covalently bound to other proteins that adsorb well¹³. Disadvantageous to passive adsorption is the random (and often incorrect) orientation of the ligand molecules resulting in a loss of their biological activity (e.g. antibodies bound via their variable and antigen-recognition part), which is not the case when ligands are coupled covalently. It is known that only ~10% of the antibodies might be preserved for capturing one antigen from solution, when they are passively adsorbed to the surface¹⁴.

Covalent coupling

Carboxyl polystyrene and amino polystyrene particles are very useful for covalent attachment, although hydroxyl- and epoxide microparticles are also possible (Figure 3). In fact, many strategies exist for covalent coupling, which is more precisely controllable and compatible with low ligand coating concentrations compared to passive adsorption. More ligand can be coupled, and the coated microparticles are more temperature stable¹⁵. Passive adsorption can result in overloading and leaching of bound ligands, an issue in production of tests that would be influenced by leaching of minute quantities of probes from the particles over time (such as for multiplexed tests, see later)¹⁶. In a lot of immunoassays, detergents (necessary to avoid non-specific binding) can also remove

adsorbed probes and finding the balance is rather difficult. Another advantage of covalent coupling is that it makes the use of spacer molecules possible between the microparticle and the ligand, which can increase sensitivity¹⁷ and makes flexible attachment of different probes with one chemistry possible. The most conventional method for covalent coupling makes use of water soluble carbodiimide as a coupling agent to react carboxyl groups with amines to form stable amide bonds, as will be explained in a further chapter.

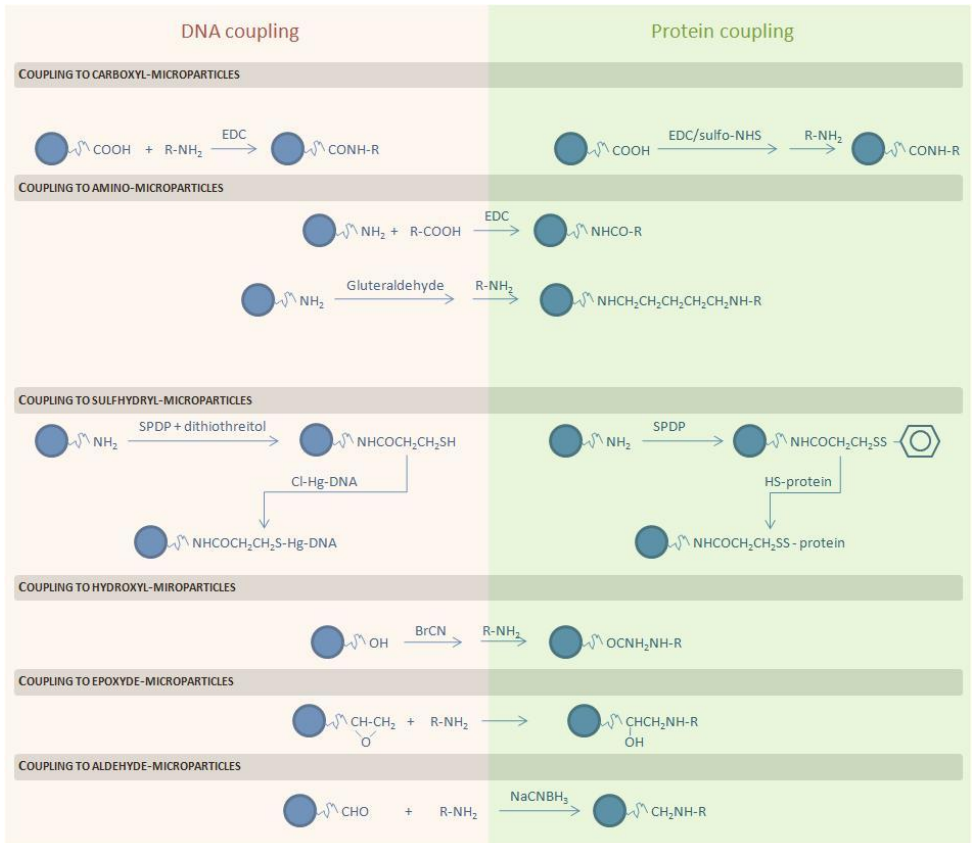


Figure 3: Main microparticle surface coatings and coupling procedures for the covalent attachment of DNA (left) and protein probes (right). Note that some strategies can be used for both types (middle).

Intermediary coated biomolecules

A third approach to couple biomolecules is by using microparticles that are pre-coated (covalently or via passive adsorption) with binding proteins, such as protein A or G, and streptavidin. Although the latter one is very user-friendly, it necessitates the biotinylation of the probes, which can affect the reactivity of the probes. Another drawback that we have observed with our study is the non-specific interaction of target DNA molecules with streptavidin-coated microspheres, making this approach less efficient for nucleic acid tests than covalent attachment.

Magnetic PS microparticles

Biological and biomedical applications of magnetic-particle technology have been employed widely for DNA, RNA, protein, and cell separations in genomic, proteomic, and immunological research. Many reviews have been published on the use of magnetic-particle technology in genomics and proteomics, drug discovery, biomedicine, and clinical applications¹⁸. For the fabrication of magnetic PS microparticles, magnetically responsive material is added to a polystyrene matrix by either of two processes: either it is entrapped during the polystyrene polymerization process (or during the polymerization process on core particles, Figure 4), or it is attached to, or incorporated in the microparticles after polymerization, for instance by means of the '*swelling method*' (as explained in a previous paragraph)¹⁰. The particles are then usually overgrown in either case, in order to encapsulate the magnetic material and to provide functional groups on the surface. Instead of the addition of magnetic material to polystyrene microparticles, the opposite case in which a thin layer of polystyrene is coated onto a magnetic crystal is also possible, but then the microparticles are not spherical and not uniform in size. With both types of magnetic microparticles, it is important that the magnetic material is completely encapsulated in order to prevent leaching of the iron complexes, which can cause problems in biological applications. In our study, polystyrene microparticles are made magnetic by incorporation of magnetic nanoparticles on the surface of the particles by means of the LbL approach (Chapter 2)¹⁹. An extra coating with polymer layers fully encapsulates the magnetic nanoparticles.

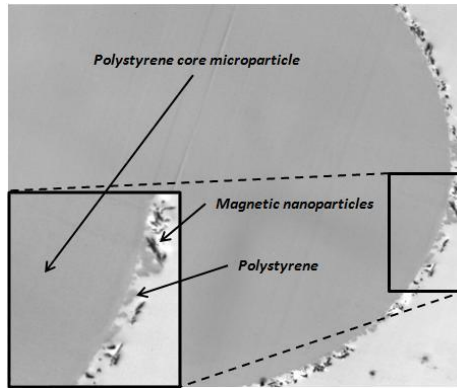


Figure 4: Electron microscopy of a transversal section of a magnetic microsphere with a diameter of 40 μm . The magnetic nanoparticles were entrapped during the polymerization of monostyrene on top of polystyrene core particles. As a result, the magnetic nanoparticles are only present at the outer layer of the microsphere.

This short overview demonstrates that multiple functionalities (fluorescence, magnetism, functional groups) can be easily introduced in PS microparticles. Note that we have focused on PS microparticles, because they form the backbone of our work. Nonetheless, a lot of those strategies can be used on microparticles that are made from other materials as well. Although the functionalities are listed separately in the previous paragraphs, several of them can be applied at once. As an example, in our study the Layer-by-Layer approach has been used to achieve multifunctional microparticles that are magnetic, as well as functionalized (Chapter 2).

New functions of microparticles in molecular diagnostics.

Due to the substantially amount of research and development in microparticle technology, new types of microparticle-based assays have emerged during the last decade, where the analysis of target molecules is performed on the surface of a single particle, often combined with advanced optical detection technologies: flow cytometric assays, fluorometric microvolume assays (FMAT), luminescent oxygen channeling assays (LOCI), and multi-analyte detection assays^{20,21}. The latter one forms the backbone of our study. Before we go into detail on this topic, we first introduce the multiplexing concept in biomolecular research and clinical diagnostics.

MULTIPLEXING

Multiplexing tests.

Healthcare providers and governments world-wide increasingly recognize the power of diagnostics to reduce the cost and enhance the efficiency of total health management: rapid, adequate, highly sensitive, targeted diagnostic tests are the key to successful and cost-effective modern treatment options and provide the means to monitor diseases at various stages, because the costs of treatment are often high. Current molecular diagnostics are primarily single-analyte tests designed around a single analyte associated with a disease state (also called 'monoplex assays'). Those kind of test are usually performed in single test tubes or separate wells of a microtiterplate or on single test strips.

The intent of multiplexing is to measure several analytes simultaneously²². A multiplex diagnostic assay is at the simplest level a combination of **independent assays**. In this case, the addition or withdrawal of individual tests has no effect on the previous results. Those kind of tests increase efficiency (lower reagent consumption, faster analysis etc), which provides a significant cost benefit (see Figure 5 left side).

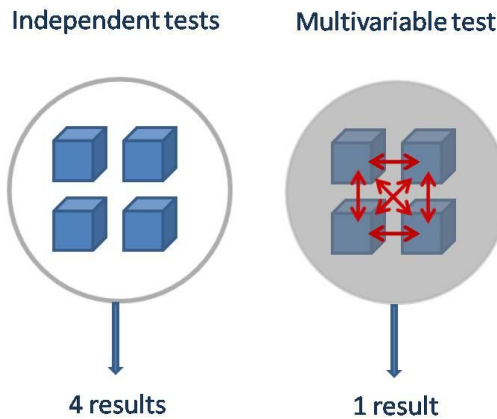


Figure 5: Multiplexing of tests is used to increase the efficiency (in case of independent tests) or to achieve results with higher quality (dependent tests) or both.

At the more complex level, however, a multiplexed diagnostic assay combines variables to provide one single result (***multivariable tests***, see Figure 5 right side). Multivariable tests are enabling new advanced diagnostics: several variables are combined to provide a single disease-specific result that no single variable could provide. Those kind of tests increase the diagnostic range of a test. Their power is the combination of variables that do not have sufficient diagnostic power on their own into an integrated result that does. The next examples support this assertion:

- Pattern recognition methods are increasingly used (by means of cluster analysis): this is a computer-assisted technique to unravel complex and high-density data, in order to make associations between multiple analytes and diseases/symptoms. The use of cluster analysis, for instance, has yielded promising results in the understanding of the function of autoantibodies²³.
- Cytokine biology provides the perfect example of the inadequacy of individual monoplex protein measurements^{24,25}. The complexity of cytokine networks, arise from their multifunctionality: they show properties as *redundancy* (different cytokines share similar functions depending on the situation) and *pleiotropy* in their activity (a particular cytokine may have different effects in different circumstances and can act on a number of different cell types rather than on a single one); they often are produced in a *cascade reaction* in which one cytokine stimulates or inhibits its target cells to produce additional cytokines or to express receptors for other cytokines (receptor transmodulation by up- and down-regulation of several genes and their transcription factors). Cytokines are also characterized by considerable *ambiguity*, meaning that they tend to have multiple target cells and multiple actions. They can act *synergistically* (acting together and increasing the effect of one another) or *antagonistically* (opposite activities). Because the activity of an individual cytokine is not only determined by its abundance, but depends also on the effects of interacting cytokines, the measurement of a general cytokine profile has a more intrinsic value than the analysis of a single one²⁴.
- A particular area in which the importance of multiplexing in biomarker research has been demonstrated is heart disease assessment. The cardiac risk has been evaluated in the past by the total cholesterol amount. Later on, other biomarkers were added (HDL, LDL, etc.) and it was seen that the more markers were taken into account, the more accurate the assessment of the cardiac risk was.
- In genomics testing, it is known that single (monoplex) nucleic-acid measurements can lead to false conclusions, such as for example in studies of transcriptional regulation or heritability of complex traits²⁶.

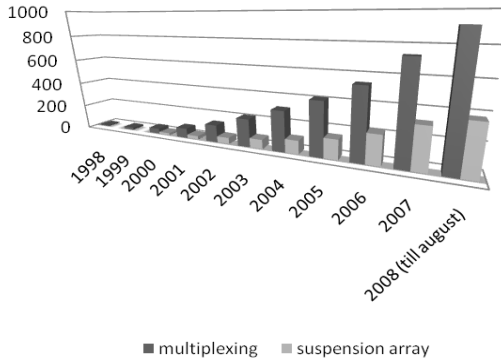
Growth of multiplexing.

Figure 6: The growing interest in multiplexing thinking. Cumulative number of manuscripts, yearly published in the Pubmed database, containing the keywords 'multiplexing' or 'suspension array' (as on September 2th, 2008).

Multivariable tests enable the analysis of patterns of results. This is very important, because, as explained in the previous paragraph, many disease-related processes are multi-factorial, involving the abnormal expression of multiple genes or the activity of multiple proteins. This field became very important, since the sequencing of the human genome had produced an enormous amount of genomic data, in which diagnostic and prognostic biomarkers were, and still are, exponentially discovered. Biomarkers provide a deeper insight into the molecular biology of diseases and move healthcare to a more efficient level in which a disease is not only recognized by its phenotype, but also understood at the molecular level. Theranostics was born, which provides the potential for an individual patient to be diagnosed according to his genetic background profile and, based on the diagnosis, treated with therapeutics designed to work on specific molecular targets²⁷.

A biomarker can be defined as a characteristic that is objectively measured and evaluated as an indicator of normal biologic or pathogenic processes or pharmacological responses to a therapeutic intervention.^a

^a FDA Office of Biostatistics, 2006

In the past, the detection of multiple biomarkers was done by performing multiple monoplex assays in parallel, but, besides that those tests were very expensive and required a lot of sample material (with the chance that there was not enough material to measure all analytes of interest), the inter-assay variation often made correct interpretation almost impossible. To this end, next-generation molecular diagnostics were needed based on novel automated & miniaturized technologies, advanced detection technologies and ultra-sensitive quantitative multiplexing platforms to perform the correct parallel screening of a large number of biomarkers simultaneously²⁸. Because such biomarkers provide direct information about genotypic and/or phenotypic changes associated with specific diseases or responses to treatment, multiplexed biomarker analysis has also become an important tool in preclinical drug development, and patient monitoring during clinical trials. Biomarker assays are indeed increasingly used throughout the process of disease management. A well-developed example is the use of HIV tests, including probe-based nucleic acid tests (NATs) and immunotests for viral genotyping, in the management of AIDS patients. The growth in multiplex thinking in biomolecular research is reflected in the increasing amount of published papers regarding multiplexing (Figure 6), and its importance in molecular diagnostics is proven by its compound annual growth rate of 26%^b. To this end it has become the most dynamic market segment in medical diagnostics.

Impact of miniaturization on multiplexing.

Multiplexing is a term derived from the telecommunication and computer sciences, where it refers to a process where multiple analog message signals or digitally data streams are combined into one signal over a shared medium. The aim is to share an expensive resource and to avoid using too many wires. For example, in telecommunications, several phone calls may be transferred using only one wire. In biological molecular research, drug discovery, and *in vitro* molecular diagnostics, multiplexed assays have been introduced by the same driving forces: they lower the expenditures by reducing the amount of material and reagents needed, and they offer an alternative for existing labor-intensive procedures. Reduced sample volume is of great importance for all those applications where only minimal amounts of samples are available (e.g. analysis of multiple tumor markers from a minimum amount of biopsy material, analysis of minimum amount of blood from newborns, prenatal diagnosis...). Besides those aspects, however, the key to the success of multiplexing in those fields was miniaturization. Miniaturization of analytical techniques has become a dominant trend in life

^b From market report 'Multiplexed Diagnostics 2008' (Select Biosciences).

sciences, primarily driven by the need to minimize costs by reducing the consumption of expensive reagents and by increasing throughput through automation ²⁹.

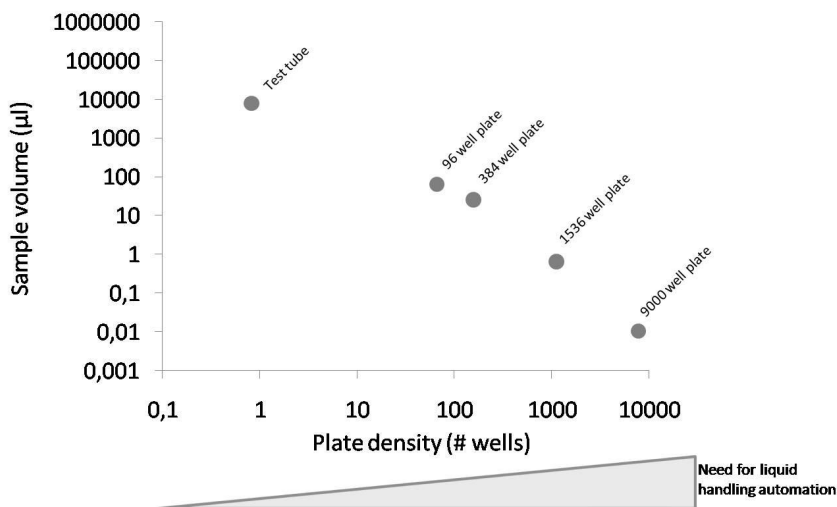


Figure 7: Evolution of micro-well plate technology. Correlation between sample volume and plate density (adapted from ³⁰). As the density of the wells increases, more and more robotics are needed for the liquid handling.

The trend of miniaturization is clearly demonstrated by the evolution that the micro-well plate underwent in high-throughput screening (HTS) ³⁰; this established field within the pharmaceutical industry has undergone a progression from 96-well plates through to 1536-well plates thanks to many technological advances in micro-well plate fabrication methods, liquid handling robotics and detection technology. Interestingly, the size of the plate didn't change (meaning that the sample density increased), but the volume of the wells significantly decreased ³¹, and as a result, reagent costs are typically 100 times lower and assay volumes have dropped to a few micro-liters (Figure 7) ³². The development of micro-plate technology is very innovative and dynamic, and many companies are involved: even extremely low-volume 3456-well plates have meanwhile been reported ³³. This evolution made it possible that more tests can be handled in the same amount of time and space, while using less reagents per test. But, although the throughput is significantly increased, leading corporations are still only capable of screening some 100 000 compounds per day. Thereby, micro-well plates have their limitations too: first of all, the miniaturization process of those plates in the way it occurred during the past is limited by the physical constraints of delivering small volumes to wells. Fluid handling becomes extremely difficult at smaller scales; advanced robotics are

already needed to deliver micro-liter amounts to high-density micro-well plates. Secondly, not all assays can be miniaturized; some assays will suffer degradation in signal-to-noise ratio upon miniaturization. Thirdly, advanced robotic systems that handle those plates require a lot of space³³. Fourthly, evaporation becomes a significant issue in open low-volume wells, which can cause more sample-to-sample variability. Another drawback is “wicking” and bridging of liquid between wells due to capillary action³⁴. To this end, emerging methods in the field of multiplexing, that have the potential to dramatically increase the amount of data, were developed without the restriction of micro-well plates.

Multiplexing summary

Previous paragraphs have demonstrated the importance of multiplexing in biomolecular research and diagnostics, due to the benefits that have been arisen with the introduction of this technology. Table 3 summarizes the advantages of a multiplex analysis. However, before a multiplex test is accepted, a lot of challenges have to be overcome during its development, from which an overview is shown in Table 4.

Table 3: Advantages of multiplexing

<i>Parameters</i>	<i>Reason</i>
Internal quality control	The nature of multiplexing methods supports the use of internal quality control checks
Patient benefit	Less sample needed
Adequacy	Cytokines are the perfect example of inadequacy of monoplex measurements Single nucleic-acid measurements can lead to spurious conclusions ²⁶
Efficiency	Much less reagent consumption No need to aliquot samples Much less hands-on time, e.g. for a 10-plex tenfold less
Flexibility	Technology can be easily customized to user's specific bioassay
Versatility	Versatility increases dramatically, as bioassays (including, nucleic acids, antigen-antibody binding, enzymes, and receptor-ligand) can be assayed simultaneously on one instrument

Table 4: Disadvantages of multiplexing

Parameters	Reason
Cross-reactivity / Non-specificity	The more targets that have to be multiplexed, the higher the risk for cross-reactivity. Cross-reactivity is one of the most important issues that has to be circumvented when developing a multiplexed protein detection assay
One condition for all targets	All targets have to react optimally in the same conditions (pH, protein content, surfactant content, ionic strength,...)
Sensitivity (*)	Sometimes, monoplex assays are more sensitive Sometimes there is no good multiplex alternative (e.g. sensitive gene-expression via monoplex qPCR compared to less sensitive gene-expression via multiplex microarrays)
Failure	If a multiplex assay fails (e.g. a ten-plex), the whole assay has to be repeated. When one monoplex assay out of ten fails, only that one has to be repeated

(*) *Important remark!* Strictly speaking, the term ‘sensitivity of an assay’ is defined as the **capability of the assay to detect differences in concentration** of the analyte of interest. As shown in Figure 8A, assay A is more sensitive than assay B, because a certain increase in concentration results in a higher increase in response in case of assay A, compared to assay B. In this thesis, however, the term ‘sensitivity of an assay’ refers to the **lower limit of detection (LOD)** of this assay. This is shown in Figure 8B. Assay A is more sensitive than assay B, because assay A detects lower concentrations of the analyte of interest than assay B (although the two standard curves have the same slope). We have used the latter definition, because it is commonly used in this way in the literature.

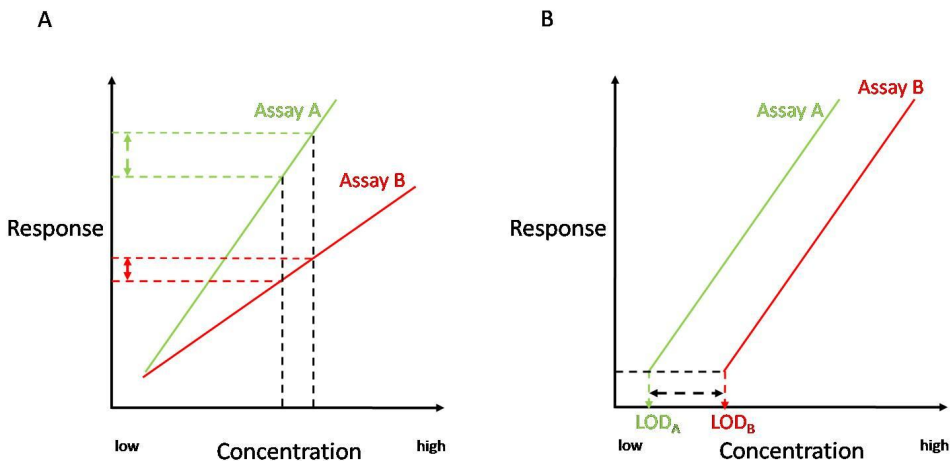


Figure 8: The term ‘sensitivity’ as it should be theoretically used (A, the capability of an assay to detect differences in concentrations), and as it is used in this thesis (B, the capability of an assay to detect lower concentrations).

MULTIPLEXING TECHNOLOGIES

Several multiplexing technologies have been developed during the last twenty years for genomics and proteomics applications. This section categorizes the most important technologies: the principal multiplexing methods for nucleic acid detection are multiplex PCR and DNA-array, and for protein detection, protein-arrays and mass spectrometry, although some other platforms exist (such as two-dimensional gel electrophoresis used for protein identification ³⁵). Note that there is not always a clear separation between those categories, because some of those technologies are often combined in order to increase the level of multiplexing, or the sensitivity of the assays.

Multiplex qPCR.

PCR (polymerase chain reaction) is an enzymatic target amplification method in which an undetectable single copy or a few copies of a piece of DNA are exponentially amplified into millions or more copies that are detectable via post-PCR processing (Figure 9). Real-time quantitative PCR (qPCR), in which the amplification process is followed by means of fluorescent dyes or probes and does not need post-PCR processing, has been established in many diagnostic situations (viral titer estimations, GMOs detection) and procedures as a quick and extremely sensitive method. Real-time qPCR makes use of one primer set (unique to a single sequence of DNA in a mixture of total DNA) in order to amplify that sequence.

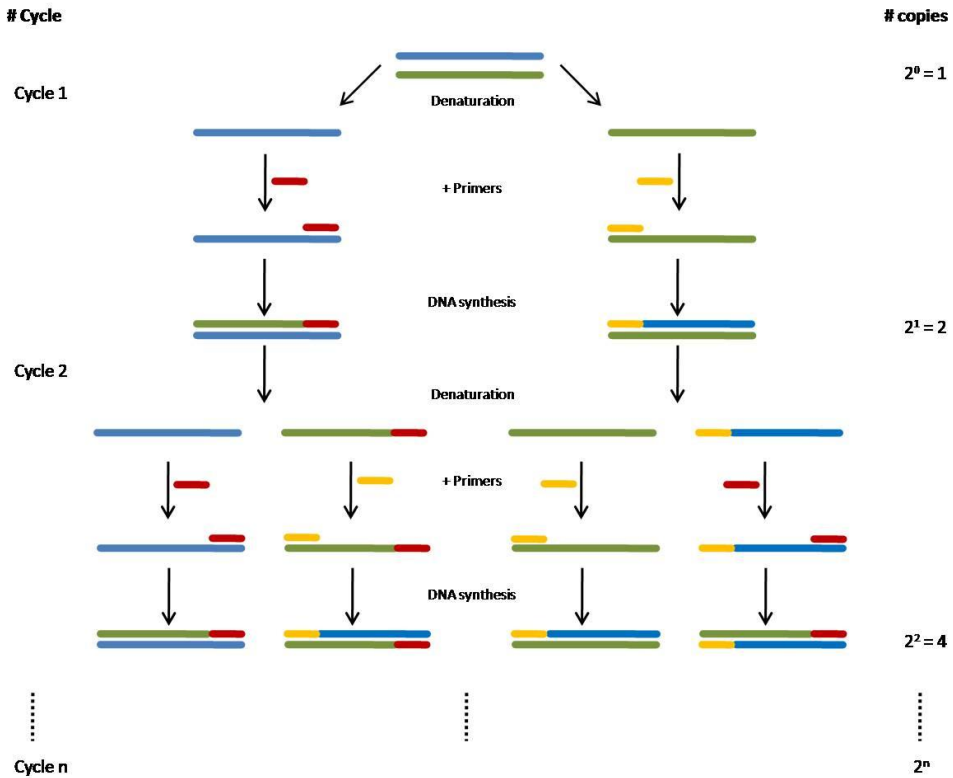


Figure 9: Schematic overview of the PCR reaction. The reaction consist of a series of 20 to 40 repeated cycles. Each cycle consist of 2-3 discrete temperature steps. First step: denaturation at 94-98°C; second step: annealing of the primers at 50-65 °C; third step: extension/elongation around 70-75°C. The DNA fragment is exponentially amplified, resulting in 2^n copies after n cycles. Amplified DNA fragments can be detected using for instance post-PCR gel electrophoresis or in real-time using fluorescent dyes or probes during the PCR reaction.

Multiplex PCR is a variant of PCR which enables simultaneous amplification of many targets of interest in one reaction by using more than one pair of primers^{36,37}. Multiplex PCR often requires an extra post-PCR step for fragment analysis. One technique uses multiple, unique primer sets within a single PCR mixture to produce amplicons of varying sizes specific to the different DNA sequences of interest. Those PCR amplicons are distinguished by fractionation by size and visualized and quantified after separation by gel electrophoresis (e.g. using ethidiumbromide or fluorescent dyes)³⁶. Drawbacks of this (labor-intensive) procedure is that annealing temperatures for each of the primer sets must be optimized to work correctly within a single reaction, and amplicon sizes, i.e., their base pair length, should be different enough to form distinct bands when visualized by gel electrophoresis. Several other methods have been introduced to perform size fractionation, such as multiplex amplifiable probe hybridization (MAPH)³⁸, Quantitative multiplex PCR of Short fluorescent

Fragments (QMPSF)³⁹, multiplex ligation-dependent probe amplification (MLPA)⁴⁰, and non-fluorescent multiplex PCR coupled to high performance liquid chromatography (NFMP-HPLC)⁴¹, from which some employ capillary electrophoresis (usually with fluorescence detection)^{38-40,42}, others high-performance liquid chromatography (HPLC, fluorescence or non-fluorescence detection)⁴¹. Tens of targets can be multiplexed with those methods. A theoretical higher degree of multiplexing can be achieved by a recently described strategy which detects PCR amplicons by hybridization on microarrays: the advantage is that the fragments don't have to be differently sized, because discrimination is based on their sequence⁴³. Other methods analyze multiplex PCR amplicons carefully by sequencing or by MALDI-TOF Mass Spectrometry⁴⁴. A more accurate quantitative estimation of products can be obtained by the use of different fluorescently labeled primers for each unique sequence (no post-PCR fragment analysis)⁴⁵. Apart from issues of cost-efficiency, the major problem of this so-called 'color multiplexing' is the limited multiplexing capacity, because the current availability of only four to five channels for the simultaneous detection of different fluorophores. This degree of multiplexing can be somewhat enhanced by combining color multiplexing with T_m (melting temperature) multiplexing, which has been demonstrated by Wittwer et al.⁴⁶. Although it is probably the most sensitive multiplexing technique for genomics applications, multiplex PCR assays are unfortunately tedious and time-consuming to establish, requiring lengthy optimization procedures. Obviously, each additional target also adds another level of complexity to the assay when it comes to primer dimerization and mispriming⁴⁷.

Mass spectrometry.

'Shotgun' mass spectrometry is the technology of choice for rapid, and cost-effective proteomic surveys today, and is based on the conversion of intact proteins into fragments of different peptides, which is then followed by their volatilization, and by the measurement of their mass-to-charge ratio (m/z ratio) and their intensity. Finally, off-line protein identification occurs by comparison with a database of peptides⁴⁸. Mass spectrometry is ideal for initial proteomic surveys - it is semi-quantitative and therefore only used for identification of gross differences in expression (\geq fivefold!) -, but has some limitations for quantitative protein measurements: 1) The usefulness of the technology for measuring low abundant or 'rare' proteins, such as cytokines, is limited because its analytical sensitivity for multiplexed measurement is much lower than ELISA. 2) Although it is applicable to many sample types, extensive sample preparation is often necessary. 3) Furthermore, labile proteins can degrade during sample preparation or storage greatly impairs protein identification. 4) Databases often contain false positives, due to incomplete or inaccurate database

entries, imprecision in m/z ratio measurement, or non-specific peptide cleavage. 5) Due to some technical and experimental variation, mass spectrometry is limited in use to experiments in which all the samples are run in a single batch. Significant improvement in sensitivity and variation, however, is obtained by using 'multiplexed reaction monitoring'. This approach has the potential to extend the applicability of mass spectrometry to multiplexed protein measurement in human samples⁴⁹. Although mass spectrometry is mainly used for protein research, genomics applications were also described. It has been used in several SNP detection methods (hybridization, invasive cleavage, and single base extension), often in combination with multiplex PCR^{50,51}. In order to overcome current multiplexing limitations of multiplex PCR for instance, recently, MassTag PCR has been proposed, which uses primers that are conjugated by a photocleavable linker to commercial available molecular tags of different molecular weight (a library of 64 distinct tags has been established). After separating amplified products from unincorporated primers, tags are released by UV irradiation and analysed by mass spectrometry. The identity of the amplified sequence is determined by its tag⁵². This approach has been commercialized as the iPlex genotyping technology from Sequenom, Inc (www.sequenom.com).

Planar (micro)arrays

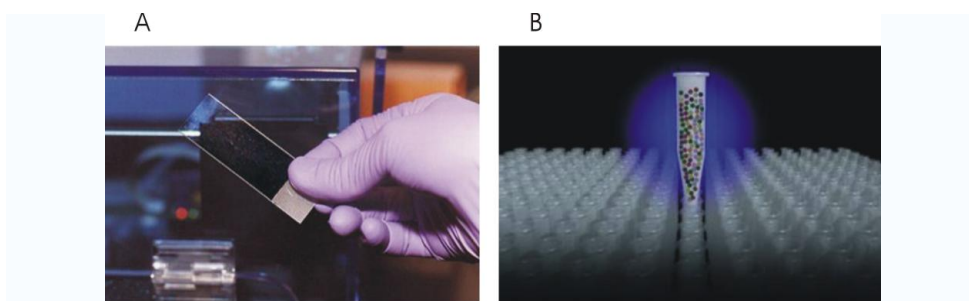


Figure 10: Multiplexing by means of A/ planar microarrays with microspots of probes, and B/ encoded microparticles. For a critical comparison between the two technologies, we refer to Table 6.

Multiplexed nucleic acid solution reactions, such as multiplex PCR, necessitates separation of the analytes for their identification. Although they benefit from optimal reaction kinetics (due to the free mobility of the molecules), their degree of multiplexing is rather low. In order to monitor the expression of many genes at once, DNA microarrays were designed, which consist of a fixed array of thousands of microscopic spots of DNA oligonucleotides, often called features or probes, each

containing picomoles of a specific DNA sequence^{53,54}. The identity of the probe is determined by its location on the chip (Figure 10A). DNA microarray assays are based on the principle of the specific recognition of nucleic acids for complementary sequences. The solid surface can be glass, plastic or a silicon chip. Multiple technologies exist for the fabrication of microarrays, including (non contact ink-jet) printing or spotting, photolithography using pre-made masks, and photolithography using dynamic micromirror devices⁵⁵. In spotted microarrays, such as the non contact ink-jet spotting developed by Agilent, the probes are oligonucleotides, cDNA or small fragments of PCR products that correspond to mRNAs. The probes are synthesized prior to deposition on the array surface and are then "spotted" onto the glass. Although oligonucleotide probes are often used in "spotted" microarrays, they are mainly produced by synthesizing short oligonucleotide sequences directly onto the array surface using photolithography instead of depositing premade intact sequences: light and light-sensitive masking agents are used to create a sequence one nucleotide at a time across the entire array. Each applicable probe is selectively "unmasked" prior to bathing the array in a solution of a single nucleotide, then a masking reaction takes place and the next set of probes are unmasked in preparation for a different nucleotide exposure. After many repetitions, the sequences of every probe become fully constructed. Photolithography can be done using pre-made masks, as done by Affymetrix (GeneChips), or using dynamic micromirrors, as done by Roche (NimbleGen technology). DNA microarrays are now available to detect DNA by comparative genomic hybridization, to probe the entire genome at the level of RNA expression by gene expression profiling, and to probe large segments of the genome for mutation analysis by single nucleotide polymorphism analysis (genotyping). In contrast to multiplex PCR, microarrays have a much higher multiplexing power, but suffer from lower sensitivity. To this end the two technologies are often combined: pre-screening by means of microarrays to detect important features, followed by sensitive PCR analysis of those features.

Table 5: Short list of notably DNA and/or protein microarray manufacturers.

Company	Website	DNA/protein array
Affymetrix	www.affymetrix.com	Yes/ No
Arrayit	www.arrayit.com	Yes/No
Agilent technologies	www.agilent.com	Yes/ No
Asper Biotech	www.asperbio.com	Yes/ No
Biacore (GE Healthcare)	www.biacore.com	Yes/Yes
CombiMatrix	www.combimatrix.com	Yes/ Yes
Eppendorf	www.eppendorf-biochip.com	Yes/ No
Febit	www.geniom.com	Yes/ No

Nimblegen Systems (Roche)	www.nimblegen.com	Yes/ No
Pamgene	www.pamgene.com	Yes/Yes
XCeed Molecular (former MetriGenix)	www.xceedmolecular.com	Yes/No
Zyomyx	www.zyomyx.com	No/Yes

The goal of DNA microarrays was initially to offer an answer on the limitation of multiplexing genomic tools such as Southern, Northern or Western blots, but its basic concepts have been applied during the last decade in proteomics for the determination and quantification of a large number of proteins⁵⁶⁻⁵⁹. Meanwhile, some protein microarray platforms are already commercially available (Table 5). The development of protein arrays, however, has been slower than DNA arrays due to the complexity of protein immobilization and interactions as compared to the principles of DNA hybridization⁶⁰⁻⁶². Protein microarrays can be considered as the next-generation high-throughput successor of the conventional protein array systems with a low multiplexing level, which include multiplex microspots on polystyrene microplates and nitrocellulose membranes, and linear immunoblot systems on nitrocellulose membranes (LIA tests). Multiplex microspot assays are based on the technique originally devised by Ekins⁶³. Genometrix pioneered the printing of dot-arrays in 96-well plate format⁶⁴. This technology is commercially available as the SearchLight platform from Pierce Biotechnology Inc. (www.piercenet.com).

Microarray technology, and in general every planar array platform, struggles with at least two important shortcomings, including: 1) the interaction process (hybridization or immunoaffinity) between the probes and targets requires very long incubation times, because of slow reaction kinetics due to the lay-out of the assay (one of the probes is attached to a fixed surface)^{65,66}. In addition molecules in low concentration have to travel large distances in order to find their appropriate probes and it is known that probes can be released during these prolonged incubation by solution-dependent cleavage⁶⁷. This issue can be partially solved by the use of slides coated with a three-dimensional gel in which the probe/target interaction kinetics are more similar to solution-phase⁶⁸, or by applying sample fluid flows instead of a fixed sample on top of the array, which is achieved by the use of active mixing chambers^{(69, www.biomico.com)}, and the use of flow trough devices^{(70, www.pamgene.com)} and microchannels^{(71,72, www.xceedmolecular.com)}, but the kinetics are still far from solution kinetics. 2) microarrays need a large amount of sample material, because the array has to be completely covered with sample to interact with all probes.

Suspension arrays

Microparticles can also be used as solid-supports in multiplexed analysis to detect several target molecules at once. By uniquely encoding microcarriers for each analyte, the analytes can be tracked by decoding and identifying individual microparticles (Figure 10B).

In combinatorial chemistry, 'active' encoding is often used: in a split-and-mix synthesis, individual microparticles take independent pathways through a series of reaction vessels, and by actively encoding the microparticles during each step of the reaction, it is possible to record the reaction history and thereby identifying the products attached to them. Active encoding is possible by the covalent attachment of detectable chemical tags (such as DNA oligonucleotides, peptides, secondary amines, haloaromatics molecules) to the support microparticles during each step of the split-and-mix synthesis (chemical encoding)⁷³. DNA is for instance often used to encode peptide libraries, because the chemistries for synthesizing both are similar. The microparticles are often called 'biobarcodes', because they are encoded by biomolecules, that need to be released and analyzed at the moment of decoding: encoding DNA molecules are detected on a planar array or by sequencing after PCR amplification. Although those biobarcodes can be produced in high amounts and high multiplexing levels can be achieved, the decoding methods are time-consuming, expensive, and complicated compared with the decoding of optically encoded microparticles. Another drawback is the occurrence of falsely encoded particles, because the synthesizing methods produce sometimes artifacts. The group of Trau demonstrated another way for 'actively' encoding combinatorial libraries: during each step of the split-and-mix synthesis, a specific amount of fluorescent nanospheres (which code for that specific step) was adsorbed via colloidal forces onto the 100 μm sized support microspheres on which the compounds are synthesized. This type of encoding was called 'colloidal encoding'⁷⁴⁻⁷⁶. They demonstrated this encoding principle by adsorbing different combinations of 20 differently dyed nanospheres.

'Active' encoding, which can only be used in the field of combinatorial chemistry, is a totally different approach for the encoding of microparticles than 'fixed' encoding which is applied in diagnostics. Although some well-written reviews were published on this matter⁷⁷⁻⁸⁰, the next section gives a brief overview^{81,82}. Instead of summarizing them by type of encoding (optical, chemical, graphical or digital, electronic, and physical encoding), we have tried to categorize suspension arrays by the technologies that are used to decode them. In general three decoding platforms are used: flow (cyto)meter platforms, optical reading platforms and fibre optic platforms.

Flow (cyto)meter platform

Most of the suspension arrays described in literature are composed of polymer microparticles that are internally doped with one or more fluorophores or chromophores. Those dyes become entrapped by the 'swelling method' as described previously. Microspheres with unique spectral properties are obtained by trapping dyes with different emission spectra at different concentrations⁸³⁻⁸⁶. Optical encoding, as this is called, is the basis for different commercially available platforms. Such optically encoded particles are analysed by flow (cyto)meters⁸⁷. Particle analysis rates as high as 10 000 s⁻¹ are possible. The flow (cyto)meter measures both the spectrum and/or the intensity of the colors/fluorophores which make up the code of a particle as well as a (spectrally different) fluorescence signal at the surface of a particle (in case of a positive reaction). Flow (cyto)meters identify individual particles at high speed^{88,89}. At this moment the xMAP[®] technology (Luminex Corp) is being used in a wide range of applications, as in the screening for and detection of single nucleotide polymorphisms, human cytokines, viruses, infectious diseases, cystic fibrosis, allergens, and kinases^{82,90 87,91-97}. By encoding 5.6 µm polystyrene microparticles with two different dyes at ten different concentrations, they compose a set of 100 unique microparticles⁹⁸ (Figure 11A). Those particles are decoded by a flexible analyzer based on the principles of flow cytometry. Although this technology has been used for a lot of applications, other applications need a higher level of throughput, thus a higher amount of microparticles that can be distinguished. In theory, more codes can be generated by incorporating more than two dyes and/or by using more intensity levels (the number of codes = N^{m-1} , where N is the number of intensity levels and m is the number of dyes), but remaining problems include finding enough encoding elements and the logistics of manufacturing so many different encoded microparticles in large amounts⁸². In practice, this number is indeed much lower by a lot of parameters: the dyes have to be compatible with the swelling process, meaning that not every dye can be used, and the doping process is not always perfectly reproducible, because small differences in bead diameter or composition alter the dyeing efficiency, and it becomes even more difficult with a higher number of dyes and concentrations⁹⁹. Some of these issues could be circumvented by the introduction of new manufacturing methods, for instance using flow focusing methods, as recently described by the group of Flores-Mosquera¹⁰⁰. Note, however, that the costs of the decoding instrument (which is in fact a flow cytometer that has been adapted to be compatible with the dyes), also increases with the number of dyes that is used, making this decoding method probably too expensive for a high-throughput level. A similar encoding strategy has been developed and distributed by Becton Dickinson (BD) Biosciences, but in this case one dye is incorporated at different concentrations¹⁰¹. Although the level of multiplexing that can be achieved is almost 10 times lower than that of the xMAP[®] technology, this technology has also been

used in many applications, because the customer doesn't need an extra bead analyzer for the decoding the microparticles, but can use conventional flow cytometers that are equipped with a 488nm laser and 576 and 670 emission filters. Optical encoding can also be achieved by incorporation of semiconductor quantum dots (QD) into or on the surface of microspheres¹⁰². This can be done during synthesis, or after synthesis by means of the 'swelling method', or by adsorption. QDs have a lot of advantages compared to organic dyes: they can be excited with one excitation wavelength and have narrow emission peaks of about 30 nm with almost no overlap, are brighter, and more resistant against photobleaching. The result is that a less expensive flow cytometer instrument can be used with only one excitation light source^{103,104}. This technology has been commercialized by Qunam Dot Corp (meanwhile acquired by Invitrogen). Organic dyes, fluorescent nanoparticles and/or QDs can also be coated in concentric shells around a core microparticle by means of the Layer-by-Layer technology. This has been shown by the group of Caruso¹². Nanoplex Technologies uses a totally different approach to spectrometric encode microparticles. SERS-Nanotags are silica-encapsulated gold nanoparticles, with a defined Raman-active optical reporter molecule attached, that deliver the superior detection performance of Surface-Enhanced Raman Spectroscopy¹⁰⁵.

By using more advanced flow (cyto)meters, not only fluorescence but also the size and the refractive index can be detected.¹⁰⁶ Note that particles may also be identified by use of their physical characteristics, such as their size and refractive index ("physical encoding"). DiaSorin manufactured the Copalis system, in which particles are encoded by their size and detected in an advanced flow cytometer. 3D Molecular Sciences manufacturers FloCodes, which are particles with different shapes for multiplexing goals. With physical encoding, however, only a low level of multiplexing can be achieved.

Sometimes several encoding methods are used at once in a single particle in order to increase the level of multiplexing¹⁰⁷. As an example, the group of Klimant recently incorporated four encoding features in microparticles: bead size, luminescence brightness of beads, luminescence lifetime, and dual lifetime referencing, and could create bead libraries with an estimated number of 840 different classes^{108,109}.

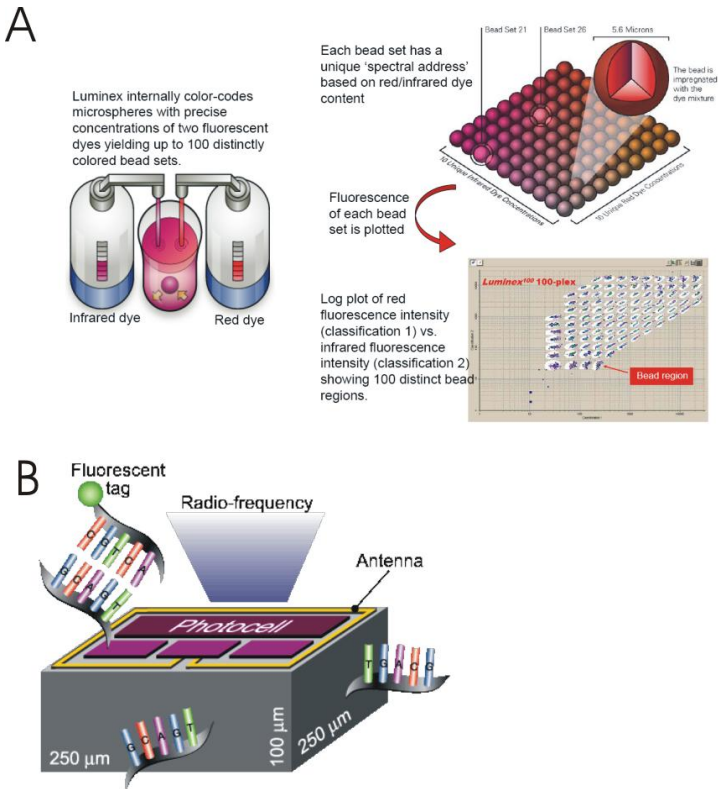


Figure 11: A The Luminex xMAP system consist of a set of 100 microspheres, each microsphere having a unique ratio of two fluorescent dyes. The microspheres are identified individually in a rapidly flowing fluid stream that passes by two laser beams: one reveals the colour code of the bead, and one quantifies the biomolecular reaction by measuring the fluorescence intensity of the reporter molecule. B Electronic radio frequency microchips from PharmaSeq coated with oligonucleotide probes. Each microtransponder is an integrated circuit composed of photocells, memory, clock and antenna. The microtransponder stores information identifying the sequence of an attached oligonucleotide probe in its electronic memory. Detection occurs with a high-speed flow fluorometer modified to detect radio frequency. (a is reproduced with permission from <http://www.luminexcorp.com>, and b with permission from <http://www.pharmaseq.com>)

A totally different approach is the use of light-powered $100\ \mu\text{m} \times 250\ \mu\text{m} \times 250\ \mu\text{m}$ microtransponders, called electronic radio frequency microchips, which comprises an integrated circuit connected to a photovoltaic cell and an antenna (Figure 11B). This type of encoding is called “electric encoding”. A serial number is stored electronically and allows identifying the probe which is attached to the surface of a transponder. Such electronically encoded microcarriers are also analysed by high-speed flow (cyto)meters modified to detect radio frequencies¹¹⁰. Because the memory capacity of such transpondors is very high, other information than ‘barcodes’ can be stored: to this end those microparticles have been used as anti-counterfeiting agents too.

A flow (cyto)meter can rapidly process optically/ physically/ electronically encoded particles making it a popular reading platform for multiplexing. However, it has also several disadvantages, including (i) the lack of portability as flow meters are bulky, (ii) the cost (especially when multiple lasers and detectors are needed) and (iii) the potential interference between the fluorescence from the fluorophores which make up the code and the fluorescence generated at the surface of the particles in case of a positive reaction.

(Fluorescence) Microscope platform.

Flow cytometry based platforms are often based on optical encoding methods, which rely on the detection of one or more optical signals and their translation in a 'code'. Because the encoding (doping) process always causes some errors, microparticles that are fabricated in the same batch, always show some variation in fluorescence intensity of one or more dyes, and therefore variation too in the ratio between the dyes; hence there is uncertainty on the code. When analyzing those particles by flow cytometry, particles with the same code appear as a cloud of dots, not as a single dot. In order to avoid overlap between two clouds (and thus misclassification), the number of intensity levels and dyes is limited. Therefore, optical encoding is limited to low multiplexing level.

An alternative approach to analyze particles is the use of a (fluorescence) microscope, especially when the particles are graphically encoded. Graphically encoded particles rely on the patterning of optical elements in or at the surface of the microcarriers. Because the code is 'digital', each particle is absolutely distinguishable from another. This means that those particles are applicable to medium and high level multiplexing levels, as far as the fabrication methods admit to generate high amount of encoded particles.

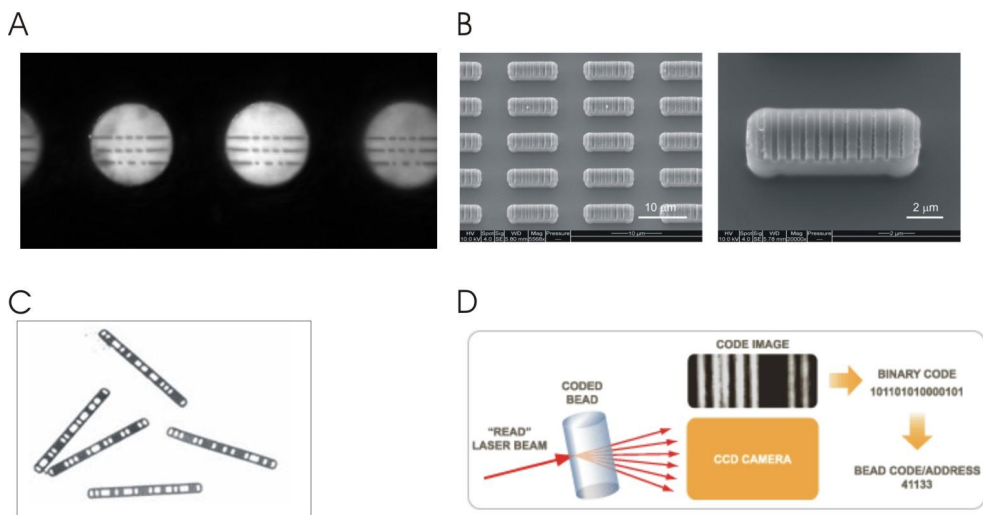


Figure 12: A/ Confocal fluorescent microscopy image of particles, internally barcoded by means of spatial selective photobleaching. The particles are 40 μm in diameter. B/ SEM image of 100 μm particles, encoded by fabrication of a nanostructured pattern on the surface; the pattern is read by detecting the spatial distribution of laser light diffracted by the tag. C/ The UltraPlex platform; a mixture of differently encoded aluminum rods, bar-coded by a dry-etching technique. The particles are 100 μm in length. D/ VeraCode, a cylindrical glass particle measuring 240 microns in length by 28 microns in diameter, inscribed with a unique digital holographic code. (B is reproduced with permission from ref [64], and C with permission from <http://www.illumina.com>)

As Figure 12 shows, different graphically encoded carriers have been reported^{111-115, 116,117, 117-120}. In contrast to optically encoded microcarriers, graphically encoded ones are often ten to some hundreds of microns in diameter or length, because the size needs to fit the 'digital' code (see Figure 12). Most of them do not use fluorescent dyes for the encoding. Hence, a broader range of fluorescence wavelengths remains available for target labeling. Graphically encoded particles often require a well defined orientation to become accurately decoded while some types also require decoding at high resolution. This makes optical reading platforms, which decode the microcarriers in rest, more suitable than flow (cyto)meters in which the carriers flow through the detection area.¹²¹ Microbarcodes, produced by Corning, are made by fusing glass blocks doped with rare-earth ions in a predetermined order and drawing out the product into a ribbon fiber with a cross-section of 20x100 μm which is thereafter cut into micrometer sized sections. An advantage is that all colors can be excited with only one wavelength (the number of codes corresponds to $N^s/2$ where N is the number of colors and s is the number of glass blocks). Nanoplex technologies (meanwhile acquired by Oxonica) has developed striped metal nanobarcode particles (NBCs) of about 500 nm by sequential electrochemical deposition of gold and silver in mesoporous aluminium templates¹²². The power of this technology is that the particles are intrinsically encoded by virtue of the difference in reflectivity

of adjacent metal stripes. Just as a conventional barcode is read by measuring the differential contrast between adjacent black and white lines using an optical scanner, individual NBC are read by measuring the differential reflectivity between adjacent metal stripes within a single particle using a conventional optical microscope. The production rate is much higher than for microbarcodes, but because of their relatively high density vigorous mixing is required in order to keep them in suspension, which can damage them. Besides gold and silver also other metals can be used, which increases the number of codes that can be generated with this technology (the number of codes corresponds to $N^s/2$ where N is the number of metals and s is the number of stripes). Pronostics (former Smartbead Technologies Ltd) fabricated patterned holes in aluminum rods ($100 \times 10 \times 1 \mu\text{m}$) with semiconductor microfabrication methods (UltraPlex platform, Figure 12C)¹²³. The production rate is very high (one wafer makes up millions of particles at once), theoretically millions of codes can be generated, and decoding is done with simple light microscopy, making this approach very attractive. 3D Molecular Sciences designed polymer particles that are encoded via lithographic technology: they use UV light to optically burn a pattern of holes into polymer wafers that are coated with a negative photoresist. Different patterns are obtained using different masks. A disadvantage, however, is the size of the particles ($500 \times 300 \times 25 \mu\text{m}$). Using holographic techniques, Illumina developed a cylindrical glass particle measuring 240 microns in length by 28 microns in diameter that is inscribed with a unique digital holographic code (VeraCode system, Figure 12D). Diffractive encoding was also developed by the group of Morgan, where the surface of $100 \mu\text{m}$ sized SU-8 particles was provided with a nanostructured pattern (Figure 12B); the pattern is read by detecting the spatial distribution of laser light diffracted by the tag¹²⁴. Our group has reported “spatial selective photobleaching” as a new method to digitally encode fluorescent microspheres. Digital codes (such as a bar code, a dot code...) can be written in the *central plane* of fluorescent polystyrene microspheres (called memobeads, Figure 12A) by localized photobleaching of the fluorescent molecules¹²⁵. Clearly, as microspheres are free to rotate in the assay tube, to be able to read the digital code (at the end of the assay) the microspheres must be properly oriented with respect to the focal plane of the microscope. For this purpose we have suggested loading the microspheres with ferromagnetic particles (e.g. CrO_2). In theory, an unlimited number of codes can be generated by the latter two techniques. Recently, an innovative technology that combines particle synthesis and encoding and probe incorporation into a single process using continuous-flow lithography has been proposed by Pregibon et al. The authors use a simple dot-coding scheme to generate particles that can bear over a million (2^{20}) codes¹²⁶. As explained by Wilson et al., besides using a static microscopy platform, theoretically, graphically encoded microcarriers could also be decoded and analyzed by means of flow cytometry. Amnis Corporation combined flow cytometry with imaging hardware in their ImageStream 100, which is like a flow cytometer, but the traditional detectors have been

replaced by a sensitive CCD camera that acquires up to six independent images (brightfield, darkfield, and four colors) at a rate of 100 particles per second. Such instrument could be used to analyze graphically encoded microparticles⁸² (Figure 13).

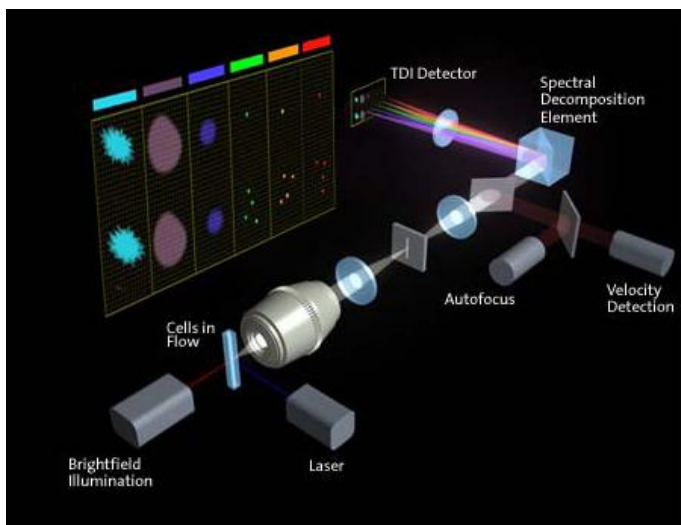


Figure 13: The ImageStream100 is a novel technology that combines the fluidics of a flow cytometer with a method that allows individual cells and particles to be imaged as they pass the detector. It is designed to image objects in flow with high sensitivity, image fidelity, and in multiple simultaneous imaging modes. Fluorescence, side scatter, and transmitted light from cells are imaged by an objective lens and relayed to a spectral decomposition element, which divides the imagery into 6 spectral bands located side-by-side across the CCD camera. The ImageStream 100 could be used to read graphical codes and detect fluorescent reporter molecules bound to their surface (Courtesy of Amnis – www.amnis.com).

Note that not only graphically encoded microcarriers but also the optically and physically encoded carriers described above can be analysed by optical reading platforms. As an example, recently Gao and Nie described the use of QD encoded particles read out by a (conventional) optical imaging platform.⁸⁵ A special technology has been developed by Swartzman et al., which was called ‘fluorometric microvolume assay technology’ (FMAT) and employs a unique macro confocal imaging system that automatically focuses and scans fluorescently encoded microparticles at the bottom of a well-plate¹²⁷. Note that graphically encoded microparticles have already shown potential in different application fields^{114,118,128,129}.

Optical fibre platform.

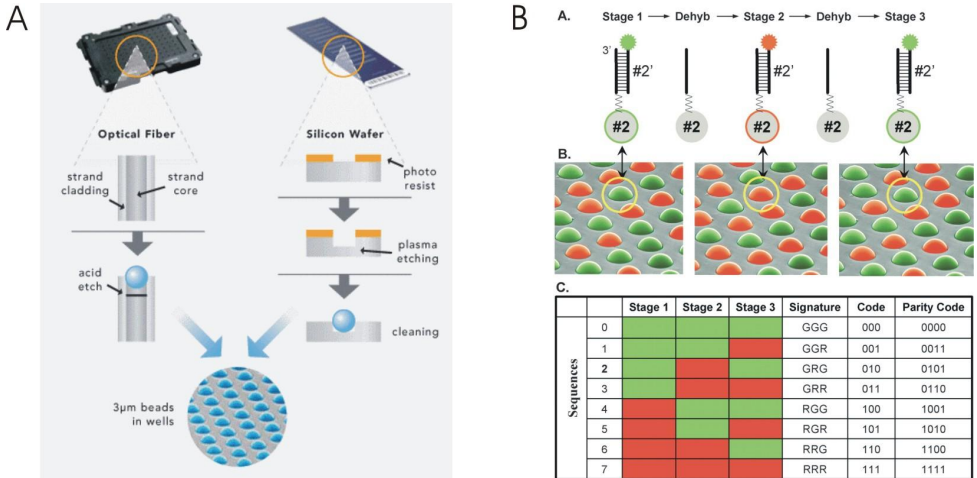


Figure 14: A/ Overview of the Illumina Inc. fibre-optic platform: 3 micron particles self assemble in uniform microwells etched into the surface of fiber optic bundles (96-sample Array Matrix) or planar silica slides (multi-sample BeadChip). B/ Decoding process of Illumina's BeadArray technology. (A) Schematic of the sequential hybridization process for a single particle. In stage 1, a complementary fluorescently labeled decoder oligonucleotide hybridizes to the oligonucleotide capture probe that is attached to the particle. The fluorescent signal is read by imaging the entire array. The array is then dehybridized, and the process is repeated for two more stages. (B) A scanning electron micrograph of an array of particles, artificially colored to represent three sequential hybridization stages (note that the particle circled in yellow has the color signature GRG or code 010). (C) Colors are assigned to individual decoder oligonucleotides in each stage to produce a unique combination across stages. (Part A with permission from www.illumina.com and part B with permission from ref [73])

Illumina developed particle-based fibre optic arrays which make use of 'optical fibres' to decode color encoded 3 micron silica particles. An optical imaging fibre consists of thousands of hexagonally packed, micrometer-sized individual optical fibres (Figure 14)^{130,131}. By dipping the etched end of the fibre directly in the sample of encoded particles, the wells are filled with particles by self-assembling. The other end of the fibre bundle is coupled to an imaging fluorescence system that independently resolves each fibre, while simultaneously viewing the entire array (Figure 14A). Although the encoded particles are positioned in an array, their identities are known from their spectral properties¹³². To overcome some encoding limitations, recently Illumina devised a novel approach (randomly ordered high-density DNA arrays, the 'Beadarray')¹³³. A different set of oligonucleotide 'tag' sequences is coupled to each particle (the "code"); after self-assembling of the particles on the array, decoding of the particles occurs by sequential hybridizations with different dye-labeled decoding (complementary anti-tag) solutions (Figure 14B)¹³⁴. This Beadarray competes with the flat surface microarrays for high-throughput analysis of genes and gene products. The main

problem is that the location of the microspheres is random and to this end the array has to be decoded before it can be used. Another issue is that this method is very time-consuming and required a lot of oligonucleotides to be synthesized.

MEMOBEAD TECHNOLOGY

As described in previous section, our group proposed spatial selective photobleaching as an alternative encoding method for the production of a suspension array. Because of the importance of this method related to the present study, this section describes the principle behind it in more detail.

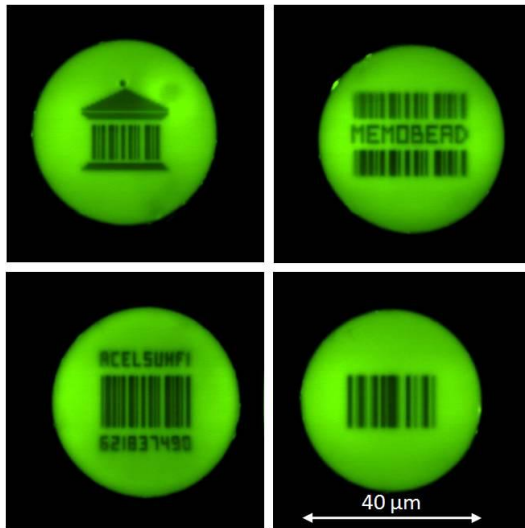


Figure 15: Encoding microcarriers by spatial selective photobleaching. Examples of several geometries that are bleached at the central plane of 40 μm sized fluorescent microcarriers. Figure adapted from ¹²⁵.

Photobleaching is a photo-induced process where fluorescent molecules lose their fluorescent properties, resulting in a fading of the fluorescent color. *Spatial selective photobleaching* refers to the photobleaching of certain regions in a fluorescent material, such as in a fluorescent microcarrier. Any geometry can be bleached, at a certain depth in that microcarrier by using a confocal scanning laser microscope (CSLM) modified for this purpose (Figure 15). There are only two requirements for the microcarrier. First, it has to be sufficiently transparent for the laser light to get inside the microsphere. Second, the fluorescent molecules should be fixed in the material.

Otherwise, the bleached code will fade away over time because of diffusion of the fluorescent and bleached molecules.

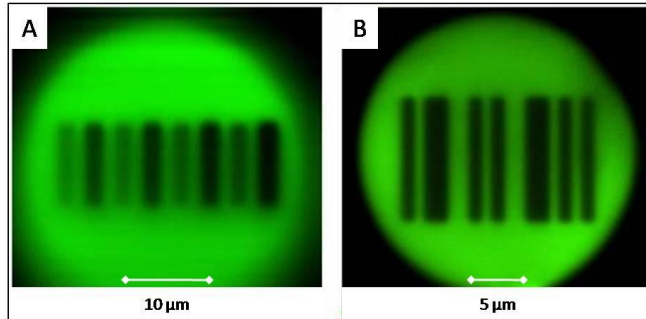


Figure 16: Encoding microcarriers by means of spatial selective photobleaching. A/ To demonstrate the possibility of intensity encoding, a barcode was bleached at the central plane of a 45 μm microcarrier using eight different bleaching levels. B/ A barcode was bleached at the central plane of a 28 μm microsphere using two intensities (bleached and unbleached) and two widths (1.06 μm and 2.12 μm). Figure adapted from ¹²⁵.

The method of spatial selective photobleaching has been applied in the past to microcarriers made of several materials, such as polystyrene, argogel (polyethylene glycol grafted polystyrene), and dextran (and other common polymer bead materials are also expected to work well). This encoding technology has important advantages. As the encoding method is applicable to regular polystyrene microspheres that have been common to screening applications for many years, it has a major advantage in that users can benefit from the current extensive knowledge on performing bead-based assays, eliminating the need for the development of new special chemistries. Because the code is written inside the microcarriers, it is protected from the environment. The code is digital, meaning that it does not carry any uncertainty, or in other words, if at time zero 'code 1' is photobleached, exactly the same code will appear as a 'code 1' that is photobleached on another moment, which is not the case with the previously mentioned 'color encoding' methods. The number of unique codes that can be generated is virtually unlimited and depends on three aspects, the first obviously being the space available inside the microsphere. The second aspect is the resolution of the writing beam primarily depending on the characteristics of the CLSM. Finally, the number of codes is determined by the number of different widths and intensities that are employed in the encoding scheme, as demonstrated in Figure 16. This minimal encoding time is not a fundamental limit to the bleaching process, but an instrument dependent parameter.

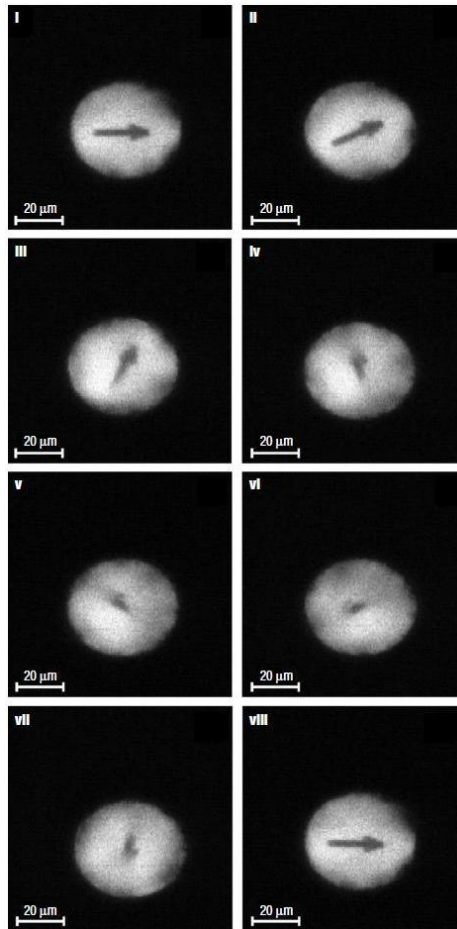


Figure 17: Magnetic orientation of a magnetized ferromagnetic microcarrier, encoded with an arrow.(i) An arrow was bleached at the central plane of a magnetized ferromagnetic microcarrier to visualize its orientation.(ii–viii) Subsequently, a sequence of confocal images (1 image every 2 seconds) was taken to record the movement of the microcarrier while being subjected to an external randomly moving magnetic field. The microcarrier follows precisely the movement of the external magnetic field. When the magnetic field returns to its original orientation, the microcarrier is observed to do the same (compare images i and viii). Images ii to vii represent the situation of the microcarrier being subjected to an assay during which it will be randomly oriented. Image viii demonstrates the possibility at readout time to correctly reorient the microcarrier such that the encoded pattern becomes clearly visible again.

Because two-dimensional codes are written inside three-dimensional microcarriers, the microcarriers have to be oriented in the appropriate position for a correct read-out of the code. This is possible by using microcarriers that are coated with ferromagnetic nanoparticles. By applying an external magnetic field at the encoding step, those magnetic nanoparticles are magnetized, so that there exists a relationship between the direction of the code and the direction of the magnetic moment. At the decoding step, the microcarriers can obtain the same orientation by applying a weak external magnetic field with the same orientation relative to the laser light, thus bringing the code to

the correct readout position (Figure 17). Chapter 2 of this thesis describes the optimal magnetic coating procedure of polystyrene microcarriers.

TO BEAD OR NOT TO BEAD?

It is widely accepted that microparticle technology has several advantages to flat surface microarray technology, regarding for instance the flexibility in test panel, the reproducibility of attached probes, and improved kinetics. Table 6 summarizes the main dissimilarities between the two multiplexing platforms. The previous paragraph has demonstrated the tremendous increase in microparticle encoding methods and applications during the last decade. The question remains, however, whether microparticle technology will replace the flat microarray technology, as the latter one did in past with the micro-wellplate technology (Figure 18).

Table 6: Flat surface microarray versus suspension arrays (adapted from ²⁸). Commercially systems are indicated with [x].

Feature	Flat surface microarrays	Suspension microarrays
Substrate	Glass (¹³⁵ , [A]) Silicon ([B]) Plastic ([C], [D], [E]) Gold ¹³⁶ PDMS ¹³⁷	Polystyrene beads (^{98,125} , [M], [N], [O], [P]) Metal (aluminium) nanoparticles (^{122,123} [Q] [R]) Semiconductor nanocrystals ([S]) Silicon ([T]) Glass ([U], [V]) SU-8 ¹²⁴
Surface modification	Polymer coating Metal coating Gel coating ⁶⁸ Membrane layer (Schleicher & Schuell) Direct derivatization	Polymer coating [P]
Probe deposition	In situ synthesis: mask-guided [B] In situ synthesis: maskless [Z] Contact printing Noncontact spotting [D]	Affinity or covalent binding in solution (batch) [several]

Probe identification	X,y coordinates	Particle encoding <ul style="list-style-type: none"> - Optical (⁸⁸, [N], [S], [M]) - Chemical ([W]) - Graphical (¹²²⁻¹²⁵, [P] [Q] [R] [X]) - Electronic ([T]) - Physical ([Y], [Z])
Incubation	Static [several] Mixing [several]	Mixing [several]
Detection	Confocal scanning (Genetix, Axon, Affymetrix) Resonance light scattering ([F]) Surface plasmon resonance ([G]; [H]) Cantilever technology ([I]) Planar waveguide detection ([J]) Mass spectrometry MALDI ([K]) SELDI ([L])	Flow cytometry ([O] [T], [N]) Fibre optics ([M] [W]) Imaging system (¹²³ [P], [S], [R], [V]) Raman spectroscopy (¹⁰⁵) Time resolved fluorometry (¹³⁸)
Production at the same time	Relatively low number	Hundreds till millions of microparticles
Reproducibility of attached probes	Relatively low; variation in spot density with spotting methods	High; produced in batches of millions of microparticles
Surface chemistry	Same for all probes on one array	Probes attached in separate batches via a variety of methods before mixing
Flexibility for adding probes	Low	High
Binding kinetics	Limited by diffusion (partly solved by some adaptations)	Efficient mixing
Degree of multiplexing	High (> 100 000)	Low [several] / Medium [several] / High [W]
Sample throughput	Low	Medium
Statistics	Each feature = datapoint; only few features per analyte	Each microparticle = datapoint; many microparticles for each analyte -> high quality
Know-how	A lot of know-how; lots of references	Rather new technology; less references
Costs	Relatively expensive for medium and low throughput	Cheaper for medium and low throughput

[A], ArrayIT; [B], Affymetrix; [C]: Nanogen, [D]: Agilent; [E]: Caliper; [F]: Genicon Sciences; [G]: Biacore, [H]: XanTec, [I]: Protiveris, [J]: Zeptosens, [K]: Sequenom, [L]: CIPHERGEN, [M]: Illumina old system, [N]: BD Cytometric BeadArray, [O]: Luminex corp.; [P]: Biocartis SA (former Memobead technologies); [Q]: Smartbead

technologies; [R]: Nanoplex; [S]: Quantum Dot Corp; [T]: PharmaSeq; [U]: Veracode from Illumina; [V]: Corning's microbarcodes; [W]: Illumina new system; [X]: 3D Molecular Sciences; [Y]: Copalis from DiaSorin; [Z]: FloCodes from 3D Molecular Sciences; [Z]: Nimblegen.

In genomics, following the decoding of the human genome, we were and still are looking for technologies that are capable to obtain more and more information from smaller sample volumes. At this moment, the most popular approach to quantify an enormous amount of DNA targets is the planar array technology. In genomics, nowadays planar microarrays can be considered as the most popular tool for whole genome screening. Regarding the multiplexing level, so far, none of the suspension array systems can compete with the planar microarray technology, and regardless of the advantages of suspension array technology with respect to hybridization kinetics, planar arrays will remain the method of choice to this purpose as long as no efforts are undertaken in the field of suspension arrays to generate an ultrahigh amount of encoded microcarriers efficiently and at an acceptable time scale¹³⁹. Those suspension arrays, however, provide the potential for probing segments of the genome (instead of the whole genome) in a customized way, using capture tags that locate specific oligonucleotide sequences to specific array elements¹⁴⁰ and are therefore recognized as an economical alternative for the high-cost planar microarray technology at the medium throughput screening level. Because suspension arrays have the potential to accommodate the simultaneous detection of some tens of SNPs, they are well suited for the detection of heterogeneous genetic disorders caused by numerous mutations (such as cystic fibrosis). They can also be useful for studying highly polymorphic systems (such as the human major histocompatibility system, HLA), for testing risk panels (cancer, infectious diseases, thrombosis,...), and for newborn screening panels¹⁴¹. To this end, planar microarrays are nowadays mainly applied in high-throughput research and only few examples were found in literature where commercially available planar microarray platforms were applied at the medium throughput level (Nanogen, Osmetech, Randox, MetriGenix, PamGene, Biosite, High Throughput Genomics, and Panomics). We believe that within the next years, both technologies will be used next to each other in the genomics field depending on the application: high or medium throughput.

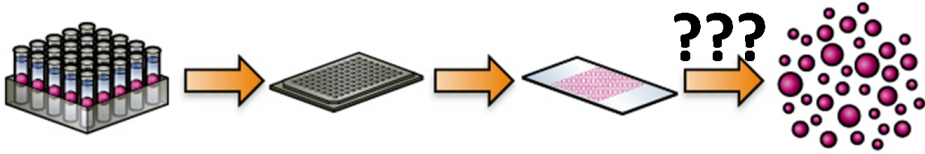


Figure 18: Evolution of tests from single-tube monoplex assays, via monoplex microwell-plate assays, to multiplex planar microarray assay and multiplex suspension array assays. The question remains whether suspension arrays are going to replace the planar microarray technology in future.

There are indications that future diagnostics will involve measuring several types of biomarkers (DNA, RNA and protein) simultaneously. This need the development of DNA/RNA/protein microarrays that are capable of assaying proteins and nucleic acid molecules simultaneously, in order to get information at the genomics, transcriptomics, and proteomics level. Because of the flexibility in chemistry for the attachment of probes, suspension arrays will become very important tools for this matter. As will be overviewed in the next paragraph, tests can made more sensitive via target-and/or signal amplification. Target amplification of DNA is for instance possible by means of PCR as described previously (Figure 9). So far, however, no target-amplification methods exist for proteins, and in order to make immunoassays more sensitive, signal amplification methods have to be used (see next paragraph). To this purpose, immunoassays using nucleic acid labels were developed, where the results are amplified and read via PCR. Because such tests would allow immunoassays and nucleic acid tests to be performed on a single platform using the same detection strategy, flexible platforms as suspension array will play a critical role.

Instead of the threat of innovative suspension arrays, the question is whether planar microarrays will not be replaced in future by other advanced technologies. Multiplexing is indeed very challenging, and for some applications it might be never as successful as their monoplex counterparts. The use of microarrays for instance as high-throughput platform for gene expression analysis is well-known, and the only reason therefore is that qPCR technology nowadays still is a low-throughput technology. But novel qPCR technologies in the field of microfluidics are under

development that have an incredible high throughput capacity and the sensitivity and accuracy of conventional qPCR platforms. Those monoplex technologies rely on the parallel qPCR analysis of hundreds till thousands of samples against hundreds till thousands of genes. Examples are the OpenArray system from Biotrove (www.biotrove.com)¹⁴², the Biomark system from Fluidigm (www.fluidigm.com)¹⁴³, the Smartchip from Wafergen (www.wafergen.com), and the 384 XHTS from StokesBio (www.stokesbio.com). Highly likely, those platforms, and not suspension arrays, will become the method of choice for high density gene expression analysis and will replace conventional flat microarrays in this field. The reason that those parallel monoplex microfluidic gene expression tests will replace planar arrays, is the quality (sensitivity) of the data, which will be of greater importance than the advantages of multiplex microarray tests (such as less sample consumption etc). Microfluidics will also be introduced in the proteomics field, but as in this field no technology exist that relies on target amplification, it will continue to benefit from the advantages of multiplex assays. To this end it is expected that microfluidics technologies will not replace multiplex assays, but instead thereof, their combination will be promising in order to bring this proteomics field to a higher level of sensitivity and efficiency. Chapter 6 overviews this integration in more detail.

TARGET LABELING IN MULTIPLEXED SUSPENSION ARRAYS

A common feature of all nucleic acid and protein detection assays on planar microarrays and suspension arrays is the use of labels, which are typically molecules that fluoresce or produce a color to indicate probe-target interactions. Sensitivity might be one drawback of multiplexing, but this can be solved by the use of signal amplification methods, as it occurs in monoplex assays too (as in ELISA for instance). Although usually less potent than target amplification (such as amplicon generation in a polymerase chain reaction), signal amplification methods became very important in multiplexed suspension arrays for protein detection. With no target amplification equivalent to PCR available for proteins, the sensitivity of protein-(immune)assays is still far below that of nucleic acid tests. Signal amplification methods lead to an improved sensitivity. Considering that some of these techniques can be further combined with improved detection methods, there is a possibility that the sensitivity gap between nucleic acid assays and immunoassays will be reduced.

Some signal amplification methods can be applied simultaneously to all features on the array, DNA or protein. Most of the methods have been developed specifically for signal amplification

on planar microarrays, such as the use of liposomes, nanoparticles, magnetic beads, and gold nanoparticles. Signal amplification systems for suspension arrays, however, are more challenging, because the microparticles randomly move through the sample. To this end only those methods in which the product of the amplification reaction is localized in the region where the reaction is initiated (and not diffuses), can be applied simultaneously to planar microarrays and suspension arrays. This section overviews labeling methods that have been applied on suspension arrays, and also labeling methods that might be compatible with suspension arrays, but not yet proven.

In bead-based immunoassays, immobilized antibodies trap their specific corresponding antigens from the sample solution. The bound antigens can be detected through a direct labeling approach (fluorophores are covalently attached to the antigen) or through a sandwich immunoassay approach (using a pair of capture and detection antibodies that recognize two non-overlapping epitopes of the antigen). In the latter approach, the detection antibody can be directly linked with a fluorophore. This is, however, a rather expensive and difficult approach (all detection antibodies in a multiplex assay have to be efficiently conjugated with fluorescent molecules), and in order to avoid this, other strategies have been proposed.

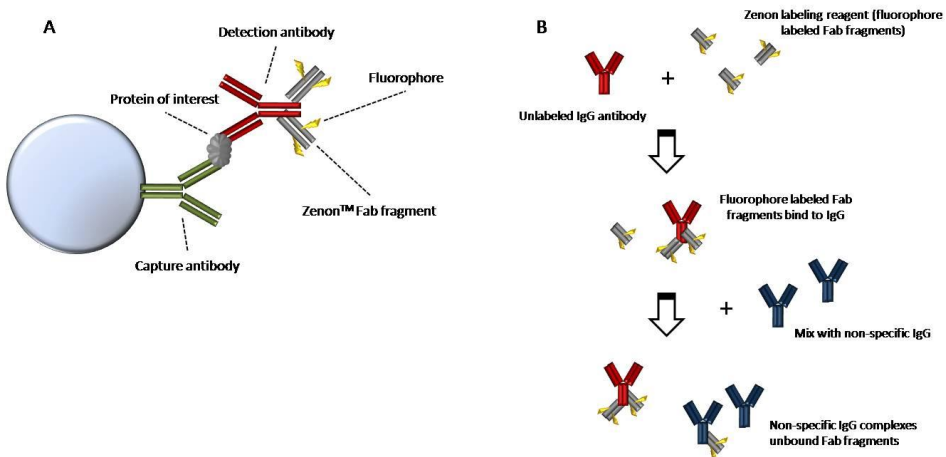


Figure 19: Target labeling by means of the Zenon™ labeling method. A/ Fluorophore conjugated Fab fragments bind to the Fc portion of the detection antibody. B/ The Zenon labeling scheme. An unlabeled IgG is incubated with the Zenon labeling reagent. The labeled Fab fragment binds and unbound Fab fragments are bound by the addition of a nonspecific IgG. The addition of nonspecific IgG prevents cross-labeling of the Fab fragment in later steps. Note that the Fab fragment used for labeling could also be coupled to a biotin, instead of a fluorophore, so that final labeling can occur with fluorescent streptavidin. Because this method makes use of a mechanism inherent to protein interactions, it cannot be used for DNA analysis.

The Zenon™ technology uses fluorescently labeled Fab fragments of antibodies to label detection antibodies all at once with the same fluorophore (Figure 19). Although this approach is geared for labeling multiplex assays, in our research we observed a relatively high amount of non-specific (background) labeling, probably because the Fab fragment were transferred from ‘positive’ microparticles to the detection antibodies at the surface of ‘negative’ microparticles, and the sensitivity was therefore troublesome. A better choice is the use of biotinylated detection antibodies which can react on their turn in a final step with fluorescently labeled streptavidin (Figure 20). An additional advantage is the little gain in signal amplification, because one streptavidin molecule is labeled with 3 fluorophores on average. Meanwhile, this approach has been applied already many times to several suspension array platforms and has become the standard method in microcarrier-based multiplex analysis¹⁴⁴.

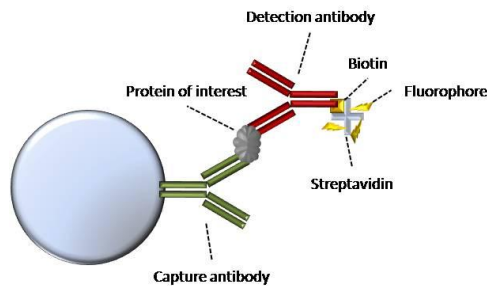


Figure 20: Target labeling by means of biotinylated detection antibodies and fluorophore conjugated streptavidin. Note that the biotin/streptavidin affinity can be used for DNA analysis, for instance for labeling captured biotinylated target sequences on microcarriers.

The same method is more or less applied to microparticle-based hybridization assays: immobilized capture probes (oligonucleotides, cDNA...) hybridize with complementary (parts of) target molecules. The bound target molecules can be detected through a direct labeling approach by the incorporation of fluorophores into the target strand (for instance fluorescently labeled polymerase chain reaction products obtained by using fluorescent probes in the PCR reaction) or indirectly via biotinylation of the target molecule and fluorophore-conjugated streptavidin⁹⁰.

Rolling circle amplification (RCA)

In its original formulation, the **rolling circle amplification** reaction (RCA), which was used for mutation detection, involves numerous rounds of isothermal enzymatic synthesis in which DNA polymerase extends a primer that is hybridized to a circular DNA probe of several dozen nucleotides, by continuously progressing around the DNA minicircle probe to replicate its sequence over and over again. This process easily yields in one hour up to several thousands of sequence-complementary tandem repeats of the original DNA minicircle ^{145,146}. Some years ago, the RCA strategy has been proposed as an alternative to conventional multiplex immunoassays on microparticles with an improvement in detection limit for human cytokines up to 100-fold ¹⁴⁷. In this so-called immunoRCA (Figure 21), the 5' end of an RCA primer is attached to the detection antibody. After formation of the sandwich construct, this short DNA sequence anneals to a single-stranded DNA circle. In the presence of RCA DNA polymerase and nucleotides, the rolling circle reaction extends the double-stranded annealed sequence. By including biotinylated dNTPs, biotin moieties are incorporated into the growing DNA strand, which can be detected by means of fluorophore-conjugated streptavidin. Rolling-circle amplification is a technique applicable to both nucleic acid and protein suspension arrays. Commercial suspension array kits are now available from Qiagen (LiquiChip technology).

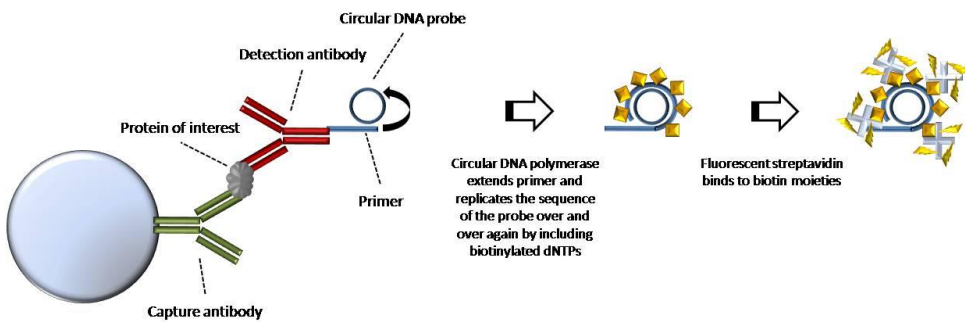


Figure 21: Target labeling by means of immuno Rolling Circle Amplification (immunoRCA). The 5' end of a primer is attached to the detection antibody. Obviously, RCA can also be used for DNA detection on microcarriers.

Nanoparticles

Kim and Park have used **magnetic nanoparticles** for a duplex detection of proteins immobilized via a sandwich assay on two different fluorescent one micrometer sized microparticles (Figure 22 B). Binding of the protein of interest resulted in deflection of the microparticles in a magnetic field, and because the velocity of the microparticles was proportional to the protein concentration, quantitative measurements were possible over a dynamic range of about 3 logs¹⁴⁸. Hall et al. demonstrated one decade ago the use of **fluorescent particulate labels** to enhance the sensitivity of sandwich immunoassays at the bottom of 96-well plates¹⁴⁹. The group of Haugland applied such nanospheres to solution-phase amplifications for the detection of cell surface receptors by flow cytometry¹⁵⁰. Although it has never been demonstrated before, particulate nanolabels could be applied to microparticle-based protein and DNA assays too as depicted in Figure 22 A. In this context, we can also refer to the use of QDs and other types of semi-conductor nanocrystals as nanolabels (commercialized by Invitrogen).

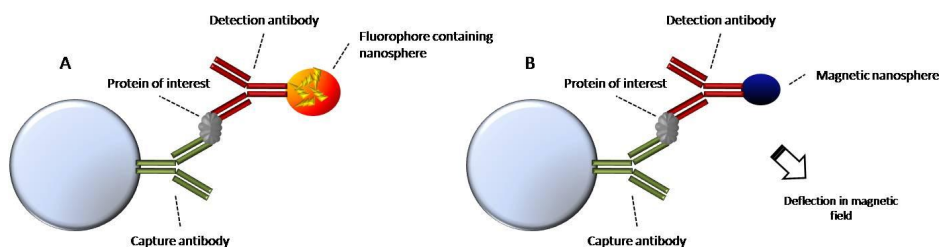


Figure 22: Target labeling by means of fluorescent nanoparticles (A), and magnetic nanoparticles (B). In the latter case, the microcarriers are deflected in a magnetic field if the protein of interest was present in the sample, with a velocity that is proportional to the concentration of the protein. The detection antibodies can be directly covalently linked to the nanoparticles, or indirectly via biotin moieties to streptavidin coated nanoparticles. Note that nanoparticles can also be coupled to oligonucleotides, so that this labeling method can be used for DNA analysis too.

Liposome signal amplification

Excellent reviews are available in literature that describe the use of liposomes to amplify the signal in immunoassays¹⁵¹. Liposomes are phospholipid vesicles that entrap hundreds of thousands of marker molecules to provide a large signal amplification and enhanced sensitivity, three orders of magnitude greater than conventional single fluorophore detection. **Liposome signal amplification** has been demonstrated on microparticle-based immunoassays too (Figure 23)¹⁵². Although the

application in multiplexed system to our knowledge has never been described, it should be applicable to both nucleic acid and protein suspension arrays.

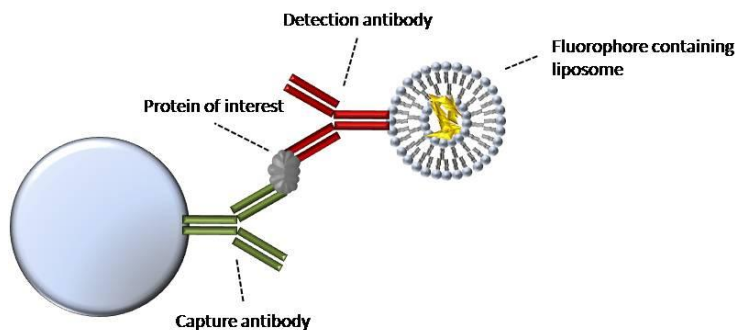


Figure 23: Target labeling by means of liposome signal amplification. Note that liposomes can also be coupled to oligonucleotides, so that this labeling method can be used for DNA analysis too.

Branched DNA

Branched DNA (bDNA) or **DNA dendrimers** are complex, branched molecules built from interconnected DNA monomeric subunits that were originally developed to detect DNA or RNA targets sensitively in a micro-well format. Meanwhile, important commercial platforms were developed based on the bDNA technology for testing HIV-1 and HCV viral load¹⁵³. Lowe et al. demonstrated the use of 3DNA dendrimers in order to increase the signal-to-noise ratio for fluorescence detection of multiple target DNA molecules captured on different microparticles in a multiplex assay. A 3DNA dendrimer is composed of two DNA strands that share a region of sequence complementarity located in the central portion of each strand. When the two strands anneal to form the monomer the resulting structure has a central double-stranded 'waist' bordered by four single-stranded 'arms'. This 'waist' plus 'arms' structure comprises the basic 3DNA monomer. The assay resulted in a 10-fold fluorescence amplification compared to single-step labeling method with fluorophore-conjugated streptavidin¹⁵⁴. The group of Lohman have adapted the branched DNA (bDNA) technology to flow cytometry and suggested the possibility of performing multiplex analysis (Figure 24)¹⁵⁵. This bDNA technology has been recently successful applied to the xMAP[®] platform for parallel quantitative gene expression profiling¹⁵⁶ and is in meanwhile commercially available (distributed by Panomics). To our knowledge, no multiplex protein detection assays exist based on the bDNA technology.

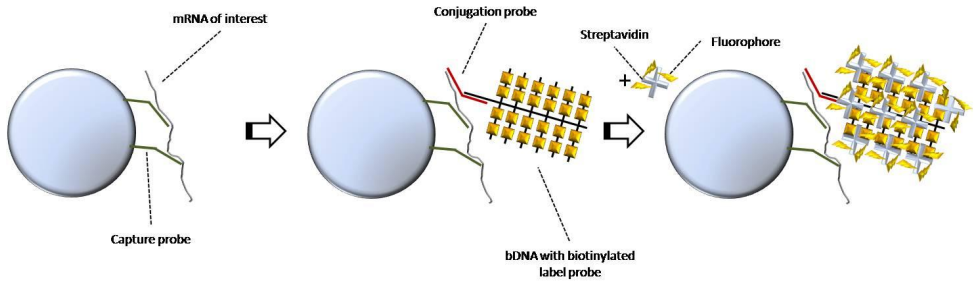


Figure 24: Target labeling by means of branched DNA (bDNA) technology. mRNA of interest hybridizes to capture probes that are coupled to the surface of the microcarrier. Conjugation probes, bDNA, and biotinylated probes are then added, which forms a complex at the surface. Finally fluorophore conjugated streptavidin is added which binds to the biotin residues and labels the surface. Note that this technology can also be used for the detection of DNA molecules.

Molecular beacons

For the detection of nucleic acids by flow cytometry, Horejsh et al. suggested the use of 'BeadCons arrays' (molecular beacon-conjugated beads), generated using different bead sizes and **molecular beacons** in different fluorophore colors⁴⁷. Molecular beacons are single-stranded oligonucleotides possessing a probing loop sequence (usually 15 to 30 nucleotides in length) embedded within complementary arm sequences (usually 5 or 6 nucleotides long). The probe sequence is chosen to be complementary to a specific target sequence that is present in the nucleic acid to be detected. The arm sequences form a hairpin stem that keeps a terminal fluorophore (covalently linked to one end of the oligonucleotide) and a terminal quencher molecule (covalently linked to the other end of the oligonucleotide) in close proximity in the absence of nucleic acid molecules that are complementary to the loop. Due to the close proximity, a FRET reaction occurs, and as a result, no fluorescence occurs. When a molecular beacon encounters a target molecule, however, a probe-target hybrid with the loop will be formed, that results in a conformational reorganization that forces the quencher and fluorophore away from each other, restoring fluorescence (Figure 25)¹⁵⁷.

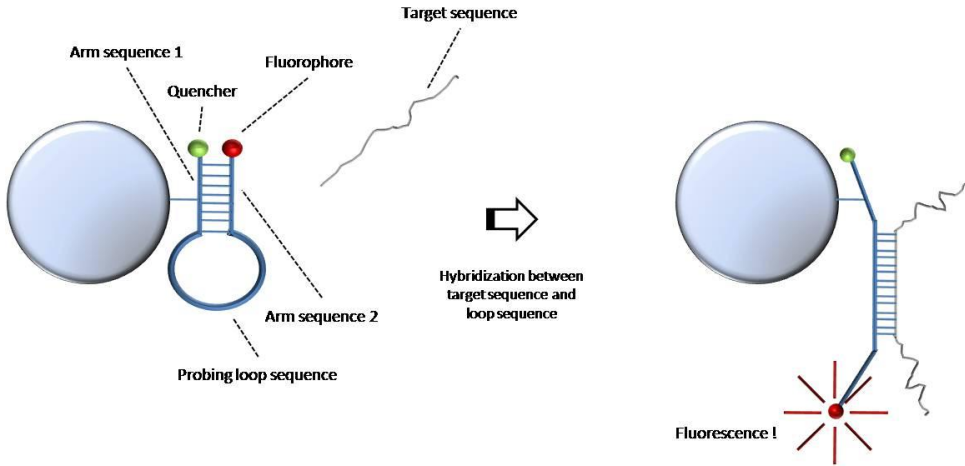


Figure 25: Target labeling by means of molecular beacons. As long as no target sequence is present that is complementary to the loop sequence, the complementary arm sequences are hybridized bringing the fluorophore and the quencher molecule in close proximity. A FRET reaction occurs, that results in no fluorescence. If a complementary arm sequence is present, it will hybridize to the loop sequence, that forces the fluorophore and the quencher molecule away from each other, resulting in fluorescence.

Catalyzed reporter deposition (CARD)

The group of Walt developed the use of imaging fibres for multiplexed assays, and in order to increase the sensitivity, they applied the **enzyme-catalyzed reporter deposition (CARD)** method to this platform¹⁵⁸. This method relies on the use of horseradish peroxidase (HRP) conjugated detection antibodies that catalyze the deposition of a substantially amount of fluorescent tyramine residues on the bead surface around the site of enzyme activity, which result in a substantially amount of fluorescence (Figure 26). A detailed description of this method, which is also called **Tyramide signal amplification (TSA)**, is given in chapter 4. Because this strategy makes use of the affinity between biotin and streptavidin, and because biotin residues can be easily build in DNA sequences, this enzymatic amplification method is applicable to nucleic acid analysis too.

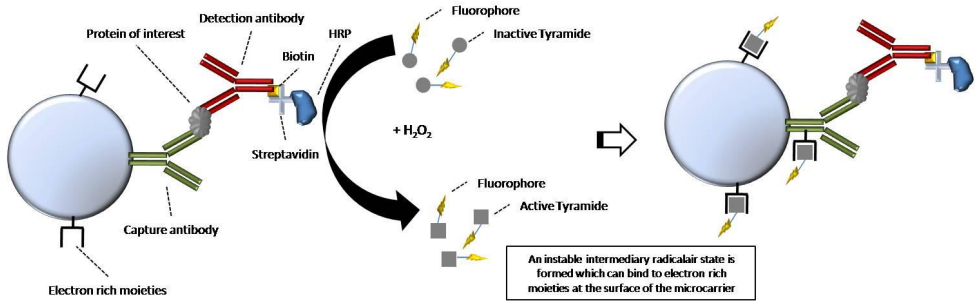


Figure 26: Target labeling by means of the enzyme-catalyzed reporter deposition technology. Horse radish peroxidase (HRP) conjugated streptavidin binds to biotinylated detection antibodies. In the next step, HRP converts inactive fluorophore conjugated tyramide residues in the presence of H_2O_2 to an activated intermediary radical state. In this unstable state, the residues can interact with electron rich moieties that are present in the proximity of the enzyme. Electron rich moieties can be found in proteins (antibodies or other proteins that are used as a blocking agent in the assay and which bound therefore to the surface of the microcarrier).

Summary of the labeling methods

Table 7 briefly summarizes the application fields of the main target labeling methods that can be applied to suspension arrays.

Table 7: Labeling technologies that are compatible with multiplex microparticle-based assays.

Labeling technology	Application		Signal enhancement
	protein	DNA	
Direct labeling of biomolecule	*	*	-
Zenon™ technology	*	-	-
Fluorescent streptavidin	*	*	+
3DNA dendrimers	*	*	+++
Branched DNA	-	*	+++
Molecular beacons	-	*	-
CARD/TSA	*	*	+++
Magnetic nanoparticles	*	*	na
Fluorescent particulate labels	*	*	++
Fluorescent Liposomes	*	*	++
Rolling circle amplification	*	*	+++

REFERENCES

1. PLOTZ, C. M.; SINGER, J. M. The latex fixation test. I. Application to the serologic diagnosis of rheumatoid arthritis. *Am. J. Med.* **1956**, *21* (6), 888-892.
2. Ortega-Vinuesa, J. L.; Bastos-Gonzalez, D. A review of factors affecting the performances of latex agglutination tests. *Journal of Biomaterials Science-Polymer Edition* **2001**, *12* (4), 379-408.
3. Piskin, E.; Tuncel, A.; Denizli, A.; Ayhan, H. Monosize microbeads based on polystyrene and their modified forms for some selected medical and biological applications. *J. Biomater. Sci. Polym. Ed* **1994**, *5* (5), 451-471.
4. Vetvicka, V.; Fornusek, L. Polymer microbeads in immunology. *Biomaterials* **1987**, *8* (5), 341-345.
5. Kawaguchi, H. Functional polymer microspheres. *Progress in Polymer Science* **2000**, *25* (8), 1171-1210.
6. Tuncel, A.; Piskin, E. Polystyrene latex particles: preparation and properties. *Biomater. Artif. Cells Immobilization Biotechnol.* **1991**, *19* (1), 229-253.
7. Zhang, P. F.; Dou, H. J.; Li, W. W.; Tao, K.; Xing, B.; Sun, K. Fabrication of fluorescent and magnetic multifunctional polystyrene microbeads with carboxyl ends. *Chemistry Letters* **2007**, *36* (12), 1458-1459.
8. Mori, H.; Haruyama, S.; Shinozaki, Y.; Okino, H.; Iida, A.; Takanashi, R.; Sakuma, I.; Hussein, W. K.; Payne, B. D.; Hoffman, J. I. New nonradioactive microspheres and more sensitive X-ray fluorescence to measure regional blood flow. *Am. J. Physiol* **1992**, *263* (6 Pt 2), H1946-H1957.
9. Sathe, T. R.; Agrawal, A.; Nie, S. M. Mesoporous silica beads embedded with semiconductor quantum dots and iron oxide nanocrystals: Dual-function microcarriers for optical encoding and magnetic separation. *Analytical Chemistry* **2006**, *78* (16), 5627-5632.
10. Mulvaney, S. P.; Mattoussi, H. M.; Whitman, L. J. Incorporating fluorescent dyes and quantum dots into magnetic microbeads for immunoassays. *Biotechniques* **2004**, *36* (4), 602-609.
11. Mulvaney, S. P.; Mattoussi, H. M.; Whitman, L. J. Incorporating fluorescent dyes and quantum dots into magnetic microbeads for immunoassays. *Biotechniques* **2004**, *36* (4), 602-+.
12. Wang, D. Y.; Rogach, A. L.; Caruso, F. Semiconductor quantum dot-labeled microsphere bioconjugates prepared by stepwise self-assembly. *Nano Letters* **2002**, *2* (8), 857-861.
13. Shah, D.; Chandra, T.; Chang, A.; Klosterman, K.; Richerson, R.; Keller, C. Acridinium-Labeling to Latex Microparticles and Application in Chemiluminescence-Based Instrumentation. *Clinical Chemistry* **1994**, *40* (9), 1824-1825.
14. Wild, D. *The Immunoassay Handbook*; Nature Publishin Group London: 2001.

15. Douglas, A. S.; Monteith, C. A. Improvements to Immunoassays by Use of Covalent Binding Assay Plates. *Clinical Chemistry* **1994**, *40* (9), 1833-1837.
16. Osipov, A. P.; Zaitseva, N. V.; Egorov, A. M. Studies on antigen-antibody interactions by flow injection chemiluminescent sensor. *J. Biolumin. Chemilumin.* **1997**, *12* (1), 37-39.
17. Halperin, A.; Buhot, A.; Zhulina, E. B. Hybridization at a surface: the role of spacers in DNA microarrays. *Langmuir* **2006**, *22* (26), 11290-11304.
18. Pankhurst, Q. A.; Connolly, J.; Jones, S. K.; Dobson, J. Applications of magnetic nanoparticles in biomedicine. *Journal of Physics D-Applied Physics* **2003**, *36* (13), R167-R181.
19. Derveaux, S.; De Geest, B. G.; Roelant, C.; Braeckmans, K.; Demeester, J.; De Smedt, S. C. Multifunctional layer-by-layer coating of digitally encoded microparticles. *Langmuir* **2007**, *23* (20), 10272-10279.
20. Miraglia, S.; Swartzman, E. E.; Mellentin-Michelotti, J.; Evangelista, L.; Smith, C.; Gunawan, I., I.; Lohman, K.; Goldberg, E. M.; Manian, B.; Yuan, P. M. Homogeneous Cell- and Bead-Based Assays for High Throughput Screening Using Fluorometric Microvolume Assay Technology. *J. Biomol. Screen.* **1999**, *4* (4), 193-204.
21. Beaudet, L.; Bedard, J.; Breton, B.; Mercuri, R. J.; Budarf, M. L. Homogeneous assays for single-nucleotide polymorphism typing using AlphaScreen. *Genome Res.* **2001**, *11* (4), 600-608.
22. Ling, M. M.; Ricks, C.; Lea, P. Multiplexing molecular diagnostics and immunoassays using emerging microarray technologies. *Expert. Rev. Mol. Diagn.* **2007**, *7* (1), 87-98.
23. Hoffman, I. E.; Peene, I.; Meheus, L.; Huizinga, T. W.; Cebecauer, L.; Isenberg, D.; De, B. K.; Hulstaert, F.; Veys, E. M.; De, K. F. Specific antinuclear antibodies are associated with clinical features in systemic lupus erythematosus. *Ann. Rheum. Dis.* **2004**, *63* (9), 1155-1158.
24. O'Garra, A.; Murphy, K. Role of cytokines in determining T-lymphocyte function. *Curr. Opin. Immunol.* **1994**, *6* (3), 458-466.
25. Kellar, K. L.; Douglass, J. P. Multiplexed microsphere-based flow cytometric immunoassays for human cytokines. *J. Immunol. Methods* **2003**, *279* (1-2), 277-285.
26. Kingsmore, S. F. Multiplexed protein measurement: technologies and applications of protein and antibody arrays. *Nat. Rev. Drug Discov.* **2006**, *5* (4), 310-320.
27. Bissonnette, L.; Bergeron, M. G. Next revolution in the molecular theranostics of infectious diseases: microfabricated systems for personalized medicine. *Expert. Rev. Mol. Diagn.* **2006**, *6* (3), 433-450.
28. Petrik, J. Diagnostic applications of microarrays. *Transfus. Med.* **2006**, *16* (4), 233-247.
29. McGlennen, R. C. Miniaturization technologies for molecular diagnostics. *Clin. Chem.* **2001**, *47* (3), 393-402.
30. Burbaum, J. J. The evolution of miniaturized well plates. *J. Biomol. Screen.* **2000**, *5* (1), 5-8.

31. Kricka, L. J. Miniaturization of analytical systems. *Clin. Chem.* **1998**, *44* (9), 2008-2014.
32. Kell, D. Screensavers: trends in high-throughput analysis. *Trends Biotechnol.* **1999**, *17* (3), 89-91.
33. Battersby, B. J.; Trau, M. Novel miniaturized systems in high-throughput screening. *Trends Biotechnol.* **2002**, *20* (4), 167-173.
34. Dove, A. Drug screening--beyond the bottleneck. *Nat. Biotechnol.* **1999**, *17* (9), 859-863.
35. Wittmann-Liebold, B.; Graack, H. R.; Pohl, T. Two-dimensional gel electrophoresis as tool for proteomics studies in combination with protein identification by mass spectrometry. *Proteomics* **2006**, *6* (17), 4688-4703.
36. Chamberlain, J. S.; Gibbs, R. A.; Ranier, J. E.; Nguyen, P. N.; Caskey, C. T. Deletion screening of the Duchenne muscular dystrophy locus via multiplex DNA amplification. *Nucleic Acids Res.* **1988**, *16* (23), 11141-11156.
37. Edwards, M. C.; Gibbs, R. A. Multiplex PCR: advantages, development, and applications. *PCR Methods Appl.* **1994**, *3* (4), S65-S75.
38. Armour, J. A.; Sismani, C.; Patsalis, P. C.; Cross, G. Measurement of locus copy number by hybridisation with amplifiable probes. *Nucleic Acids Res.* **2000**, *28* (2), 605-609.
39. Charbonnier, F.; Raux, G.; Wang, Q.; Drouot, N.; Cordier, F.; Limacher, J. M.; Saurin, J. C.; Puisieux, A.; Olschwang, S.; Frebourg, T. Detection of exon deletions and duplications of the mismatch repair genes in hereditary nonpolyposis colorectal cancer families using multiplex polymerase chain reaction of short fluorescent fragments. *Cancer Res.* **2000**, *60* (11), 2760-2763.
40. Schouten, J. P.; McElgunn, C. J.; Waaijjer, R.; Zwijnenburg, D.; Diepvens, F.; Pals, G. Relative quantification of 40 nucleic acid sequences by multiplex ligation-dependent probe amplification. *Nucleic Acids Res.* **2002**, *30* (12), e57.
41. De, L. L.; Curia, M. C.; Catalano, T.; De, T. S.; Bassi, C.; Mareni, C.; Bertario, L.; Battista, P.; Mariani-Costantini, R.; Radice, P.; Cama, A. Combined use of MLPA and nonfluorescent multiplex PCR analysis by high performance liquid chromatography for the detection of genomic rearrangements. *Hum. Mutat.* **2006**, *27* (10), 1047-1056.
42. Carrera, P.; Barbieri, A. M.; Ferrari, M.; Righetti, P. G.; Perego, M.; Gelfi, C. Rapid detection of 21-hydroxylase deficiency mutations by allele-specific in vitro amplification and capillary zone electrophoresis. *Clin. Chem.* **1997**, *43* (11), 2121-2127.
43. Gibbons, B.; Datta, P.; Wu, Y.; Chan, A.; Al, A. J. Microarray MAPH: accurate array-based detection of relative copy number in genomic DNA. *BMC Genomics* **2006**, *7*, 163.
44. Ross, P.; Hall, L.; Smirnov, I.; Haff, L. High level multiplex genotyping by MALDI-TOF mass spectrometry. *Nat. Biotechnol.* **1998**, *16* (13), 1347-1351.
45. Persson, K.; Hamby, K.; Ugozzoli, L. A. Four-color multiplex reverse transcription polymerase chain reaction--overcoming its limitations. *Anal. Biochem.* **2005**, *344* (1), 33-42.

46. Wittwer, C. T.; Herrmann, M. G.; Gundry, C. N.; Elenitoba-Johnson, K. S. Real-time multiplex PCR assays. *Methods* **2001**, *25* (4), 430-442.
47. Horejsh, D.; Martini, F.; Poccia, F.; Ippolito, G.; Di, C. A.; Capobianchi, M. R. A molecular beacon, bead-based assay for the detection of nucleic acids by flow cytometry. *Nucleic Acids Res.* **2005**, *33* (2), e13.
48. Reddy, G.; Dalmaso, E. A. SELDI ProteinChip(R) Array Technology: Protein-Based Predictive Medicine and Drug Discovery Applications. *J. Biomed. Biotechnol.* **2003**, *2003* (4), 237-241.
49. Anderson, L.; Hunter, C. L. Quantitative mass spectrometric multiple reaction monitoring assays for major plasma proteins. *Molecular & Cellular Proteomics* **2006**, *5* (4), 573-588.
50. Kim, S.; Edwards, J. R.; Deng, L.; Chung, W.; Ju, J. Solid phase capturable dideoxynucleotides for multiplex genotyping using mass spectrometry. *Nucleic Acids Res.* **2002**, *30* (16), e85.
51. Yang, H.; Wang, H.; Wang, J.; Cai, Y.; Zhou, G.; He, F.; Qian, X. Multiplex single-nucleotide polymorphism genotyping by matrix-assisted laser desorption/ionization time-of-flight mass spectrometry. *Anal. Biochem.* **2003**, *314* (1), 54-62.
52. Briese, T.; Palacios, G.; Kokoris, M.; Jabado, O.; Liu, Z.; Renwick, N.; Kapoor, V.; Casas, I.; Pozo, F.; Limberger, R.; Perez-Brena, P.; Ju, J.; Lipkin, W. I. Diagnostic system for rapid and sensitive differential detection of pathogens. *Emerg. Infect. Dis.* **2005**, *11* (2), 310-313.
53. Lockhart, D. J.; Winzeler, E. A. Genomics, gene expression and DNA arrays. *Nature* **2000**, *405* (6788), 827-836.
54. Brown, P. O.; Botstein, D. Exploring the new world of the genome with DNA microarrays. *Nat. Genet.* **1999**, *21* (1 Suppl), 33-37.
55. Venkatasubbarao, S. Microarrays--status and prospects. *Trends Biotechnol.* **2004**, *22* (12), 630-637.
56. Joos, T. O.; Stoll, D.; Templin, M. F. Miniaturised multiplexed immunoassays. *Curr. Opin. Chem. Biol.* **2002**, *6* (1), 76-80.
57. Stoll, D.; Templin, M. F.; Schrenk, M.; Traub, P. C.; Vohringer, C. F.; Joos, T. O. Protein microarray technology. *Front Biosci.* **2002**, *7*, c13-c32.
58. Templin, M. F.; Stoll, D.; Schrenk, M.; Traub, P. C.; Vohringer, C. F.; Joos, T. O. Protein microarray technology. *Trends Biotechnol.* **2002**, *20* (4), 160-166.
59. Wiese, R.; Belosludtsev, Y.; Powdrill, T.; Thompson, P.; Hogan, M. Simultaneous multianalyte ELISA performed on a microarray platform. *Clin. Chem.* **2001**, *47* (8), 1451-1457.
60. Kusnezow, W.; Hoheisel, J. D. Antibody microarrays: promises and problems. *Biotechniques* **2002**, *Suppl*, 14-23.

61. Kusnezow, W.; Syagailo, Y. V.; Ruffer, S.; Baudenstiel, N.; Gauer, C.; Hoheisel, J. D.; Wild, D.; Goychuk, I. Optimal design of microarray immunoassays to compensate for kinetic limitations: theory and experiment. *Mol. Cell Proteomics* **2006**, *5* (9), 1681-1696.
62. Perlee, L.; Christiansen, J.; Dondero, R.; Grimwade, B.; Lejnine, S.; Mullenix, M.; Shao, W.; Sorette, M.; Tchernev, V.; Patel, D.; Kingsmore, S. Development and standardization of multiplexed antibody microarrays for use in quantitative proteomics. *Proteome Sci.* **2004**, *2* (1), 9.
63. Ekins, R.; Chu, F. Multianalyte microspot immunoassay. The microanalytical 'compact disk' of the future. *Ann. Biol. Clin. (Paris)* **1992**, *50* (5), 337-353.
64. Mendoza, L. G.; McQuary, P.; Mongan, A.; Gangadharan, R.; Brignac, S.; Eggers, M. High-throughput microarray-based enzyme-linked immunosorbent assay (ELISA). *Biotechniques* **1999**, *27* (4), 778-6, 788.
65. Kusnezow, W.; Syagailo, Y. V.; Goychuk, I.; Hoheisel, J. D.; Wild, D. G. Antibody microarrays: the crucial impact of mass transport on assay kinetics and sensitivity. *Expert. Rev. Mol. Diagn.* **2006**, *6* (1), 111-124.
66. Henry, M. R.; Stevens, P. W.; Sun, J.; Kelso, D. M. Real-time measurements of DNA hybridization on microparticles with fluorescence resonance energy transfer. *Analytical Biochemistry* **1999**, *276* (2), 204-214.
67. Situma, C.; Hashimoto, M.; Soper, S. A. Merging microfluidics with microarray-based bioassays. *Biomolecular Engineering* **2006**, *23* (5), 213-231.
68. Angenendt, P.; Glöckler, J.; Konthur, Z.; Lehrach, H.; Cahill, D. J. 3D protein microarrays: performing multiplex immunoassays on a single chip. *Anal. Chem.* **2003**, *75* (17), 4368-4372.
69. Adey, N. B.; Lei, M.; Howard, M. T.; Jensen, J. D.; Mayo, D. A.; Butel, D. L.; Coffin, S. C.; Moyer, T. C.; Slade, D. E.; Spute, M. K.; Hancock, A. M.; Eisenhoffer, G. T.; Dalley, B. K.; McNeely, M. R. Gains in sensitivity with a device that mixes microarray hybridization solution in a 25- μ m-thick chamber. *Analytical Chemistry* **2002**, *74* (24), 6413-6417.
70. van Beuningen, R.; van Damme, H.; Boender, P.; Bastiaensen, N.; Chan, A.; Kievits, T. Fast and specific hybridization using flow-through microarrays on porous metal oxide. *Clinical Chemistry* **2001**, *47* (10), 1931-1933.
71. Benoit, V.; Steel, A.; Torres, M.; Lu, Y. Y.; Yang, H. J.; Cooper, J. Evaluation of three-dimensional microchannel glass biochips for multiplexed nucleic acid fluorescence hybridization assays. *Analytical Chemistry* **2001**, *73* (11), 2412-2420.
72. Muggerud, A. A.; Johnsen, H.; Barnes, D. A.; Steel, A.; Lonning, P. E.; Naume, B.; Sorlie, T.; Borresen-Dale, A. L. Evaluation of MetriGenix custom 4D (TM) arrays applied for detection of breast cancer subtypes. *Bmc Cancer* **2006**, *6*.
73. Czarnik, A. W. Encoding strategies in combinatorial chemistry. *Proceedings of the National Academy of Sciences of the United States of America* **1997**, *94* (24), 12738-12739.

74. Battersby, B. J.; Lawrie, G. A.; Johnston, A. P.; Trau, M. Optical barcoding of colloidal suspensions: applications in genomics, proteomics and drug discovery. *Chem. Commun. (Camb.)* **2002**, (14), 1435-1441.
75. Grondahl, L.; Battersby, B. J.; Bryant, D.; Trau, M. Encoding combinatorial libraries: A novel application of fluorescent silica colloids. *Langmuir* **2000**, *16* (25), 9709-9715.
76. Trau, M.; Battersby, B. J. Novel colloidal materials for high-throughput screening applications in drug discovery and genomics. *Advanced Materials* **2001**, *13* (12-13), 975-+.
77. Braeckmans, K.; De Smedt, S. C.; Leblans, M.; Pauwels, R.; Demeester, J. Encoding microcarriers: present and future technologies. *Nat. Rev. Drug Discov.* **2002**, *1* (6), 447-456.
78. Yingyongnarongkul, B. E.; How, S. E.; az-Mochon, J. J.; Muzerelle, M.; Bradley, M. Parallel and multiplexed bead-based assays and encoding strategies. *Comb. Chem. High Throughput. Screen.* **2003**, *6* (7), 577-587.
79. Venkatasubbarao, S. Microarrays--status and prospects. *Trends Biotechnol.* **2004**, *22* (12), 630-637.
80. Wilson, R.; Cossins, A. R.; Spiller, D. G. Encoded microcarriers for high-throughput multiplexed detection. *Angew. Chem. Int. Ed Engl.* **2006**, *45* (37), 6104-6117.
81. Braeckmans, K.; De Smedt, S. C.; Leblans, M.; Pauwels, R.; Demeester, J. Encoding microcarriers: present and future technologies. *Nat. Rev. Drug Discov.* **2002**, *1* (6), 447-456.
82. Wilson, R.; Cossins, A. R.; Spiller, D. G. Encoded microcarriers for high-throughput multiplexed detection. *Angew. Chem. Int. Ed Engl.* **2006**, *45* (37), 6104-6117.
83. Cook, E. B.; Stahl, J. L.; Lowe, L.; Chen, R.; Morgan, E.; Wilson, J.; Varro, R.; Chan, A.; Graziano, F. M.; Barney, N. P. Simultaneous measurement of six cytokines in a single sample of human tears using microparticle-based flow cytometry: allergics vs. non-allergics. *J. Immunol. Methods* **2001**, *254* (1-2), 109-118.
84. Fulton, R. J.; McDade, R. L.; Smith, P. L.; Kienker, L. J.; Kettman, J. R., Jr. Advanced multiplexed analysis with the FlowMetrix system. *Clin. Chem.* **1997**, *43* (9), 1749-1756.
85. Gao, X.; Nie, S. Quantum dot-encoded beads. *Methods Mol. Biol.* **2005**, *303*, 61-71.
86. Han, M.; Gao, X.; Su, J. Z.; Nie, S. Quantum-dot-tagged microbeads for multiplexed optical coding of biomolecules. *Nat. Biotechnol.* **2001**, *19* (7), 631-635.
87. Vignali, D. A. Multiplexed particle-based flow cytometric assays. *J. Immunol. Methods* **2000**, *243* (1-2), 243-255.
88. Gao, X.; Nie, S. Quantum dot-encoded mesoporous beads with high brightness and uniformity: rapid readout using flow cytometry. *Anal. Chem.* **2004**, *76* (8), 2406-2410.
89. Nolan, J. P.; Sklar, L. A. Suspension array technology: evolution of the flat-array paradigm. *Trends Biotechnol.* **2002**, *20* (1), 9-12.

90. Dereg, D.; Gilbert, S. A.; Dudas, S.; Pasick, J.; Baxi, S.; Burton, K. M.; Baxi, M. K. A multiplex DNA suspension microarray for simultaneous detection and differentiation of classical swine fever virus and other pestiviruses. *J. Virol. Methods* **2006**, *136* (1-2), 17-23.
91. Dunbar, S. A.; Jacobson, J. W. Application of the luminex LabMAP in rapid screening for mutations in the cystic fibrosis transmembrane conductance regulator gene: A pilot study. *Clin. Chem.* **2000**, *46* (9), 1498-1500.
92. Dunbar, S. A.; Vander Zee, C. A.; Oliver, K. G.; Karem, K. L.; Jacobson, J. W. Quantitative, multiplexed detection of bacterial pathogens: DNA and protein applications of the Luminex LabMAP system. *J. Microbiol. Methods* **2003**, *53* (2), 245-252.
93. Dunbar, S. A.; Jacobson, J. W. Rapid screening for 31 mutations and polymorphisms in the cystic fibrosis transmembrane conductance regulator gene by Luminex xMAP suspension array. *Methods Mol. Med.* **2005**, *114*, 147-171.
94. Oliver, K. G.; Kettman, J. R.; Fulton, R. J. Multiplexed analysis of human cytokines by use of the FlowMetrix system. *Clin. Chem.* **1998**, *44* (9), 2057-2060.
95. Prabhakar, U.; Eirikis, E.; Davis, H. M. Simultaneous quantification of proinflammatory cytokines in human plasma using the LabMAP assay. *J. Immunol. Methods* **2002**, *260* (1-2), 207-218.
96. Prabhakar, U.; Eirikis, E.; Miller, B. E.; Davis, H. M. Multiplexed cytokine sandwich immunoassays: clinical applications. *Methods Mol. Med.* **2005**, *114*, 223-232.
97. Taylor, J. D.; Briley, D.; Nguyen, Q.; Long, K.; Iannone, M. A.; Li, M. S.; Ye, F.; Afshari, A.; Lai, E.; Wagner, M.; Chen, J.; Weiner, M. P. Flow cytometric platform for high-throughput single nucleotide polymorphism analysis. *Biotechniques* **2001**, *30* (3), 661-669.
98. Fulton, R. J.; McDade, R. L.; Smith, P. L.; Kienker, L. J.; Kettman, J. R. Advanced multiplexed analysis with the FlowMetrix(TM) system. *Clinical Chemistry* **1997**, *43* (9), 1749-1756.
99. Kettman, J. R.; Davies, T.; Chandler, D.; Oliver, K. G.; Fulton, R. J. Classification and properties of 64 multiplexed microsphere sets. *Cytometry* **1998**, *33* (2), 234-243.
100. Ganan-Calvo, A. M.; Martin-Banderas, L.; Gonzalez-Prieto, R.; Rodriguez-Gil, A.; Berdun-Alvarez, T.; Cebolla, A.; Chavez, S.; Flores-Mosquera, M. Straightforward production of encoded microbeads by Flow Focusing: potential applications for biomolecule detection. *Int. J. Pharm.* **2006**, *324* (1), 19-26.
101. Varro, R.; Chen, R.; Sepulveda, H.; Apgar, J. Bead-based multianalyte flow immunoassays: the cytometric bead array system. *Methods Mol. Biol.* **2007**, *378*, 125-152.
102. Han, M.; Gao, X.; Su, J. Z.; Nie, S. Quantum-dot-tagged microbeads for multiplexed optical coding of biomolecules. *Nat. Biotechnol.* **2001**, *19* (7), 631-635.
103. Wang, H. Q.; Liu, T. C.; Cao, Y. C.; Huang, Z. L.; Wang, J. H.; Li, X. Q.; Zhao, Y. D. A flow cytometric assay technology based on quantum dots-encoded beads. *Anal. Chim. Acta* **2006**, *580* (1), 18-23.

104. Wang, H. Q.; Huang, Z. L.; Liu, T. C.; Wang, J. H.; Cao, Y. C.; Hua, X. F.; Li, X. Q.; Zhao, Y. D. A feasible and quantitative encoding method for microbeads with multicolor quantum dots. *J. Fluoresc.* **2007**, *17* (2), 133-138.
105. Mulvaney, S. P.; Musick, M. D.; Keating, C. D.; Natan, M. J. Glass-coated, analyte-tagged nanoparticles: A new tagging system based on detection with surface-enhanced Raman scattering. *Langmuir* **2003**, *19* (11), 4784-4790.
106. Battersby, B. J.; Lawrie, G. A.; Trau, M. Optical encoding of microbeads for gene screening: alternatives to microarrays. *Drug Discovery Today* **2001**, *6* (12), S19-S26.
107. Park, M. K.; Briles, D. E.; Nahm, M. H. A latex bead-based flow cytometric immunoassay capable of simultaneous typing of multiple pneumococcal serotypes (Multibead assay). *Clin. Diagn. Lab Immunol.* **2000**, *7* (3), 486-489.
108. Moser, C.; Mayr, T.; Klimant, I. Microsphere sedimentation arrays for multiplexed bioanalytics. *Analytica Chimica Acta* **2006**, *558* (1-2), 102-109.
109. Mayr, T.; Moser, C.; Klimant, I. Luminescence decay time encoding of magnetic micro spheres for multiplexed analysis. *Anal. Chim. Acta* **2007**, *597* (1), 137-144.
110. Mandecki, W.; Ardel, B.; Coradetti, T.; Davidowitz, H.; Flint, A.; Huang, Z.; Kopacka, M.; Lin, X.; Wang, Z.; Darzynkiewicz, Z. Microtransponders, the miniature RFID electronic chips, as platforms for cell growth in cytotoxicity assays. *Cytometry A* **2006**, *69* (11), 1097-1105.
111. Dames, A.; England, J.; Colby, E. Bio-assay technique. 2000.
112. Nicewarner-Pena, S. R.; Freeman, R. G.; Reiss, B. D.; He, L.; Pena, D. J.; Walton, I. D.; Cromer, R.; Keating, C. D.; Natan, M. J. Submicrometer metallic barcodes. *Science* **2001**, *294* (5540), 137-141.
113. Penn, S. G.; He, L.; Natan, M. J. Nanoparticles for bioanalysis. *Curr. Opin. Chem. Biol.* **2003**, *7* (5), 609-615.
114. Sha, M. Y.; Walton, I. D.; Norton, S. M.; Taylor, M.; Yamanaka, M.; Natan, M. J.; Xu, C. J.; Drmanac, S.; Huang, S.; Borcharding, A.; Drmanac, R.; Penn, S. G. Multiplexed SNP genotyping using nanobarcode particle technology. *Analytical and Bioanalytical Chemistry* **2006**, *384* (3), 658-666.
115. Walton, I. D.; Norton, S. M.; Balasingham, A.; He, L.; Oviso, D. F., Jr.; Gupta, D.; Raju, P. A.; Natan, M. J.; Freeman, R. G. Particles for multiplexed analysis in solution: detection and identification of striped metallic particles using optical microscopy. *Anal. Chem.* **2002**, *74* (10), 2240-2247.
116. Braeckmans, K.; De Smedt, S. C.; Roelant, C.; Leblans, M.; Pauwels, R.; Demeester, J. Encoding microcarriers by spatial selective photobleaching. *Nat. Mater.* **2003**, *2* (3), 169-173.
117. Dendukuri, D.; Pregibon, D. C.; Collins, J.; Hatton, T. A.; Doyle, P. S. Continuous-flow lithography for high-throughput microparticle synthesis. *Nature Materials* **2006**, *5* (5), 365-369.

118. Galitonov, G. S.; Birtwell, S. W.; Zheludev, N. I.; Morgan, H. High capacity tagging using nanostructured diffraction barcodes. *Optics Express* **2006**, *14* (4), 1382-1387.
119. Pregibon, D. C.; Toner, M.; Doyle, P. S. Multifunctional encoded particles for high-throughput biomolecule analysis. *Science* **2007**, *315* (5817), 1393-1396.
120. Zhi, Z. L.; Morita, Y.; Hasan, Q.; Tamiya, E. Micromachining microcarrier-based biomolecular encoding for miniaturized and multiplexed immunoassay. *Anal. Chem.* **2003**, *75* (16), 4125-4131.
121. Derveaux, S.; Geest, B. G.; Roelant, C.; Braeckmans, K.; Demeester, J.; Smedt, S. C. Multifunctional Layer-by-Layer Coating of Digitally Encoded Microparticles. *Langmuir* **2007**, *23* (20), 10272-10279.
122. Freeman, R. G.; Raju, P. A.; Norton, S. M.; Walton, I. D.; Smith, P. C.; He, L.; Natan, M. J.; Sha, M. Y.; Penn, S. G. Use of nanobarcode particles in bioassays. *Methods Mol. Biol.* **2005**, *303*, 73-83.
123. Smith, J.; Onley, D.; Garey, C.; Crowther, S.; Cahir, N.; Johanson, A.; Painter, S.; Harradence, G.; Davis, R.; Swarbrick, P. Determination of ANA specificity using the UltraPlex platform. *Ann. N. Y. Acad. Sci.* **2005**, *1050*, 286-294.
124. Banu, S.; Birtwell, S.; Galitonov, G.; Chen, Y. F.; Zheludev, N.; Morgan, H. Fabrication of diffraction-encoded micro-particles using nano-imprint lithography. *Journal of Micromechanics and Microengineering* **2007**, *17* (7), S116-S121.
125. Braeckmans, K.; De Smedt, S. C.; Roelant, C.; Leblans, M.; Pauwels, R.; Demeester, J. Encoding microcarriers by spatial selective photobleaching. *Nat. Mater.* **2003**, *2* (3), 169-173.
126. Pregibon, D. C.; Toner, M.; Doyle, P. S. Multifunctional encoded particles for high-throughput biomolecule analysis. *Science* **2007**, *315* (5817), 1393-1396.
127. Swartzman, E. E.; Miraglia, S. J.; Mellentin-Michelotti, J.; Evangelista, L.; Yuan, P. M. A homogeneous and multiplexed immunoassay for high-throughput screening using fluorometric microvolume assay technology. *Anal. Biochem.* **1999**, *271* (2), 143-151.
128. Freeman, R. G.; Raju, P. A.; Norton, S. M.; Walton, I. D.; Smith, P. C.; He, L.; Natan, M. J.; Sha, M. Y.; Penn, S. G. Use of nanobarcode particles in bioassays. *Methods Mol. Biol.* **2005**, *303*, 73-83.
129. Smith, J.; Onley, D.; Garey, C.; Crowther, S.; Cahir, N.; Johanson, A.; Painter, S.; Harradence, G.; Davis, R.; Swarbrick, P. Determination of ANA specificity using the UltraPlex platform. *Ann. N. Y. Acad. Sci.* **2005**, *1050*, 286-294.
130. Walt, D. R. Techview: molecular biology. Bead-based fiber-optic arrays. *Science* **2000**, *287* (5452), 451-452.
131. Epstein, J. R.; Walt, D. R. Fluorescence-based fibre optic arrays: a universal platform for sensing. *Chem. Soc. Rev.* **2003**, *32* (4), 203-214.
132. Michael, K. L.; Taylor, L. C.; Schultz, S. L.; Walt, D. R. Randomly ordered addressable high-density optical sensor arrays. *Analytical Chemistry* **1998**, *70* (7), 1242-1248.

133. Gunderson, K. L.; Kruglyak, S.; Graige, M. S.; Garcia, F.; Kermani, B. G.; Zhao, C.; Che, D.; Dickinson, T.; Wickham, E.; Bierle, J.; Doucet, D.; Milewski, M.; Yang, R.; Siegmund, C.; Haas, J.; Zhou, L.; Oliphant, A.; Fan, J. B.; Barnard, S.; Chee, M. S. Decoding randomly ordered DNA arrays. *Genome Res.* **2004**, *14* (5), 870-877.
134. Shen, R.; Fan, J. B.; Campbell, D.; Chang, W.; Chen, J.; Doucet, D.; Yeakley, J.; Bibikova, M.; Wickham, G. E.; McBride, C.; Steemers, F.; Garcia, F.; Kermani, B. G.; Gunderson, K.; Oliphant, A. High-throughput SNP genotyping on universal bead arrays. *Mutat. Res.* **2005**, *573* (1-2), 70-82.
135. Joos, B.; Kuster, H.; Cone, R. Covalent attachment of hybridizable oligonucleotides to glass supports. *Analytical Biochemistry* **1997**, *247* (1), 96-101.
136. Csaki, A.; Moller, R.; Straube, W.; Kohler, J. M.; Fritzsche, W. DNA monolayer on gold substrates characterized by nanoparticle labeling and scanning force microscopy. *Nucleic Acids Research* **2001**, *29* (16), art-e81.
137. Moorcroft, M. J.; Meuleman, W. R. A.; Latham, S. G.; Nicholls, T. J.; Egeland, R. D.; Southern, E. M. In situ oligonucleotide synthesis on poly(dimethylsiloxane): a flexible substrate for microarray fabrication. *Nucleic Acids Research* **2005**, *33* (8).
138. Kurner, J. M.; Klimant, I.; Krause, C.; Pringsheim, E.; Wolfbeis, O. S. A new type of phosphorescent nanospheres for use in advanced time-resolved multiplexed bioassays. *Anal. Biochem.* **2001**, *297* (1), 32-41.
139. Gibson, N. J. Application of oligonucleotide arrays to high-content genetic analysis. *Expert Rev. Mol. Diagn.* **2006**, *6* (3), 451-464.
140. Salas, V. M.; Edwards, B. S.; Sklar, L. A. Advances in multiple analyte profiling. *Adv. Clin. Chem.* **2008**, *45*, 47-74.
141. Ugozzoli, L. A. Multiplex assays with fluorescent microbead readout: a powerful tool for mutation detection. *Clin. Chem.* **2004**, *50* (11), 1963-1965.
142. Morrison, T.; Hurley, J.; Garcia, J.; Yoder, K.; Katz, A.; Roberts, D.; Cho, J.; Kanigan, T.; Ilyin, S. E.; Horowitz, D.; Dixon, J. M.; Brenan, C. J. H. Nanoliter high throughput quantitative PCR. *Nucleic Acids Research* **2006**, *34* (18).
143. Spurgeon, S. L.; Jones, R. C.; Ramakrishnan, R. High throughput gene expression measurement with real time PCR in a microfluidic dynamic array. *PLoS. ONE.* **2008**, *3* (2), e1662.
144. Fulton, R. J.; McDade, R. L.; Smith, P. L.; Kienker, L. J.; Kettman, J. R., Jr. Advanced multiplexed analysis with the FlowMetrix system. *Clin. Chem.* **1997**, *43* (9), 1749-1756.
145. Demidov, V. V. 10 years of rolling the minicircles: RCA assays in DNA diagnostics. *Expert Rev. Mol. Diagn.* **2005**, *5* (4), 477-478.
146. Lizardi, P. M.; Huang, X.; Zhu, Z.; Bray-Ward, P.; Thomas, D. C.; Ward, D. C. Mutation detection and single-molecule counting using isothermal rolling-circle amplification. *Nat. Genet.* **1998**, *19* (3), 225-232.

147. Mullenix, M. C.; Sivakamasundari, R.; Feaver, W. J.; Krishna, R. M.; Sorette, M. P.; Datta, H. J.; Morosan, D. M.; Piccoli, S. P. Rolling circle amplification improves sensitivity in multiplex immunoassays on microspheres. *Clinical Chemistry* **2002**, *48* (10), 1855-1858.
148. Kim, K. S.; Park, J. K. Magnetic force-based multiplexed immunoassay using superparamagnetic nanoparticles in microfluidic channel. *Lab Chip*. **2005**, *5* (6), 657-664.
149. Hall, M.; Kazakova, I.; Yao, Y. M. High sensitivity immunoassays using particulate fluorescent labels. *Anal. Biochem.* **1999**, *272* (2), 165-170.
150. Bhalgat, M. K.; Haugland, R. P.; Pollack, J. S.; Swan, S.; Haugland, R. P. Green- and red-fluorescent nanospheres for the detection of cell surface receptors by flow cytometry. *J. Immunol. Methods* **1998**, *219* (1-2), 57-68.
151. Edwards, K. A.; Baeumner, A. J. Liposomes in analyses. *Talanta* **2006**, *68* (5), 1421-1431.
152. Zaytseva, N. V.; Goral, V. N.; Montagna, R. A.; Baeumner, A. J. Development of a microfluidic biosensor module for pathogen detection. *Lab Chip*. **2005**, *5* (8), 805-811.
153. Tsongalis, G. J. Branched DNA technology in molecular diagnostics. *Am. J. Clin. Pathol.* **2006**, *126* (3), 448-453.
154. Lowe, M.; Spiro, A.; Zhang, Y. Z.; Getts, R. Multiplexed, particle-based detection of DNA using flow cytometry with 3DNA dendrimers for signal amplification. *Cytometry A* **2004**, *60* (2), 135-144.
155. Van, C. M.; Ostrerova, N.; Tietgen, K.; Cao, W.; Chang, C.; Collins, M. L.; Kolberg, J.; Urdea, M.; Lohman, K. Direct quantitation of HIV by flow cytometry using branched DNA signal amplification. *Mol. Cell Probes* **1998**, *12* (4), 243-247.
156. Flagella, M.; Bui, S.; Zheng, Z.; Nguyen, C. T.; Zhang, A.; Pastor, L.; Ma, Y.; Yang, W.; Crawford, K. L.; McMaster, G. K.; Witney, F.; Luo, Y. A multiplex branched DNA assay for parallel quantitative gene expression profiling. *Anal. Biochem.* **2006**, *352* (1), 50-60.
157. Tyagi, S.; Kramer, F. R. Molecular beacons: probes that fluoresce upon hybridization. *Nat. Biotechnol.* **1996**, *14* (3), 303-308.
158. Szurdoki, F.; Michael, K. L.; Walt, D. R. A duplexed microsphere-based fluorescent immunoassay. *Anal. Biochem.* **2001**, *291* (2), 219-228.

CHAPTER Two

MULTIFUNCTIONAL LAYER-BY- LAYER COATING OF MICROCARRIERS

Parts of this chapter were published in:

Derveaux S.,¹ De Geest, B.G.,¹ Roelant, C.,² Braeckmans, K.,¹ Demeester, J.,¹ De Smedt, S.C.¹ *Langmuir* **2007**, 23 (20), 10272-10279.

WO/2008/034275, EP20060019661. Coating for microcarriers. De Smedt S., Derveaux S., Demeester J., De Geest B.G., Biocartis SA. Publication date: 26 maart 2008.

¹ Laboratory of General Biochemistry and Physical Pharmacy, Department of Pharmaceutics, Ghent University, 9000 Ghent, Belgium.

² Memobead Technologies NV, Rupelweg 10, 2850 Boom, Belgium.

ABSTRACT

In the field of medical diagnostics there is a growing need for inexpensive, accurate and quick “multiplexing” assays. By making use of encoded microparticles, such assays allow simultaneously determining the presence of several analytes in a biological sample. The microparticles under investigation in this study are encoded by writing a digital dot- or barcode in their central plane. This chapter evaluates to what extent a “multifunctional” coating can be applied around the digitally encoded microparticles by the layer-by-layer (LbL) technology. We show that a LbL coating containing CrO₂ nanoparticles allows (a) an optimal (optical) readout of the dot- and bar codes, (b) a perfect orientation of the microparticles, necessary to be able to read the code and (c) an optimal coupling of capture probes to the surface of the microparticles.

CHAPTER 2

MULTIFUNCTIONAL LAYER-BY-LAYER COATING OF MICROCARRIERS

INTRODUCTION

Driven by the human genome project, an increasing number of genes related to diseases have been discovered. As a result, tools are needed to carry out inexpensive, accurate and quick genetic diagnostic analyses. In recent years, “multiplexing” diagnostic assays have been developed. While a “monoplex” assay aims to measure the binding of a single analyte in the biological sample to its receptor, a multiplexing assay aims to measure *simultaneously* the binding of several analytes in the biological sample to their respective receptors¹.

Multiplex technologies are divided into two categories, “flat surface arrays” and “suspension arrays”². To the first category belong the well known DNA microarrays, using the x,y -coordinates of spots of single-stranded DNA (called probes) on a glass plate to identify which DNA targets are present in a sample³. Despite the success of DNA microarrays, they lack efficient reactions between the probes and the targets due to, among other reasons, slow diffusion of the target DNA molecules towards the probes on the flat surface⁴. Furthermore, flat microarray technology struggles with localization problems upon miniaturization while its use has also been limited by the high cost of the microarray consumables and the instruments. Suspension arrays have a number of advantages compared to flat microarrays, regarding for instance the attachment of probes, the flexibility in composing a test panel, improved kinetics⁵⁻⁸.

The second category, suspension arrays, uses *encoded* micron sized particles for multiplexing; the code identifies which probe is bound to the surface of the microparticles. Targets

present in the biological sample will bind to their corresponding microparticles that are added to the sample. By decoding the microparticles that show a positive reaction, the target molecules that are present in the sample can be identified.

Various strategies have been applied to encode microparticles: spectrometric⁶, electronic⁶, physical⁹⁻¹¹, and graphical encoding^{12,13}. Each of the encoding technologies has its strengths and weaknesses, as reviewed by Braeckmans et al.¹⁴ Our group has reported “spatial selective photobleaching” as a new method to digitally encode fluorescent microspheres¹⁵. As Figure 1A and Figure 1B show, digital codes (like a bar code, a dot code...) can be written in the *central plane* of fluorescent polystyrene microspheres (called memobeads) by localized photobleaching of the fluorescent molecules. Clearly, as microspheres are free to rotate in the assay tube, to be able to read the digital code (at the end of the assay) the microspheres must be properly oriented with respect to the focal plane of the microscope (Figure 1C). For this purpose we have suggested loading the microspheres with ferromagnetic particles (e.g. CrO₂)¹⁵. Ferromagnetic materials become magnetized in an external magnetic field and remain magnetized for a period after the material is no longer in the field (a net magnetic moment is present in the absence of the external magnetic field, called remanence, or “magnetic memory”). The encoding process of the microspheres in this study consists of two steps, a writing step (i.e. the photobleaching process) and a magnetizing step, during which the CrO₂ loaded microspheres are exposed to an external magnetic field sufficient to provide them with a magnetic memory. The microspheres are fixed on a grid during the encoding process to avoid rotation between the two steps. At the decoding step, the ferromagnetic microspheres are again exposed to a (weak) magnetic field with the same orientation as the first one (relative to the direction of the laser light). In the presence of this weak magnetic field, the ‘remanent’ nanoparticles tend to align with the magnetic field, so they will turn the microspheres at which surface they are fixed. The magnetic forces enable the orientation of the microspheres into such a position that the code can be read (the code is present in a plane perpendicular to the direction of the laser light).¹⁵ A software program can detect the orientation of the code within that plane, so that one magnetic field component is enough for the orientation of the microspheres.

Various methods have been developed for the production of magnetic microspheres. They include the deposition of nanoparticles in polymer particles by dispersion copolymerization of polymers in the presence of magnetic nanoparticles¹⁶ or by ‘activated swelling’¹⁷. Some groups reported the use of block copolymer systems for the controlled formation of a homogeneous nanoparticle pattern on a planar surface^{18,19}; the pattern formation of nanoparticles on flat surfaces seemed to be perfectly tunable via this approach²⁰. Bhat et al. reported another interesting method to fine-tune the number density of nanoparticles on a planar substrate by tailoring of attachment

points on that substrate²¹. To our knowledge none of these last two approaches has been applied to microspheres. Skirtach et al. could control the distribution of nanoparticles within polyelectrolyte capsules by polymers²².

With the aim of properly orient digitally encoded microspheres, we examine in this chapter whether memobeads can be coated with sub 500 nm CrO_2 nanoparticles by Layer-by-Layer (LbL) technology which is based on the alternate adsorption of oppositely charged polyelectrolytes/nanoparticles onto a charged substrate²³⁻²⁵. The major aims are to evaluate whether the magnetic LbL coating is indeed multifunctional in the sense that the LbL coating (a) allows positioning the memobeads for decoding, (b) does not optically interfere with the encoding and reading process and (c) allows a high and homogeneous loading of the surface of the microspheres with probes.

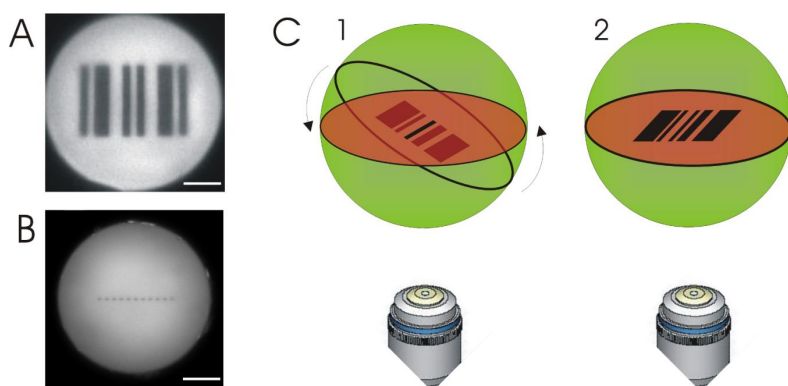


Figure 1: Confocal images of the central plane of non-magnetic fluorescent microspheres encoded with respectively a bar code (A) and a dot code (B). The scale bar is 10 μm . (C) The encoded microsphere has to be properly oriented at the time of decoding in order to be able to read the entire code; At position 1, the code is tilted with respect to the microscope focal plane and only the intersection of the code with the focal plane will be visible. At position 2, the entire code is visible because it coincides with the focal plane.

MATERIALS & METHODS

Materials.

Non-magnetic and ferromagnetic green fluorescent carboxylated polystyrene microspheres (39 μm in diameter) were purchased from Spherotech (Libertyville, Illinois, USA). Poly (allylamine hydrochloride) (PAH, MW $\sim 70\ 000$ g/mol), sodium poly (styrene sulfonate) (PSS, MW $\sim 70\ 000$ g/mol) and poly (acrylic acid) (PAA, MW $\sim 450\ 000$ g/mol) were obtained from Sigma Aldrich (Steinheim, Germany). A 5'-Cy5-terminal 3'-amino-terminal labeled 29-mer oligonucleotide was purchased from Eurogentec (Seraing, Belgium). Bovine serum albumine (BSA) and 2-[N-morpholino]ethanesulfonic acid (MES) were purchased from Sigma, PBS Dulbecco's from Invitrogen (Merelbeke, Belgium) and Tween-20 from Calbiochem (Darmstadt, Germany). EDC (1-ethyl-3-(3-dimethyl aminopropyl) carbodiimide HCl) was obtained from Perbio Science (Erembodegem, Belgium). Tris(hydroxymethyl)-aminomethan-hydrochlorid (Tris-HCl), p-nitrophenyl phosphate disodium salt (hexahydrate) and disodium carbonate were purchased from Merck (Darmstadt, Germany). Inulin solution: 10% (w/v); degree of polymerization = 11. Biotinylated alkaline phosphatase was purchased from New England BioLabs Inc. (Ipswich, Boston, USA).

Layer-by-Layer coating of the microspheres.

PAH and PSS stock solutions were prepared in 0.5M NaCl (2 mg/ml). PAA was dissolved in 0.5M NaCl to a final concentration of 1 mg/ml. 1 ml of the (stock) suspension of non-magnetic (green fluorescent, carboxylated, 39 μm) microspheres (approx. 400 000 microspheres/ml) was centrifuged at 450 rpm for 1 minute. The supernatant was aspirated and the microspheres were washed with a 0.05% Tween-20 solution (in deionized water). After resuspension of the microspheres, the centrifugation and washing procedure was repeated a second time.

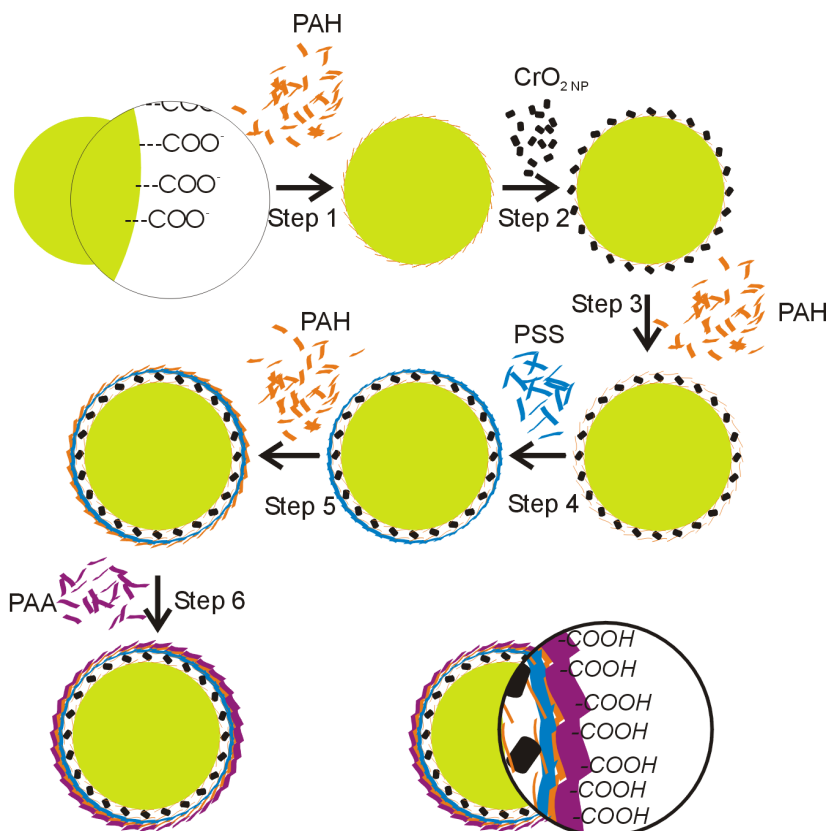


Figure 2: Schematic representation of the LbL coating of microspheres. Oppositely charged polyelectrolytes are sequentially adsorbed on the negatively charged non-magnetic polystyrene microspheres (PAH = poly (allylaminehydrochloride); PSS = poly (styrenesulfonate); PAA = poly (acrylic acid)). Ferromagnetic chromium dioxide nanoparticles (CrO_2 NP, <450 nm) are added in between two PAH layers.

As illustrated in Figure 2 the non-magnetic microspheres were LbL coated by suspending them in 1 ml PAH solution; the suspension was continuously vortexed (1000 rpm, 25°C) for 15 min. The non-adsorbed PAH was removed by repeated centrifugation and washing. Subsequently, the microspheres were dispersed in deionized water containing the sub 500 nm chromium dioxide nanoparticles (CrO_2 NP) which were obtained by filtration of a chromium dioxide nanoparticle dispersion through a membrane filter with 450 nm pores. The size of the CrO_2 NP was measured with a Zetasizer Nano ZS (Malvern, Worcestershire, UK). The microsphere dispersion was continuously shaken for 15 min and the excess of CrO_2 NP was removed by repeated centrifugation/washing steps. The third, fourth... polyelectrolyte layer was applied in a way similar to the first layer. Finally the microspheres are coated with 6 layers in the following order: PAH / CrO_2 NP / PAH / PSS / PAH / PAA.

These LbL coated microspheres were resuspended in 1 ml of deionized water and subsequently encoded (see below).

Encoding of the microspheres.

The LbL coated microspheres were encoded by spatial selective photobleaching as previously described¹⁵. An in-house-developed encoding device was used, being a microscopy platform equipped with an Aerotech ALS3600 scanning stage, a SpectraPhysics 2060 Argon laser and an Acousto-Optic-Modulator (AA.MQ/A0.5-VIS, A.A-Opto-Electronique, Orsay Cedex, France). The encoding process consists of two steps, a writing step (i.e. the photobleaching process) and a magnetizing step, during which the CrO₂ loaded microspheres are exposed to an external magnetic field sufficient to provide them with a magnetic memory. The microspheres are fixed on a grid during the encoding process to avoid rotation of the microspheres between the two steps.

Coupling of oligonucleotides to the LbL coated microspheres.

5'-amino-terminal oligonucleotides were covalently attached to the (PAA) carboxyl groups at the surface of the microspheres by one-step carbodiimide chemistry. In brief, approximately 10 000 microspheres were washed three times with 100 μ l 0.4M MES buffer (0.05% Tween-20, pH of 5) and centrifuged. The oligonucleotides were coupled by incubating the microspheres in 7.5 μ l EDC solution (100 mg/ml in 0.4M MES buffer, immediately used after preparation) to which 3 μ l oligonucleotides (33 μ M) and 7 μ l MES buffer were added. The reaction was allowed to proceed for one hour in an Eppendorf thermomixer (at 1500 rpm, 20°C). Subsequently, the microspheres were washed three times with 100 μ l "assay buffer" (1% BSA, 0.05% Tween-20 in PBS, "blocking step"). They were finally washed another three times with 100 μ l hybridization buffer (5 mM Tris-HCl, 0.5 mM EDTA, 1.0 M NaCl) and stored in 200 μ l hybridization buffer (\pm 50 000 microspheres/ml) at 4°C.

Confocal and scanning electron microscopy imaging of the microspheres.

The memobeads were analyzed using a Bio-Rad MRC 1024 confocal laser scanning system (Bio-Rad, Hemel Hempstead, UK) equipped with an inverted microscope (Eclipse TE300D, Nikon, Japan). Images were captured with a Nikon Plan Apochromat 60x water immersion objective lens (NA of 1.2, collar rim correction) and with a Nikon Plan Apochromat 10x objective lens (NA of 0.45)

using the 488 nm laser line from the argon-ion laser and the 647 nm laser line from the Ar/Kr laser. For the orientation of the memobeads, a weak external magnetic field was applied with the same orientation as the magnetic field applied during the encoding process (relative to the direction of the laser light). In the presence of this weak magnetic field, the ‘remanent’ nanoparticles tend to align with the magnetic field, so they will turn the microspheres (at which surface they are fixed) into a position that the code can be read (the code is present in a plane perpendicular to the direction of the laser. The average contrast of the dot code can be defined by the following equation:

$$\text{Contrast} = \frac{1}{n} * \sum_{i=0}^n \left(\frac{C_{\max,i} - C_{\min,i}}{C_{\max,j}} \right)$$

where i = a code segment (i.e. a dot)
 n = total number of code segments (i.e. number of dots)
 C = fluorescence intensity ($C_{\max,i}$ and $C_{\min,i}$ as shown in Figure 8)

The coefficient of variation (CV; in %) equals the standard deviation (SD) divided by the average contrast (expressed as a percent). The standard deviation on the average contrast was calculated as:

$$SD = \sqrt{\frac{\sum_{i=1}^n (x_i - \bar{x})^2}{(n-1)}}$$

where i = a code segment (i.e. a dot)
 n = total number of code segments (i.e. number of dots)
 x = contrast per segment (i.e. contrast per dot) = $\left(\frac{C_{\max,i} - C_{\min,i}}{C_{\max,j}} \right)$

To determine the average red fluorescence of one microsphere (due to coupled Cy5-conjugated oligonucleotides) a region of interest (ROI) was drawn around the microsphere and the red fluorescence within the ROI was measured using the Matlab 7.1 version equipped with home-made imaging processing software. The average red fluorescence of each microsphere was defined as the average of the fluorescence of all pixels within the ROI. The intra-microsphere coefficient of variation (CV; in %) equals the intra-microsphere standard deviation (SD) divided by the average red fluorescence (expressed as a percent). The intra-microsphere standard deviation on the red fluorescence was calculated as:

$$SD = \sqrt{\frac{\sum_{i=1}^n (x_i - \bar{x})^2}{(n-1)}}$$

where i = a pixel within the ROI
 n = number of pixels within the ROI
 x = fluorescence of a pixel within ROI

Scanning electron microscopy (SEM) measurements on memobeads were carried out using a Quanta 200 FEG FEI scanning electron microscope operated at an accelerating voltage of 3 kV. A drop of memobeads suspension was deposited onto a silicon wafer and dried under nitrogen stream followed by sputtering with gold before analysis.

Coupling of streptavidin and biotinylated alkaline phosphatase to LbL coated microspheres and lyophilization of the microspheres.

Streptavidin molecules were covalently attached to the (PAA) carboxyl groups at the surface of the microspheres by the two-step carbodiimide-method. In brief, approximately 400 000 microspheres (in 800 μ l of “activation buffer”: 0.1M $\text{Na}_2\text{HPO}_4/\text{NaH}_2\text{PO}_4$, 0.05% Tween-20, pH 6.3) were activated with 100 μ l EDC (50 mg/ml); at the same time the active intermediate was stabilized with 100 μ l sulfo-NHS (50 mg/ml). Note that the storage and handling of EDC has to be done under proper conditions (EDC is very sensitive to moisture). The microspheres were then washed twice with 0.05 M MES-buffer (0.05% Tween-20, pH 5) and centrifuged (4000 rpm, 30 seconds). Subsequently the streptavidin molecules were coupled by incubating the microspheres in 1 ml streptavidin solution (1 mg/ml) for 2 hours in an Eppendorf Thermomixer (250 rpm). Finally the microspheres were washed twice with “assay buffer” (1% BSA and 0.05% Tween-20 in PBS) to avoid non-specific binding to un-reacted coupling places later on (“blocking step”). The streptavidin coated microspheres were stored in 2 ml “assay buffer” (\pm 200 000 microspheres/ml) at 4 °C. A sample of 100 000 microspheres was added to 100 μ l biotinylated alkaline phosphatase (0.5 mg/ml), and incubated during 1 hour on a rocker at 250 rpm. The microspheres were then washed for 3 times with 200 μ l assay buffer in order to remove any excess of free phosphatase molecules. They were then washed twice with 100 μ l Tris-buffer, resuspended in 100 μ l Tris-buffer, and finally diluted with 100 μ l inulin solution (10% w/v in distilled water) or with distilled water. The microspheres were subsequently immersed into liquid nitrogen for 10 seconds, and immediately thereafter lyophilized in a Lyovac GT4 lyophilisator with the conditions described in Table 1.

Table 1: Procedure and settings of the lyophilization process.

Process	Temperature (°C) / pressure (mBar)	Duration (minutes)
Start	-45	-
First drying	-45 / 0.8 - 1.0	800
Second drying	0 / 0.1 - 0.2	120
	10 / 0.1- 0.2	420

Alkaline phosphatase quality control test.

The lyophilized microspheres were resuspended into 200 μ l assay buffer (100 000 microspheres/200 μ l) and, subsequently, 2 μ l of this suspension was added to 150 μ l of substrate solution (p-nitrophenyl phosphate disodium salt (hexahydrate) dissolved in 0.1M Tris-HCl at 0.1% w/v and pH=8.4). They were allowed to incubate for exactly thirty minutes. The reaction was stopped by adding 20 μ l of 2 M Na_2CO_3 , which immediately changes the pH of the solution so that the enzyme is not active anymore. The microspheres were then centrifuged, and a volume of 120 μ l of the supernatant of was transferred to one well of a 96-well plate. The absorbance was read out in a plate reader by excitation with 405 nm wavelength light.

Coupling of human TNF- α antibodies to LbL coated microspheres and lyophilization of the microspheres.

'Capture' antibodies were covalently attached to the (PAA) carboxyl groups at the surface of the microspheres by the two-step carbodiimide-method. In brief, approximately 10 000 microspheres (in 80 μ l of "activation buffer": 0.1M $\text{Na}_2\text{HPO}_4/\text{NaH}_2\text{PO}_4$, 0.05% Tween-20, pH 6.3) were activated with 10 μ l EDC (50 mg/ml); at the same time the active intermediate was stabilized with 10 μ l sulfo-NHS (50 mg/ml). The microspheres were then washed twice with 0.05 M MES-buffer (0.05% Tween-20, pH 5) and centrifuged (4000 rpm, 30 seconds). Subsequently the antibodies were coupled by incubating the microspheres in 30 μ l antibody solution (83 μ g/ml) for 2 hours in an Eppendorf Thermomixer (250 rpm). Finally the microspheres were washed twice with "assay buffer" (1% BSA and 0.05% Tween-20 in PBS) to avoid non-specific binding to un-reacted coupling places later on ("blocking step"). The microspheres were stored in 200 μ l "assay buffer" (\pm 50 000 microspheres/ml) at 4 °C. Approximately 500 microspheres were resuspended into 200 μ l assay buffer. The tubes were then submersed during a few seconds in liquid nitrogen, and immediately

thereafter freeze-dried following conditions described above in Table 1. They were then stored at 4°C. Instead of assay buffer (BSA), several other cryoprotectants (lactose, sucrose, glycerol, trehalose dihydrate) and distilled water were also used. The same procedure was followed for those vials.

Quality control test with AF647® labeled antibodies.

A volume of 100 μl AlexaAFluor® 647 labeled goat anti-mouse antibody solution (2 $\mu\text{g}/\text{ml}$) was added to 100 microspheres and incubated during 1 hour on a rocker at 250 rpm. The red fluorescence was detected as described above.

RESULTS AND DISCUSSION

Ferromagnetic coating of the microspheres by surface polymerization.

Figure 3 shows confocal images of a ferromagnetic fluorescent polystyrene microsphere which was commercially available. According to the manufacturer's information, the magnetic surface-polymerized microspheres are prepared by entrapping CrO_2 particles mixed with styrene (monomer) at the surface of pre-made polystyrene microspheres by polymerization of the styrene.

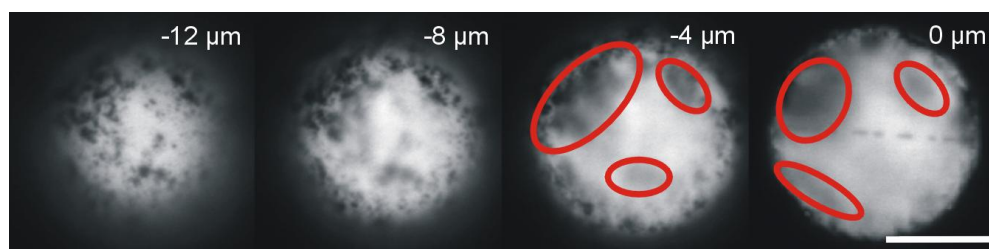


Figure 3: Confocal optical sections of a magnetic surface-polymerized encoded microsphere ($\phi = 39 \mu\text{m}$). The dot code is written in the central plane of the microsphere (0 μm). Magnetic particles at the surface of the microspheres (leftmost image) result in shaded areas (indicated by the circles), even in the central plane (rightmost image). The scale bar is 20 μm .

Clearly, the surface of such 'surface-polymerized' microspheres is not homogeneously covered with the magnetic particles; at certain locations even large aggregates of CrO_2 particles can

be present. It is important for both encoding and decoding, that the microspheres are sufficiently transparent to the laser light and the emitted fluorescence. The CrO_2 aggregates, however, locally attenuate the laser light and fluorescence. In addition, the chromium dioxide aggregates also cause the appearance of “shadows” in the inner part of the microspheres. Figure 4B shows an electron microscopy image of those microspheres. CrO_2 particles are indeed present at the surface of magnetic surface-polymerized microspheres, with polystyrene units in-between, but they are, however, not totally covered with polystyrene, and the surface is rather rough compared to the smooth surface of non-magnetic microspheres (Figure 4A).

Figure 5 shows the result of the decoding of both a non-magnetic (Figure 5A) and a magnetic (surface-polymerized) (Figure 5B) microsphere carrying a dot code in its central plane. Note that both microspheres were decoded immediately after the encoding process, thus without any movement/rotation of the microspheres between the encoding and decoding step. The fluorescence intensity is measured along the dot code (right panels). While the dot code can be read perfectly in Figure 5A, in Figure 5B, the shadows partially obscure the bleached code segments and do not allow clear visualization of the code.

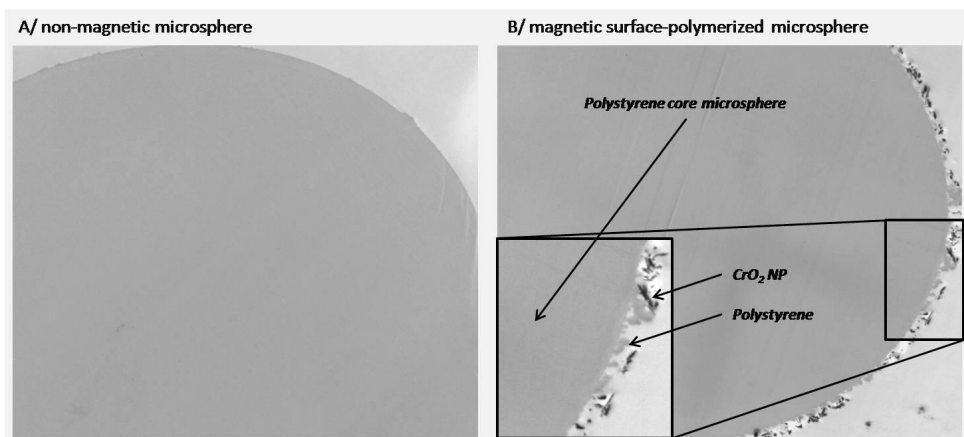


Figure 4: Electron microscopy images of A/ Non-magnetic PS microsphere, and B/ Magnetic surface-polymerized microsphere. The latter one has a rough surface due to the presence of the magnetic nanoparticles.

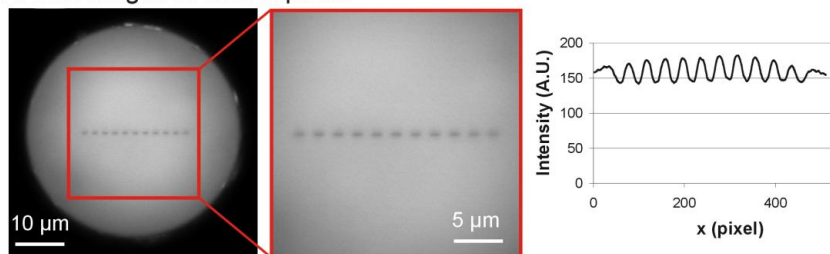
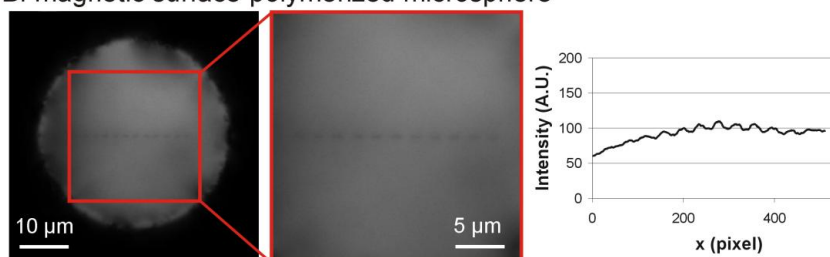
A: non-magnetic microsphere**B: magnetic surface-polymerized microsphere**

Figure 5: Decoding of non-magnetic (A) and magnetic surface-polymerized (B) microspheres. Left column: confocal images of the central plane of the microspheres. Middle column: magnification of the encoded area. Right column: fluorescence intensity profile measured along the code. In Figure B, the shadows partially obscure the bleached code segments and do not allow clear visualization of the code. Decoding was performed immediately after the encoding process, thus without any movement/rotation of the microspheres between the encoding and decoding step.

Figure 6 shows red fluorescent images of both non-magnetic (Figure 6A, left panel) and magnetic (surface-polymerized) microspheres (Figure 6B, left panel) loaded at their surface with red (Cy5) labeled 29-mer oligonucleotides. Compared to the surface of the non-magnetic spheres (Figure 6A), the red fluorescence at the surface of the magnetic (surface-polymerized) microspheres (Figure 6B) seems less homogeneous. It indicates that the surface of the magnetic spheres was not homogeneously covered with the red labeled 29-mer oligonucleotides. The right panels in Figure 6 show scanning electron microscopy images of the surface of the microspheres; chromium dioxide particles seem present in the outer surface of the magnetic surface-polymerized microspheres, which was also observed in Figure 4B; hence we expect no polystyrene (and thus no carboxyl groups) at those regions in the surface, which very likely explains why their surface is not homogeneously covered with 29-mer oligonucleotides (Figure 6, left panel).

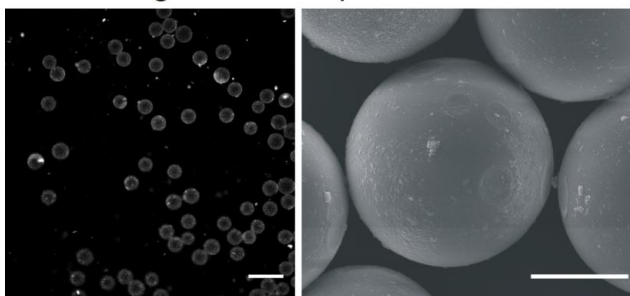
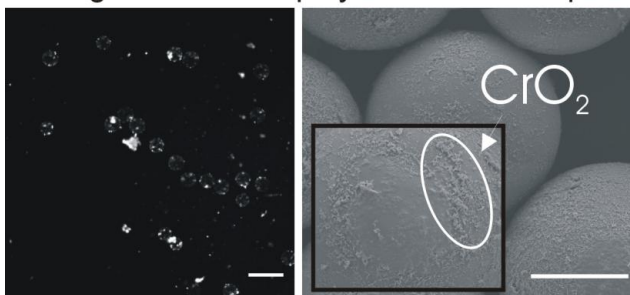
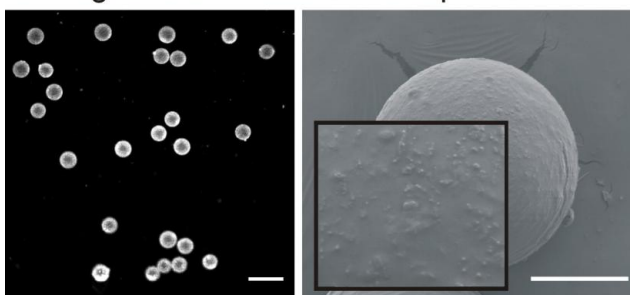
A: non-magnetic microsphere**B: magnetic surface-polymerized microsphere****C: magnetic LbL coated microsphere**

Figure 6: Red fluorescence microscopy images (left) and SEM images (right) of non-magnetic microspheres (A), magnetic surface-polymerized microspheres (B) and magnetic LbL coated microspheres (C) after the coupling of Cy5-labeled 29-mer oligonucleotides. The scale bar in fluorescence microscopy images is 100 μm while it is 20 μm in the SEM images. Even though the laser power to excite Cy5 was approximately 7.5 times less in A and C (compared to B), the red fluorescence at the surfaces of the carriers is less intense in the case of the magnetic surface-polymerized microspheres (B). In B aggregated CrO_2 NP are heterogeneously spread over the surface and partially present outside the surface. The CrO_2 NP at the surface of LbL coated microspheres (C) are not as sharp as those at the surface of magnetic surface-polymerized microspheres (B), very likely due to the fact that they are covered with extra polyelectrolyte layers.

Ferromagnetic coating of the microspheres by layer-by-layer technology.

The observations in Figure 5 and Figure 6 clearly show the need to design polystyrene microspheres that (a) are sufficiently magnetic without having chromium dioxide aggregates at their surface (to avoid shadows) and (b) can be homogeneously loaded with capture probes. Therefore, as schematically shown in Figure 2, six layers of poly-electrolytes and ferromagnetic chromium dioxide nanoparticles were applied by layer-by-layer (LbL) technology on the surface of the polystyrene microspheres²⁵. CrO₂ NP, smaller than 0.45 μm (as obtained by the filtration of a chromium dioxide nanoparticle dispersion through a 0.45 μm pore-filter), were added in between two PAH layers; in order to obtain carboxyl groups at the surface, the final layer in the LbL coating was PAA.

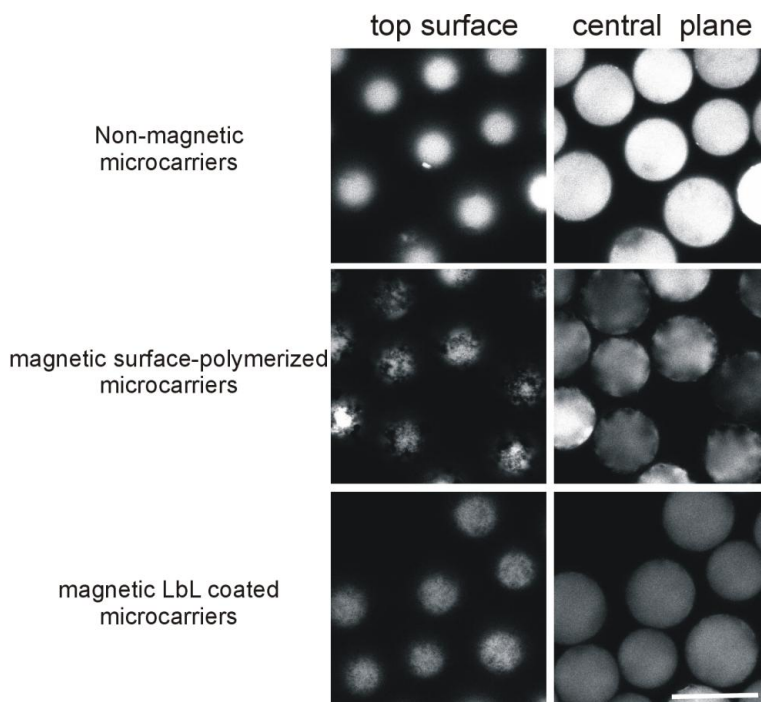


Figure 7: Confocal images of the top surface and the central plane of non-magnetic, magnetic surface-polymerized and magnetic LbL coated microspheres. Not-aggregated CrO₂ NP are homogeneously distributed over the surface of magnetic LbL coated microspheres. Hence, shaded areas are not present in the central plane. The scale bar is 50 μm.

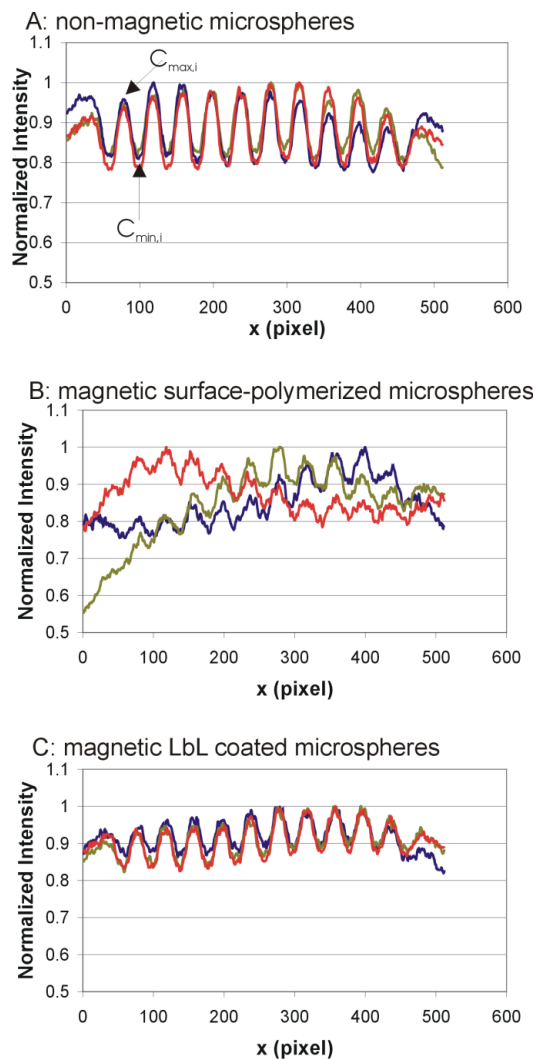


Figure 8: Normalized fluorescence intensity profiles of identical dot codes written in the central plane of non-magnetic microspheres (A; 3 spheres were encoded), magnetic surface-polymerized microspheres (B; 3 spheres were encoded) and magnetic LbL coated microspheres (C; 3 spheres were encoded). Normalized values were calculated as the ratio between the fluorescence intensity and the maximum fluorescence intensity along the dot code. Decoding was performed immediately after the encoding process, thus without any movement/rotation of the microspheres between the encoding and decoding step.

As the confocal microscopy images of the top surface of the microspheres (Figure 7, left panels) show, when applied by LbL coating the CrO_2 NP seem more homogeneously distributed over the surface of microspheres, without the occurrence of aggregates. This was confirmed by SEM images (see Figure 6, right panel). Especially, shadows in the central plane of the LbL coated microspheres were not observed (Figure 7, right panels) which facilitates a correct decoding. Figure

8 shows the (normalized) fluorescence intensity profiles of a dot code written in both non-magnetic, magnetic surface-polymerized and magnetic LbL coated microspheres. Note that all microspheres were decoded immediately after the encoding process, thus without any movement/rotation of the microspheres between the encoding and decoding step. Clearly, the dotcode written in magnetic LbL coated microspheres (Figure 8C) is much more uniform compared to the dot code written in magnetic surface-polymerized microspheres (Figure 8B). This observation is supported quantitatively by the information in Table 2.

Table 2: Contrast values (and corresponding coefficients of variation, CV) measured along the dot code intensity profiles of Figure 8.

Non-magnetic microspheres			Magnetic surface-polymerized microspheres			Magnetic LbL coated microspheres		
Contrast	CV (%)	Normalized minimum	Contrast	CV (%)	Normalized minimum	Contrast	CV (%)	Normalized minimum
0.153	18	0.112	0.079	27	0.051	0.083	15	0.062
0.141	16	0.100	0.068	46	0.005	0.094	11	0.077
0.171	12	0.133	0.066	38	0.017	0.105	9	0.086

Normalized minimum = code segment which minimal differs from un-bleached local background fluorescence=

$$\left(\frac{C_{\max j} - C_{\min j}}{C_{\max j}} \right)_{\min}$$

The average contrast for the different kinds of beads is reported together with the corresponding coefficient of variation. Table 2 also shows the “normalized minimum”, which is the lowest contrast value found in the dot code. The profiles of the codes written in the central plane of the surface-polymerized microspheres exhibit a very high CV (37% on average), compared to that of non-magnetic microspheres (15% on average), due to the presence of code segments that are almost indistinguishable from the unbleached background fluorescence (which can also be seen in Table 2 from the ‘normalized minimum’ values). The CVs along the dot code profiles measured in the magnetic LbL coated microspheres, however, are 12% on average, which is far below that of the magnetic surface-polymerized microspheres and similar to the non-magnetic microspheres. Here all code segments are clearly distinguishable from the unbleached local background fluorescence, as can be seen in Table 2 from the ‘normalized minimum’ values.

Note that in these experiments, 39µm sized polystyrene microspheres are used. The LbL coating procedure can be applied on microspheres with other sizes as well. The minimal size of the microspheres is especially determined by the length of the code which has to be written in the

microspheres. For more information regarding the length of the code, we refer to Braeckmans et al.

15

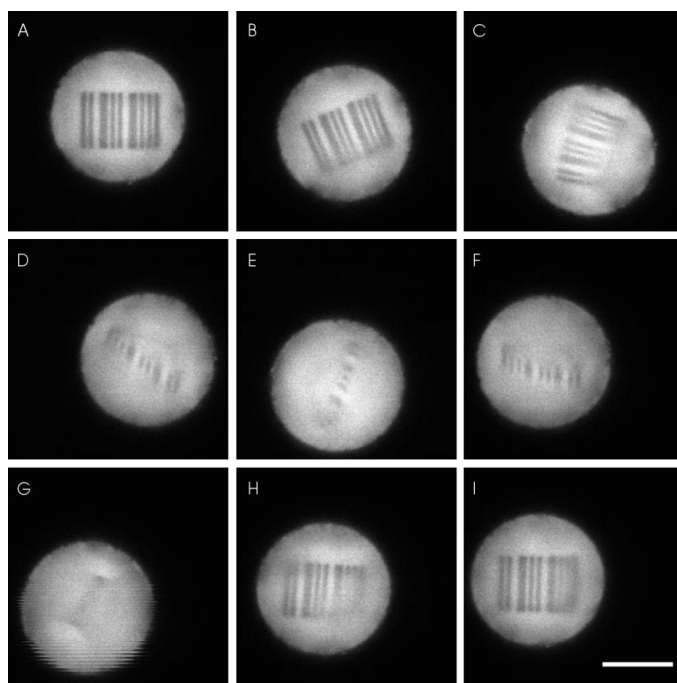


Figure 9: A magnetic LbL coating of the microspheres allows bringing the microspheres into a correct readout position. (a) Confocal image of the central plane of a magnetic LbL coated microsphere just after being encoded with a bar code; during the encoding process the microspheres were exposed to a strong magnetic field in order to provide them with a remanent magnetic direction. (b-h) Confocal images of the central plane of the microsphere while randomly moving. (i) Confocal image of the central plane of the microsphere upon bringing the microsphere back in a (weak) magnetic field: it turns to its original orientation (compare images A and I) which permits reading the code. The scale bar is 20 μm .

Positioning of magnetic LbL coated microspheres in a magnetic field.

Figure 9 shows a magnetic LbL coated barcoded polystyrene microsphere exposed to a magnetic field: the CrO_2 NP in the LbL coating and the magnetic field bring the bar code to the position allowing readout of the code. We note that the CrO_2 NP (a) keep their magnetic memory, as expected, and (b) are immobilized in the LbL coating which is also a requirement to be able to properly orient the microspheres upon applying the magnetic field for decoding. The fact that the CrO_2 NP are sufficiently fixed on the microspheres is not surprising since they are strongly bound by electrostatic interactions with the polycations of the LbL coating (Figure 2).

On one hand, smaller CrO₂ NP allow a more uniform readout of the code because the shadows in the central plane are less pronounced. On the other hand, the force required to turn the microspheres into the appropriate position, which is related to the size and amount of the magnetic CrO₂ NP, should be strong enough to overcome the interaction forces between the microsphere and the glass surface of the recipient. Figure 10 shows polystyrene microspheres that were LbL coated with CrO₂ NP differing in size (respectively < 100 nm, < 220 nm and < 450 nm). The CrO₂ NP were obtained by filtration of a chromium dioxide nanoparticle dispersion through respectively a 100 nm, 220 nm and a 450 nm pore-filter. When coated with CrO₂ NP smaller than 220 nm, the positioning of the microspheres, upon applying a magnetic field, did not always work perfectly. This means that the total magnetic force of the sub 220 nm sized nanoparticles, coated on one microparticle, was not high enough to turn around the relative huge microparticle. Conversely to the positioning of microspheres coated with larger CrO₂ NP, which took place immediately upon applying the magnetic field. We concluded that the preferred size range of the CrO₂ NP is between 220 and 450 nm.

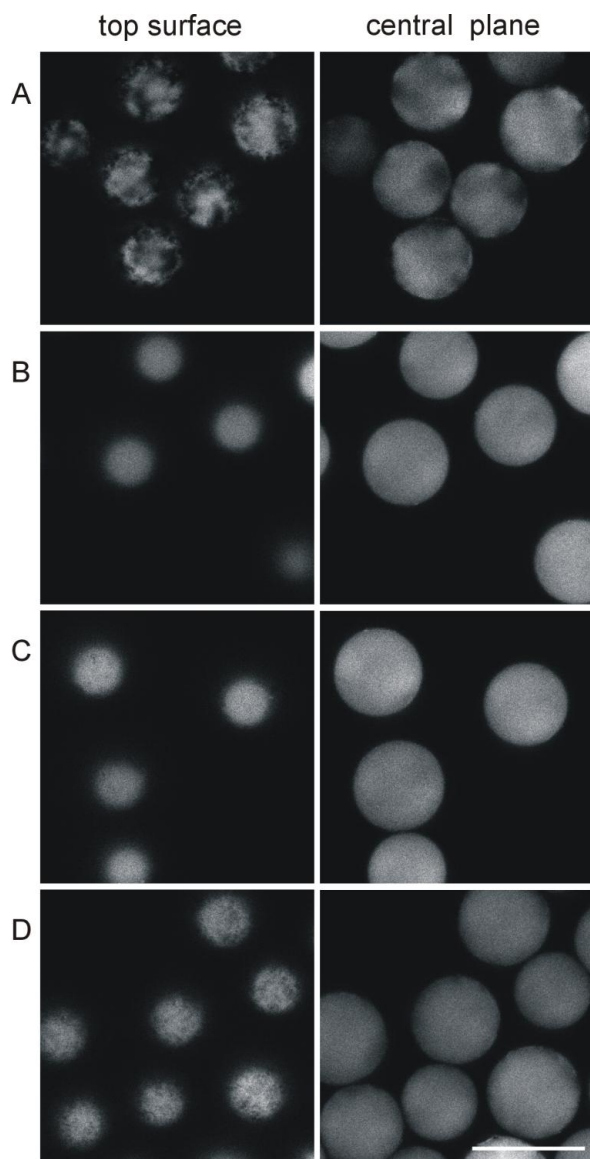


Figure 10: Confocal images of the top surface and the central plane of magnetic surface-polymerized microspheres (A) and magnetic LbL coated microspheres (B,C and D). The latter ones were coated with CrO₂ NP with different sizes (B: < 100 nm; C: < 220 nm and D: < 450 nm). The smaller the CrO₂ NP, the fewer shadows at the central plane. However, when coated with CrO₂ NP, smaller than 220 nm, the positioning of the microspheres did not always work perfectly. The scale bar is 50 μm .

Capturing oligonucleotides at the surface of LbL coated encoded microspheres.

Figure 6B and Figure 6C (left panels) show fluorescence images of both magnetic surface-polymerized and magnetic LbL coated microspheres loaded at their surfaces with Cy5 labeled 29-mer oligonucleotides. Unlike the surfaces of surface-polymerized microspheres, the surfaces of the LbL coated ones seem more homogeneously covered with Cy5 labeled oligonucleotides. This is most likely due to the fact that the CrO₂ NP at the surface of the microspheres were also coated with PAA (Figure 2), providing the whole surface of the beads with carboxyl groups. From the SEM images in Figure 6 one can clearly see that the CrO₂ NP are coated with extra polymer layers: the particles do not look so sharp (Figure 6C, right panel) as when they are not covered (Figure 6B, right panel). This is also confirmed in Table 3, where the red fluorescence intensity values at the surfaces of non-magnetic, magnetic surface-polymerized and magnetic LbL coated microspheres is analyzed. The magnetic LbL coated microspheres have an intra-microsphere CV on their red fluorescent signal around 40%, which is similar to that of the non-magnetic microspheres. The magnetic surface-polymerized ones, however, show CVs of approximately 70-90%, indicating that the probes are inhomogeneously loaded across the surface. The magnetic LbL coated microspheres also have an increased loading capacity, as can be seen from the average red fluorescence which is 4 times higher than that of the non-magnetic ones. While the non-magnetic and LbL coated microspheres have a similar inter-microsphere CV (respectively 14.2% and 13.8%), the magnetic surface-polymerized microspheres show a higher inter-microsphere CV of around 27%. In addition, the average red fluorescence of the latter ones is approximately 50 times less than that of the magnetic LbL coated microspheres. Clearly, besides the improved visibility of the code, the LbL coating of the microspheres also increases the capacity (and quality) to load probes (like oligonucleotides) at the surface, which can be easily explained by the fact that LbL coating results in a higher number of carboxyl groups at the surface.

Table 3: Analysis of the coupling of Cy5-labeled 29-mer oligonucleotides to the carboxyl groups at the surface of 7 surface-polymerized microspheres and 7 LbL coated microspheres. Although the power of the laser to excite Cy5 was approximately 7.5 times less in the case of the non-magnetic and the magnetic LbL coated microspheres (compared to the magnetic surface-polymerized microspheres), the red fluorescence at the surface is less intense in case of the magnetic surface-polymerized microspheres.

Non-magnetic microspheres		Magnetic surface-polymerized microspheres		Magnetic LbL coated microspheres	
Average fluorescence	CV (%)	Average fluorescence ^a	CV (%)	Average fluorescence	CV (%)
40.5	39.3	39.0	80.1	179.3	37.4

49.3	39.9	24.4	65.1	130.7	42.9
47.4	37.7	27.0	84.3	172.3	37.5
42.6	38.0	22.3	68.6	176.3	38.3
56.1	36.1	27.1	60.8	167.2	41.1
40.0	33.0	38.2	96.6	138.4	47.8
40.8	39.1	26.3	90.5	118.4	40.8
41.0	31.4	20.1	81.6	175.6	47.5

^a 7.5 times higher excitation

The stability of the LbL coated microspheres.

The stability of the LbL coated microspheres can be seen from different points of view. First of all, regarding their use in multiplex assays, they should be decodable at any time. Degradation or loss of the code must not happen at all. In the past, chemical and light stability experiments that were performed on non-magnetic microspheres have shown that the code was resistant against several chemical solvents, and that the code was stable for at least several months when the microspheres were continuously exposed to daylight, respectively. This in contrast to color-encoded microcarriers (such as xMAP microparticles) that have to be handled in the dark as bleaching of the fluorophores by prolonged exposure to light results in false codes²⁶. Another issue of such microcarriers is the possibility of misclassification due to storage²⁷. Meanwhile we have introduced the LbL modification of those microspheres. Because this modification does not affect the fluorescence properties of the core microspheres (the coating is only applied at the surface of the microspheres), we can presume that those results also hold for the LbL coated microspheres. Secondly, one has to be concerned also about the stability of the LbL coated surface. Because the latter one is functionalized, any damage by external factors could influence the coupling of biomolecules, which could directly affect their use in multiplex assays, even if the code would still be readable.

In order to get an idea about the strength of the LbL coated microspheres, they were challenged by autoclaving and freeze-drying. The autoclaving of those microspheres is important when they would be used as cell-carriers (for the development of cell libraries on a suspension array), as has been demonstrated by Fayazpour et al.²⁸ In order to allow the growth of cells at the surface of the encoded microspheres, it would be recommended to make use of sterile batches of encoded microspheres. Figure 11 shows the decoding of LbL coated memobeads before and after an autoclaving process during 20 minutes, and demonstrates that the autoclaving has no negative effect on the decoding of the memobeads, which indicates that neither the polystyrene core matrix

of the microspheres, nor the LbL coating and the magnetic orientation of the CrO₂ NP have been destroyed. Indeed, changes in the LBL coating or displacement of the magnetic nanoparticles would have led to problematic orientation of the beads in the magnetic field, making the read-out of the code impossible. As is shown by Fayazpour et al., cells can easily bind to and grow at the surface of the microspheres²⁸.

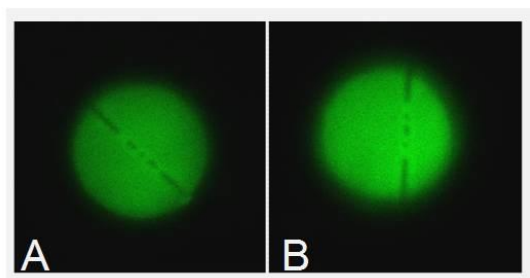


Figure 11: Confocal image of encoded memobeads (A) before and (B) after autoclaving.

Lyophilization on the other hand is a process that is often applied for the preparation of research and diagnostic reagent kits for prolongation of their storage time period by protecting them against hydrolysis and contamination, and for their flexible transport. The basic principle of lyophilization is the removal of water molecules from materials via sublimation (at a critical temperature/pressure point, a solid state of a material can be converted into its gas state). The composition and structure of the material will stay intact, when this dehydration process is carefully applied. Lyophilization of the LbL coated microspheres was done as described above (Table 1). Different parameters were tested, such as the physical properties of the microspheres, the resistance of the code, and the activity of coupled biomolecules (alkaline phosphatase, antibodies).

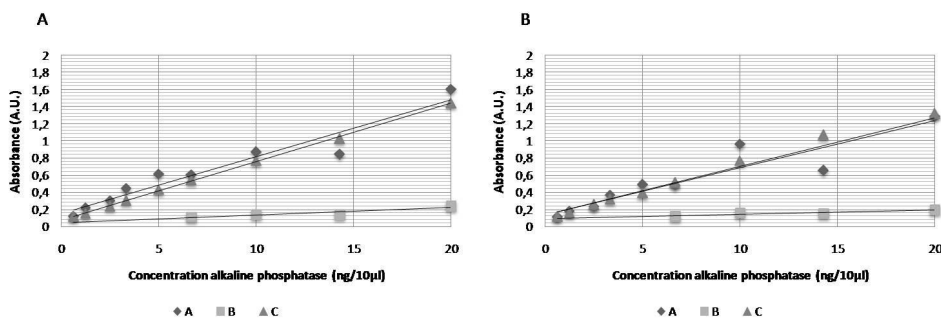


Figure 12: Absorbance as a function of the concentration of alkaline phosphatase (ng /10 µl) which was prior to the quality test lyophilized in 5% inulin (A) or water (B), or non-lyophilized (C). Two different batches were analyzed (A and B).

To test the activity of ‘free’ alkaline phosphatase (AP) after free-drying, several AP dilutions (diluted in water or 5% inulin solution) were lyophilized, and their activity was subsequently tested and compared with no lyophilized control samples by means of the AP quality test: 150 μ l substrate solution was added to 10 μ l of each dilution. Linear fittings were applied to the data points, as shown in Figure 12 (Left and right graphs show two independent replications for each condition). As expected, when lyophilized without any protecting agent (samples B), the activity of the enzyme decreased enormously and the enzyme is almost totally destroyed. In the presence of a protecting agent such as 5% inulin (samples A), however, the enzyme activity equaled that of fresh made non-lyophilized enzyme dilutions (samples C), meaning that the lyophilization did not destroy the enzyme activity at all. Table 4 shows the activity of immobilized AP that is coupled to LbL coated microspheres, after they were a) lyophilized in a 5% inulin solution and then stored for 2 days at 4°C, b) lyophilized in water and then stored for 2 days at 4°C, and c) not lyophilized but only stored for two days at 4°C. The activity was compared with that of control microspheres, which were microspheres that were tested for AP activity, immediately after immobilization of AP. The activity decreased in all cases, but lyophilization seems to be the best option; up to 70% of the activity of freshly made microspheres could be maintained when lyophilization was performed in the presence of a protecting agent such as 5% inulin. Remarkably, lyophilization in water still preserves half of the activity, while free enzyme molecules were almost totally destroyed when they were lyophilized in water (Figure 12). This means that the surface of the microspheres protects the enzymes in one or another way, probably due to the fact that the enzyme molecules are densely packed near each other.

Table 4: Activity of alkaline phosphatase coupled to microspheres as a function of their storage condition.

Types of microspheres	Absorbance ratio's between the microspheres and control microspheres ^a
Microspheres lyophilized in 5% inulin solution and stored for 2 days at 4°C	69.7
Microspheres lyophilized in water and stored for 2 days at 4°C	47.5
Non-lyophilized microspheres that are immediately stored for 2 days at 4°C	30.4

^a Fresh made microspheres that were immediately tested for their enzymatic activity.

It was also tested whether lyophilized LbL coated microspheres maintain their ability to capture antigens. To this end, LbL coated microspheres were coupled with mouse IgG antibodies,

subsequently lyophilized and immediately thereafter stored for 2 days at 4°C. They were then incubated with a solution of red fluorescently labeled goat anti-mouse IgG antibodies. As a control, non-lyophilized LbL coated microspheres were used, that were stored for 2 days at 4°C. Figure 13 shows red fluorescent images of the microspheres. More or less the same amount of red fluorescence can be observed on the lyophilized and non-lyophilized microspheres in the figure (this was confirmed by image analysis), meaning that an equal amount of goat antibodies was caught on both types. This differs from the AP results (Table 4), which showed that the enzyme (coupled to non-lyophilized microspheres) probably degraded during the 2 days storage period at 4°C, while the activity of antibodies might be less affected by this storage. More qualitative results are shown in Figure 14. Three different batches of LbL coated microspheres were coupled with mouse IgGs and each batch was then stored in three different ways for 2 days (4°C, -20°C, and 4°C after lyophilization) before quality control, which was done again by testing the affinity reaction with red fluorescently labeled goat anti-mouse IgG antibodies. No significant differences were observed between the three batches and between the different storage conditions of each batch, which shows that the storage condition does not remarkably influence the affinity of the coupled antibodies, at least after 2 days of storage.

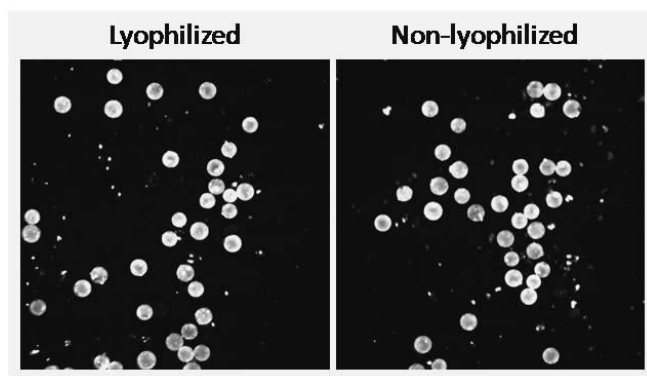


Figure 13: Binding of red fluorescent goat anti-mouse antibodies to lyophilized and non-lyophilized microspheres that were coupled with mouse antibodies.

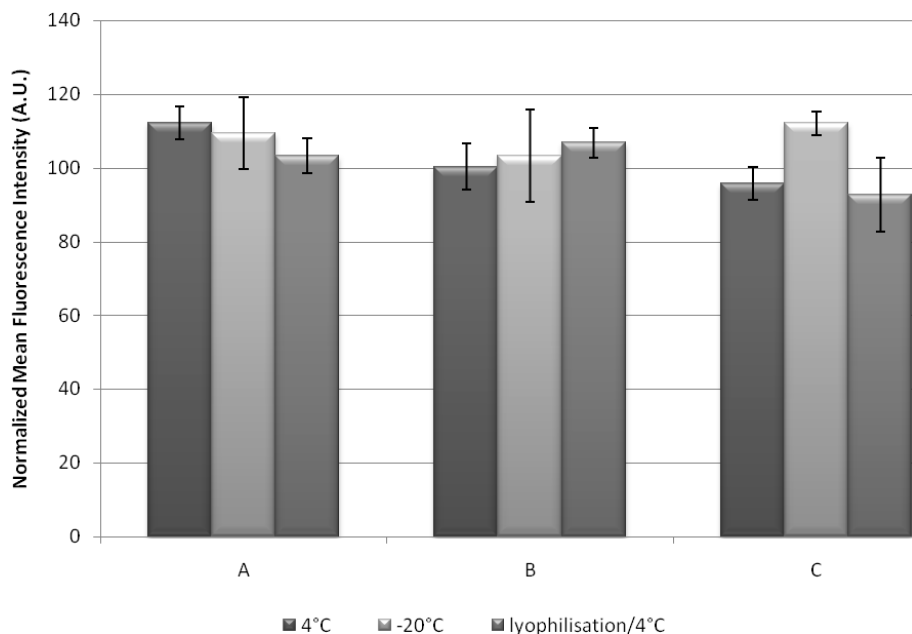


Figure 14: Stability of three different batches lyophilized LbL coated microspheres, coupled with mouse IgGs (A, B, C). Affinity of the antibodies for coupling red fluorescently labeled goat anti-mouse IgG antibodies was determined immediately after storage for 2 days at 4°C, at -20°C, and at 4°C after lyophilization of the microspheres. Note that the measurements were normalized to the measurement of red fluorescent control microspheres, that stably emit red fluorescence.

It has been shown so far that LbL coated microspheres, coupled with antibodies, can be lyophilized with preservation of their affinity for corresponding biomolecules ('antigens'). The storage was carried out, however, only for 2 days, and much longer storage periods might be expected when applying such microspheres in research and/or diagnostic kits. In order to get an idea about the impact of the storage time after lyophilization, four different batches of lyophilized microspheres, previously coated with mouse antibodies, were stored at 4 °C. After one, two, and three weeks, a sample of each batch was tested for its activity to bind to red fluorescently labeled goat anti-mouse IgGs. Figure 15 shows that no significant difference could be observed within this time period for any of the batches.

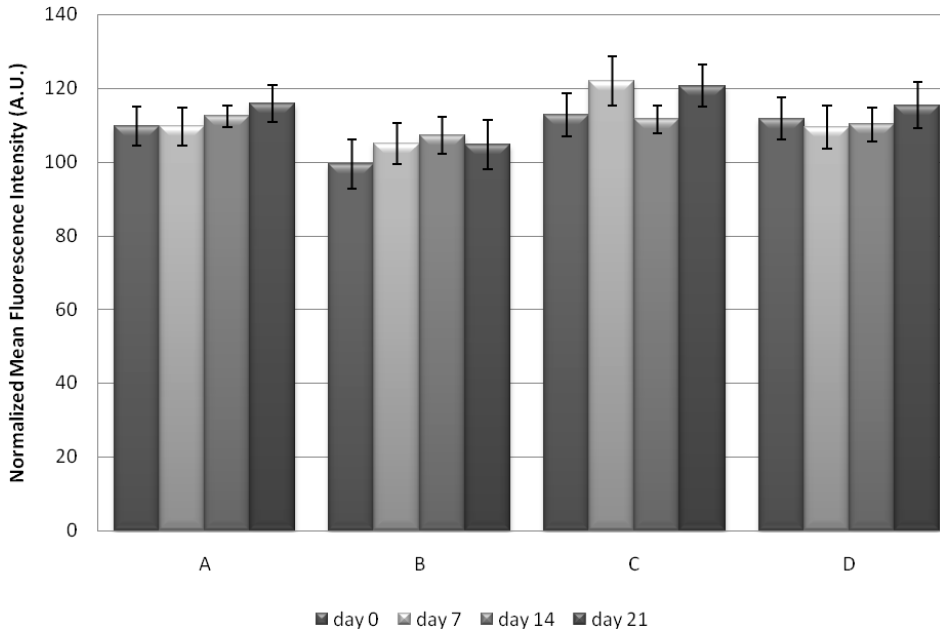


Figure 15: Stability of four different batches lyophilized LbL coated microspheres, coupled with mouse antibodies (A, B, C and D). Affinity of the antibodies for coupling fluorescently labeled anti-mouse antibodies was determined immediately after lyophilization, and after one, two, and three weeks storage at 4°C. Note that the measurements were normalized to the measurement of red fluorescent control microspheres, that stably emit red fluorescence.

Finally, the capacity of several other cryoprotectants (5% solutions), to protect LbL coated mouse IgG coupled microspheres during the lyophilization process, was tested. As can be seen in Figure 16, the activity of the microspheres to catch goat anti-mouse IgGs was in each case maintained for at least 2 weeks after lyophilization. Based on the fluorescent signals in Figure 16, the optimal cryoprotectant for the microspheres seems to be the bovine serum albumin, although this experiment was only performed once. No real differences can be observed between the other cryoprotectants, which is not remarkable since even lyophilization in distilled water maintains the activity.

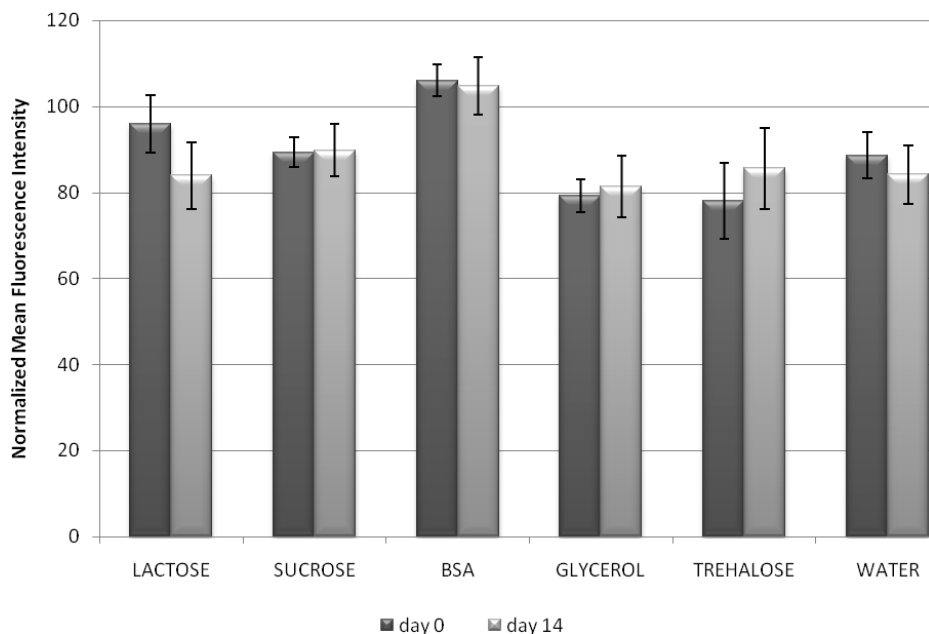


Figure 16: Stability of LbL coated microspheres, coupled with mouse antibodies (A, B, C) and lyophilized in 5% solutions of different cryoprotectants. Affinity of the antibodies for coupling fluorescently labeled anti-mouse antibodies was determined immediately after lyophilization and after a storage for 2 weeks. Note that the measurements were normalized to the measurement of red fluorescent control microspheres, that stably emit red fluorescence.

CONCLUSIONS

A 'multifunctional' layer-by-layer coating, containing CrO₂ NP, was applied at the surface of digitally encoded microspheres. We showed that the LbL coating allows (a) an optimal (optical) read out of the codes, (b) a perfect orientation (within pixel accuracy (0.7 μm/pixel) of the microspheres (leading to a correct decoding) and (c) an optimal coupling of capture probes to the surface. Thus far the potential of LbL coating has been explored in a number of scientific fields like e.g. drug delivery^{29,30,30,31}, for corrosion protection³², and for the production of biosensors³³. To our knowledge this is one of the first studies that experimentally demonstrate that LbL technology indeed allows the application of coatings with various advanced functionalities. The LbL coated microspheres can be

autoclaved and lyophilized without degradation of the code, and their capacity to react with biomolecules remained after lyophilization. We are currently investigating whether the LbL coatings surrounding the microspheres would also allow us to quantitatively measure analytes (like proteins and nucleic acids) in biological samples such as serum and blood.

REFERENCES

1. Ling, M. M.; Ricks, C.; Lea, P. Multiplexing molecular diagnostics and immunoassays using emerging microarray technologies. *Expert. Rev. Mol. Diagn.* **2007**, *7* (1), 87-98.
2. Venkatasubbarao, S. Microarrays--status and prospects. *Trends Biotechnol.* **2004**, *22* (12), 630-637.
3. Southern, E. M. DNA microarrays. History and overview. *Methods Mol. Biol.* **2001**, *170*, 1-15.
4. Vainrub, A.; Pettitt, B. M. Coulomb blockage of hybridization in two-dimensional DNA arrays. *Phys. Rev. E. Stat. Nonlin. Soft. Matter Phys.* **2002**, *66* (4 Pt 1), 041905.
5. Henry, M. R.; Wilkins, S. P.; Sun, J.; Kelso, D. M. Real-time measurements of DNA hybridization on microparticles with fluorescence resonance energy transfer. *Anal. Biochem.* **1999**, *276* (2), 204-214.
6. Czarnik, A. W. Encoding methods for combinatorial chemistry. *Curr. Opin. Chem. Biol.* **1997**, *1* (1), 60-66.
7. Wilson, R.; Cossins, A. R.; Spiller, D. G. Encoded microcarriers for high-throughput multiplexed detection. *Angew. Chem. Int. Ed Engl.* **2006**, *45* (37), 6104-6117.
8. Nolan, J. P.; Sklar, L. A. Suspension array technology: evolution of the flat-array paradigm. *Trends Biotechnol.* **2002**, *20* (1), 9-12.
9. McHugh, T. M.; Miner, R. C.; Logan, L. H.; Stites, D. P. Simultaneous detection of antibodies to cytomegalovirus and herpes simplex virus by using flow cytometry and a microsphere-based fluorescence immunoassay. *J. Clin. Microbiol.* **1988**, *26* (10), 1957-1961.
10. Scillian, J. J.; McHugh, T. M.; Busch, M. P.; Tam, M.; Fulwyler, M. J.; Chien, D. Y.; Vyas, G. N. Early detection of antibodies against rDNA-produced HIV proteins with a flow cytometric assay. *Blood* **1989**, *73* (7), 2041-2048.
11. Martens, C.; Bakker, A.; Rodriguez, A.; Mortensen, R. B.; Barrett, R. W. A generic particle-based nonradioactive homogeneous multiplex method for high-throughput screening using microvolume fluorimetry. *Anal. Biochem.* **1999**, *273* (1), 20-31.
12. Pantano, P.; Meek, C. C.; Wang, J.; Coutinho, D. H.; Balkus Jr, K. J. Optical encoding with shaped DAM-1 molecular sieve particles. *Lab Chip.* **2003**, *3* (2), 132-135.
13. Nicewarner-Pena, S. R.; Freeman, R. G.; Reiss, B. D.; He, L.; Pena, D. J.; Walton, I. D.; Cromer, R.; Keating, C. D.; Natan, M. J. Submicrometer metallic barcodes. *Science* **2001**, *294* (5540), 137-141.
14. Braeckmans, K.; De Smedt, S. C.; Leblans, M.; Pauwels, R.; Demeester, J. Encoding microcarriers: present and future technologies. *Nat. Rev. Drug Discov.* **2002**, *1* (6), 447-456.
15. Braeckmans, K.; De Smedt, S. C.; Roelant, C.; Leblans, M.; Pauwels, R.; Demeester, J. Encoding microcarriers by spatial selective photobleaching. *Nat. Mater.* **2003**, *2* (3), 169-173.
16. Horak, D.; Rittich, B.; Safar, J.; Spanova, A.; Lenfeld, J.; Benes, M. J. Properties of RNase a immobilized on magnetic poly(2-hydroxyethyl methacrylate) microspheres. *Biotechnology Progress* **2001**, *17* (3), 447-452.
17. Ugelstad, J.; Stenstad, P.; Kilaas, L.; Prestvik, W. S.; Herje, R.; Berge, A.; Hornes, E. Monodisperse magnetic polymer particles. New biochemical and biomedical applications. *Blood Purif.* **1993**, *11* (6), 349-369.
18. Aizawa, M.; Buriak, J. M. Nanoscale patterning of two metals on silicon surfaces using an ABC triblock copolymer template. *J. Am. Chem. Soc.* **2006**, *128* (17), 5877-5886.
19. Minelli, C.; Geissbuehler, I.; Hinderling, C.; Heinzelmann, H.; Vogel, H.; Pugin, R.; Liley, M. Organization of nanoparticles on hard substrates using block copolymer films as templates. *J. Nanosci. Nanotechnol.* **2006**, *6* (6), 1611-1619.

20. Krishnamoorthy, S.; Hinderling, C.; Heinzelmann, H. Nanoscale patterning with block copolymers. *Materials Today* **2006**, *9* (9), 40-47.
21. Bhat, R. R.; Fischer, D. A.; Genzer, J. Fabricating planar nanoparticle assemblies with number density gradients. *Langmuir* **2002**, *18* (15), 5640-5643.
22. Skirtach, A. G.; Déjugnat, C.; Braun, D.; Susha, A. S.; Rogach, A. L.; Sukhorukov, G. B. Nanoparticles Distribution Control by Polymers: Aggregates versus Nonaggregates. *J. Phys. Chem. C* **2007**, *111* (2), 555-564.
23. Decher, G. Fuzzy nanoassemblies: Toward layered polymeric multicomposites. *Science* **1997**, *277* (5330), 1232-1237.
24. Caruso, F.; Caruso, R. A.; Mohwald, H. Nanoengineering of inorganic and hybrid hollow spheres by colloidal templating. *Science* **1998**, *282* (5391), 1111-1114.
25. Sukhorukov, G. B.; Donath, E.; Lichtenfeld, H.; Knippel, E.; Knippel, M.; Budde, A.; Mohwald, H. Layer-by-layer self assembly of polyelectrolytes on colloidal particles. *Colloids and Surfaces A-Physicochemical and Engineering Aspects* **1998**, *137* (1-3), 253-266.
26. Carson, R. T.; Vignali, D. A. Simultaneous quantitation of 15 cytokines using a multiplexed flow cytometric assay. *J. Immunol. Methods* **1999**, *227* (1-2), 41-52.
27. Pang, S.; Smith, J.; Onley, D.; Reeve, J.; Walker, M.; Foy, C. A comparability study of the emerging protein array platforms with established ELISA procedures. *J. Immunol. Methods* **2005**, *302* (1-2), 1-12.
28. Fayazpour, F.; Lucas, B.; Huyghebaert, N.; Braeckmans, K.; Derveaux, S.; Vandenbroucke, R.; Remon, J. P.; Demeester, J.; Vervaet, C.; De Smedt, S. Opportunities for digitally encoded microcarriers in pharmacy and cell-based assays. *European Journal of Pharmaceutical Sciences* **2008**, *34* (1), S29.
29. Ai, H.; Jones, S. A.; Lvov, Y. M. Biomedical applications of electrostatic layer-by-layer nano-assembly of polymers, enzymes, and nanoparticles. *Cell Biochemistry and Biophysics* **2003**, *39* (1), 23-43.
30. Wood, K. C.; Boedicker, J. Q.; Lynn, D. M.; Hammon, P. T. Tunable drug release from hydrolytically degradable layer-by-layer thin films. *Langmuir* **2005**, *21* (4), 1603-1609.
31. De Geest, B. G.; Dejugnat, C.; Sukhorukov, G. B.; Braeckmans, K.; De Smedt, S. C.; Demeester, J. Self-rupturing microcapsules. *Advanced Materials* **2005**, *17* (19), 2357-+.
32. Shchukin, D. G.; Zheludkevich, M.; Yasakau, K.; Lamaka, S.; Ferreira, M. G. S.; Mohwald, H. Layer-by-layer assembled nanocontainers for self-healing corrosion protection. *Advanced Materials* **2006**, *18* (13), 1672-+.
33. Ferreira, M.; Fiorito, P. A.; Oliveira ON Jr; Cordoba de Torresi, S. I. Enzyme-mediated amperometric biosensors prepared with the Layer-by-Layer (LbL) adsorption technique. *Biosens. Bioelectron.* **2004**, *19* (12), 1611-1615.

C H A P T E R Three

LAYER-BY-LAYER COATED DIGITALLY ENCODED MICROCARRIERS ALLOW SENSITIVE QUANTIFICATION OF PROTEINS IN SERUM AND PLASMA

Parts of this chapter were published in:

Derveaux S.,¹ Stubbe, B.G.,¹ Roelant, C.,² Leblans, M.,¹ De Geest, B.G.,¹ Demeester, J.,¹ De Smedt, S.C.¹
Analytical Chemistry **2008**, 80, 85-94.

¹ Laboratory of General Biochemistry and Physical Pharmacy, Department of Pharmaceutics, Ghent University, 9000 Ghent, Belgium.

² Memobead Technologies NV, Rupelweg 10, 2850 Boom, Belgium.

ABSTRACT

Since a couple of years the “Layer-by-Layer” (LbL) technology is widely investigated for the coating of flat substrates and capsules with polyelectrolytes. In this chapter, LbL polyelectrolyte coatings applied at the surface of digitally encoded microcarriers were evaluated for the quantitative, sensitive and simultaneous detection of proteins in complex biological samples like serum, plasma and blood. LbL coated microcarriers were to this end coupled to capture antibodies which were used as capturing agents for the detection of tumor necrosis factor (TNF- α), P24 and follicle stimulating hormone (FSH). It was found that the LbL coatings did not disassemble upon incubating the microcarriers in serum and plasma. Also, non-specific binding of target analytes to the LbL coating was not observed. We showed that the LbL coated microcarriers can repeatedly detect TNF- α , P24 and FSH down to the pg/ml level, not only in buffer, but also in serum and plasma samples. Microcarrier-to-microcarrier intra-tube variations were less than 30% and inter-assay variations less than 8% were observed. This chapter shows also evidence that the LbL coated digitally encoded microcarriers are ideally suited for assaying proteins in “whole” blood in microfluidic chips which are of high interest for “point-of-care” diagnostics.

CHAPTER 3

LAYER-BY-LAYER COATED DIGITALLY ENCODED MICROCARRIERS ALLOW SENSITIVE QUANTIFICATION OF PROTEINS IN SERUM AND PLASMA

INTRODUCTION

Immunoassays, like radio-immunoassays, immunoprecipitation assays and enzyme-linked immunosorbent assays (ELISAs), are routinely used in medical diagnostics. ELISAs can be considered as the golden immunoassay assay to quantify soluble analytes (antigens) in human samples. As more and more protein disease markers are discovered there is a growing need to analyze more types of (diagnostic) proteins. ELISAs, however, are not convenient to answer this growing need because (a) each protein marker has to be analyzed individually, (b) there is a high consumption of reagents and biological samples and (c) it is a labor-intensive and time-consuming technique. To this end, fast, inexpensive, accurate immunoassays with increased sensitivity using smaller sample volumes are under development.

Over the last decade, “multiplexing” immunoassays were developed ¹. While a “monoplex” immunoassay aims to measure the binding of one analyte, present in the biological sample, to its receptor, a multiplexing immunoassay aims to measure simultaneously the binding of several analytes in the biological sample to their respective receptors. This multiplex approach allows faster analysis of a high number of protein markers and both the sample and reagent consumption is considerably reduced.

Multiplex immunoassay-technologies are divided into respectively “flat surface arrays” and “suspension arrays”. To the first category belong the protein microarrays, which use the x,y-coordinates of the spots of capture probes (antibodies) on a glass plate to identify which targets (antigens) are present in a sample²⁻⁴. Like DNA microarrays, protein microarrays, however, struggle with localization problems of the capture antibodies upon miniaturization and slow reaction kinetics (as the diffusion of the antigens in the sample to the capture antibodies is time-consuming)⁵⁻⁷. The use of protein microarrays has also been limited by the high cost of both the microarray consumables and the instruments. Suspension arrays may have a number of advantages compared to the flat microarrays regarding for instance the reproducibility of the attachment of probes, the flexibility in surface chemistry, the flexibility in panel of tests, and improved kinetics^{5,8,9}. Suspension arrays use encoded micron sized particles for multiplexing; the code allows knowing which capture antibody is bound to the surface of the microcarriers^{8,10,11}. Antigens present in the biological sample will bind to their corresponding microcarriers which are added to the sample. Fluorescent labeling of the bound antigens can be obtained in different ways, e.g. ‘directly’ by fluorescently labeled detection antibodies or ‘indirectly’ by using fluorescently labeled or enzyme-labeled reporter molecules that bind to the detection antibodies¹²⁻¹⁴. Decoding of the ‘positive’ microcarriers (i.e. those microcarriers which show fluorescently labeled antigens at their surface) subsequently allows knowing which antigens are present in the sample. The microcarrier-based platforms are gaining popularity because they can detect antigens as sensitively and as reproducibly as the traditional ELISAs¹⁵⁻²⁰. Current applications of microcarrier-based assays include detection of immunoglobulins²¹ and cytokines^{16,18-20,22,23}, the analysis of single nucleotide polymorphisms²⁴, DNA methylation profiling²⁵ and gene expression²⁶.

Our group introduced the encoding of fluorescent polystyrene microspheres (of about 40 μm in size) with a digital barcode by means of “spatial selective photobleaching” (Figure 1, B and C)²⁷. The thus encoded microspheres were called “memobeads”. To optimize the surface characteristics of memobeads we recently proposed to coat their surface with poly-electrolytes by the “Layer-by-Layer” (LbL) approach²⁸. The LbL coating is based on the alternate adsorption of oppositely charged polyelectrolytes onto a charged substrate (Figure 1 A)²⁹⁻³². The LbL coating of the surface of the memobeads was proven to be “multifunctional” in the sense that it (a) allows positioning of the memobeads for decoding, (b) does not optically interfere with the encoding and reading process and (c) allows a high loading of the surface of the microparticles with capture probes (like proteins and DNA molecules)³³.

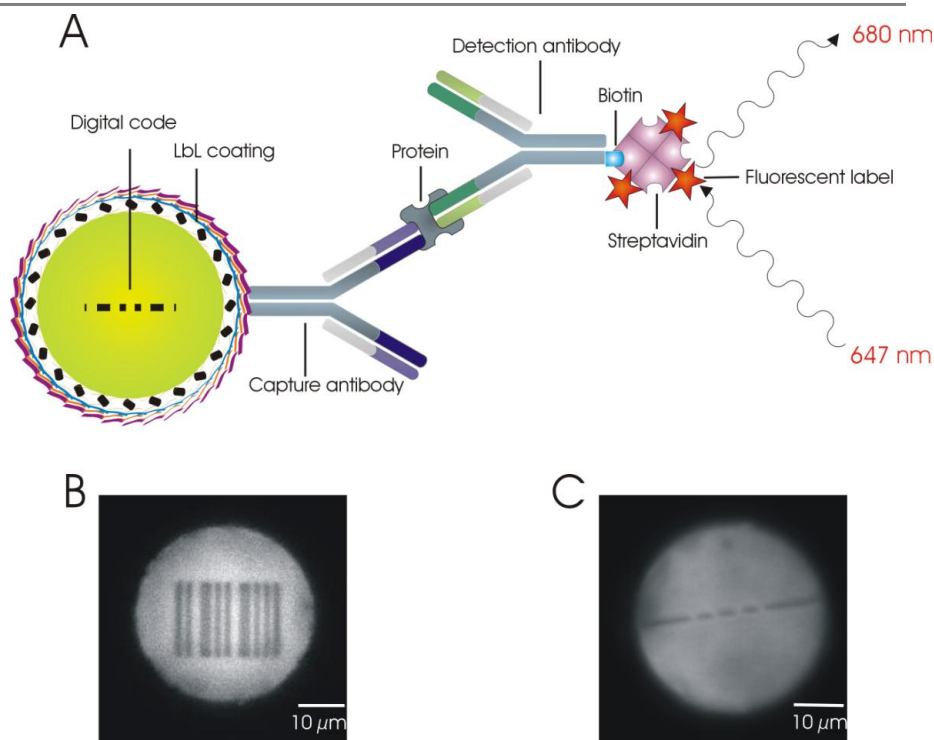


Figure 1: (A) Schematic representation of the detection of proteins with LbL coated memobeads. Proteins (antigens) are captured from the medium by means of capture antibodies bound to the surface of the encoded microcarriers. To detect the bound proteins biotinylated detection antibodies are used. The detection antibodies are labeled with AlexaFluor 647 conjugated streptavidin. (B) Example of a 39µm sized microcarrier digitally encoded with a barcode. (C) Example of a 39µm sized microcarrier digitally encoded with a dotcode.

A major aim of the encoded memobeads is to use them in protein multiplexing. To our knowledge it has never been evaluated whether LbL coatings are suitable to bind capture probes (antibodies) in such a way that they allow quantitative protein (antigen) analysis. To this end, in this chapter we investigate whether LbL coated memobeads allow sensitive and precise detection of proteins, not only in buffer but also in complex biological samples like serum and plasma. Clearly, for this purpose the LbL coating should remain stable in the serum/plasma which contains many types of charged compounds that may interfere with the LbL coating. Also, non-specific binding to the LbL coating should be avoided. In addition we investigate whether the LbL coated memobeads allow performing protein multiplexing in “whole” blood without “washing” (separating) the memobeads from the blood at the time of read out of the microcarriers. “Whole blood analysis” is a challenging objective in the field of diagnostics.

MATERIALS & METHODS

Materials.

Non-magnetic fluorescent carboxylated microspheres (CFP-40052-100, $\phi = 39 \mu\text{m}$) were purchased from Spherotech (Libertyville, Illinois, USA). Poly (allylamine hydrochloride) [PAH; 28,322-3], sodium poly (styrene sulfonate) [PSS, MW $\sim 70\,000$; 24,305-1] and poly (acrylic acid) [PAA, MW $\sim 45\,000$; 18,128-5] were obtained from Sigma Aldrich (Steinheim, Germany). The polymers were dissolved into 0.5 M sodium chloride (31434, Sigma Aldrich, Seelze, Germany). Bovine serum albumine (BSA, A-7906) and 2-[N-Morpholino]ethanesulfonic acid (MES, M-8259) were purchased from Sigma (Bornem, Belgium), PBS Dulbecco's (14190-094) from Gibco and Tween-20 (655204) from Calbiochem. EDC (1-ethyl-3-(3-dimethyl aminopropyl) carbodiimide HCl, 22980) was obtained from Perbio Science (Erembodegem, Belgium); desiccated and stored at -20°C . Sulfo-NHS (N-hydroxysulfosuccinimide sodium salt, 106627-54-7) was purchased from Sigma Aldrich (Steinheim, Germany); desiccated and stored at 4°C . Purified anti-human TNF α (551220), recombinant human TNF α (551838) and biotinylated mouse anti-human TNF α (554511) were purchased from BD Pharmingen (Erembodegem, Belgium). AlexaFluor[®] 647 labeled streptavidin (S21374) was purchased from Molecular Probes (Inc. Invitrogen[™], Eugene, Oregon, USA). Rat Follicle Stimulating Hormone (FSH), purified anti-rat FSH antibody, biotinylated anti-rat FSH antibody, blanc and unknown serum samples and ELISA buffer were a gift from Biocode-Hyclon[™] (Luik, Belgium). P24, purified anti-P24 antibody, biotinylated anti-P24 antibody and blanc plasma samples were a gift from BioMaric[™] (Ghent, Belgium).

Layer-by-Layer coating of the microspheres.

A schematic overview, as well as the procedure of the Layer-by-Layer modification is described in Chapter 2.

Encoding of the microspheres.

The encoding process is described in Chapter 2.

Coupling of capture antibodies to the LbL coated microspheres.

'Capture' antibodies were covalently attached to the (PAA) carboxyl groups at the surface of the microspheres by the two-step carbodiimide-method³⁴. In brief, approximately 10 000 microspheres (in 80 μ l of "activation buffer": 0.1M Na₂HPO₄/NaH₂PO₄, 0.05% Tween-20, pH 6.3) were activated with 10 μ l EDC (50 mg/ml); at the same time the active intermediate was stabilized with 10 μ l sulfo-NHS (50 mg/ml). Note that the storage and handling of EDC has to be done under proper conditions³⁵. The microspheres were then washed twice with 0.05 M MES-buffer (0.05% Tween-20, pH 5) and centrifuged (4000 rpm, 30 seconds). Subsequently the antibodies were coupled by incubating the microspheres in 30 μ l antibody solution (83 μ g/ml) for 2 hours in an Eppendorf Thermomixer (250 rpm). Finally the microspheres were washed twice with "assay buffer" (1% BSA and 0.05% Tween-20 in PBS) to avoid non-specific binding to un-reacted coupling places later on ("blocking step"). The microspheres were stored in 200 μ l "assay buffer" (\pm 50 000 microspheres/ml) at 4 °C.

As described above, the microspheres were incubated in a 83 μ g/ml antibody solution. This seemed to be the optimal antibody concentration as a higher antibody concentration did not result in a higher loading of the microspheres with antibodies (as observed from measurements using AlexaFluor 647 labeled antibodies; data not shown). All of the coupling reactions described above were performed at room temperature.

Assay procedure.

As described below in detail, proteins (antigens) were captured on the LbL coated microspheres carrying the capture antibodies. The bound proteins were detected by means of biotinylated detection antibodies and AlexaFluor 647 (AF647) conjugated streptavidin, as illustrated in Figure 1A. The concentration of biotinylated detection antibody and AF647 conjugated streptavidin used for detecting the bound proteins was optimized (data not shown): lower concentrations resulted in a decrease of the fluorescence intensity, while higher concentrations did not further increase the signal. Note that incubations with AF647 conjugated streptavidin were performed protected from light. All of the following steps were performed at room temperature.

For the detection of TNF- α and P24 in a monoplex assay, approximately 100 microspheres, coated with capture antibody, were incubated for 1 hour in 100 μ l of standard dilutions spiked with respectively TNF- α and P24 (Eppendorf Thermomixer, 250 rpm, 25°C). The dilutions were made in

assay buffer, serum or a plasma/buffer mixture, respectively. After 1 hour incubation the microspheres were washed with assay buffer. As illustrated in Figure 1, the microspheres were subsequently incubated for 1 hour in 100 µl of a biotinylated detection antibody solution (8 µg/ml in assay buffer). Finally, the microspheres were washed three times with assay buffer. The labeling of the bound detection antibodies with AF647 conjugated streptavidin was done as described below.

For the simultaneous detection of TNF-α and P24 in the duplex assay, approximately 300 (encoded) microspheres were used; one third of the microspheres (bearing a dotcode encoding for TNF- α) was coated with capture antibody against TNF- α, one third (bearing a dotcode encoding for P24) with capture antibody against P24 and one third of the microspheres (bearing a dotcode encoding for a control) did not bear antibodies (“control microspheres”). The rest of the procedure was done as described above.

For the detection of FSH, approximately 100 microspheres, coated with capture antibodies, were incubated for 2 hours in respectively 25 µl standard dilutions spiked with FSH (in ELISA buffer) or 25 µl of unknown serum samples. 100 µl of biotinylated detection antibodies (8 µg/ml in assay buffer) was added. The microspheres were subsequently washed three times with assay buffer.

Labeling of the bound detection antibodies was always done with AF647 conjugated streptavidin. The microspheres were incubated for 1 hour in the dark in 100 µl AF647 conjugated streptavidin solution (8 µg/ml). Next, the microspheres were washed three times with 100 µl PBS.

Calibration curves.

Lyophilized TNF-α, P24 and FSH was reconstituted in respectively assay buffer, ELISA buffer, serum or plasma. For each protein, 6 to 9 serial dilutions were made.

The calibration curves were calculated by the GraphPad Prism software. The 4-parameter logistic equation (4-PL) was used to obtain the most precise determination of the protein concentration³⁶:

$$y = a + \frac{b - a}{1 + 10^{[(d-x)*c]}}$$

where x is the logarithmic of the protein concentration, y is the response (i.e. the red fluorescence at the surface of the microcarriers), a is the estimated response at zero protein

concentration (i.e. the “zero calibrator”), b is the estimated response at infinite protein concentration, c is the slope of the tangent midpoint and d is the logarithmic of the midrange protein concentration.

The R^2 -value of the calibration curves together with back-calculations of the standards were used to measure the “goodness of fit”. The latter is done by calculating the concentration of each standard and then comparing it to the expected concentration using the formula: calculated concentration/expected concentration * 100.

The lower limit of detection (LOD) of a protein was defined as the concentration corresponding to the median fluorescence intensity (MFI) plus 3 times the standard deviation of the “zero calibrator”. The inter-assay variability was defined as the coefficient of variation (CV; in %) on the average value of repeated measurements on identical samples performed at different days.

Microscopy on the microspheres.

The LbL coated encoded microspheres were decoded using a pseudo-confocal Perkin-Elmer CSU-10 scanning unit mounted to an inverted Zeiss microscope equipped with an objective 40x lens (NA 0.6) and a cooled Hamamatsu ORCA-ER charge coupled device (CCD) camera. Excitation took place with laser light (488nm). Imaging Technology PC-DIG framegrabber boards took care of image transfer from the CCD camera to the computer.

The (red) AlexaFluor 647 fluorescence at the surface of the microcarriers was measured with the same instrument, but excitation took place with a halogen lamp. A 647nm LP filter was put in front of the lamp to obtain the optimal wavelength. To determine the red fluorescence of a microcarrier, a region of interest (ROI) was drawn around the microcarrier and the red fluorescence within the ROI was measured using the Matlab 7.1 version equipped with home-made imaging processing software. The red fluorescence of each microsphere was defined as the mean of the intensity of all pixels within the ROI.

RESULTS

Detection of TNF- α in buffer by LbL coated microcarriers.

LbL coated microspheres, carrying TNF- α (capture) antibodies, were incubated in different TNF- α standard solutions, prepared in buffer. Following the procedure as depicted in Figure 1, they were further incubated with biotinylated detection antibodies and AlexaFluor 647 conjugated streptavidin. This is the preferred detection method in bead-based assays as (a) biotinylation of antibodies is well-known chemistry^{37,38}, (b) approximately three dyes per streptavidin molecule are present which results in a (small) amplification of the signal, compared to the use of fluorochrome conjugated antibodies, and (c) conjugates with streptavidin give much lower background than those with neutralite-avidin³⁹.

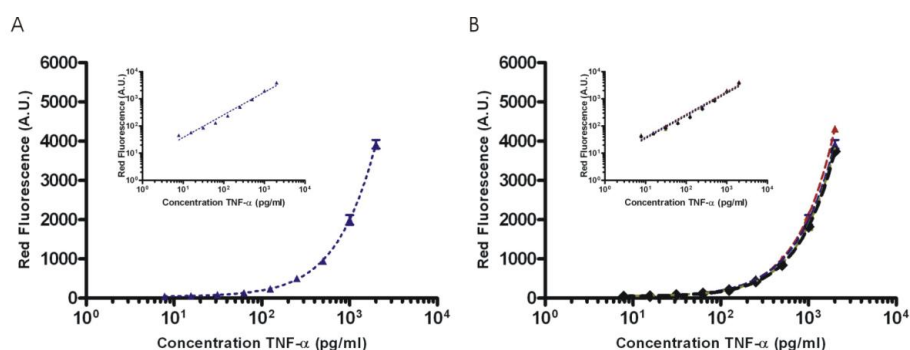


Figure 2: Quantitative analysis of TNF- α spiked in buffer. A) Red fluorescence at the surface of the LbL coated microcarriers as a function of the TNF- α concentration (A.U. = arbitrary units). Each datapoint is the average value of the red (surface) fluorescence of about 20 LbL coated microcarriers (CV's varied between 4% and 26%). A non-linear four-parameter plot accurately fits the data. The lower limit of detection (LOD) equaled 10 pg/ml. B) The red fluorescence of the microspheres was measured immediately (\blacktriangle), 5 (\blacklozenge), 10 (\blacksquare) and 20 days (\bullet) after the assay, respectively. R^2 values of the non-linear four-parameter plots range from 0.97 to 0.99 and standard recovery was between 70% and 130% for all standards. Inset: representation on a log-log plot: F-tests on the slopes ($p=0.9992$) and Y-intercepts ($p=0.549$) of the 4 fitted linear curves yielded no significant differences between the curves measured at the different time points. The pooled slope equaled 0.90 and the pooled Y-intercept equaled 3.72.

As Figure 2A shows, the red fluorescence at the surface of the LbL coated microspheres is proportional to the TNF- α concentration in the sample. A non-linear four-parameter logistic plot was proven to accurately fit the values. Other immunodetection methods reveal the same type of trend

in the relation between the signal and the antigen concentration⁴⁰. The inset in Figure 3A shows a linear fitting applied on the data.

In Figure 2A the red fluorescence at the surface of the microspheres was measured immediately after the assay. To test the stability of the LbL coating and the “capture antibody/TNF- α /detection antibody/AlexaFluor 647 conjugated streptavidin” construct at the surface of the microcarriers, the red fluorescence of the microcarriers was also measured at 5, 10 and 20 days after the assay (instead of immediate read out as in Figure 2A). Figure 2B shows that the microcarriers keep their red fluorescence indirectly indicating that the antibody-antigen construct remains stable at the surface of the microcarriers for at least 20 days. It also indicates that the LbL coating does not disassemble within this time interval which is not surprising since LbL coatings have been reported to be very stable⁴¹.

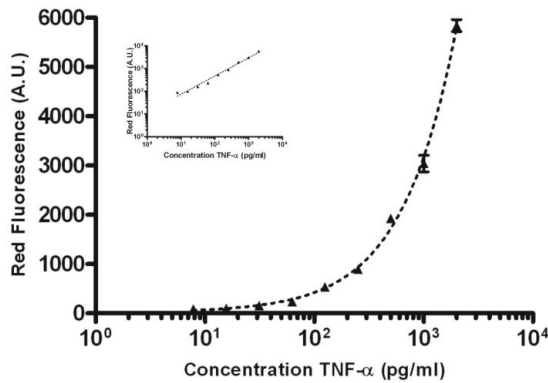


Figure 3: Quantitative analysis of TNF- α spiked in serum. Each datapoint is the average value of the red (surface) fluorescence of 4 to 13 LbL coated microcarriers (CV's between 6% and 28%). A non-linear four-parameter plot accurately fits the data ($R^2 = 0.98$ and standard recovery was between 77% and 117% for all standards). The LOD equaled 16 pg/ml. Inset: representation on a log-log plot.

Detection of TNF- α in serum and plasma by LbL coated microcarriers.

For diagnostic purposes, the stability of the LbL coated microcarriers in more complex media like serum and plasma is important, as well as their ability to detect antigens in those media. Figure 3 shows the outcome of TNF- α measurements by LbL coated microcarriers in not diluted sera spiked with TNF- α . A non-linear four-parameter logistic plot was again proven to accurately fit the values ($R^2 = 0.98$). As expected, a slightly lower sensitivity was observed than in buffer; the LOD in serum

equaled 16 pg/ml compared to 10 pg/ml in buffer, because serum contents generally suppress the antibody-antigen interaction ⁴².

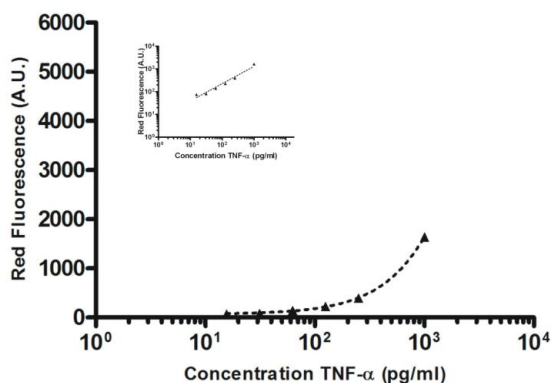


Figure 4: Quantitative analysis of TNF- α spiked in plasma/buffer matrix (50/50; v/v). Each datapoint is the average value of the red (surface) fluorescence of 9 to 16 microspheres (CV's between 7% and 29%); so there seems no significant difference in intra-tube variation whether the LbL coated memobeads are used in buffer, serum or plasma. A non-linear four-parameter logistic plots accurately fits the data ($R^2 = 0.98$ and standard recovery was between 70% and 130% for all standards). The LOD equaled 23 pg/ml. Inset: representation on a log-log plot.

It is well known that during the separation of serum from blood one may lose some proteins of interest which should obviously be avoided in the case of low-abundant proteins. It is therefore preferred to analyze plasma (or even “whole” blood) instead of serum. Figure 5 shows the outcome of TNF- α measurements by LbL coated microcarriers in a plasma/buffer mixture (50/50; v/v) spiked with TNF- α . Clearly, compared to buffer and serum (respectively Figure 2 and Figure 3), in plasma the red fluorescence measured at the surface of the microcarriers is lower while also the sensitivity is not as high as in buffer and serum (the LOD equals 23 pg/ml). Indeed, plasma compounds may non-specifically interfere with the antibody-antigen binding, a phenomenon that was also observed with other cytokines and in other bead-based assays.

As can be concluded from the low LOD values, there is almost no red fluorescence on the LbL coated microspheres (carrying TNF- α capture antibodies) incubated in the “zero calibrator”, indicating that biotinylated antibodies and AlexaFluor 647 labeled streptavidine do not bind aspecifically to the surface of the microcarriers. Also, control experiments in which microcarriers without capture antibodies were dispersed in TNF- α spiked in buffer, serum, and plasma, respectively, all showed the same negligible red fluorescence after adding biotinylated TNF- α

antibodies and AlexaFluor 647 labeled streptavidin (data not shown). It indicates that, even in serum and plasma, the LbL coating itself does not aspecifically bind detection antibodies and/or fluorescently labeled streptavidin molecules.

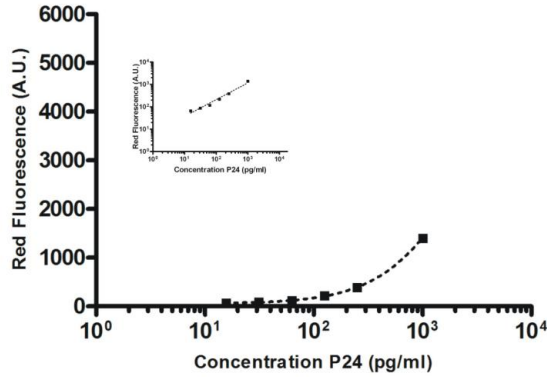


Figure 5: Quantitative analysis of P24 spiked in plasma/buffer matrix (50/50; v/v). Each datapoint is the average value of the red (surface) fluorescence of 11 to 14 microspheres (CV's between 12% and 29%); this means that the variation seems target independent. A non-linear four-parameter logistic plot accurately fits the data (R^2 value = 0.95 and standard recovery was between 92% and 106% for all standards). The LOD equaled 34 pg/ml. Inset: representation on a log-log plot.

Detection of P24 in plasma/buffer mixtures by LbL coated microcarriers.

P24 is a major core protein of the human immunodeficiency virus encoded by the HIV gag gene. It is of interest to detect P24 at a very early stage of the infection in order to start drug therapy. P24 is currently analyzed by ELISA⁴³. Figure 5 shows the outcome of P24 measurements in plasma/buffer mixtures (50/50; v/v) spiked with P24. As was the case for TNF- α , the red fluorescence at the surface of the LbL coated microspheres is proportional to the P24 concentration in the sample. A non-linear four-parameter logistic plot was proven to accurately fit the values. The LOD equals 34 pg/ml.

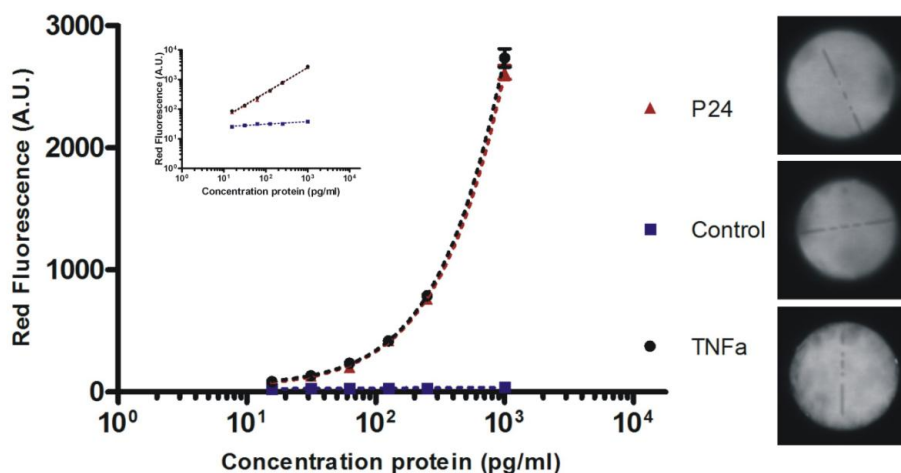


Figure 6: Quantitative duplex analysis of P24 (▲, code 9) and TNF- α (●, code 23) spiked in plasma/buffer matrix (25/75; v/v). Negative control microspheres without capture antibody were included in the test (■, code 14). Each datapoint is the average value of the red (surface) fluorescence of 6 to 13 microspheres (CV's between 4% and 22%). A non-linear four-parameter logistic plots accurately fit the data (R^2 value = 0.95 and standard recovery was between 92% and 106% for all standards). The LOD equaled 15 and 18 pg/ml for respectively P24 and TNF- α . Inset: representation on a log-log plot.

TNF- α and P24 multiplex measurements in plasma/buffer mixtures by LbL coated microcarriers.

As described in the introduction, the purpose the LbL coated encoded microcarriers is to use them for multiplexing. We subsequently evaluated the potential of LbL coated microcarriers to measure simultaneously TNF- α and P24 in a plasma/buffer mixture (25/75; v/v). To this end 3 types of encoded LbL coated microcarriers were simultaneously dispersed in the TNF- α , P24 spiked plasma/buffer mixtures: to one type of microcarriers (with a “TNF- α dot code”; see inset in Figure 6) TNF- α antibodies were coupled, the second type of microcarriers (with a “P24 dot code”; see inset in Figure 6) was loaded with P24 antibodies while the third type of microcarriers (with a “control dot code”) did not carry antibodies.

Figure 6 shows the outcome of the simultaneous measurement of TNF- α and P24 in spiked plasma/buffer (25/75; v/v) samples. As observed in the monoplex assays (Figure 4 and Figure 5), a quantitative relationship is seen between the red fluorescence at the surface of the P24 and TNF- α microcarriers and the P24 and TNF- α concentration in the samples. The specificity was confirmed under monoplex conditions; microcarriers bearing TNF- α capture antibodies showed negligible red fluorescence after being dispersed in P24 spiked plasma samples, while microcarriers bearing P24

capture antibodies showed negligible red fluorescence after being dispersed in TNF- α spiked plasma (results not shown). It seems that, for a given P24 and TNF- α concentration in the sample, the red fluorescence of the microcarriers in the duplex assay (Figure 6) exceeds the one of the microcarriers in the monoplex assay (Figure 4 and Figure 5). This is probably due to less interference with plasma proteins as a 25/75 (v/v) plasma/buffer mixture was used in Figure 6 while a 50/50 (v/v) plasma/buffer mixture was used in Figure 4 and Figure 5.

FSH measurements in clinical serum samples by LbL coated microcarriers.

In the experiments above the potential of LbL coated microcarriers was evaluated in buffer/serum/plasma samples which were spiked with respectively P24 and TNF- α . We subsequently tested whether the LbL coated microcarriers can specifically and precisely measure a protein target (FSH) in (“real, unknown”) serum samples.

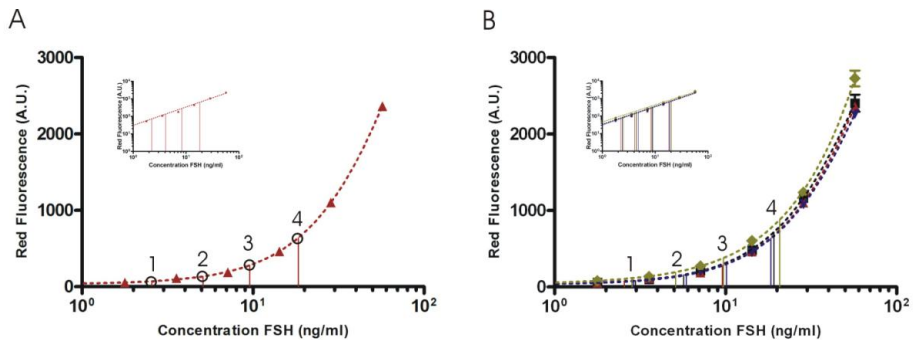


Figure 7: A) Quantitative analysis of FSH spiked in ELISA buffer (\blacktriangle) and determination of FSH concentration in 4 unknown samples (\circ) (extrapolation process: 4 vertical lines). B) The same assay was repeated 4 times (\blacktriangle , \blacksquare , \blacktriangledown and \blacklozenge). Each datapoint is the average value of the red (surface) fluorescence of 15 to 34 microspheres (CV's between 8% and 23%). Four-parameter logistic plots accurately fit the data (R^2 between 0.9999 and 1 and standards recovery was between 92 and 120% for each standard). The LOD equaled between 0.9 and 1.5 ng/ml. Inset: representation on a log-log plot.

Table 1: The FSH concentration in four different mouse serum samples measured with the LbL coated microcarriers (by the extrapolation process visualized in Figure 7B).^a

Samples	A	B	C	D	Average (ng/ml)	SD	CV%
1	3.0	2.6	2.9	2.8	2.8	0.2	7.1
2	5.7	5.1	5.9	5.1	5.4	0.4	7.4
3	10.1	9.6	10.1	9.7	9.9	0.3	3.0
4	19.1	18.4	18.3	20.8	19.2	1.1	5.7

^a Each sample was analysed four times (A, B, C and D). SD is the standard deviation on the average concentration; CV (in %) is the coefficient of variation (i.e. the standard deviation divided by the mean).

Typically, when quantitatively assaying an analyte in serum samples by ELISA, an internal calibration curve is first made by the use of sera spiked with (known) concentrations of the analyte of interest. The same procedure is applied in bead-based assays¹⁸. The concentration of the analyte in the “unknown” sample is then extrapolated from the calibration curve. Figure 7A shows the FSH calibration curve and the extrapolation of the signal as measured in the 4 unknown samples (1 to 4 in Figure 7A). The whole assay was repeated 4 times to test its repeatability. Figure 7B shows the 4 calibration curves and the 4 measurements on the 4 unknown samples. Clearly, the calibration curves do not differ significantly. The inter-assay variability for each of the unknown samples was very low (CV below 8%, see Table 1) which is comparable with the variability observed in other bead-based assays^{18,44,45}. All together Figure 7B indicates that the LbL coated microspheres can measure repeatedly the FSH concentrations in sera. Note that only 25 µl serum was needed to obtain those repeatable results.

Influence of the number of LbL coated microcarriers on the sensitivity of the analysis.

It has been reported that the number of microcarriers used in a (bead-based) assay may profoundly affect the sensitivity and the dynamic range of the assay. This is explained by the fact that the proteins (antigens) present in the sample will be distributed over a larger surface in case a higher number of microcarriers is used, which lowers the average (red) surface fluorescence per microcarrier.

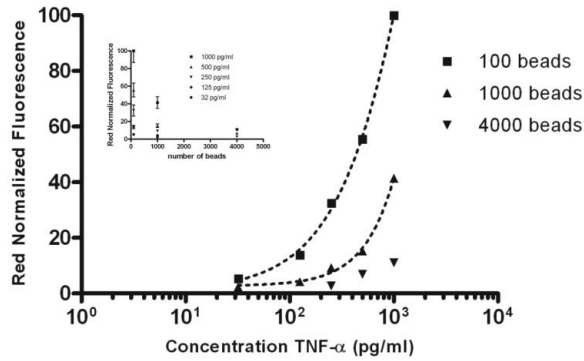


Figure 8: The influence of the number of LbL beads used in the assay on the red fluorescence at the surface of LbL coated memobeads incubated with different dilutions of TNF- α . Main graph: red fluorescence intensity as a function of the spiked concentrations of TNF- α ; respectively 4000 (\blacktriangledown), 1000 (\blacktriangle) and 100 (\blacksquare) memobeads were used. In the case of 4000 memobeads, there are too few data points to fit a 4-parameter logistic equation. Inset: fluorescence as a function of the number of memobeads for different TNF- α concentrations.

Figure 8 shows the red fluorescence at the surface of the LbL coated microcarriers dispersed in TNF- α solutions (in buffer); the number of LbL microcarriers in the assay was varied (between 100 and 4000). Clearly, for a given TNF- α concentration, the lower the number of beads used in the assay, the higher the red fluorescence at the surface of the LbL coated microcarriers. Thus, the number of LbL microcarriers used strongly determines both the sensitivity and the dynamic range of the assay. For example, with 1000 memobeads in the assay, a significant difference between 32 and 125 pg/ml can not be detected anymore, while this remains possible when only 100 memobeads are used in the assay.

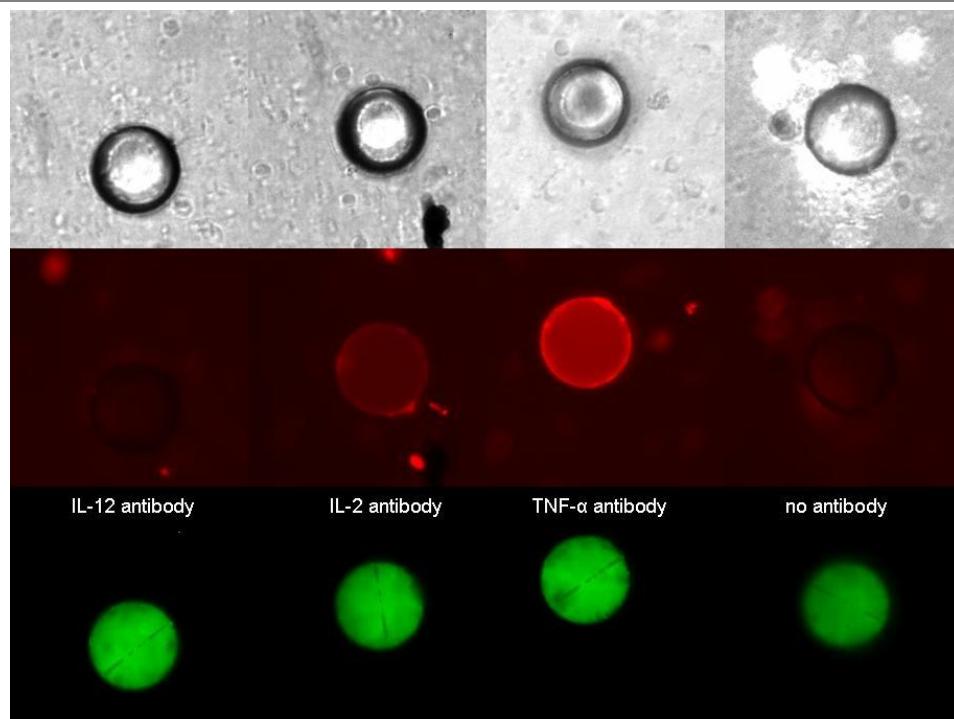


Figure 9: Multiplexing in “whole” blood using LbL coated (encoded) microcarriers. The analysis of the microcarriers was performed while the microcarriers remained in the blood (thus without prior wash steps). Differently encoded LbL coated microspheres were coupled to IL-12 capture antibodies, IL-2 capture antibodies or TNF- α capture antibodies. A mixture of encoded TNF- α -, IL-2-, IL-12- and blanco-microcarriers (i.e. microcarriers without capture antibody) was incubated during 3 hours in a whole blood sample spiked with TNF- α and IL-2 (together with the biotinylated detection antibodies and the AF647 conjugated streptavidin). Top row: transmission image showing the microcarriers suspended between blood cells. Middle row: red fluorescence image of the microcarriers; only the surface of the TNF- α and IL-2 microcarriers turns red fluorescent as the samples where only spiked with TNF- α and IL-2. Bottom row: green fluorescence confocal image of the microcarriers which reveals the code.

Potential use of LbL coated microcarriers for protein analysis in “whole” blood.

As outlined in the introduction, the encoded LbL coated microcarriers under investigation in this study can be easily decoded by means of a fluorescence microscope (equipped with a semi-confocal module). To this end, for decoding it is sufficient to put the microcarriers in a glass bottomed recipient under a microscope; for this type of encoded microcarriers, microcapillaries are not needed to align the microcarriers to pass in front of the detector. Such microcapillaries (like in a flow cytometry apparatus) are used e.g. in the decoding of spectrometrically encoded microcarriers¹⁴. As assaying in “whole” blood, instead of in serum or plasma, would be a clear advantage for different reasons we subsequently studied whether the code in the LbL coated microcarriers and the

red fluorescence at their surface could be detected with this easy read-out system while the microcarriers remain in blood.

Figure 9 shows the outcome of a multiplex assay in whole blood spiked with TNF- α and IL-2 without separating (washing) the LbL coated microcarriers from the blood sample. The encoded microcarriers, the biotinylated detection antibodies and the AlexaFluor 647 streptavidin were simultaneously incubated for 3 hours in the blood samples spiked with TNF- α and IL-2. Note that in Figure 2 to Figure 8 detection antibodies and AlexaFluor 647 conjugated streptavidin were added step per step while in Figure 9 an “all-in-one” procedure was used as the microcarriers, detection antibodies and fluorescent streptavidin were simultaneously added to the blood sample. We observed the following. (a) The digital code of the microcarriers could be still accurately decoded while the microcarriers were in blood (bottom row in Figure 9); (b) It was still possible to measure the red fluorescence at the surface of the microcarriers (middle row in Figure 9). Thus, the blood cells and blood plasma did not hinder the decoding and the quantification process.

Discussion

Bead-based assays become more and more attractive for the analysis of proteins because, compared to ELISAs, they are faster and less-expensive and have a broader dynamic range, while they have the same specificity and reproducibility^{18,42,46}. Also, less sample is needed^{19,47}. This study shows that microcarriers Layer-by-Layer coated with poly-electrolytes, as shown in Figure 1, allow quantitative measurements of TNF- α , down to 10 pg/ml in buffer, 16 pg/ml in serum and 23 pg/ml in a plasma/buffer mixture which comes close to the LOD reported for commercially available humane cytokine bead-based assays which can detect concentrations down to a few picograms cytokine per ml^{16,48}. One could wonder what the advantage of the Layer-by-Layer coating then is. The LbL technology is a flexible approach to modify surfaces, e.g. in this study the LbL coating is bifunctional: the LbL coating incorporates magnetic nanoparticles (needed to properly orient the carriers for decoding) without the formation of aggregates while it also provides the surface of the carriers with a large number of carboxylgroups homogeneously spread over their surface, which improves the intra-tube variation. We have proven that the LbL coated microcarriers can repeatedly measure other proteins like P24 and FSH in complex samples as well; The lower limit of detecting P24 in the

plasma samples was 34 pg/ml which is certainly an acceptable value when compared with the commercially available fourth-generation P24 ELISA assays which measure down to 10 pg/ml⁴⁹. We observed inter-assay variation coefficients below 8%, which is comparable with other bead-based assays^{18,44,45}. Note that there remains room to further improve the sensitivity of the LbL coated beads, e.g. by making use of other antibody kits (it is well known that both the LOD as well as the dynamic range of a multiplex bead-assay is highly dependent of the quality of the capture and detection antibody)¹⁵. For diagnostic purposes, besides the sensitivity also the stability of the LbL coated microcarriers in serum and plasma is important. However, the LbL coated microcarriers did not show non-specific interactions with the serum/plasma proteins; no degradation of the LbL coating has been observed.

We showed that the number of LbL coated microspheres in the protein assay may affect profoundly the sensitivity. The same finding was observed by Kohara et al.⁵⁰ who used microcarriers for DNA assaying, while other authors did not experience significant differences in sensitivity when changing the number of microcarriers³⁹. The higher sensitivity when lowering the number of microcarriers is due to the fact that a higher number of antigens become coupled per microcarrier which results in a stronger red fluorescence of the microcarrier. Some authors argue, however, that a sufficiently high number of microcarriers should be used to precisely determine the concentration of the antigen, especially in low antigen concentrations, and to shorten the confidence interval⁵¹. In our study the red surface fluorescence of only some tens of microcarriers was measured per antigen concentration. Though, the inter-bead variation for beads incubated within the same well was acceptable (CV between 4 and 30%) and comparable to bead-based assays in which a higher number of beads was used^{42,52}.

We observed that the LbL coated microcarriers are stable for at least 20 days after the assay. This means that the red fluorescence of the surface of the microcarriers has not to be read out immediately after the assay, as long as the microcarriers are kept in the dark. We found before that the code in the microcarriers is very light stable when the memobeads are stored in day light (this period is even longer when the beads are stored in the dark; unpublished results). Hence, the stability of the code is not the limiting factor. It has been reported that spectrometrically encoded beads (which are loaded with a mixture of fluorophores which encodes the beads) lack stability: in this study the decoding of such beads becomes problematic after 1-month storage at 4°C after antibody coupling, although no other literature confirms this observation⁵². Furthermore, such beads should also be handled in the dark as bleaching of the fluorophores by prolonged exposure to light results in false codes³⁹.

The detection of antigens in “whole blood” instead of in serum and plasma is highly desirable in the field of diagnostics. Indeed, assaying in whole blood would shorten the processing-time and lower the costs, two main issues in diagnostic and research settings. Additionally, in whole blood the assay was performed in a more physiological environment as during the preparation of serum and plasma, the antigen may be degraded or adsorbed and even antigen cellular production is possible¹⁵. This study (Figure 10) showed that the red fluorescence at the surface of the LbL coated microcarriers can be measured even when the beads remain in whole blood. Importantly, while being in blood, also the digital code in the beads can be perfectly read out; Although blood is significantly more viscous than water and blood cells are extensively present, the orientation of the LbL coated microcarriers in blood by applying a magnetic field (which is necessary for the decoding of the microcarriers) remains possible. We conclude that the digitally encoded LbL coated memobeads are good candidate materials to be used in near-patient testing which aims at rapid and simultaneous diagnosis of many antigens in whole blood while the patient is in the doctor’s cabinet.

Importantly, the encoding of microcarriers by means of photobleaching provides them with a digitally accurate code. As the decoding of such microcarriers occurs with 100% certainty, it means that, theoretically, one microcarrier per antigen type in the assay would be sufficient. Other bead encoding technologies do not permit the use of a very small number of microcarriers as errors may occur in the decoding process which necessitates a statistical analysis of the decoding result of a larger number of microcarriers to obtain the correct code. It means that, typically, at least 100 microcarriers per antigen type are used in the assay. Considering the fact that a low number of digitally encoded microcarriers per antigen in the assay is sufficient and considering the increase in sensitivity when performing assays with a very small number of microcarriers (see above), one may conclude that the LbL coated microcarriers described in this chapter are well suited for assaying biological samples in microfluidic chips⁵³ which are loaded with a limited number of the encoded beads. Assaying in microfluidic chips may have a number of advantages. It is for instance well-known that (bio)chemical reactions occur much faster in a microfluidic environment⁵⁴⁻⁵⁶. Those chips, however, often lack multiplexing capabilities. The use of the digitally encoded LbL coated microcarriers in microfluidic based devices could give new opportunities for “point-of-care” micro total analysis systems (μ TAS).

CONCLUSION

This study shows that LbL coatings, loaded with capture antibodies, at the surface of digitally encoded microcarriers allow the quantitative and sensitive detection of proteins, like TNF- α , P24 and FSH, not only in buffer but also in complex media like serum and plasma. When incubated in serum or plasma the LbL coatings remain stable at the surface of the microcarriers while non-specific binding of serum/plasma molecules to the capture antibody loaded LbL layers was not observed. Importantly, we observed that (a) the digital code of the microcarriers could be still accurately decoded and (b) the red fluorescence at their surface could be quantified even when the microcarriers remained in “whole blood”. These properties make the LbL coated digitally encoded microcarriers investigated in this study ideally suited for the simultaneous (multiplexing) assaying of proteins in “whole” blood instead of in serum or plasma. We showed that using a lower number of LbL coated microcarriers in the protein assay even profoundly improves the sensitivity of the assay, an interesting feature when one wants to make use of the microcarriers for assaying in microchips which only allow using a rather low number of microcarriers. Based on the observations in this study we suggest that the LbL coated digitally encoded microcarriers may be ideally suited for protein multiplexing in whole blood making use of microchips.

REFERENCES

1. Joos, T. O.; Stoll, D.; Templin, M. F. Miniaturised multiplexed immunoassays. *Curr. Opin. Chem. Biol.* **2002**, *6* (1), 76-80.
2. Knight, P. R.; Sreekumar, A.; Siddiqui, J.; Laxman, B.; Copeland, S.; Chinnaiyan, A.; Remick, D. G. Development of a sensitive microarray immunoassay and comparison with standard enzyme-linked immunoassay for cytokine analysis. *Shock* **2004**, *21* (1), 26-30.
3. Templin, M. F.; Stoll, D.; Schrenk, M.; Traub, P. C.; Vohringer, C. F.; Joos, T. O. Protein microarray technology. *Trends Biotechnol.* **2002**, *20* (4), 160-166.
4. Wiese, R.; Belosludtsev, Y.; Powdrill, T.; Thompson, P.; Hogan, M. Simultaneous multianalyte ELISA performed on a microarray platform. *Clin. Chem.* **2001**, *47* (8), 1451-1457.
5. Henry, M. R.; Wilkins, S. P.; Sun, J.; Kelso, D. M. Real-time measurements of DNA hybridization on microparticles with fluorescence resonance energy transfer. *Anal. Biochem.* **1999**, *276* (2), 204-214.
6. Kusnezow, W.; Syagailo, Y. V.; Ruffer, S.; Klenin, K.; Sebald, W.; Hoheisel, J. D.; Gauer, C.; Goychuk, I. Kinetics of antigen binding to antibody microspots: strong limitation by mass transport to the surface. *Proteomics.* **2006**, *6* (3), 794-803.
7. Kusnezow, W.; Syagailo, Y. V.; Goychuk, I.; Hoheisel, J. D.; Wild, D. G. Antibody microarrays: the crucial impact of mass transport on assay kinetics and sensitivity. *Expert. Rev. Mol. Diagn.* **2006**, *6* (1), 111-124.
8. Wilson, R.; Cossins, A. R.; Spiller, D. G. Encoded microcarriers for high-throughput multiplexed detection. *Angew. Chem. Int. Ed Engl.* **2006**, *45* (37), 6104-6117.
9. Nolan, J. P.; Sklar, L. A. Suspension array technology: evolution of the flat-array paradigm. *Trends Biotechnol.* **2002**, *20* (1), 9-12.
10. Braeckmans, K.; De Smedt, S. C.; Leblans, M.; Pauwels, R.; Demeester, J. Encoding microcarriers: present and future technologies. *Nat. Rev. Drug Discov.* **2002**, *1* (6), 447-456.
11. Pregibon, D. C.; Toner, M.; Doyle, P. S. Multifunctional encoded particles for high-throughput biomolecule analysis. *Science* **2007**, *315* (5817), 1393-1396.
12. Szurdoki, F.; Michael, K. L.; Walt, D. R. A duplexed microsphere-based fluorescent immunoassay. *Anal. Biochem.* **2001**, *291* (2), 219-228.
13. Hall, M.; Kazakova, I.; Yao, Y. M. High sensitivity immunoassays using particulate fluorescent labels. *Anal. Biochem.* **1999**, *272* (2), 165-170.
14. Fulton, R. J.; McDade, R. L.; Smith, P. L.; Kienker, L. J.; Kettman, J. R., Jr. Advanced multiplexed analysis with the FlowMetrix system. *Clin. Chem.* **1997**, *43* (9), 1749-1756.
15. De Jager, W.; Rijkers, G. T. Solid-phase and bead-based cytokine immunoassay: a comparison. *Methods* **2006**, *38* (4), 294-303.
16. Ray, C. A.; Bowsher, R. R.; Smith, W. C.; Devanarayan, V.; Willey, M. B.; Brandt, J. T.; Dean, R. A. Development, validation, and implementation of a multiplex immunoassay for the simultaneous determination of five cytokines in human serum. *J. Pharm. Biomed. Anal.* **2005**, *36* (5), 1037-1044.

17. Elshal, M. F.; McCoy, J. P. Multiplex bead array assays: performance evaluation and comparison of sensitivity to ELISA. *Methods* **2006**, *38* (4), 317-323.
18. De Jager, W.; te, V. H.; Prakken, B. J.; Kuis, W.; Rijkers, G. T. Simultaneous detection of 15 human cytokines in a single sample of stimulated peripheral blood mononuclear cells. *Clin. Diagn. Lab Immunol.* **2003**, *10* (1), 133-139.
19. Tarnok, A.; Hamsch, J.; Chen, R.; Varro, R. Cytometric bead array to measure six cytokines in twenty-five microliters of serum. *Clin. Chem.* **2003**, *49* (6 Pt 1), 1000-1002.
20. Kellar, K. L.; Douglass, J. P. Multiplexed microsphere-based flow cytometric immunoassays for human cytokines. *J. Immunol. Methods* **2003**, *279* (1-2), 277-285.
21. Dasso, J.; Lee, J.; Bach, H.; Mage, R. G. A comparison of ELISA and flow microsphere-based assays for quantification of immunoglobulins. *J. Immunol. Methods* **2002**, *263* (1-2), 23-33.
22. Cook, E. B.; Stahl, J. L.; Lowe, L.; Chen, R.; Morgan, E.; Wilson, J.; Varro, R.; Chan, A.; Graziano, F. M.; Barney, N. P. Simultaneous measurement of six cytokines in a single sample of human tears using microparticle-based flow cytometry: allergics vs. non-allergics. *J. Immunol. Methods* **2001**, *254* (1-2), 109-118.
23. Heijmans-Antonissen, C.; Wesseldijk, F.; Munnikes, R. J.; Huygen, F. J.; van der, M. P.; Hop, W. C.; Hooijkaas, H.; Zijlstra, F. J. Multiplex bead array assay for detection of 25 soluble cytokines in blister fluid of patients with complex regional pain syndrome type 1. *Mediators. Inflamm.* **2006**, *2006* (1), 28398.
24. Hurley, J. D.; Engle, L. J.; Davis, J. T.; Welsh, A. M.; Landers, J. E. A simple, bead-based approach for multi-SNP molecular haplotyping. *Nucleic Acids Res.* **2004**, *32* (22), e186.
25. Bibikova, M.; Lin, Z.; Zhou, L.; Chudin, E.; Garcia, E. W.; Wu, B.; Doucet, D.; Thomas, N. J.; Wang, Y.; Vollmer, E.; Goldmann, T.; Seifart, C.; Jiang, W.; Barker, D. L.; Chee, M. S.; Floros, J.; Fan, J. B. High-throughput DNA methylation profiling using universal bead arrays. *Genome Res.* **2006**, *16* (3), 383-393.
26. Yang, L.; Tran, D. K.; Wang, X. BADGE, Beads Array for the Detection of Gene Expression, a high-throughput diagnostic bioassay. *Genome Res.* **2001**, *11* (11), 1888-1898.
27. Braeckmans, K.; De Smedt, S. C.; Roelant, C.; Leblans, M.; Pauwels, R.; Demeester, J. Encoding microcarriers by spatial selective photobleaching. *Nat. Mater.* **2003**, *2* (3), 169-173.
28. Derveaux, S.; Geest, B. G.; Roelant, C.; Braeckmans, K.; Demeester, J.; Smedt, S. C. Multifunctional Layer-by-Layer Coating of Digitally Encoded Microparticles. *Langmuir* **2007**.
29. Decher, G. Fuzzy nanoassemblies: Toward layered polymeric multicomposites. *Science* **1997**, *277* (5330), 1232-1237.
30. Caruso, F.; Caruso, R. A.; Mohwald, H. Nanoengineering of inorganic and hybrid hollow spheres by colloidal templating. *Science* **1998**, *282* (5391), 1111-1114.
31. Sukhorukov, G. B.; Donath, E.; Lichtenfeld, H.; Knippel, E.; Knippel, M.; Budde, A.; Mohwald, H. Layer-by-layer self assembly of polyelectrolytes on colloidal particles. *Colloids and Surfaces A-Physicochemical and Engineering Aspects* **1998**, *137* (1-3), 253-266.
32. De Geest, B. G.; Sanders, N. N.; Sukhorukov, G. B.; Demeester, J.; De Smedt, S. C. Release mechanisms for polyelectrolyte capsules. *Chemical Society Reviews* **2007**, *36* (4), 636-649.

33. Derveaux, S.; Geest, B. G.; Roelant, C.; Braeckmans, K.; Demeester, J.; Smedt, S. C. Multifunctional Layer-by-Layer Coating of Digitally Encoded Microparticles. *Langmuir* **2007**.
34. Staros, J. V.; Wright, R. W.; Swingle, D. M. Enhancement by N-hydroxysulfosuccinimide of water-soluble carbodiimide-mediated coupling reactions. *Anal. Biochem.* **1986**, *156* (1), 220-222.
35. Giavedoni, L. D. Simultaneous detection of multiple cytokines and chemokines from nonhuman primates using luminex technology. *J. Immunol. Methods* **2005**, *301* (1-2), 89-101.
36. Baud, M. In *Methods of Immunological Analysis*, VCH Publishers: New York, 1993; p 671.
37. McHugh, T. M.; Miner, R. C.; Logan, L. H.; Stites, D. P. Simultaneous detection of antibodies to cytomegalovirus and herpes simplex virus by using flow cytometry and a microsphere-based fluorescence immunoassay. *J. Clin. Microbiol.* **1988**, *26* (10), 1957-1961.
38. Diamandis, E. P.; Christopoulos, T. K. The biotin-(strept)avidin system: principles and applications in biotechnology. *Clin. Chem.* **1991**, *37* (5), 625-636.
39. Carson, R. T.; Vignali, D. A. Simultaneous quantitation of 15 cytokines using a multiplexed flow cytometric assay. *J. Immunol. Methods* **1999**, *227* (1-2), 41-52.
40. Koertge, T. E.; Butler, J. E. The relationship between the binding of primary antibody to solid-phase antigen in microtiter plates and its detection by the ELISA. *J. Immunol. Methods* **1985**, *83* (2), 283-299.
41. Li, B.; Rozas, J.; Haynie, D. T. Structural stability of polypeptide nanofilms under extreme conditions. *Biotechnol. Prog.* **2006**, *22* (1), 111-117.
42. Kellar, K. L.; Kalwar, R. R.; Dubois, K. A.; Crouse, D.; Chafin, W. D.; Kane, B. E. Multiplexed fluorescent bead-based immunoassays for quantitation of human cytokines in serum and culture supernatants. *Cytometry* **2001**, *45* (1), 27-36.
43. Brust, S.; Duttman, H.; Feldner, J.; Gurtler, L.; Thorstensson, R.; Simon, F. Shortening of the diagnostic window with a new combined HIV p24 antigen and anti-HIV-1/2/O screening test. *J. Virol. Methods* **2000**, *90* (2), 153-165.
44. Camilla, C.; Mely, L.; Magnan, A.; Casano, B.; Prato, S.; Debono, S.; Montero, F.; Defoort, J. P.; Martin, M.; Fert, V. Flow cytometric microsphere-based immunoassay: analysis of secreted cytokines in whole-blood samples from asthmatics. *Clin. Diagn. Lab Immunol.* **2001**, *8* (4), 776-784.
45. Gordon, R. F.; McDade, R. L. Multiplexed quantification of human IgG, IgA, and IgM with the FlowMetrix system. *Clin. Chem.* **1997**, *43* (9), 1799-1801.
46. Kellar, K. L.; Iannone, M. A. Multiplexed microsphere-based flow cytometric assays. *Exp. Hematol.* **2002**, *30* (11), 1227-1237.
47. Bellisario, R.; Colinas, R. J.; Pass, K. A. Simultaneous measurement of antibodies to three HIV-1 antigens in newborn dried blood-spot specimens using a multiplexed microsphere-based immunoassay. *Early Hum. Dev.* **2001**, *64* (1), 21-25.
48. Khan, S. S.; Smith, M. S.; Reda, D.; Suffredini, A. F.; McCoy, J. P., Jr. Multiplex bead array assays for detection of soluble cytokines: comparisons of sensitivity and quantitative values among kits from multiple manufacturers. *Cytometry B Clin. Cytom.* **2004**, *61* (1), 35-39.
49. Ly, T. D.; Laperche, S.; Brennan, C.; Vallari, A.; Ebel, A.; Hunt, J.; Martin, L.; Daghfal, D.; Schochetman, G.; Devare, S. Evaluation of the sensitivity and specificity of six HIV combined p24 antigen and antibody assays. *J. Virol. Methods* **2004**, *122* (2), 185-194.

50. Kohara, Y.; Noda, H.; Okano, K.; Kambara, H. DNA probes on beads arrayed in a capillary, 'Bead-array', exhibited high hybridization performance. *Nucleic Acids Res.* **2002**, *30* (16), e87.
51. Jacobson, J. W.; Oliver, K. G.; Weiss, C.; Kettman, J. Analysis of individual data from bead-based assays ("bead arrays"). *Cytometry A* **2006**, *69* (5), 384-390.
52. Pang, S.; Smith, J.; Onley, D.; Reeve, J.; Walker, M.; Foy, C. A comparability study of the emerging protein array platforms with established ELISA procedures. *J. Immunol. Methods* **2005**, *302* (1-2), 1-12.
53. Lim, C. T.; Zhang, Y. Bead-based microfluidic immunoassays: The next generation. *Biosens. Bioelectron.* **2006**.
54. Kartalov, E. P.; Zhong, J. F.; Scherer, A.; Quake, S. R.; Taylor, C. R.; Anderson, W. F. High-throughput multi-antigen microfluidic fluorescence immunoassays. *Biotechniques* **2006**, *40* (1), 85-90.
55. Kim, J.; Heo, J.; Crooks, R. M. Hybridization of DNA to Bead-Immobilized Probes Confined within a Microfluidic Channel. *Langmuir* **2006**, *22* (24), 10130-10134.
56. Schulte, T. H.; Bardell, R. L.; Weigl, B. H. Microfluidic technologies in clinical diagnostics. *Clin. Chim. Acta* **2002**, *321* (1-2), 1-10.

C H A P T E R Four

FASTER AND MORE SENSITIVE BEAD BASED MULTIPLEXING BY TYRAMIDE SIGNAL AMPLIFICATION

Parts of this chapter are submitted:

Derveaux S.,¹ Fayazpour, F.,¹ Adibkia, K.,² Demeester, J.,¹ De Smedt, S.C.¹

¹ Ghent Research Group on Nanomedicines, Laboratory of General Biochemistry and Physical Pharmacy, Ghent University, Harelbekestraat 72, 9000 Ghent, Belgium

² Department of Pharmaceutics, Faculty of Pharmacy, Tabriz University of Medical Sciences, Tabriz,Iran

ABSTRACT

This chapter introduces the use of the Tyramide Signal Amplification (TSA) method in multiplex bead-based immunoassays. Multiple target proteins (cytokines, HIV-1 P24) were analyzed with memobeads and *xMAP*[®] beads. For both types of beads it was found that the TSA method deposits tyramide residues only on the surface of the beads which have bound target proteins, a clear requirement in a multiplex assay. The amount of tyramide deposited on the bead's surface was in concordance with the amount of target protein captured at the surface of the beads, being a requirement for quantitative multiplex-assays with beads. The TSA method significantly amplifies the fluorescence signals on the beads (up to 100 times) resulting in (much) higher signal-to-noise ratios which makes it especially attractive for the rapid analysis of target proteins. It was found that TSA on beads is applicable as well in real (serum) samples - sub-pg detection of P24 was possible - and works perfectly in a multiplex (quadruplex) format.

CHAPTER 4

FASTER AND MORE SENSITIVE BEAD BASED MULTIPLEXING BY TYRAMIDE SIGNAL AMPLIFICATION

INTRODUCTION

Antibody based immunoassays, like radio-immunoassays (RIA), western blots, immunoprecipitation assays, and enzyme-linked immunosorbent assays (ELISAs), are routinely used in clinical laboratories for the diagnosis of diseases. Due to improved specificity (by the use of monoclonal antibodies instead of polyclonal antibodies) ELISA has become the standard method for the sensitive quantification of various soluble analytes ¹. The detection limit for ELISA assays usually lies between 0.01 and 50 ng/ml of antigen, depending upon the affinity of the (capture) antibody for the antigen ². Because of (a) long incubation times and (b) (sometimes) too low sensitivity, various alternative strategies have been developed to improve microplate and membrane based immunoassays. One strategy aimed to amplify the detection signal ^{3,4}. As an example, in the 'catalyzed reporter deposition technology' (CARD), as developed more than fifteen years ago by Bobrow *et al* ^{5,6}, the biotinylated detection antibodies are labeled with the streptavidin-horseradish peroxidase (HRP) conjugate (Figure 1A). HRP oxidizes biotinylated tyramide residues in the presence of hydrogen peroxide resulting in radical species. The activated tyramide residues are then deposited on the solid phase by reaction with electron rich moieties of protein molecules (tyrosine, tryptophan,...) present in the vicinity of the streptavidin-HRP conjugate at the surface of the solid phase. The deposited biotins are subsequently reacted with streptavidin-labeled HRP, thereby resulting in the deposition of additional HRP. The net effect is that a single HRP molecule becomes surrounded by many HRP molecules.

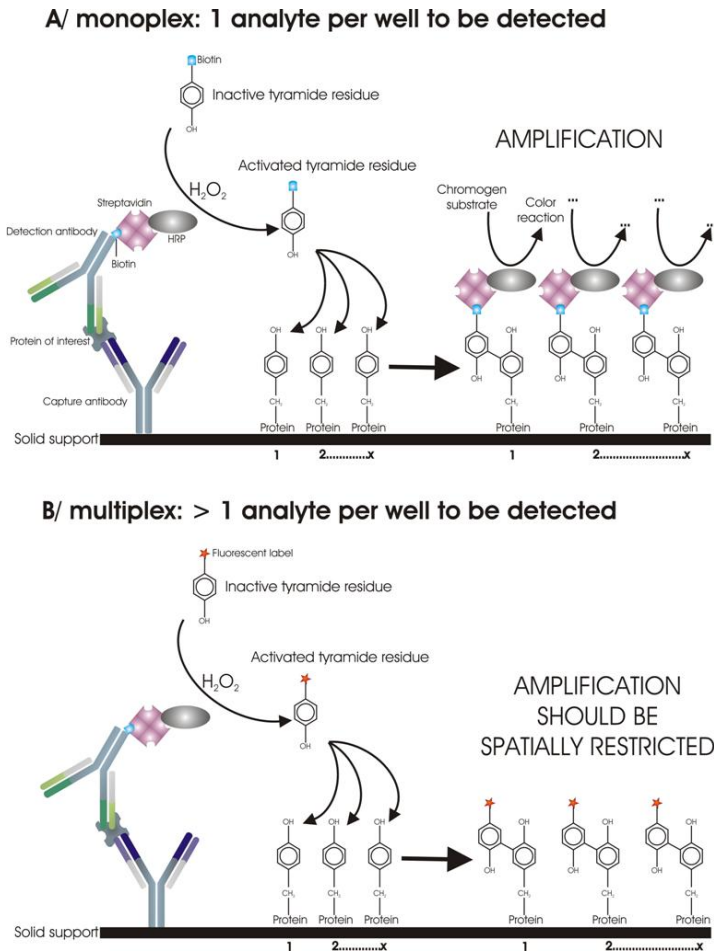


Figure 1: Schematic overview of Tyramide Signal Amplification (TSA) on a flat surface. A) In a monoplex assay the protein of interest (antigen) is detected by the appearance of a color in the well which contains the sample to be analyzed. B) When TSA is applied in a multiplex assay the activated tyramide residues have to be bind specifically to the surface of the microarray or microcarrier where the analyte is caught.

This technique, which is also called ‘tyramide signal amplification’ (TSA), improved the detection limit of membrane immunoassays 25-fold. Meanwhile TSA has been reported by many other authors to be a valuable tool for blotting methods, immunohistochemical staining, gene expression microarray labeling and in situ hybridization techniques (FISH)⁷⁻⁹. The CARD method has been optimized by Bhattacharya *et al.*, resulting in a detection sensitivity of as few as 800 IgG molecules that were blotted on a membrane. The authors introduced to this end high electron rich groups in the proteins that were used as blocking agents.¹⁰ The same group could measure down to 0.1 pg aflatoxin B₁ per well in a total incubation time of 16 minutes by using this super-CARD approach¹¹ and recently they up-graded their approach resulting in a rapid (12 minutes) detection

with much lower reagent consumption and the same sensitivity¹². The group of Schüpbach recently demonstrated the ultrasensitivity of a CARD based ELISA method for the quantification of HIV-1 P24 and stated that this boosted ELISA, the costs of which are expected to amount to 10-20% of those of HIV-1 RNA tests, could be used to improve treatment monitoring in low-resource settings^{13,14}.

As more and more protein disease markers are discovered there is a growing need to analyze more types of (diagnostic) proteins. ELISAs, however, are not convenient to answer this high-throughput need because (a) each protein marker has to be analyzed individually, (b) there is a high consumption of reagents and biological samples and (c) it is a labor-intensive and time-consuming technique. To this end, fast, inexpensive, accurate immunoassays with increased sensitivity, using smaller sample volumes, are under development. Over the last decade, “multiplex” immunoassays have been developed¹⁵. While a “monoplex” immunoassay aims to measure the binding of one analyte, present in the biological sample, to its receptor, a multiplex immunoassay aims to measure *simultaneously* the binding of several analytes in a biological sample to their respective receptors. This multiplex approach allows faster analysis of a high number of protein markers while both the sample and reagent consumption are considerably reduced.

Multiplex immunoassay-technologies are divided into “flat surface arrays” and “suspension arrays”, respectively. To the first category belong the protein microarrays, which use the x,y-coordinates of the spots of capture probes (capture antibodies) on a glass plate to identify which analytes (antigens) are present in a sample¹⁶⁻²⁰. The use of protein microarrays has been limited by the high cost of the microarray consumables and the instruments. Suspension arrays use *encoded* micron sized particles for multiplexing; the code allows knowing which capture antibody is bound to the surface of the microcarriers²¹⁻²³. Antigens present in the biological sample will bind to their corresponding microcarriers which are added to the sample; finally the antigens become fluorescently labeled by means of fluorescent detection antibodies. Decoding of the ‘positive’ microcarriers (i.e. those microcarriers which show fluorescently labeled antigens at their surface) subsequently allows knowing which antigens are present in the sample. The microcarrier-based platforms are gaining popularity²⁴⁻²⁹. Current applications of microcarrier-based assays include the detection of immunoglobulins³⁰ and cytokines^{31,32}, the analysis of single nucleotide polymorphisms³³, DNA methylation profiling³⁴ and gene expression³⁵. Compared to flat microarrays, suspension arrays may have a number of advantages like for instance a more reproducible attachment of the capture probes, a higher flexibility in both surface chemistry and composition of the test panel, and improved (‘near-solution’) kinetics^{23,36,37}.

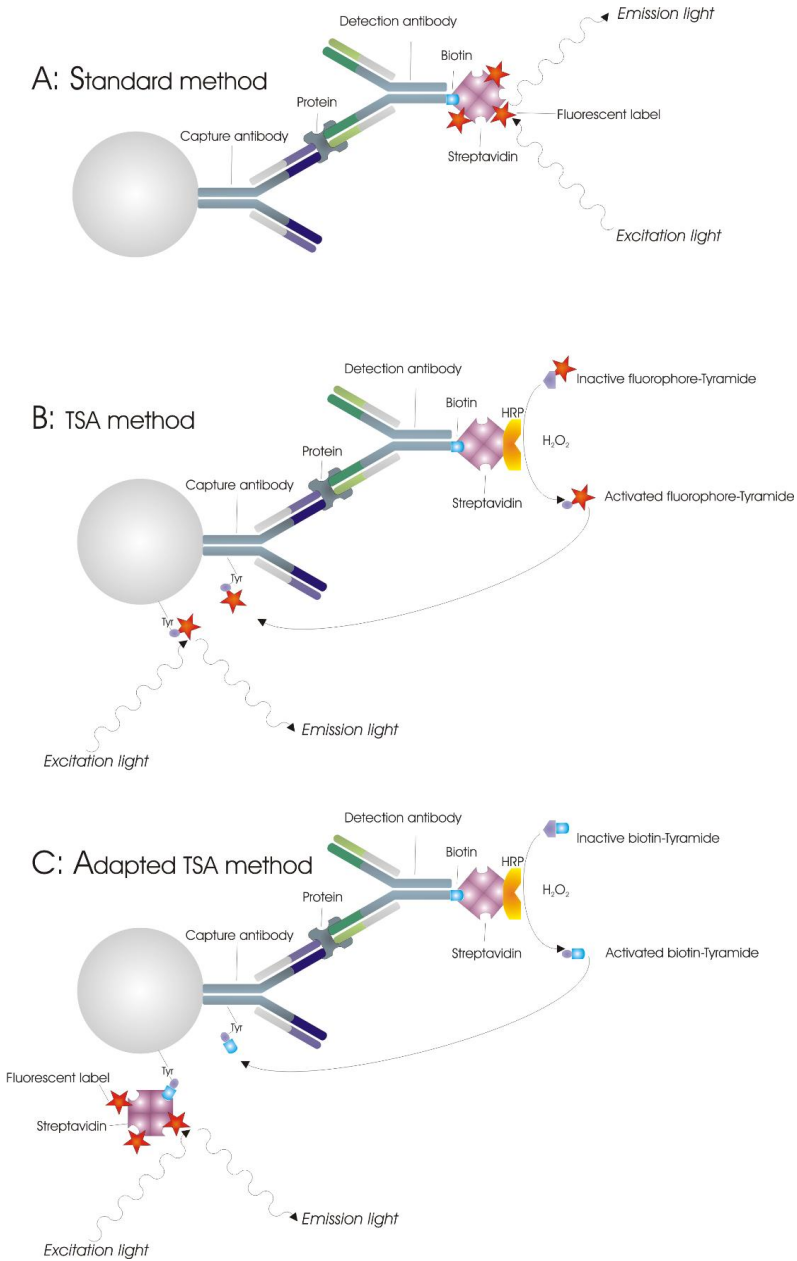


Figure 2: Schematic overview of the detection of antigens (proteins) with microcarriers coated with capture antibodies. A) Detection by the 'standard method' making use of fluorophore conjugated streptavidin which binds to the biotinylated detection antibodies. B) Detection by TSA method: Horse Radish Peroxidase (HRP) conjugated streptavidin binds to the biotinylated detection antibodies. Subsequently fluorophore conjugated tyramide (induced by the HRP to an activated state) binds to electron rich moieties at the surface of the microcarrier. C) Detection by the adapter TSA method: HRP conjugated streptavidin binds to the biotinylated detection antibodies. Subsequently biotin conjugated tyramide (induced by the HRP to an activated state) binds to electron rich moieties at the surface of the microcarrier. Finally, fluorophore conjugated streptavidin binds to the biotin molecules deposited at the surface of the microcarrier.

In 1994 already Ekins stated that an "*ultrasensitive*" *simultaneous* detection of multiple analytes in one sample would be a methodological challenge³⁸. Meanwhile multiplex immunoassays have become a valuable technique being as sensitive, accurate and reproducible as conventional monoplex ELISA, but requiring much lower reagent and sample volumes while reaching, in some case, broader dynamic ranges^{30,39}. However, one challenge remains the application of "ultrasensitive" detection methods in multiplexed assays.

Analytes captured on the microcarriers are usually detected by fluorophore conjugated (detection) antibodies or biotinylated (detection) antibodies (which, on their turn, react with strongly fluorescent streptavidin) (Figure 2A)^{4,40-42}. As is the case for monoplex ELISA, sensitivity could be improved by amplifying the signal that is generated at the surface of the solid support upon binding of an analyte^{43,44}. Little research has been done, however, on signal amplification in multiplex assays. Indeed, in contrast to monoplex ELISA's in which all the reactions occur in separated wells, one major challenge for signal amplification in multiplex assays is that the (amplified) detection signal should be spatially restricted to the surface (on an array or a microcarrier) where the analyte is captured.

So far, only very few reports mention the use of CARD technology in a multiplexed immunoassay (Figure 1B). Bacarese-Hamilton *et al.* demonstrated higher signals in the detection of allergen-specific IgE by a flat protein microarray when the bound allergens were detected by the CARD method instead of by conventional fluorophore-conjugated detection antibodies or by biotinylated detection antibodies in combination with fluorophore -conjugated streptavidin⁴⁵. In another study Varnum *et al.* could detect antigens with a sensitivity as low as sub pg/ml by immunoassays on a flat microarray and signal amplification by tyramide deposition⁴⁶. Applying CARD technology on multiplex bead-based immunoassays, which to our knowledge has been only done by Szurdoki *et al.*⁴¹ for a duplex competitive immunoassay, is even more challenging considering the mobility of the microcarriers and thus the higher risk for false positive results; indeed, on an (immobile) flat microarray, false positive results may arise through the diffusion of activated tyramide molecules to other zones on the array, however, in case of a microcarrier platform (not reacted) microcarriers can move to activated tyramide molecules as well.

Previously our group introduced 'memobeads' which are polystyrene beads, surrounded by a polyelectrolyte coating, encoded by means of spatial selective photobleaching^{47,48}. Very recently we proved that memobeads allow to detect clinically relevant concentrations of several proteins in complex matrices like plasma^{40,47,49}. In the current paper we explore whether the sensitivity for multiplex protein detection by memobeads can be further improved by CARD technology. To evaluate whether CARD technology can be applied as well to other types of encoded microcarriers we also tested the commercially available xMAP beads and compared the CARD method with the standard labeling method used on this platform, which has never been described so far.

MATERIALS & METHODS

Materials.

Non-magnetic fluorescent carboxylated microspheres (CFP-40052-100, $\phi = 39 \mu\text{m}$) Fluorescent carboxylated microspheres (CFP-40052-100, $\phi = 39 \mu\text{m}$) were purchased from Spherotech (Libertyville, Illinois, USA). Poly (allylamine hydrochloride) [PAH; 28,322-3], sodium poly (styrene sulfonate) [PSS, MW $\sim 70\ 000$; 24,305-1] and poly (acrylic acid) [PAA, MW $\sim 45\ 000$; 18,128-5] were obtained from Sigma Aldrich (Steinheim, Germany). The polymers were dissolved into 0.5 M sodium chloride (31434, Sigma Aldrich, Seelze, Germany). Bovine serum albumine (BSA, A-7906) and 2-[N-Morpholino]ethanesulfonic acid (MES, M-8259) were purchased from Sigma (Bornem, Belgium), PBS Dulbecco's (14190-094) from Gibco and Tween-20 (655204) from Calbiochem. EDC (1-ethyl-3-(3-dimethyl aminopropyl) carbodiimide HCl, 22980) was obtained from Perbio Science (Erembodegem, Belgium), desiccated and stored at -20°C . Sulfo-NHS (N-hydroxysulfosuccinimide sodium salt, 106627-54-7) was purchased from Sigma Aldrich (Steinheim, Germany), desiccated and stored at 4°C . Purified mouse anti-human TNF- α (551220) and anti-human IL-2 (555051), recombinant human TNF- α (551838) and human IL-2 (554603), biotinylated mouse anti-human TNF- α (554511) and anti-human IL-2 (555040) were purchased from BD Pharmingen. Tyramide Signal Amplification Kits (T20936 and T20931) were purchased from Invitrogen (Eugene, Oregon, USA). P24, purified anti-P24 antibody, biotinylated anti-P24 antibody and blanc plasma samples were a kind gift from BioMaricTM (Ghent, Belgium). AlexaFluor[®] 647 labeled streptavidin (S21374) was purchased from Molecular Probes (Inc. InvitrogenTM, Eugene, Oregon, USA). Fluorokine MAP Human Base Kit A (LUH000), Human IL-1 β /IL-1F2 Kit (LUH201), Human IL-4 Kit (LUH204), Human IL-5 Kit (LUH205), and Human CXCL8/IL-8 Kit (LUH208) were purchased from R&D Systems (Minneapolis, USA).

Layer-by-Layer coating of the microspheres⁴⁷

A schematic overview, as well as the procedure of the Layer-by-Layer modification is described in Chapter 2.

Encoding of the microspheres

The encoding process is described in Chapter 2.

Coupling of capture antibodies to the LbL coated microspheres

The coupling procedure has been described in Chapter 3.

Capturing TNF- α and P24 by LbL coated microspheres and detection by a “standard procedure”

As described below in detail, antigens were captured on the LbL coated microspheres carrying the capture antibodies during 1 hour incubation (unless otherwise noted). The antigens were detected by a “standard procedure” i.e. by means of biotinylated detection antibodies and AlexaFluor 647 (AF647) conjugated streptavidin, as illustrated in Figure 2A. The concentrations of biotinylated detection antibody and AF647 conjugated streptavidin used for detecting the bound antigens were optimized (data not shown): lower concentrations decreased the fluorescence signal, while higher concentrations did not further increase the signal. Note that incubations with AF647 conjugated streptavidin were done in the dark. All of the following steps were performed at room temperature.

For the detection of TNF- α and P24 by the standard procedure, approximately 100 microspheres, coated with capture antibody, were incubated for 1 hour in 100 μ l of standard dilutions spiked with TNF- α and P24, respectively (Eppendorf Thermomixer, 250 rpm, 25°C). The dilutions were made in assay buffer or serum, respectively. After 1 hour incubation the microspheres were washed with assay buffer, and subsequently incubated for 1 hour in 100 μ l of a biotinylated detection antibody solution (4 μ g/ml in assay buffer). Finally, the microspheres were washed three times with assay buffer. Labeling of the bound biotinylated detection antibodies was done by incubating the microspheres for 1 hour in the dark in 100 μ l AF647 conjugated streptavidin solution (8 μ g/ml). Next, the microspheres were washed three times with 100 μ l PBS before analysis.

Capturing TNF- α and P24 by LbL coated microspheres and detection by the TSA procedure

As described below in detail, antigens were captured by LbL coated microspheres carrying capture antibodies. The bound antigens were then detected by means of biotinylated detection antibodies and the TSA amplification system, as illustrated in Figure 2B. For detailed information regarding the TSA kit components (concentrations, buffers...) we refer to the website of the provider (<http://www.invitrogen.com>). Note that incubations with fluorescent analytes were always performed protected from light in an Eppendorf Thermomixer at 250 rpm and at room temperature.

For the detection of TNF- α and P24 in a *monoplex* assay, approximately 100 antibody coated microspheres were used. For the detection of TNF- α in the *duplex* assay, approximately 200 antibody coated microspheres were used; half of them were coated with capture antibodies against human

TNF- α , while the other ones carried capture antibodies against human IL-2. The microcarriers were incubated with standards and biotinylated antibody mixture under the same conditions as used in the standard procedure, as described above. The microspheres were then washed three times with assay buffer, and subsequently incubated for 1 hour with 100 μ l of streptavidin-HRP (2.5 μ g/ml in assay buffer), protected from light. The washing procedure was repeated and the microspheres were finally incubated with 10 μ l of AlexaFluor Tyramide (one-step TSA method) or 10 μ l of the Biotin Tyramide (two-step TSA method), both at a 1/10 dilution of the stock solution (in amplification buffer/0.0015% H₂O₂), unless otherwise noted. In case of the one-step TSA method, after washing, the microcarriers were resuspended in 100 μ l PBS/Tween20 before analysis. In case of the two-step TSA method, the microcarriers were washed for another three times, before they were resuspended in 100 μ l AF647 conjugated streptavidin solution (8 μ g/ml). After 15 minutes of incubation, the washing procedure was repeated and the microcarriers were resuspended in 100 μ l PBS/Tween20.

Calibration curves.

Lyophilized antigens were reconstituted in assay buffer or serum; 6 to 10 serial dilutions were made. The calibration curves were calculated by the GraphPad Prism software. The 4-parameter logistic equation (4-PL) was used to obtain the most accurate determination of the protein concentration:

$$y = a + \frac{b - a}{1 + 10^{[(d-x)*c]}}$$

where x is the logarithmic of the protein concentration, y is the response (i.e. the red fluorescence at the surface of the microcarriers), a is the estimated response at zero protein concentration (i.e. the “zero calibrator”), b is the estimated response at infinite protein concentration, c is the slope of the tangent midpoint and d is the logarithmic of the midrange protein concentration.

The lower limit of detection (LOD) of a protein was defined as the concentration corresponding to the median fluorescence intensity (MFI) plus 3 times the standard deviation of the “zero calibrator”. The inter-bead variability was defined as the coefficient of variation (CV; in %) on the average value of measurements on approximately 20 beads.

(Confocal) fluorescent microscopy imaging of the microspheres.

The memobeads were analyzed using a Bio-Rad MRC 1024 confocal laser scanning system (Bio-Rad, Hemel Hempstead, UK) equipped with an inverted microscope (Eclipse TE300D, Nikon, Japan). Images were captured with a Nikon Plan Apochromat 60x water immersion objective lens (NA of 1.2, collar rim correction) and with a Nikon Plan Apochromat 10x objective lens (NA of 0.45) using the 488 nm laser line from the argon-ion laser and the 647 nm laser line from the Ar/Kr laser. For the orientation of the memobeads, a weak external magnetic field was applied with the same orientation as the magnetic field applied during the encoding process (relative to the direction of the laser light). In the presence of this weak magnetic field, the 'remanent' nanoparticles tend to align with the magnetic field, so they will turn the microspheres (at which surface they are fixed) into a position that the code can be read (the code is present in a plane perpendicular to the direction of the laser).

Capturing IL-1 β , IL-4, IL-5 and IL-8 by Luminex microcarriers and detection by the standard procedure (Figure 2A)

The assays below were carried out in a 96-well plate, protected from light at all times. Standards of IL-1 β , IL-4, IL-5 and IL-8 were prepared in calibrator diluent RD6-40. The four Luminex microcarrier stock suspensions were mixed by dilution 1/100 in diluents RD6-40 and 50 μ l of the Luminex microcarrier mixture was incubated with 50 μ l of each standard for 2 hours on a microplate shaker. Meanwhile, biotinylated detection antibodies were diluted 1/100 in diluent RD6-40. After washing the plate three times with 100 μ l wash buffer using a vacuum manifold, 50 μ l of the diluted biotinylated antibody mixture was added to the wells and the plate was incubated for 1 hour. Meanwhile, streptavidin-PE was diluted 1/100 in wash buffer. The plate was washed another three times, and the Luminex microcarriers were incubated for 30 minutes with 50 μ l of the diluted streptavidin-PE. The microcarriers were then washed three times and resuspended in 100 μ l wash buffer. The Luminex microcarriers were subsequently analyzed following the instructions of the provider.

Capturing IL-1 β , IL-4, IL-5 and IL-8 by xMAP[®] microcarriers and detection by the TSA procedure (Figure 2C)

The xMAP[®] microcarriers were incubated with standards and biotinylated antibody mixture as described above. After washing three times with 100 μ l wash buffer, the microcarriers were incubated with 50 μ l streptavidin-HRP (2 ng/ μ l) for 30 minutes. The xMAP[®] microcarriers were then washed three times with 100 μ l PBS-Tween20 and subsequently incubated with 50 μ l of biotin-

tyramide (1/25 in amplification buffer/0.0015% H₂O₂) for 30 minutes. After washing with 100 µl wash buffer, the *xMAP*[®] microcarriers were incubated for another 30 minutes with 50 µl of streptavidin-PE (1/100 diluted in wash buffer, same concentration as described above). The microcarriers were then washed three times with wash buffer and finally resuspended in 100 µl wash buffer. The Luminex microcarriers were subsequently analyzed following the instructions of the provider.

RESULTS AND DISCUSSION

Applying TSA to multiplex assays.

First we investigated whether the tyramide signal amplification only occurs at the surface of 'positive' memobeads being beads to which antigens became bound; Indeed, in multiplex assays one has to avoid that TSA would also occur at the surface of the 'negative' (i.e. 'cross-reaction'). Equal amounts of two differently encoded memobeads, carrying respectively (capture) antibodies against TNF- α and IL-2, were mixed. Two hundred memobeads of this mixture were subjected to respectively 100 pg/ml TNF- α in assay buffer, 100 pg/ml IL-2 in assay buffer and a control sample (being assay buffer without cytokines). They were subsequently incubated with biotinylated detection antibodies, HRP conjugated streptavidin and the AF647 conjugated tyramide substrate solution (following the method described in Figure 2B).

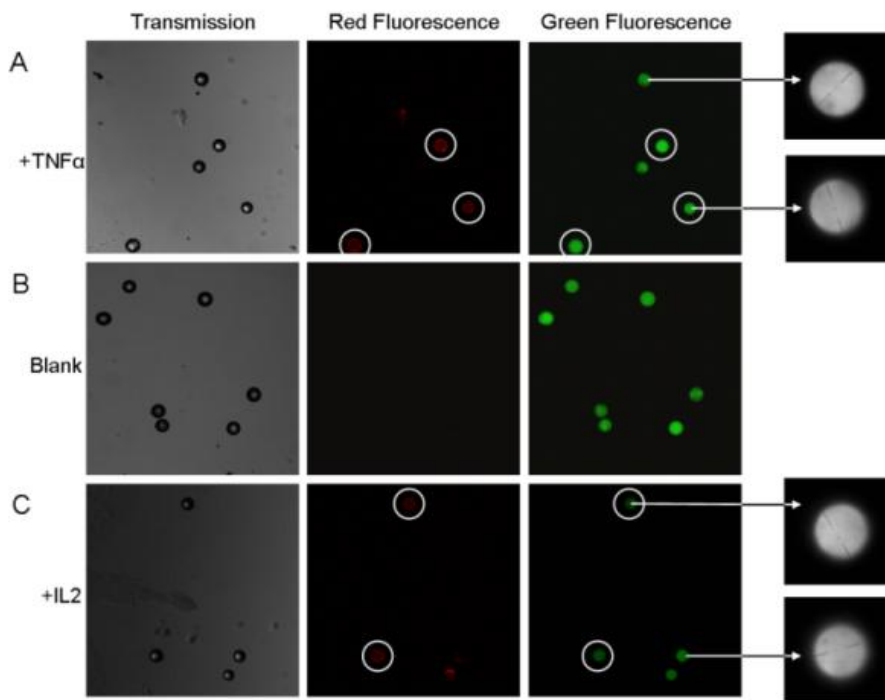


Figure 3: Two types of differently (dot) encoded memobeads were coupled with respectively antibodies against TNF- α and antibodies against IL-2, mixed and subsequently incubated in respectively a 100 pg/ml TNF- α solution (A), a control sample (i.e. buffer without cytokines) (B) and a 100 pg/ml IL-2 solution (C). First column: transmission image showing (all) the memobeads. Second column: red fluorescence image showing (only) the positive memobeads. Third column: green fluorescence image of (all) the memobeads (as explained in Figure 3A memobeads are polystyrene beads stained with a green fluorophore). The positive memobeads, as detected by the image analysis software, are stressed with white circles. The arrows show confocal images of the middle plane of some beads, which makes the code visible.

Row A in Figure 3 clearly shows that, as expected, half of the (200) memobeads become red fluorescent (i.e. those ones carrying TNF- α antibodies) upon incubating the memobeads in the TNF- α solution; the memobeads carrying IL-2 antibodies do not exhibit any signal (and therefore any antigen) at all at their surface. Applying the (200) memobeads to an IL-2 solution gave the opposite result (row C in Figure 3). None of the memobeads showed red fluorescence if they were incubated in the control sample (row B in Figure 3). When the images were analysed by the software program, only those memobeads for which a corresponding antigen was present in the solution revealed red fluorescence (and became identified as positive memobeads). The TSA method thus accurately works in this duplex assay, in agreement with the previous observation by Szudoki *et al.* with other microcarriers⁴¹. It shows that the activated AF647-tyramide molecules only interact with the surface of those microcarriers at which the HRP (and thus the antigen) is present; activated AF647-tyramide

molecules do not seem to diffuse into the solution and do not seem to bind to the surface of surrounding (negative) microcarriers.

Characterizing the optimal TSA conditions

Part 1: Optimal volume of the tyramide solution

About one hundred memobeads were incubated for one hour in respectively a 50 and 500 pg/ml TNF- α solution and subsequently labeled using equal amounts of Tyramide. However, in one experiment 25 μ l of a 1/100 diluted tyramide stock solution was added (light grey bars in Figure 4A) while in another experiment 50 μ l of a 1/200 diluted tyramide stock solution was used (dark grey bars in Figure 4A). Figure 4A shows higher signals when using the more concentrated tyramide solution, both in the 50 as well as in the 500 pg/ml TNF- α solution. It suggests that the diffusion of tyramide molecules to the surface of the microcarriers is a limiting factor. In later experiments the volume of the diluted tyramide stock solution was kept at 10 μ l (as a lower volume did not significantly further increase the signal on the memobeads; data not shown)

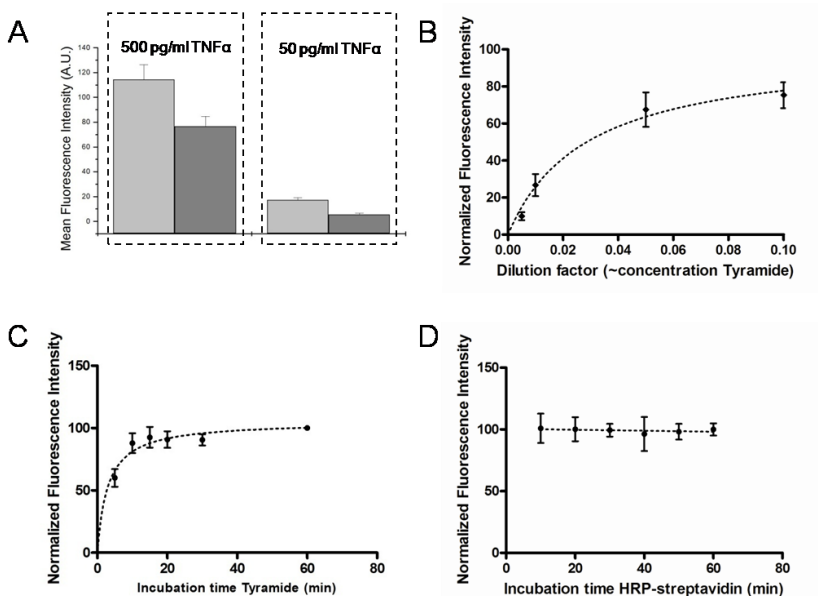


Figure 4: Characterizing the optimal TSA conditions; the y-axis shows the mean red fluorescence signal of the memobeads. (A) About 100 memobeads were subjected for 1 hr to a 500 pg/ml (left part) and 50 pg/ml (right part) TNF- α spiked buffer solutions and then detected with either a 25 μ l 1/100 diluted tyramide stock solution (light grey bars) or a 50 μ l 1/200 diluted

tyramide stock solution (dark grey bars). (B) About 100 memobeads were subjected for 1 hr to a 63 pg/ml TNF- α spiked buffer solution and detected with 10 μ l of a diluted tyramide stock solution. The data were normalized to the maximal fluorescent signal, as it was obtained from the hyperbolic fitting procedure. (C) About 100 memobeads were subjected for 1 hr to a 63 pg/ml TNF- α spiked buffer solution. Subsequently they were incubated with 10 μ l of a 1/10 diluted tyramide stock solution; the incubation time varied between 5 and 60 min. The data were normalized to the maximal fluorescent signal. (D) About 100 memobeads were subjected for 1 hr to a 63 pg/ml TNF- α spiked buffer solution and then labeled with 10 μ l of a 1/10 diluted tyramide stock solution; the incubation time with the HRP conjugated streptavidin ranged from 10 to 60 min. The data were normalized to the maximal fluorescent signal.

Part 2: Optimal concentration of the tyramide concentration

In a next step we determined which tyramide concentration is the most optimal. About one hundred memobeads were incubated in a 63 pg/ml TNF- α solution and detected using 10 μ l of tyramide solution with varying concentration. Figure 4B shows an increasing fluorescence signal on the beads with increasing tyramide concentration; a hyperbolic fitting has been applied to the data, showing that 75% of the maximum signal is obtained with a 1/10 dilution of the tyramide stock solution which was used in further experiments.

Part 3: Optimal time for incubating the memobeads and the tyramide solution

About one hundred memobeads were incubated in a 63 pg/ml TNF- α solution and detected by the use of 10 μ l of a 1/10 diluted tyramide stock solution which was in contact with the memobeads for different times. Figure 4C clearly shows that an incubation time of 10 minutes is sufficient to allow an optimal signal.

Part 4: Optimal time for incubating the memobeads with HRP-streptavidin

The incubation of the memobeads with HRP-streptavidin in the experiments in Figure 4 A-C above was carried out after washing away not bound TNF- α and detection antibodies and took 1 hour. As the total assay time will strongly depend on the incubation step with HRP-streptavidin, we wondered how long this step should be to obtain an optimal signal on the beads. To this end, about 100 memobeads were incubated in a 63 pg/ml TNF- α solution and detected using 10 μ l of a 1/10 diluted tyramide stock solution after being incubated with HRP-streptavidin for 10 to 60 minutes. Figure 4D shows that a maximal fluorescence signal is already achieved when only incubated for 10 minutes. Based on the results in Figure 4 A-D it can be concluded that incubation for 10 minutes with HRP-streptavidin, followed by an incubation for 10 minutes with 10 μ l of a 1/10 diluted tyramide stock solution is most time-efficient to get optimal signal on memobeads. This procedure was therefore used in further experiments in this paper.

Sensitivity of memobeads/TSA for detecting TNF- α in buffer

Figure 5 shows the mean red fluorescence signal of memobeads carrying TNF- α antibodies after being dispersed in TNF- α solutions for different times. A first observation is that TSA on the beads allows quantitative measurements. Clearly, the longer the incubation in the TNF- α solutions, the higher the signal which is explained by the fact that the TNF- α molecules have longer times to diffuse (and bind) to the memobead's surfaces. Non-linear four parameter logistic equations were fitted to the data points and EC50 values ranged from 14.4 to 289.1 pg/ml for incubation times from 10 to 720 minutes. The memobead/TSA assay seems very sensitive: the minimal detectable concentration that was distinguishable from the background signal was 4 pg/ml for 720 minutes of incubation, 8 pg/ml for 180 and 60 minutes incubation, and 32.5 pg/ml for 30 and 10 minutes of incubation. We were not able to measure a signal at the surface of unreacted control microcarriers (background signal) for each of the curves; they were sometimes below the detection limit of the instrument. Because this background signal is needed to calculate the LOD (as explained in the methods section), it was impossible to define the LOD for those curves. However, in case of the 180 and 720 minutes of incubation, the LOD equaled 5.6 and 2.5 pg/ml, respectively.

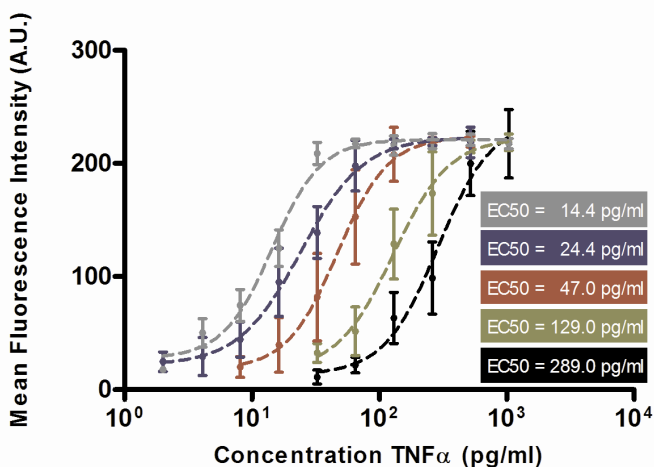


Figure 5: Quantitative analysis of TNF- α spiked in buffer. Red surface fluorescence of the memobeads as a function of the TNF- α concentration and the incubation time (\bullet = 720, \bullet = 180, \bullet = 60, \bullet = 30, and \bullet = 10 minutes) (A.U. means arbitrary units). Each data point is the average value of the red (surface) fluorescence of about 20 memobeads (inter-bead CV's varied between 12% and 61%).

Figure 6 compares the sensitivity and detection range of the TNF- α memobead assay using respectively the standard detection method (Figure 2A) and the TSA detection method (Figure 2B). In

each analysis 100 memobeads were used. The red fluorescence signal on the memobeads becomes much more intense when detection was performed by tyramide instead of by the standard detection method. This is true for both incubation times (Figure 6A: 180 minutes and Figure 6B: 720 minutes). Four-parameter logistic equations were fitted to the data points of both graphs. In case of 180 minutes of incubation the EC50 reaches 23.9 pg/ml and 931.2 pg/ml for respectively the TSA and the standard detection method, while it equals 14.2 and 691.6 pg/ml for 720 minutes of incubation.

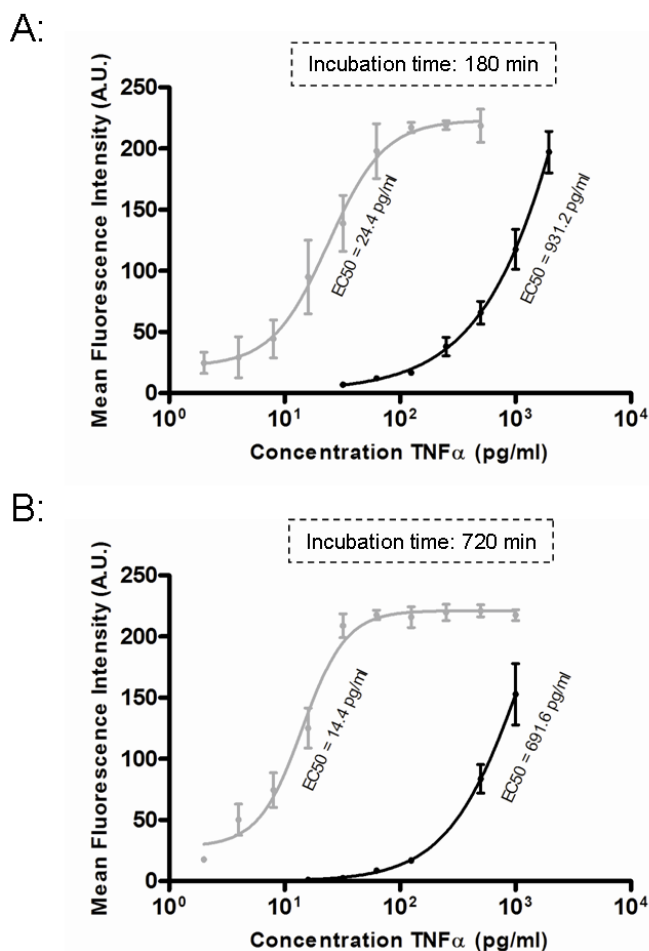


Figure 6: Quantitative analysis of TNF- α spiked in buffer by memobeads. The memobeads were incubated with the TNF- α for respectively 180 minutes (A) and 720 minutes (B). Red surface fluorescence of the memobeads as a function of the TNF- α concentration and the detection method: TSA (grey symbols) and standard method with AF647 conjugated streptavidin (black symbols; A.U. means arbitrary units). Each data point is the average value of the red (surface) fluorescence of about 20 memobeads (inter-bead CV's for standard labeling varied between 1% and 36%, while they varied between 11% and 57% for TSA).

In case the memobeads were incubated with the antigen for respectively 180 and 720 minutes and detection was done by the standard procedure, the minimal detectable concentration was respectively, 32.5 pg/ml and 16.3 pg/ml (the LOD could not be measured because of the reasons explained above). The LOD equaled respectively 5.6 pg/ml and 2.5 pg/ml when the TSA method was applied, which means at least a 5x gain in sensitivity.

Interestingly, the minimal detectable TNF- α concentration when memobeads were incubated with TNF- α for only 10 minutes and detected by TSA (i.e. 32.5 pg/ml; see Figure 5), equaled the minimal detectable concentration when memobeads were incubated with TNF- α for 3 hours but detected by the standard procedure (Figure 6A), which means almost 20x gain in speed. TSA on memobeads is thus of interest not only to obtain a more sensitive assay but also to obtain faster assays. Infectious agents like HIV have to be detected at the earliest stage after infection. This means that low abundant antigens have to be detected which necessitates ultrasensitive tests to give the fastest and most optimal treatment to infected patients. Rapid diagnosis might be also of importance in emergency departments where the remedy is dependent on the diagnosis.

Sensitivity of memobeads/TSA for detecting P24 in serum

To test the applicability of TSA on (antigen positive) microcarriers in more complex samples than buffer, negative sera were spiked with different concentrations of P24, being a major core protein of HIV encoded by the HIV gag gene. It is of interest to detect P24 at a very early stage of the infection in order to start drug therapy; P24 is currently analyzed by ELISA⁵⁰. About 100 memobeads were incubated for different times in the spiked sera and detected by TSA using the optimal conditions described above. Figure 7 clearly shows sensitive measurements on the order of some pg/ml. As also observed in Figure 5 for TNF- α , a longer incubation of the memobeads with P24 resulted in higher signals. Non-linear four parameter logistic equations were fitted to the data points: EC50 values ranged from 2.2 to 64.5 pg/ml for incubation times from 18 to 1 hour.

Simultaneous analysis of TNF- α and P24 in (spiked) sera using memobeads and TSA detection was also possible: red fluorescence only appeared on those microcarriers which carried the appropriate antibody (data not shown).

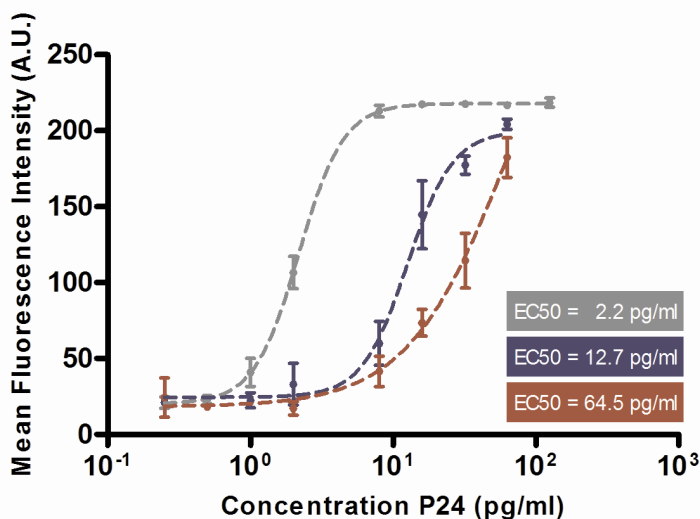


Figure 7: Quantitative analysis of P24 spiked in serum by memobeads. Red surface fluorescence of the memobeads as a function of the P24 concentration and the incubation time (\bullet = 18, \bullet = 3, and \bullet = 1 hour(s)) (A.U. means arbitrary units). Each data point is the average value of the red (surface) fluorescence of about 20 memobeads (inter-bead CV's varied between 3% and 53%).

One-step versus two-steps TSA procedure

So far a one-step TSA procedure was applied: AlexaFluor647 conjugated tyramide molecules were deposited on the surface of the microcarriers (Figure 2B). As illustrated in Figure 2C, we explored whether the TSA detection method could be made even more sensitive by deposition of biotin conjugated tyramide molecules on the surface of the microcarriers (first step) followed by the binding of AlexaFluor647 conjugated streptavidin (second step). To this end, about 100 memobeads were incubated for one hour in TNF- α solutions and subsequently detected by respectively the one-step and two-steps TSA procedure. Figure 8 shows that the extra step indeed amplifies the fluorescence signal which results in a more sensitive test: the EC₅₀ moved from 29.2 pg /ml to 3.5 pg/ml. Besides further amplifying the signal, this 2-steps approach is also attractive when one is interested in the use of other fluorophores; indeed, not all fluorophores are available as tyramide-conjugates, although they are often available as streptavidin-conjugates.

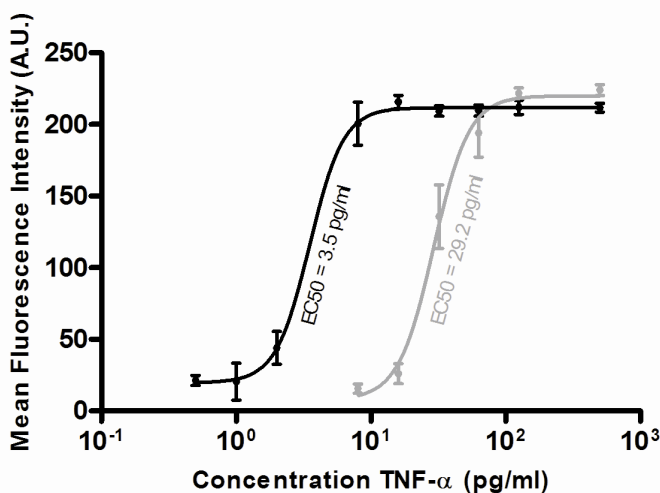


Figure 8: Quantitative analysis of TNF- α spiked in buffer by memobeads by respectively the one-step (following Figure 2B; grey symbols) and two-steps TSA procedure (following Figure 2C; black symbols). Red surface fluorescence of the memobeads as a function of the TNF- α concentration (A.U. means arbitrary units). Each datapoint is the average value of the red (surface) fluorescence of about 20 memobeads (inter-bead CV's varied between 9% and 63%).

TSA on xMAP[®] beads

The previous experiments show proof-of-concept that TSA is a sensitive and specific method to detect antigens on memobeads which are 39 μm sized polystyrene beads coated with layers of polyelectrolytes and chromiumdioxide nanoparticles (see Chapter 2). It would be attractive if TSA would be applicable as well to any other bead-based multi-parameter profiling platform. To this end we investigated whether TSA could be applied on the xMAP[®] platform from Luminex Corporation which makes use of 5.6 μm red dyed (polystyrene) microspheres and which uses biotinylated detection antibodies and phycoerythrin conjugated streptavidin to detect captured antigens (i.e. the standard method in Figure 2A).

First we investigated whether the signal on xMAP[®] beads as achieved by the standard method could be improved by TSA. xMAP[®] beads were incubated in IL-1 β and IL-4 solutions in duplicate. In one experiment the beads were further incubated with phycoerythrin-streptavidin, following the instructions of the provider. In the other experiment they were incubated with streptavidin-HRP, subsequently with biotin-tyramide and finally with streptavidin-phycoerythrin (Figure 2C). Importantly, equal amounts of streptavidin-phycoerythrin were added in both experiments. Figure 9A clearly shows the enormous gain in signal upon using the TSA method: the

EC50 was around 40-50 pg/ml in case of the TSA method, while it was around 900 pg/ml in case of the standard method; unfortunately, the negative control microspheres (that do not carry any antigen) exhibited somewhat higher signals too, so that the gain in sensitivity is not so explicit. Note, however, that the TSA method as used in Figure 9A was not yet optimized for this platform. Nevertheless, as shown in Figure 9B, TSA on *xMAP*[®] beads results in much higher signal-to-noise ratios compared to the standard method, and may thus also be of interest to shorten the total assay time. Because equal amounts of fluorescent molecules were applied in both methods, the gain in signal is due to a higher deposition- and thus a more efficient use- of the fluorescent molecules.

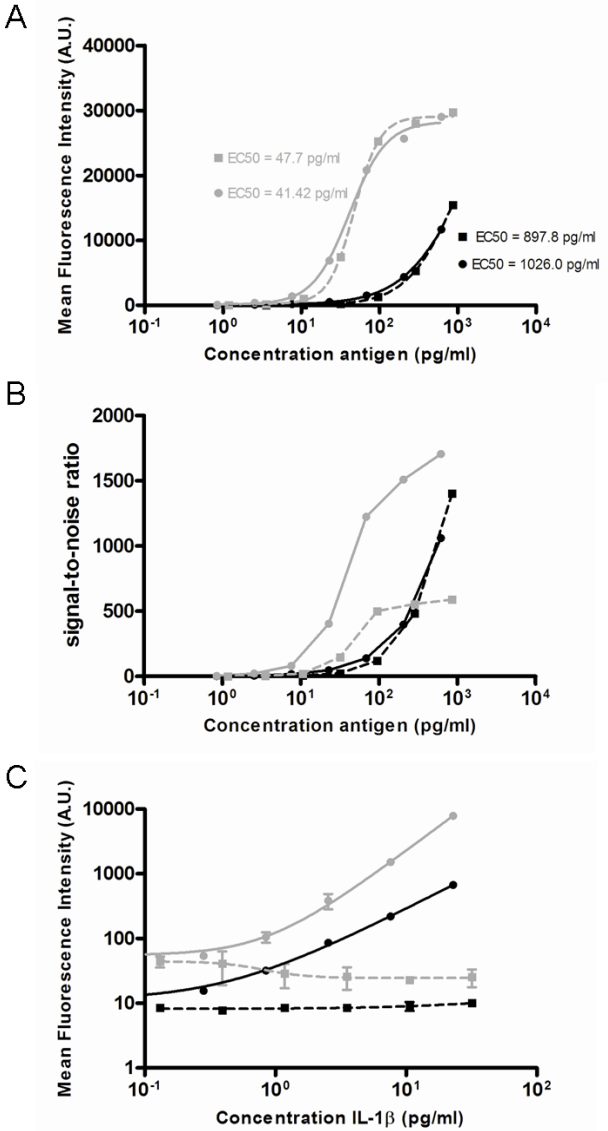


Figure 9: (A) Duplex analysis of IL-1β (●) and IL-4 (■) in buffer with xMAP® beads. Detection by TSA (following Figure 2C; grey data points) and the standard method (i.e. detection following the instructions of the provider; black data points). Each data point is the average value of the red (surface) fluorescence of about 100 microcarriers (inter-bead CV's for standard labeling varied between 14% and 54%, while they were between 5% and 96% for the TSA labeling method). (B) Mean signal-to-noise values. Detection of IL-1β with TSA method (grey solid lines), detection of IL-1β with standard method (black solid lines), detection of IL-4 with TSA method (grey dotted lines), detection of IL-4 with standard method (black dotted lines). (C) Quantitative analysis of IL-1β after adding IL-1β antibody (●) and IL-4 antibody (■) carrying xMAP® beads to the IL-1β solutions. Detection by TSA (grey data points) and the standard method (black data points). The IL-4 antibody coated microcarriers only exhibit a 'background' signal upon increasing the IL-1β concentration.

Figure 9A showed a duplex analysis of a solution containing IL-1 β using *xMAP*[®] beads. We repeated the measurements using *xMAP*[®] beads carrying IL-1 β and IL-4 antibodies but this time only IL-1 β was present in the sample (Figure 9C). Clearly, IL-1 β antibody carrying *xMAP*[®] beads light up, while the signal of the IL-4 ones is not significantly higher than the (non-specific) background signal. It suggests again that the activated tyramide molecules do not diffuse and bind to other microcarriers that are present in the surrounding medium. Figure 9C again shows higher background values when applying the TSA method so that there is almost no gain in sensitivity with the TSA method.

Figure 10 demonstrates the quadruplex analysis of IL-1 β , IL-4, IL-5, and IL-8 (spiked in buffer) with *xMAP*[®] beads. Detection was carried out by the standard method (following the instructions of the provider) and TSA, respectively. Tyramide signal amplification significantly amplifies the fluorescence signal (and signal-to-noise ratio) for each analyte. The LODs as measured by TSA (0.7, 1.5, 0.2, and 0.4 pg/ml for respectively IL-1 β , IL-4, IL-5, and IL-8) were, due to the higher background signals, again comparable with the LODs obtained by the standard labeling (as given by the provider).

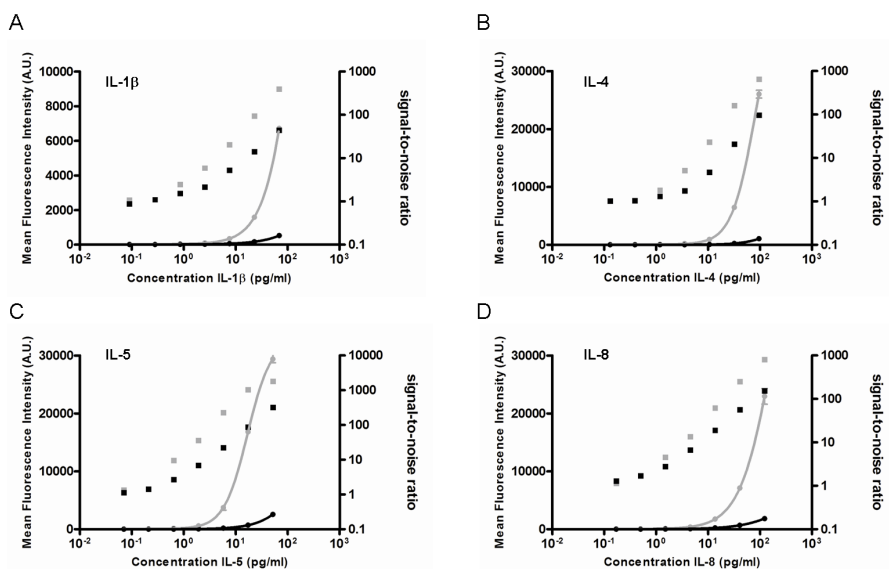


Figure 10: Quadruplex analysis of IL-1 β (A), IL-4 (B), IL-5 (C), and IL-8 (D) in buffer by *xMAP*[®] beads. The fittings indicate the mean red (surface) fluorescence of the beads (left Y-axis) while the single dots are the mean signal-to-noise values (right Y-axis). Grey symbols: detection with biotinylated tyramide and phycoerythrin conjugated streptavidin (following Figure 2C). Black symbols: detection with phycoerythrin conjugated streptavidin (following instructions of the provider). Each data point is the average value of the red (surface) fluorescence of about 100 *xMAP*[®] beads.

Effect of the Layer-by-Layer coating

In chapter 2 we already showed the impact of the LbL modification on the coupling density of biomolecules: a remarkable higher amount could be loaded on the microspheres. Because the surface characteristics of the microspheres would probably also affect the formation of the sandwich construct, and the TSA detection (which uses bound proteins to capture activated tyramide molecules), we wondered which impact the LbL modification had. To this end, not modified microcarriers were compared with LbL modified microcarriers for assaying 5 pg/ml TNF- α in buffer by means of the two-step TSA procedure. It is important to notice that exactly the same carboxylated microcarriers were used with or without LbL modification.

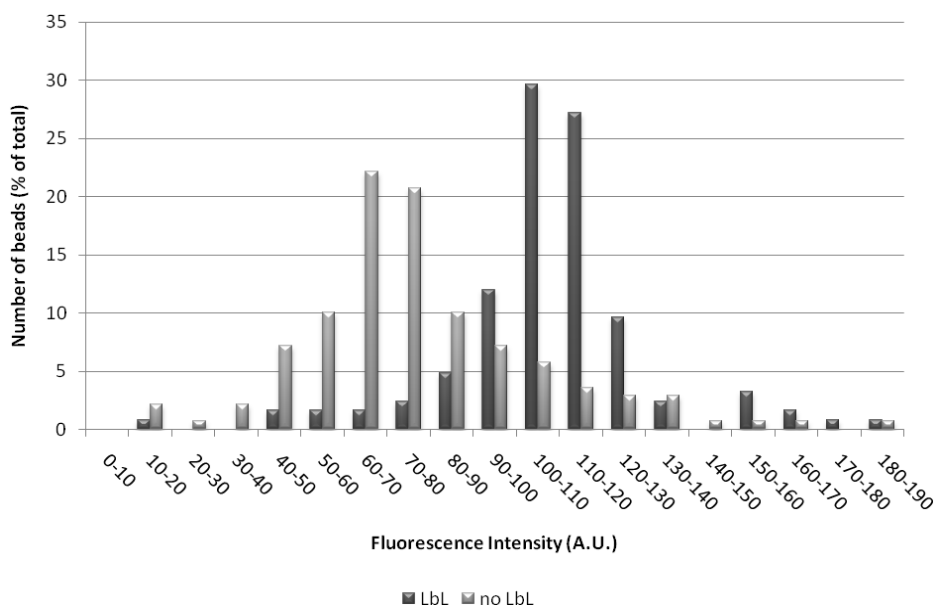


Figure 11: Number of microcarriers (expressed as % of the total amount of microcarriers) as a function of their fluorescence intensity. Two types of microcarriers were analyzed: LbL coated and not modified microcarriers. The microcarriers were incubated with 5 pg/ml TNF- α and labeled by means of the two-step TSA method.

The LbL modified microcarriers yielded higher red fluorescence (MFI: 108.1 ± 24.0 A.U.), upon incubation with the same amount of target molecules and detection reagents, than the unmodified ones (MFI: 77.0 ± 27.9 A.U.), as shown in Figure 11. This is probably due a) a more efficient reaction between antibodies and antigens at the surface of LbL coated microcarriers, or to b) a higher surface area (and thus higher amount of capture antibodies and BSA) of LbL coated

microcarriers so that more tyramide molecules can be caught, or to c) a combination of both. Important to note is that we have seen already in the past higher fluorescent signals on the surface of LbL coated microcarriers than on not modified ones (and little more sensitive results with LbL coated microcarriers than with not modified ones) when detection was done in the conventional way with fluorescent streptavidin, which means that the affinity reaction between the probes/targets were more efficiently on the LbL surface. Figure 11 also shows a more narrow fluorescence distribution in the case of the LbL coated microcarriers, meaning that LbL results in more precise measurements.

Figure 12 shows the coefficient of variation of the red fluorescence, measured at single microcarrier level (note that the red fluorescence is calculated by measuring the mean of several pixels within the ROI, as explained in the previous chapters). Less variation is observed in the case of the LbL coated microcarriers, than in the case of no LbL modified ones (respectively CV %: 38.9 ± 4.7 , and 47.9 ± 10.2), which means that the red fluorescence is more homogeneously distributed at the surface of the former ones.

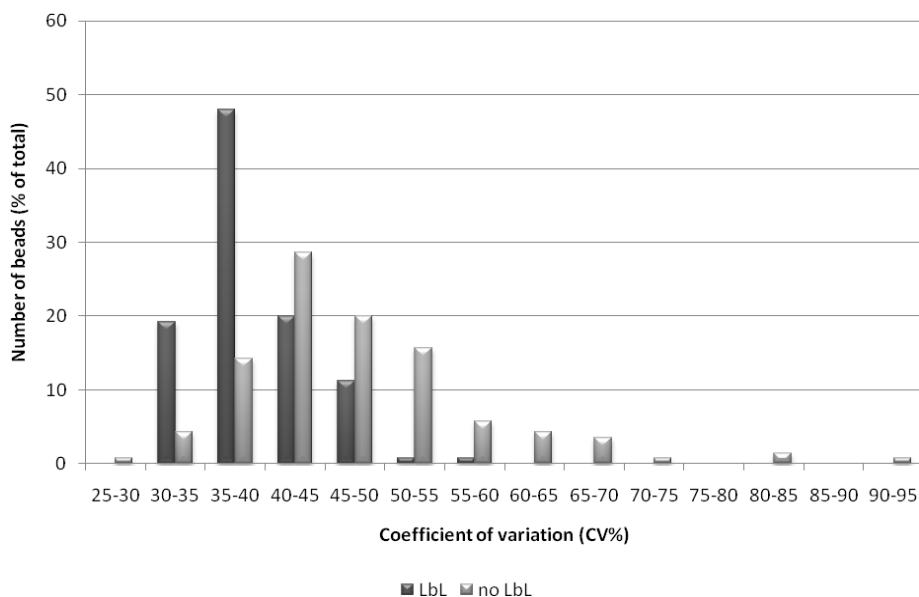


Figure 12: Number of microcarriers (expressed as % of the total amount of microcarriers) as a function the coefficient of variation of the red fluorescence that has been measured at their surface. Two types of microcarriers were analyzed: LbL coated and no modified microcarriers. The microcarriers were incubated with 5 pg/ml TNF- α and labeled by means of the two-step TSA method.

CONCLUSIONS

Multiplex assays are more and more introduced in research and diagnostic labs, because they have proven to be as accurate as their monoplex counterparts, while they have lots of advantages.⁵¹⁻⁵³ Two multiplex platforms currently exist, based on encoded beads (microcarriers) and microarrays, respectively. Detection of antigens at the surface of microcarriers is most often done through the binding of biotinylated detection antibodies which, on their turn, are recognized by fluorophore conjugated streptavidin^{40,42}. In the past enzymatic detection methods have proven to increase the sensitivity of monoplex assays performed in e.g. wells of a microtiter plate (e.g. ELISAs). However, as the converted products freely diffuse in the surrounding medium those methods cannot be applied in multiplex bead-based assays as false positive results may arise due to cross-reaction with not reacted beads. The TSA method, however, is an enzymatic method, in which the converted (fluorescent) product immediately interacts with electron rich groups in the neighborhood of the enzyme⁵. Because the resulting fluorescence is measured at the location where the targets are bound, and not in the surrounding medium, we expected TSA to be suitable in multiplex bead-based platforms. This paper shows evidence that TSA method is indeed attractive for the fast and simultaneous detection of (multiple) targets in a sample by memobeads and *xMAP*[®] beads. Compared to currently used detection methods, TSA significantly amplifies the fluorescence signals on the beads (up to 100 times) resulting in (much) higher signal-to-noise ratios. TSA on beads is applicable in real (serum) samples - sub-pg detection of P24 was possible - and worked perfectly in a multiplex (quadruplex) format.

REFERENCES

1. Kohler, G.; Milstein, C. Continuous cultures of fused cells secreting antibody of predefined specificity. *Nature* **1975**, *256* (5517), 495-497.
2. Porstmann, T.; Kiessig, S. T. Enzyme immunoassay techniques. An overview. *J. Immunol. Methods* **1992**, *150* (1-2), 5-21.
3. Dhawan, S. Signal amplification systems in immunoassays: implications for clinical diagnostics. *Expert Rev. Mol. Diagn.* **2006**, *6* (5), 749-760.
4. Hall, M.; Kazakova, I.; Yao, Y. M. High sensitivity immunoassays using particulate fluorescent labels. *Anal. Biochem.* **1999**, *272* (2), 165-170.
5. Bobrow, M. N.; Harris, T. D.; Shaughnessy, K. J.; Litt, G. J. Catalyzed reporter deposition, a novel method of signal amplification. Application to immunoassays. *J. Immunol. Methods* **1989**, *125* (1-2), 279-285.
6. Bobrow, M. N.; Shaughnessy, K. J.; Litt, G. J. Catalyzed reporter deposition, a novel method of signal amplification. II. Application to membrane immunoassays. *J. Immunol. Methods* **1991**, *137* (1), 103-112.
7. van Gijlswijk, R. P.; Zijlmans, H. J.; Wiegant, J.; Bobrow, M. N.; Erickson, T. J.; Adler, K. E.; Tanke, H. J.; Raap, A. K. Fluorochrome-labeled tyramides: use in immunocytochemistry and fluorescence in situ hybridization. *J. Histochem. Cytochem.* **1997**, *45* (3), 375-382.
8. Zwirgmaier, K. Fluorescence in situ hybridisation (FISH)--the next generation. *FEMS Microbiol. Lett.* **2005**, *246* (2), 151-158.
9. Karsten, S. L.; Van Deerlin, V. M. D.; Sabatti, C.; Gill, L. H.; Geschwind, D. H. An evaluation of tyramide signal amplification and archived fixed and frozen tissue in microarray gene expression analysis. *Nucleic Acids Research* **2002**, *30* (2).
10. Bhattacharya, R.; Bhattacharya, D.; Dhar, T. K. A novel signal amplification technology based on catalyzed reporter deposition and its application in a Dot-ELISA with ultra high sensitivity. *J. Immunol. Methods* **1999**, *227* (1-2), 31-39.
11. Bhattacharya, D.; Bhattacharya, R.; Dhar, T. K. A novel signal amplification technology for ELISA based on catalyzed reporter deposition. Demonstration of its applicability for measuring aflatoxin B(1). *J. Immunol. Methods* **1999**, *230* (1-2), 71-86.
12. Saha, D.; Acharya, D.; Roy, D.; Dhar, T. K. Filtration-based tyramide amplification technique--a new simple approach for rapid detection of aflatoxin B1. *Anal. Bioanal. Chem.* **2007**, *387* (3), 1121-1130.
13. Knuchel, M. C.; Tomasik, Z.; Speck, R. F.; Luthy, R.; Schubach, J. Ultrasensitive quantitative HIV-1 p24 antigen assay adapted to dried plasma spots to improve treatment monitoring in low-resource settings. *Journal of Clinical Virology* **2006**, *36* (1), 64-67.
14. Schubach, J. Viral RNA and p24 antigen as markers of HIV disease and antiretroviral treatment success. *Int. Arch. Allergy Immunol.* **2003**, *132* (3), 196-209.
15. Joos, T. O.; Stoll, D.; Templin, M. F. Miniaturised multiplexed immunoassays. *Curr. Opin. Chem. Biol.* **2002**, *6* (1), 76-80.

16. Knight, P. R.; Sreekumar, A.; Siddiqui, J.; Laxman, B.; Copeland, S.; Chinnaiyan, A.; Remick, D. G. Development of a sensitive microarray immunoassay and comparison with standard enzyme-linked immunoassay for cytokine analysis. *Shock* **2004**, *21* (1), 26-30.
17. Wiese, R.; Belosludtsev, Y.; Powdrill, T.; Thompson, P.; Hogan, M. Simultaneous multianalyte ELISA performed on a microarray platform. *Clin. Chem.* **2001**, *47* (8), 1451-1457.
18. Templin, M. F.; Stoll, D.; Schrenk, M.; Traub, P. C.; Vohringer, C. F.; Joos, T. O. Protein microarray technology. *Trends Biotechnol.* **2002**, *20* (4), 160-166.
19. Walter, G.; Bussow, K.; Cahill, D.; Lueking, A.; Lehrach, H. Protein arrays for gene expression and molecular interaction screening. *Current Opinion in Microbiology* **2000**, *3* (3), 298-302.
20. Cahill, D. J. Protein and antibody arrays and their medical applications. *Journal of Immunological Methods* **2001**, *250* (1-2), 81-91.
21. Braeckmans, K.; De Smedt, S. C.; Leblans, M.; Pauwels, R.; Demeester, J. Encoding microcarriers: present and future technologies. *Nat. Rev. Drug Discov.* **2002**, *1* (6), 447-456.
22. Pregibon, D. C.; Toner, M.; Doyle, P. S. Multifunctional encoded particles for high-throughput biomolecule analysis. *Science* **2007**, *315* (5817), 1393-1396.
23. Wilson, R.; Cossins, A. R.; Spiller, D. G. Encoded microcarriers for high-throughput multiplexed detection. *Angew. Chem. Int. Ed Engl.* **2006**, *45* (37), 6104-6117.
24. de, J. W.; Rijkers, G. T. Solid-phase and bead-based cytokine immunoassay: a comparison. *Methods* **2006**, *38* (4), 294-303.
25. Ray, C. A.; Bowsher, R. R.; Smith, W. C.; Devanarayan, V.; Willey, M. B.; Brandt, J. T.; Dean, R. A. Development, validation, and implementation of a multiplex immunoassay for the simultaneous determination of five cytokines in human serum. *J. Pharm. Biomed. Anal.* **2005**, *36* (5), 1037-1044.
26. Elshal, M. F.; McCoy, J. P. Multiplex bead array assays: performance evaluation and comparison of sensitivity to ELISA. *Methods* **2006**, *38* (4), 317-323.
27. de, J. W.; te, V. H.; Prakken, B. J.; Kuis, W.; Rijkers, G. T. Simultaneous detection of 15 human cytokines in a single sample of stimulated peripheral blood mononuclear cells. *Clin. Diagn. Lab Immunol.* **2003**, *10* (1), 133-139.
28. Tarnok, A.; Hamsch, J.; Chen, R.; Varro, R. Cytometric bead array to measure six cytokines in twenty-five microliters of serum. *Clin. Chem.* **2003**, *49* (6 Pt 1), 1000-1002.
29. Kellar, K. L.; Douglass, J. P. Multiplexed microsphere-based flow cytometric immunoassays for human cytokines. *J. Immunol. Methods* **2003**, *279* (1-2), 277-285.
30. Dasso, J.; Lee, J.; Bach, H.; Mage, R. G. A comparison of ELISA and flow microsphere-based assays for quantification of immunoglobulins. *J. Immunol. Methods* **2002**, *263* (1-2), 23-33.
31. de, J. W.; te, V. H.; Prakken, B. J.; Kuis, W.; Rijkers, G. T. Simultaneous detection of 15 human cytokines in a single sample of stimulated peripheral blood mononuclear cells. *Clin. Diagn. Lab Immunol.* **2003**, *10* (1), 133-139.
32. Cook, E. B.; Stahl, J. L.; Lowe, L.; Chen, R.; Morgan, E.; Wilson, J.; Varro, R.; Chan, A.; Graziano, F. M.; Barney, N. P. Simultaneous measurement of six cytokines in a single sample of human tears using microparticle-based flow cytometry: allergics vs. non-allergics. *J. Immunol. Methods* **2001**, *254* (1-2), 109-118.

33. Hurley, J. D.; Engle, L. J.; Davis, J. T.; Welsh, A. M.; Landers, J. E. A simple, bead-based approach for multi-SNP molecular haplotyping. *Nucleic Acids Res.* **2004**, *32* (22), e186.
34. Bibikova, M.; Lin, Z.; Zhou, L.; Chudin, E.; Garcia, E. W.; Wu, B.; Doucet, D.; Thomas, N. J.; Wang, Y.; Vollmer, E.; Goldmann, T.; Seifart, C.; Jiang, W.; Barker, D. L.; Chee, M. S.; Floros, J.; Fan, J. B. High-throughput DNA methylation profiling using universal bead arrays. *Genome Res.* **2006**, *16* (3), 383-393.
35. Yang, L.; Tran, D. K.; Wang, X. BADGE, Beads Array for the Detection of Gene Expression, a high-throughput diagnostic bioassay. *Genome Res.* **2001**, *11* (11), 1888-1898.
36. Henry, M. R.; Wilkins, S. P.; Sun, J.; Kelso, D. M. Real-time measurements of DNA hybridization on microparticles with fluorescence resonance energy transfer. *Anal. Biochem.* **1999**, *276* (2), 204-214.
37. Nolan, J. P.; Sklar, L. A. Suspension array technology: evolution of the flat-array paradigm. *Trends Biotechnol.* **2002**, *20* (1), 9-12.
38. Ekins, R. Immunoassay: recent developments and future directions. *Nucl. Med. Biol.* **1994**, *21* (3), 495-521.
39. Pang, S.; Smith, J.; Onley, D.; Reeve, J.; Walker, M.; Foy, C. A comparability study of the emerging protein array platforms with established ELISA procedures. *J. Immunol. Methods* **2005**, *302* (1-2), 1-12.
40. Derveaux, S.; Stubbe, B. G.; Roelant, C.; Leblans, M.; De Geest, B. G.; Demeester, J.; De Smedt, S. C. Layer-by-layer coated digitally encoded microcarriers for quantification of proteins in serum and plasma. *Anal. Chem.* **2008**, *80* (1), 85-94.
41. Szurdoki, F.; Michael, K. L.; Walt, D. R. A duplexed microsphere-based fluorescent immunoassay. *Anal. Biochem.* **2001**, *291* (2), 219-228.
42. Fulton, R. J.; McDade, R. L.; Smith, P. L.; Kienker, L. J.; Kettman, J. R., Jr. Advanced multiplexed analysis with the FlowMetrix system. *Clin. Chem.* **1997**, *43* (9), 1749-1756.
43. Dhawan, S. Signal amplification systems in immunoassays: implications for clinical diagnostics. *Expert Rev. Mol. Diagn.* **2006**, *6* (5), 749-760.
44. Porstmann, T.; Kiessig, S. T. Enzyme immunoassay techniques. An overview. *J. Immunol. Methods* **1992**, *150* (1-2), 5-21.
45. Bacarese-Hamilton, T.; Mezzasoma, L.; Ingham, C.; Ardizzoni, A.; Rossi, R.; Bistoni, F.; Crisanti, A. Detection of allergen-specific IgE on microarrays by use of signal amplification techniques. *Clin. Chem.* **2002**, *48* (8), 1367-1370.
46. Varnum, S. M.; Woodbury, R. L.; Zangar, R. C. A protein microarray ELISA for screening biological fluids. *Methods Mol. Biol.* **2004**, *264*, 161-172.
47. Derveaux, S.; Geest, B. G.; Roelant, C.; Braeckmans, K.; Demeester, J.; Smedt, S. C. Multifunctional Layer-by-Layer Coating of Digitally Encoded Microparticles. *Langmuir* **2007**, *23* (20), 10272-10279.
48. Braeckmans, K.; De Smedt, S. C.; Leblans, M.; Pauwels, R.; Demeester, J. Encoding microcarriers: present and future technologies. *Nat. Rev. Drug Discov.* **2002**, *1* (6), 447-456.
49. Braeckmans, K.; De Smedt, S. C.; Roelant, C.; Leblans, M.; Pauwels, R.; Demeester, J. Encoding microcarriers by spatial selective photobleaching. *Nat. Mater.* **2003**, *2* (3), 169-173.

50. Brust, S.; Duttmann, H.; Feldner, J.; Gurtler, L.; Thorstensson, R.; Simon, F. Shortening of the diagnostic window with a new combined HIV p24 antigen and anti-HIV-1/2/O screening test. *J. Virol. Methods* **2000**, *90* (2), 153-165.
51. Bacarese-Hamilton, T.; Gray, J.; Ardizzoni, A.; Crisanti, A. Allergen microarrays. *Methods Mol. Med.* **2005**, *114*, 195-207.
52. Kellar, K. L.; Kalwar, R. R.; Dubois, K. A.; Crouse, D.; Chafin, W. D.; Kane, B. E. Multiplexed fluorescent bead-based immunoassays for quantitation of human cytokines in serum and culture supernatants. *Cytometry* **2001**, *45* (1), 27-36.
53. De Jager, W.; Rijkers, G. T. Solid-phase and bead-based cytokine immunoassay: a comparison. *Methods* **2006**, *38* (4), 294-303.

C H A P T E R Five

MULTIPLEXED SNP GENOTYPING WITH LAYER-BY-LAYER COATED DIGITALLY ENCODED MICROCARRIERS

ABSTRACT

This chapter shows that LbL coated memobeads can quantitatively detect DNA molecules. First of all, some parameters were investigated that could influence the hybridization of target sequences to capture probes that were immobilized on the surface of the microcarriers, such as length of the spacer molecule, the direction of the probe/target complex, and the hybridization time. An important strength of the memobead platform, compared to other suspension array platforms, is that it makes dual-color target labeling possible, which is very attractive for e.g. gene expression analysis. Multiple-color labeling might even be possible with this platform, by changing the dye inside the microcarriers. Finally, the memobead platform succeeded in genotyping nine patient samples for the two single nucleotides polymorphisms of the Apolipoprotein E gene, as it was compared to microarray analysis and sequencing, which demonstrates the possibility of using the memobeads as a genotyping platform.

CHAPTER 5

MULTIPLEXED SNP GENOTYPING WITH LAYER-BY-LAYER COATED DIGITALLY ENCODED MICROCARRIERS

INTRODUCTION

Over the last decade, human genome projects have resulted in an incredible amount of genetic information. Among those data, single nucleotide polymorphisms (SNPs) were found, single base-pair mutations that occur at a specific site in the DNA sequence and represent the most common form of genetic variation and a major cause of many diseases. They are believed to uncover the reasons that individuals respond differentially to therapeutics, and further on, SNPs often determine host range of pathogens, and will be highly useful in molecular diagnostics and drug discovery ¹. But SNP analysis is used throughout other life sciences including agriculture, food testing, identity testing, and pathogen identification ². Those observations resulted in an incredible burst in research for and development of solution-phase molecular methods that could detect and type SNPs to improve clinical diagnostics. Among them are single base extension reactions (SBE), primer extension reactions, oligo ligation assays (OLA), invader assays, pyro-sequencing, real-time polymerase chain reactions (real-time PCRs) ¹⁻⁵. Because detection of multiple SNPs within a sequence offers great advantages, the combination of these SNP typing methods with multiplex technologies are of wide interest for SNP genotyping, especially because costs can be substantially reduced and throughput increased. Multiplex platforms deliver the solid support, on which the

multiple final products of the genotyping methods are caught and distinguished, so that no physical separation of those products is needed and automation is easily possible, an advance for large scale genotyping. Different platforms were developed and introduced in the field of multiplexed SNP typing, among which some of them increased revolutionarily the multiplex capability, such as the Affymetrix GeneChip array⁶ and the Illumina BeadArray genotyping technology^{7,8}. The former is the standard in the field of the ‘planar’ DNA microarrays, which use the *x,y*-coordinates of the spots of printed capture probe sequences on a glass plate to identify which SNPs were present in a sample. However, DNA microarrays cope with localization problems of the capture probes upon miniaturization and slow reaction kinetics (as the diffusion of the targets in the sample to the capture probes is time-consuming)⁹⁻¹¹. Despite the success of the DNA microarrays in whole-genome SNP analysis, their use for low density multiplexing has also been limited by the high cost of both the microarray consumables and the instruments. Instead of a glass plate, the BeadArray of Illumina makes use of micrometer-sized beads and is so far the only bead-technology suitable for high-density SNP typing. Although this array benefits from near-solution kinetics, the instrument costs are, however, too high for low and medium level multiplexing, as was the case for the planar-surface microarrays. Because multiple recent studies demonstrate that genetic testing - and more specific SNP typing – could have high impact in near-patient diagnostics (personalized medicine), with a main focus on infectious disease diagnostics and pharmacogenetic analysis, other technologies are required, that are capable to rapidly genotype multiple SNPs at low costs and at low-sample throughputs¹².

The so-called “suspension arrays” are good candidates to fulfill those different criteria¹³⁻¹⁶. Suspension arrays use *encoded* micron sized particles for multiplexing goals. Different capture probes can be covalently coupled to differently encoded microspheres; the code allows knowing which capture probe is bound to the surface of the microcarriers. They have a number of advantages compared to the planar microarrays regarding for instance the reproducibility of the attachment of the capture probes, the flexibility in surface chemistry, the flexibility in panel of tests, and improved kinetics.¹³ By encoding, each microsphere becomes the address for a single mutation^{17,18}. Specific fluorescent target sequences, that are generated by the genotyping assay, can hybridize to their corresponding (complementary) capture probe at the surface of a certain microsphere. Decoding of the ‘positive’ reacted microcarriers (i.e. those microcarriers which bound fluorescently labeled targets at their surface) subsequently allows identification of the SNPs present in the sample. Multiple strategies have been proposed to build “suspension arrays”¹⁹⁻²¹. Our group introduced the encoding of fluorescent polystyrene microspheres (of about 40 μm in size) with a digital barcode by means of “spatial selective photobleaching” (see Chapter 2). The thus encoded microspheres were

called “memobeads”.²² To optimize the surface characteristics of memobeads we recently proposed to coat their surface with poly-electrolytes by the “Layer-by-Layer” (LbL) approach.²³ As shown in Chapter 2, LbL coating is based on the alternate adsorption of oppositely charged polyelectrolytes onto a charged substrate. The LbL coating of the surface of the memobeads was proven to be “multifunctional” in the sense that it (a) allows positioning of the memobeads for decoding, (b) does not optically interfere with the encoding and reading process and (c) allows a high loading of the surface of the microparticles with capture probes (like proteins and DNA molecules). Meanwhile, those memobeads were already applied as a platform for sandwich immunoassays and enzyme screening²⁴.

In this study, we demonstrate a proof-of-concept of using memobeads for multiplexed SNP genotyping by combination with the solution-phase Oligo Ligation Assay (OLA) genotyping method, which is a ligation-dependent PCR method for the detection of known single nucleotide polymorphisms (SNPs) in genes²⁵. The OLA method, which is depicted in Figure 1, has several advantages compared to other SNP typing methods: any nucleotide variation at the ligation junction can be detected with a single set of assay conditions, the assay has a high specificity, speed, and can be automated, making it suitable for large-scale genotyping. Because of the high specificity of the ligase, SNPs can be identified with high accuracy, even at low abundance (which is often the case in e.g. cancer mutations that are present in a minority of the total target DNA)²⁶. Suitably designed common locus specific and allele specific primers are hybridized to the denatured target DNA, and are subsequently ligated to each other provided that the nucleotides are perfectly base-paired to the target at the junction (Figure 1)^{25,27}. Ligated products can be detected by a wide variety of methods, like separation with PAGE or capillary tubes, or trapping using biotin-streptavidin interactions or via disulfide bonds on microarrays, combined with fluorescent, radioactive or enzymatic detection^{28,29}. The allele specific ligation primers that are used in this chapter, however, contain at their 5'-terminus zip-codes (with a specific sequence) that are used to hybridize the OLA products, after a PCR amplification step, to corresponding zip-code addresses that are attached to the digitally encoded microcarriers (Figure 1). The use of artificially made zip-codes - which are designed in such a way that cross-hybridization is impossible - as a universal platform for molecular recognition was first described by Gerry et al.²⁶ The ligated product is then amplified and fluorescently labeled by means of a PCR which uses two universal primers, one of which is fluorescently labeled (see Figure 1). Those primers anneal to the tail sequences of the ligated product. This yields consistent results among different ligated targets and allows uniform PCR conditions to be used. Since a single base mismatch prevents ligation, it is possible to distinguish mutations with high specificity. Using the Apolipoprotein E (ApoE) gene as a model system, multiplexed OLA/PCR followed by hybridization to

digitally encoded microcarriers was used for genotyping nine clinical samples. The ApoE is a plasma protein involved in lipid transport and lipoprotein metabolism³⁰. The ApoE gene on chromosome 19 exhibits two common polymorphisms that have been associated with both coronary artery diseases (CAD) and Alzheimer's disease³¹. The polymorphisms create the 3 allelic isophorms E2, E3 and E4 which are encoded by Cysteine-Cysteine (Cys-Cys), Cysteine-Arginine (Cys-Arg) and Arginine-Arginine (Arg-Arg) at amino acid positions 112 and 158, respectively, resulting from the single base substitution of a T to a C at each of these two corresponding sites in the gene (ApoE Cys112Arg and ApoE Arg158Cys).

MATERIALS & METHODS

Materials.

Non-magnetic fluorescent carboxylated microspheres (CFP-40052-100, $\phi = 39 \mu\text{m}$) were purchased from Spherotech (Libertyville, Illinois, USA). Poly (allylamine hydrochloride) [PAH; 28,322-3], sodium poly (styrene sulfonate) [PSS, MW $\sim 70\,000$; 24,305-1] and poly (acrylic acid) [PAA, MW $\sim 45\,000$; 18,128-5] were obtained from Sigma Aldrich (Steinheim, Germany). The polymers were dissolved into 0.5 M sodium chloride (31434, Sigma Aldrich, Seelze, Germany). Bovine serum albumine (BSA, A-7906) and 2-[N-Morpholino]ethanesulfonic acid (MES, M-8259) were purchased from Sigma (Bornem, Belgium), PBS Dulbecco's (14190-094) from Gibco and Tween-20 (655204) from Calbiochem. EDC (1-ethyl-3-(3-dimethyl aminopropyl) carbodiimide HCl, 22980) was obtained from Perbio Science (Erembodegem, Belgium); desiccated and stored at -20°C . All oligonucleotide were synthesized by Eurogentec (Liege, Belgium). Capture probes were amino (NH_2)-modified for coupling to carboxylated microcarriers. Capture probes were purified by reverse-phase HPLC. Target sequences used for hybridization studies were Cy5 or TexasRed conjugated for fluorescent detection. One PCR primer used for genotyping was Cy5 conjugated, the other one unmodified. SNP specific ligation primers containing the SNP position were phosphate-modified. The other SNP specific ligation primers were unmodified. Before use, all nucleotides were reconstituted in sterile distilled, deionized water. We randomly choose 4 zipcode sequences from those described by the group of Barany for hybridizing OLA targets to the microspheres²⁶.

Layer-by-Layer coating of the microspheres.

A schematic overview, as well as the procedure of the Layer-by-Layer modification is described in Chapter 2.

Encoding of the microspheres.

The encoding process is described in Chapter 2.

Coupling of capture probes to the LbL coated microcarriers and encoded memobeads.

Aminated capture probes were covalently attached to the (PAA) carboxyl groups at the surface of the microcarriers by the one-step carbodiimide-method in a total reaction volume of 17.5 μ l. In brief, the microcarriers (suspended in 7.5 μ l 0.4M MES buffer) were activated and coupled to capture probes by incubation with 7.5 μ l EDC (100 mg/ml in 0.4M Mes-buffer – fresh made) and 2.5 μ l capture probe in a thermomixer at 20°C and at 1500 rpm for 1 hour. In order to check which coupling concentration was most optimal, 2.5 μ l of differently concentrated solutions of Cy5 red fluorescent capture probes (CP A and CP B, see Table 1) (between 40 nM and 200 μ M) were coupled to approximately 500 LbL coated microcarriers. For the coupling of TAG capture probes to the encoded memobeads, approximately 500 encoded memobeads were incubated with 2.5 μ l of the TAG probes (at 33 μ M), and for the coupling of the other capture probes to the LbL coated microcarriers, approximately 6000 microcarriers were incubated with 2.5 μ l of the probes (at 100 μ M). The sequences of the capture probes are listed in Table 1. The microcarriers were then washed three times with 100 μ l of assay buffer (1% bovine serum albumin, 0.05% Tween-20 in PBS) for 30 seconds, and they were subsequently washed twice with 100 μ l hybridization buffer (5 mM Tris-HCl, 0.5 mM Titriplex III, 1.0 M NaCl, dH₂O). Finally, the coated microcarriers were stored in 200 μ l hybridization buffer (final concentration = 2500 microspheres / ml) at 4°C.

Hybridization of target probes to the LbL coated microcarriers.

Approximately 3000 coated microcarriers (suspended in 10 μ l hybridization buffer) were incubated with 5 μ l target probes (35 μ M) for 30 minutes at room temperature, unless otherwise noted. Before that, the targets were incubated for 2 minutes at 95°C to denature their sequences.

The microcarriers were then washed twice with 1x SSC buffer, and finally stored in 40 μ l 1x SSC buffer before analysis. The sequences of the target probes (TP) are listed in Table 1.

OLA and multiplexed memobead assay.

The Oligo Ligation Assay, as explained in this section, has been developed and optimized by the group of Jurgen Del-Favero (VIB Department of Molecular Genetics, University of Antwerp). PCRs of the samples were performed in a total of 20 μ l using 20 ng aliquots of sample. The PCR master mix included final concentrations of reagents as follows: 1x TitaniumTM Taq PCR buffer (Clontech), 0.1 μ l 50x TitaniumTM Taq DNA Polymerase (Clontech), 0.25 mM of each deoxynucleoside triphosphate (Invitrogen), 0.5 μ M of each PCR primer (apoE-F and R), and 1 M betaine. Standard PCR conditions were developed: denaturation for 2 minutes at 95 °C, followed by 35 cycles for 30 seconds at 95°C, 30 seconds at 68°C, 30 seconds at 72 °C, and final extension for 6 minutes at 72°C. The samples were subsequently stored at 8°C. The PCR samples were finally purified with the QIAquick PCR Purification Kit (Qiagen). Ligation primers were designed to bind to specific sequence regions of the amplified targets on 1 strand of the double-stranded DNA amplicon (LP1, LP2, LP3, LP4, LP5 (OLA112R), and LP6 (OLA158R)). The sequences are listed in Table 1. Purified PCR product was diluted 1/5000 and 1 μ l was used for the multiplexed ligation reaction. The ligation reaction was done in a total 15 μ l volume, consisting of 0.66 fmol/ μ l of each ligation primer, 10x ampligase reaction buffer (Epicentre), and 1U ampligase (Epicentre). The DNA ligation reactions were carried out in a thermo cycler as follows: denaturation for 2 minutes at 95°C, followed by 5 minutes at 65°C, followed by 19 cycles for 1 minute at 95°C and 5 minutes at 65°C. The ligation product was finally stored at 8°C. After the multiplexed ligation reaction, the ligation product was amplified by means of a secondary PCR in a total reaction volume of 20 μ l. The ligation product was diluted 1/10 and 2 μ l was used for the PCR reaction. The PCR master mix included final concentrations of reagents as follows: 1x TitaniumTM Taq PCR buffer (Clontech), 0.2 μ l 50x TitaniumTM Taq DNA Polymerase (Clontech), 0.25 mM of each deoxynucleoside triphosphate (Invitrogen), 0.5 μ M of each PCR primer (PP2 and Cy5 conjugated PP1, Table 1). Standard PCR conditions were developed: denaturation for 2 minutes at 95 °C, followed by 35 cycles for 30 seconds at 95°C, 30 seconds at 60°C, 30 seconds at 72 °C, and final extension for 6 minutes at 72°C. The samples were subsequently stored at 8°C. For the multiplexed detection of the SNPs on the memobeads platform, approximately 125 microspheres were used in total reaction volume of 40 μ l in a 0.2 ml PCR tube; 25 microspheres (bearing a dotcode encoding for the 112T-allele) were coated with the 112T tag probe (CP F'), 25 microspheres (bearing a dotcode encoding for the 112C-allele) were coated with the 112C tag probe (CP F), 25

microspheres (bearing a dotcode encoding for the 158T-allele) were coated with the 158T tag probe (CP F^{'''}), 25 microspheres (bearing a dotcode encoding for the 158C-allele) were coated with the 158C tag probe (CP F^{''}), and 25 microspheres did not bear any probes ("control microspheres"). The target reaction mix contained 4 μ l of the ligation product, and 36 μ l of fresh made 3.33x SSC buffer + 0.33% SDS. The target reaction mix was firstly denatured at 98°C for 5 minutes, and thereafter immediately placed on ice. The target reaction mix was then added to the bead mixture, vortexed for 3 seconds, and incubated for 14 hours on a rotator in a hybridization oven at 60°C. The microspheres were finally washed twice with 100 μ l of 1x SSC buffer, and resuspended into 40 μ l of the same buffer.

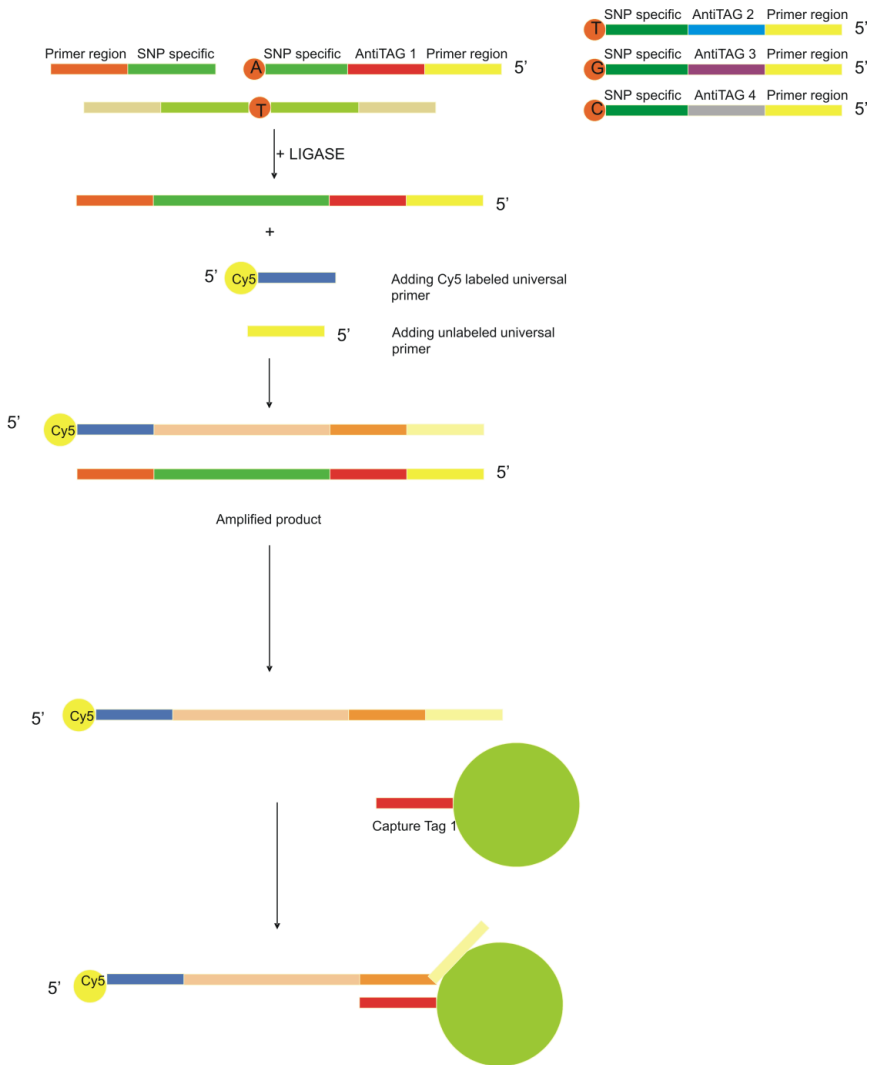


Figure 1: Procedure of single nucleotide polymorphism detection by combination of the Oligo Ligation Assay with memobeads. In a first step ligation primers hybridize to the sample DNA and are ligated to each other if they are completely complementary to the target sequence. Both ligation primers consist of an allele-specific sequence and a sequence that is specific for hybridization with a universal PCR primer. One of the ligation primers also carries an 'anti-TAG' sequence (ZIP-code) that is necessary for hybridization to complementary capture TAGs that are coupled to the memobeads. In the next step, ligated products are all together amplified and fluorescently labeled in one PCR reaction, using universal PCR primers from which one is fluorescently labeled. The fluorescent PCR amplicons are then captured on the memobeads. Different alleles are captured on different memobeads, using different TAG-sequences.

Microscopy of the microspheres.

The LbL coated encoded microspheres were decoded using a pseudo-confocal Perkin-Elmer CSU-10 scanning unit mounted to an inverted Zeiss microscope equipped with an objective 40x lens (NA 0.6) and a cooled Hamamatsu ORCA-ER charge coupled device (CCD) camera. Excitation was done with laser light (488nm). Imaging Technology PC-DIG framegrabber boards took care of image transfer from the CCD camera to the computer. The (red) AlexaFluor 647 fluorescence at the surface of the microcarriers was measured with the same instrument, but excitation was done with a halogen lamp. A 647nm LP filter was put in front of the lamp to obtain the optimal wavelength. To determine the red fluorescence of a microcarrier, a region of interest (ROI) was drawn around the microcarrier and the red fluorescence within the ROI was measured using the Matlab 7.1 version equipped with home-made imaging processing software. The red fluorescence of each microsphere was defined as the mean of the intensity of all pixels within the ROI.

RESULTS AND DISCUSSION

Optimization of probe coupling conditions to LbL coated microcarriers.

It is well-known that the coupling density of probes on microarrays and microparticles strongly influences the hybridization kinetics with target molecules^{10,32,33}. Figure 2 shows the effect of the concentration of capture probes in the coating solution on the amount of coupled probes. Several sequential dilutions of a Cy5 red fluorescently conjugated probe were used (CP A, see Table 1). It proves that the coupling density can be controlled by varying the probe concentration. An increase in red fluorescence is measured at the surface of the microcarriers, which is proportional to the amount of bound probes, as a function of increasing probe concentrations. The signal reaches thereafter a maximal value at probe concentrations around 3.3 μM , and finally decreases with higher probe concentrations. The latter one is remarkable, and not expected, because there we couldn't find any reason why higher probe concentrations result in a less dense surface occupation. As far as we know, this has never been described in the literature; in contrast, other research groups reported an increase in surface density, which finally reaches a saturation level³³. Although they have used different microparticles and coupling methods, there is no reason why this should not

happen in our case. The decrease in fluorescence is probably due to a quenching reaction. At certain coating concentration, the fluorescent probes become too densely packed at the surface of LbL coated microcarriers, which brings the fluorophores in too close proximity. LbL coated microcarriers exhibit indeed a higher loading capacity than the original non-magnetic microcarriers, as was shown in Chapter 2, which was probably the result of 1) a higher density of carboxylic acid groups per unit of surface area due to coating with PAA, and 2) a higher surface area due to the incorporation of magnetic nanoparticles (as is depicted in Figure 3). Therefore, it might be possible that the probes come in too close proximity at high surface densities. If quenching occurs, then this means that the maximal fluorescence in Figure 2 does not necessarily correlate to the maximal surface loading. Therefore, higher densities might be obtained with coating concentrations that are higher than 3.3 μM , although less fluorescence is observed. It has been postulated, however, that a too dense packaging of probe molecules impedes the hybridization of target molecules, because of steric hindrance. Quenching reactions occur when two fluorescent molecules are in close neighborhood (distance of a few Angström). As a result, a less efficient hybridization might be expected, if the coating concentration is higher than 3.3 μM . Therefore, in the following experiments, capture probe concentrations were used around this value.

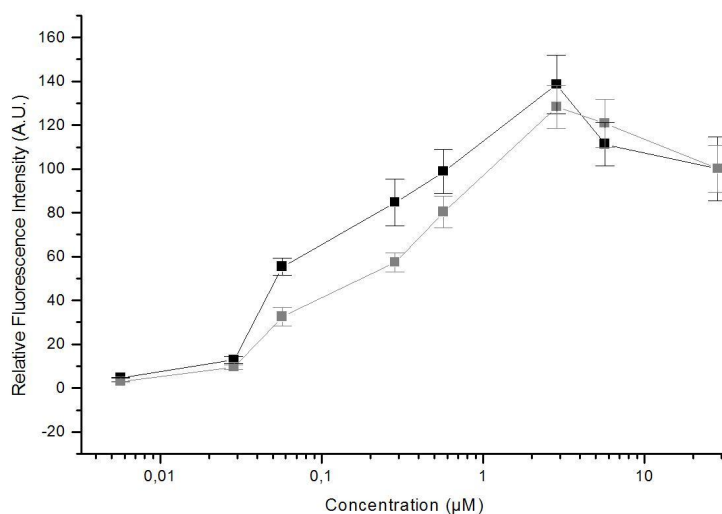


Figure 2: Titration of 3' red fluorescently labeled and 5' aminated capture probes used in the coupling procedure and its effect on surface probe densities in two independent experiments (black and grey). The decrease in fluorescence for concentrations higher than $\sim 3.3 \mu\text{M}$ is probably due to the quenching of the fluorophores at the surface of the microcarriers, because the probes are bound in too close proximity.

Note that the previous result was achieved by coupling a 5' amino and 3' fluorescently labeled capture probe (CP A). The same result has been observed, however, when coupling a 3' amino and 5' fluorescently labeled capture probe (CP B, Table 1, results not shown), which means that the result is independent of the orientation of the capture probe at the surface of the microcarriers.

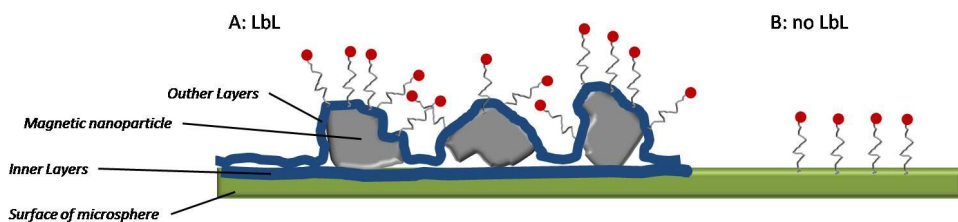


Figure 3: Coupling of probes to microspheres with and without LbL coating. The physical structure of the LbL surface probably brings fluorescently labeled probes in too close proximity, with quenching of the fluorophores as a result.

Hybridization of complementary oligonucleotides to LbL coated microcarriers.

Figure 4 shows the titration of a target probe (TP C, Table 1) against a fixed number of microcarriers that were coated with capture probes C. The volume of the hybridization mixture was kept as low as practically possible (15 μ l) in order to increase the relative probe concentration. Together with a continuously mixing condition, this improves the hybridization efficiency, as was demonstrated by Gerry et al.²⁶ As expected, a quantitative relationship was observed between the concentration of the target probe and the fluorescent signal that was measured at the surface of the microcarriers. As negative control, non-coated microspheres were incubated with the highest target concentration. No detectable non-specific binding to the LbL coating of those microcarriers was observed. This shows that LbL coatings might have potential in genetic tests, provided that sensitive measurements are possible.

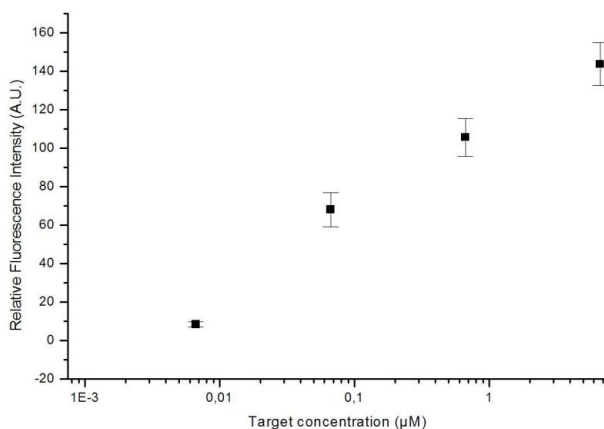


Figure 4: Relative red fluorescence intensity at the surface of the microcarriers as a function of the concentration of the target probe. Capture probe coated LbL coated microspheres were incubated with dilutions of the Cy5 labeled complementary sequence.

Optimization of hybridization: influence of the spacer length of the capture probes.

Spacer molecules play an important role in the hybridization of target sequences to probes that are fixed on a surface³⁴. The length of the spacer molecule drastically determines the mobility of the capture probes and thus the hybridization with them³⁵. Generally, the longer the spacer molecule, the more the oligonucleotide is spatially removed from the surface, the less it will interact with the surface, and thus the more the hybridization kinetics resembles solution-kinetics. Hybridization efficiencies were compared in this study between a Cy5 fluorescently labeled target probe (TP C) and a capture probe that was coupled via four different spacer molecules (three of them were coupled via their 5' end: CP C with a C6 spacer, CP C' with a C3 spacer, and CP C'' with a C12 spacer, and one was coupled via its 3' end: CP C''' with a C6 spacer) (Table 1). Three independent experiments were performed, and because it was important that each of the four tubes carried the same amount of target probe within each repetition, one dilution was made which was then equally distributed in the four tubes. To avoid irregularities due to different amounts of target probes between the three experiments, the average fluorescence of all samples was normalized to the average fluorescence of sample 1 (spacer 1) within each experiment. Figure 5 shows the highest hybridization efficiency when the capture probes were coupled via their 3' terminus to the microcarriers. Because the target sequence is labeled at its 5' end with a Cy5 fluorophore, which

comes in close proximity with the surface of the microcarrier during the hybridization of the target sequence to the bound capture probe, the higher efficiency might be explained by the fact that the Cy5 molecules are a little attracted to the surface of the microcarriers, in which way they facilitate the hybridization. This is, however, only a suggestion, and more experiments have to be performed to investigate this opinion. Since no fluorescence was observed when the target sequences were incubated with control microcarriers (which were not coupled with capture probes), the final washing steps are stringent enough to eliminate non-specifically coupled target probes, as was also observed in the previous experiment.

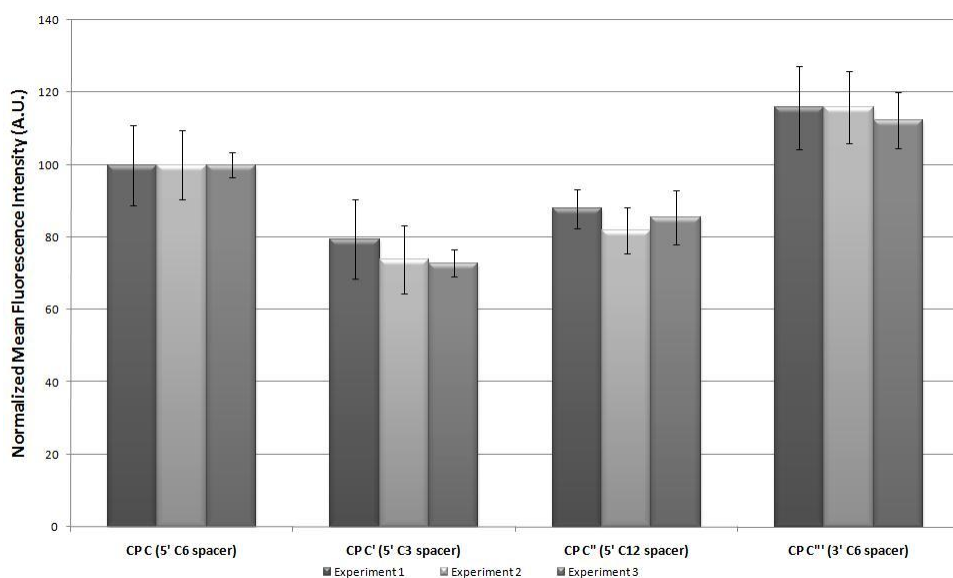


Figure 5: Influence of the length of the spacer by which the capture probes are coupled to the microcarriers, and the direction by which they are coupled, on the hybridization efficiency of target sequences. Three independent experiments were performed and to avoid irregularities due to different amounts of target probes between the three experiments, for each experiment the mean fluorescent signals were always normalized against the mean signal of the microcarriers that were coupled with the CP C capture probe (via a 5' C6 spacer). The sequences are listed in Table 1.

Comparing the probes that were coupled via their 5' terminus, it can be seen that the C6 spacer resulted in the highest hybridization, which can be explained by the fact that probes exhibit enough flexibility, while this is probably not true for probes that were coupled via a C3 spacer. On the other hand, a C12 spacer probably results in a less efficient hybridization, because, probably, the capture probes achieve too much flexibility. They start to bend and can, besides making contact via

their 5' end, also interact with the surface via other parts in their sequence, which has been also demonstrated by Southern on planar supports³⁶. Such an inconsistent, but significant effect of the length of the spacer on the hybridization efficiency was also observed by the group of Walker, when the capture microcarriers (coated with probes) were kept at room temperature before hybridization, although other immobilization strategies were used³⁵. They could circumvent this effect by pre-heating the capture microcarriers at 90°C for 10 minutes immediately before hybridization. A increase in hybridization was then observed as the length of the spacer was increased, probably because the contact points at other parts in the capture probe sequence were broken by the high temperatures³⁷.

Optimization of hybridization: influence of the hybridization time.

Different concentrations of target probes C (13 μM , 0.13 μM , and 0.013 μM) were hybridized to microcarriers that were coupled with the complementary capture probes C (5' C6 spacer). Target hybridization efficiency was measured as a function of the incubation time. It was seen that most of the target molecules hybridized already during the first minutes of incubation (Figure 6), with a neglected increase in the amount of hybridization for longer incubation times, independent of target concentration, as shown by the linear fittings.

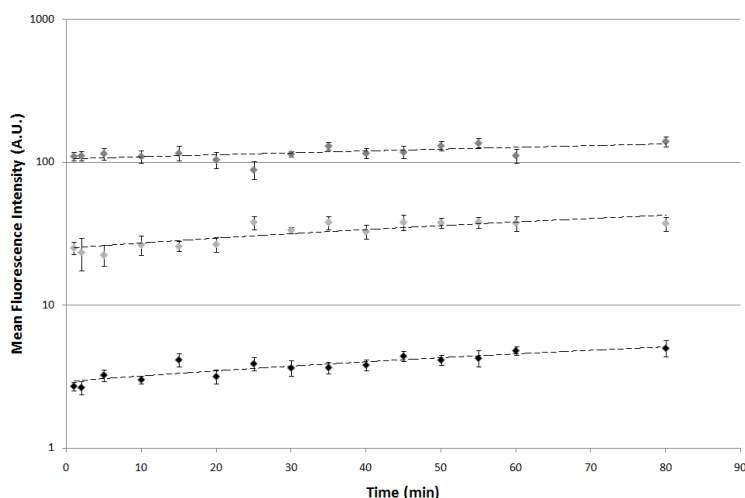


Figure 6: Influence of the hybridization time on the hybridization efficiency for three different target concentrations: 13 nM (grey circles), 0.13 μM (light grey circles) and 13 μM (dark grey circles). A linear fitting has been applied to the data points, which shows that most of the targets already hybridized during the first moments of incubation, and that additional bound targets at longer incubation times can be neglected.

Optimization of hybridization: influence of the degree of probe/target complementary.

Because most genetic applications of the LbL coated memobeads will rely on the hybridization of targets, from which only a part of their sequence is complementary to that of the capture probes, it was investigated to which extent the degree of complementarity between probes and targets influences their hybridization efficiency. As will be shown later on in this chapter, when memobeads are used to capture OLA amplicons, the target sequence is much longer than the capture probe sequence, and only a part of the target sequence is used to capture it (see Oligo Ligation Assay in Figure 1).

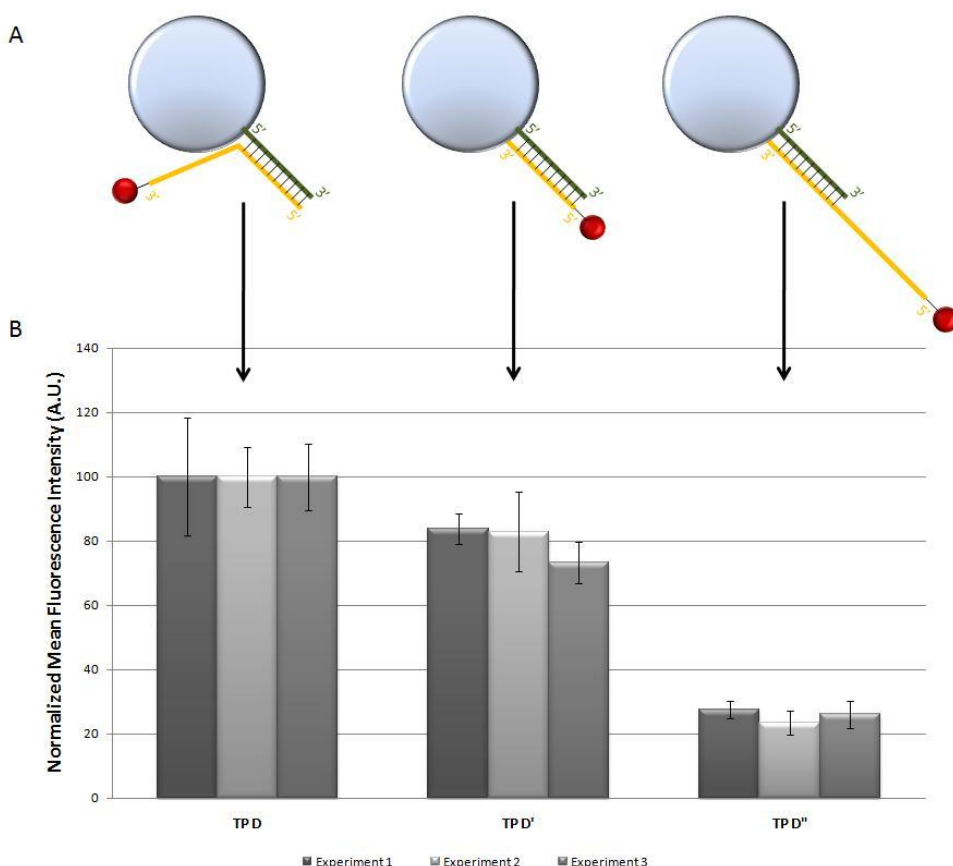


Figure 7: A/ Schematic overview of the hybridization between capture and target probes at the surface of a microcarrier. The capture probe is coupled via its 5' end with a C6 spacer molecule. Middle: capture and target probe are equally sized and fully complementary. If the target sequence is larger than the probe sequence, a part of the sequence is not complementary, and will result in an 'overhanging' part at the 5' end of the capture probe (left), or at the 3' end of the capture probe (right). B/

Influence of the degree of complementary between capture and target probes, and the position of the overlap of the not hybridized part of the target sequence, on the hybridization efficiency.

The real OLA situation was mimicked here by hybridizing two different (fluorescently labeled) 44-mer target oligonucleotides to a 20-mer capture probe (CP D), which resulted in an overhang close to the surface of the microcarrier at the 5' end of the capture probe (when TP D was used, Figure 7 A left), or far from the surface of the microcarrier at the 3' end (when target probe D'' was used, Figure 7 A right). The hybridization efficiency was compared to that of a fully complementary 20-mer target sequence (TP D', Figure 7 A middle). The sequences can be found in Table 1. Three independent experiments were performed, and in order to avoid irregularities due to different amounts of target probes between the three experiments, the average fluorescence was always normalized to the average fluorescence of one of the samples within each experiment. Figure 7 B shows that if the overlap of the non-complementary part of the target sequence occurs at the 5' end of the capture probe (which is close to the surface of the microcarrier), then the highest fluorescence signal is achieved (which is proportional to the amount of hybridized targets). This signal is even a little higher than the mean fluorescence measured at the surface of microcarriers on which hybridization occurred between two fully complementary 20-mer sequences (TP D'). As already mentioned in a previous paragraph, the reason therefore might be an attraction of the Cy5 fluorophore to the surface of the microcarrier, which facilitates the hybridization process, although this is still a suggestion. Remarkably, in case of an overlap at the 3' end of the capture probe, the fluorescence signal is significantly much lower, meaning that much less targets are hybridized.

Dual color detection with LbL coated microcarriers.

So far, target probes were always red fluorescently labeled (Cy5), in order to avoid as much as possible any cross-talk between the fluorescent reporter molecule and the green fluorescent molecule that is used to stain the memobeads (and which is necessary for the encoding technology). Cross-talk indeed results in a higher background fluorescence, which should be avoided, especially in situations where the intensity of a specific signal is low (e.g. when only a few target molecules have been hybridized). Cross-talk between the Cy5 and green fluorescent dye inside the memobeads can be avoided by using the correct excitation- and emission filters, as shown in Figure 8.

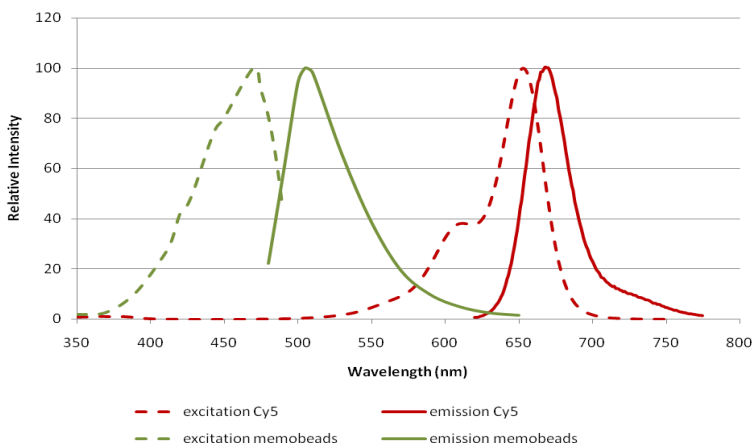


Figure 8: Excitation- (dotted lines) and emission (full lines) spectra of the green fluorescent dye that is used to stain the memobeads (green lines) and Cy5 fluorophores (red lines). Cross-talk can be avoided by using the correct excitation- and emission filters.

Besides Cy5, however, also other fluorescent dyes might be applied for target labeling, as long as their spectrum does not interfere (too much) with the spectrum of the green fluorescent memobeads. The encoding of microspheres by means of photobleaching makes use of only one fluorescent dye, independently on the number of codes that has to be generated. One encoding dye means that a broad part of the spectrum is available for reporter labeling. Therefore, multi-color reporter labeling might be an option on the memobead platform, which is not the case on certain other platforms, such as e.g. the optical encoding platform developed by Luminex Corp., which uses two different fluorescent dyes to generate only 100 codes, as shown in Chapter 1, and which will need a third/fourth/... dye to generate even a larger number of codes. Multi-color labeling is important for some NATs, such as for gene expression analysis on conventional cDNA microarrays. The latter one needs two colors; cDNA from two different conditions (e.g. normal versus disease samples) is labeled with two different fluorophores (e.g. Cy3 for normal and Cy5 for disease cDNA)³⁸. Several genes are labeled simultaneously in this way. Those differently labeled samples are subsequently co-hybridized to a microarray on which probes for the multiple genes are separately spotted. After washing, the microarray is scanned at two different wavelengths and the ratio between the Cy3 and Cy5 emission signals informs about the relative transcript abundance of each gene under investigation: if the ratio Cy3/Cy5 is high, it means that there is less expression in the disease sample compared to the normal sample. Oppositely, a low Cy3/Cy5 ratio means a higher expression of the gene in the disease samples. When this type of gene expression analysis has to be applied to suspension arrays, two color reporter labeling is necessary.

A

Target probe D	+	-	+	-	+	+	+	-	+
Target probe D'''	-	+	-	+	+	+	-	+	+
Target probe E	+	-	-	+	+	-	+	+	+
Target probe E'	-	+	+	-	-	+	+	+	+

B

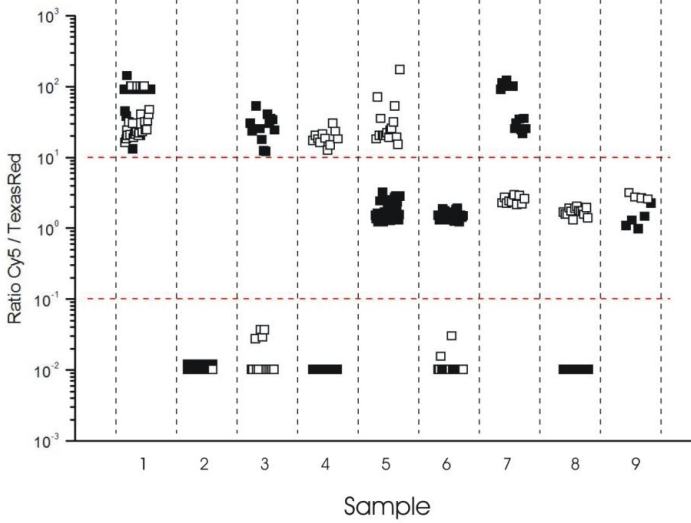


Figure 9: Dual-color target labeling. Microcarriers that are encoded with dotcode 1 (closed symbols) and with dotcode 2 (open symbols) were coupled with capture probes D and capture probes E, respectively. (A) A mixture of those microcarriers was incubated with 9 different solutions, composed of two or more Cy5 and/or TexasRed labeled target sequences (added sequences are indicated with a '+' symbol). The sequences are listed in Table 1. (B) After hybridization, the observed ratio between the Cy5 signal and the TexasRed signal is shown for several microcarriers from each code. Red lines mark-off the categories (ratio > 10: only Cy5 signal, ratio < 0.1: only TexasRed signal, 0.1 < ratio < 10: both signals).

As a proof-of-principle, a mixture of two differently encoded memobeads (each coupled with different capture probes, respectively CP D and E, Table 1), was incubated with several target solutions, composed of mixtures of target probes TP D, D''', E, and E' (Table 1). Two reporter dyes were used, Cy5 (TP D and TP E) and TexasRed (TP D''' and TP E'). The composition of the solutions, and the ratio between the Cy5 and the TexasRed fluorescence that were measured at the surface of both types of memobeads, are shown in Figure 9 A, respectively Figure 9 B.

We were able to retrieve the composition of each solution by means of the Cy5/Texas Red ratio and the code of the memobeads. The measurements could be clearly classified into three

separate categories. To the first category ($Cy5/TR > 10$) belong the memobeads to which Cy5-labeled target probes specifically hybridized, TexasRed labeled ones not (or only non-specific). The second category ($0.1 < Cy5/TR < 10$) consists of those memobeads that detected both types of targets. Finally, the third category ($Cy5/TR < 0.1$) are the memobeads that detected TexasRed labeled target sequences specifically, but not Cy5 labeled ones. Note that the Cy5/TR ratio is limited to 0.01 and 100, if no Cy5 fluorescence, respectively TexasRed fluorescence was measured (in order to avoid unlimited values).

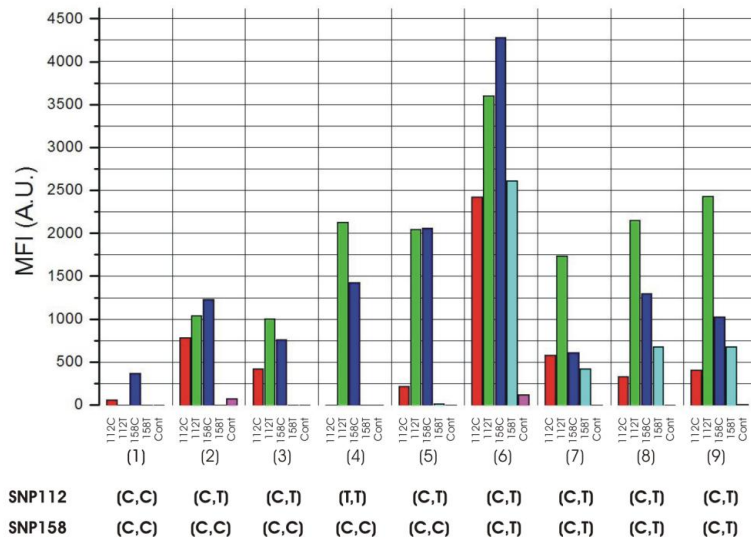
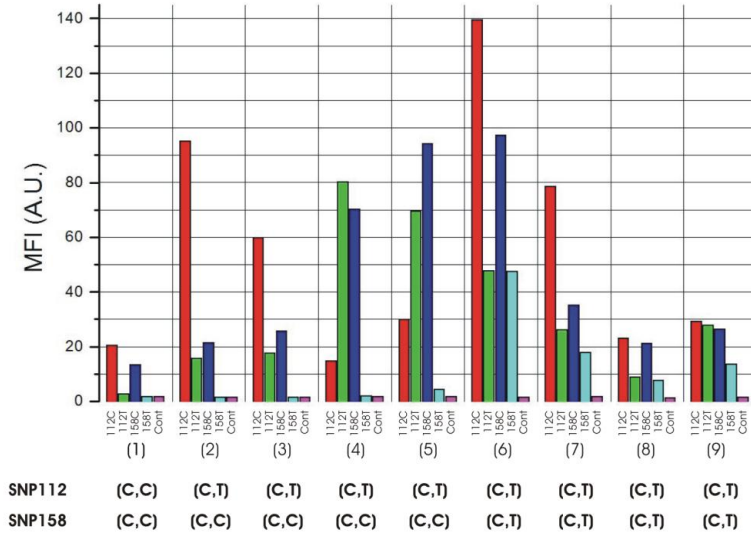
The results in Figure 9 proves that dual-color labeling on the memobead platform is possible. So far, only green fluorescently dyed memobeads were used, because of their availability. This dye, unfortunately, has a broad excitation- and emission-spectrum that is situated in the middle of the visible spectrum (Figure 8). Because a lot of commercially available dyes exhibit cross-talk in this area, they cannot be applied to the memobead platform at this moment. In other words, the memobead platform is actually limited to the use of (far) red fluorescent dyes. The encoding process by means of photobleaching, however, is in theory applicable to any other fluorescent molecule, as long as it can be incorporated in an immobile fashion inside the microcarriers, and as long as it can be bleached within acceptable times. The use of microcarriers that are fluorescently stained with fluorophores that can be excited with e.g. UV light or with far red light, could even improve the number and types of fluorophores that can be simultaneously used in one memobead-assay.

ApoE genotyping of nine clinical samples.

Besides for gene expression analysis, multiplexed platforms are ideally suitable for genotyping too, because of the high-density information. The memobead platform was therefore evaluated as genotyping platform, by combining it with the oligo ligation assay (OLA). The main advantage of the latter PCR based assay is the high specificity with which it detects, amplifies and labels single nucleotide polymorphisms, as explained in Figure 1, and in the introduction. The ligation primers (LP, Table 1) were designed with a target specific sequence, a sequence for universal primer hybridization, and an internal tag-sequence which corresponds to a ZIP-code sequence that was covalently linked to one of the microcarrier sets (see Figure 1). This assures hybridization of (allele-specific) OLA amplicons to their corresponding encoded memobeads, so that each different encoded memobead detects another allele.

As a model system, genotyping for Apolipoprotein E (ApoE) was performed. The capture probes, ligation primers and PCR primers (listed in Table 1) were designed to detect and differentiate

the two single nucleotide polymorphisms of the ApoE gene (ApoE112 and ApoE158). Nine different patient samples were evaluated, and the assay was carried out as described in the section materials & methods. Figure 10A shows the mean red fluorescence of each set of encoded memobeads, that was measured in a region of interest (ROI), as previously described. All samples were correctly genotyped (compared to the golden standard 'sequencing' results of the same patients; data not shown), although some signals do not differ that much from the background signal. Note that this problem might be avoided by calculating the correlation value between all pixels within the ROI and all pixels within a predefined ring structure that surrounds the ROI, as shown in Figure 10C. A clear separation between positive and negative measurements can be defined in this way, even for low signals. The mean red fluorescence remarkably varied between the different samples, probably due to varying yields in the PCR reactions, and/or varying incorporation of fluorophores, which has been previously described in the literature ³⁹. The result was also compared with that obtained on a microarray platform (Figure 10B). The same capture probe sequences were therefore spotted on the latter one, and the OLA amplicons were then hybridized to this microarray. Figure 10 shows a good agreement between the results that were obtained with both platforms. Only one allele was differently measured on both platforms (sample 4, 112C), probably due to a less efficient hybridization on the microarray. Figure 10B again shows remarkable variations in absolute red fluorescence between the different samples that were measured on the microarray platform, which means that the variation is not introduced by irregularities during the hybridization process, but is rather related to the OLA assay itself.



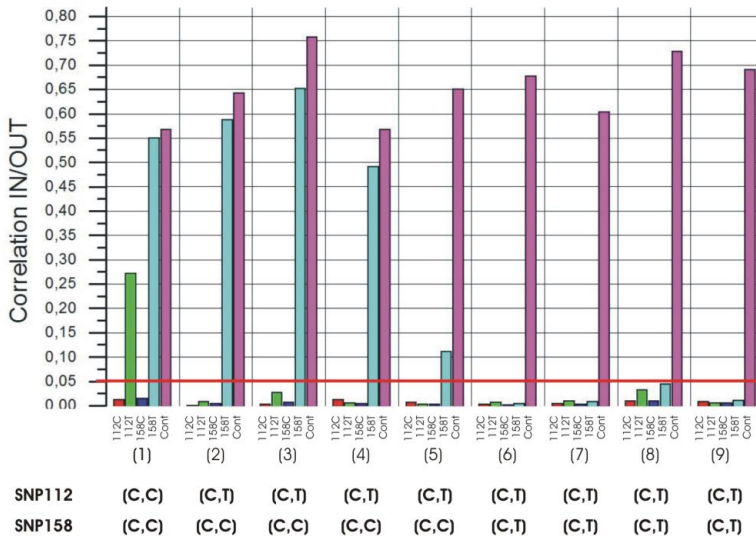


Figure 10: Simultaneous detection of SNP112 and SNP158 associated with the ApoE gene from nine different clinical samples with the memobead platform (upper graph) and with a microarray platform (middle graph). Lower graph: correlation value between all pixels measured within the ROI and all pixels measured in a predefined ring structure that surrounds the ROI, for all signals shown in the upper graph (memobead platform) (upper and lower graph) and a spot with no complementary tag-sequence in the case of the microarray (middle graph).

Table 1: ID, sequence and modification of the capture probes, the target probes and the primers used in this study.

ID (*)	Spacer	5'	3'	Sequence, 5' → 3' (')
CP A	C6 Spacer	NH ₂	Cy5	aAAAGCAggCTTCTATACgAAATTCCTggg
CP B	C6 Spacer	Cy5	NH ₂	aAAAGCAggCTTCTATACgAAATTCCTggg
CP C	C6 Spacer	NH ₂	-	aAAAGCAggCTTCTATACgAAATTCCTggg
CP C'	C3 Spacer	NH ₂	-	aAAAGCAggCTTCTATACgAAATTCCTggg
CP C''	C12 Spacer	NH ₂	-	aAAAGCAggCTTCTATACgAAATTCCTggg
CP C'''	C6 Spacer	-	NH ₂	aAAAGCAggCTTCTATACgAAATTCCTggg
CP D	C6 Spacer	NH ₂	-	CCCTATAGTGAGTCGTATTA
CP F	5' H ₂ N(CH ₂) ₆ O-3'	NH ₂	-	TGCGACCTCAGCATCGACCTCAGC (capture tag for snp112c allele)
CP F'	5' H ₂ N(CH ₂) ₆ O-3'	NH ₂	-	CAGCACCTGACCATCGATCGCAGC (capture tag for snp112t allele)
CP F''	5' H ₂ N(CH ₂) ₆ O-3'	NH ₂	-	GACCACCTTCGGATCGGGTACAGC (capture tag for snp158c allele)
CP F'''	5' H ₂ N(CH ₂) ₆ O-3'	NH ₂	-	TGCGGGTACAGCACCTACCTTGCG (capture tag for snp158t allele)
TP C		Cy5	-	CCCAggAAATTCgTATAgAAgCCCTgCTTTT
TP D		-	Cy5	TAATACGACTCACTATAGGGCTTACTTGAAAATTTATTTGGC
TP D'		Cy5	-	TAATACGACTCACTATAGGG

TP D''		Cy5	-	CTCTTACTGAAATTTATTTTGCCTAATACGACTCACTATAGGG
TP D'''		-	TR	TAATACGACTCACTATAGGGCTCTTACTTGAAATTTATTTGCC
TP E		-	Cy5	ATTTAGGTGACACTATAGAATACTACTGCACCAGGCGGCCGC
TP E'		-	TR	ATTTAGGTGACACTATAGAATACTACTGCACCAGGCGGCCGC
LP 1 (112c)		PO ₄	-	<u>ATTTAGGTGACACTATAGAATACT</u> <u>TGC</u> GACCTCAGCATCGACTCAGCCGGGACATGGAGGACGTGc
LP 2 (112t)		PO ₄	-	<u>ATTTAGGTGACACTATAGAATACT</u> CAGCACTGACCATCGATCGCAGCCGGGACATGGAGGACGTGt
LP 3 (158c)		PO ₄	-	<u>ATTTAGGTGACACTATAGAATACT</u> GACCACCTTGCGATCGGGTACAGCGATGCCGATGACCTGCAGAAAGc
LP 4 (158t)		PO ₄	-	<u>ATTTAGGTGACACTATAGAATACT</u> TGCGGGTACAGCACCTACCTTCCGGATGCCGATGACCTGCAGAAAGt
PP 1		Cy5	-	TAATACGACTCACTATAGGG
PP 2		-	-	ATTTAGGTGACACTATAGAATACT
LP 5 (OLA112R)		-	-	GCGGCCCGCTGGTGCAGTACCCCTATAGT GAGT CGTATTA
LP 6 (OLA158R)		PO ₄	-	GCTGGCAGTGTACGAGG CCCTATAGT GAGT CGTATTA

(*) CP = capture probe, TP = Target probe, LP = Ligation primer, PP = PCR primer. (#) Several colors are used to indicate the specific sequences within each ligation primer: Red = SNP112 specific sequence, yellow = SNP158 specific sequence, _ = universal primer (PP 2) specific sequence, fat = universal primer (PP1) specific sequence. Blue, green, orange and purple sequence refer to the ZIP-codes, respectively CP F, CP F', CP F'', and CP F'''.

CONCLUSION

This study shows evidence that LbL coated microcarriers can quantitatively detect DNA molecules. We showed that the length of the spacer molecule by which capture probes are attached to the microcarriers, plays an important role in the hybridization efficiency of targets probes thereto. It has been observed that hybridization occurred very fast on the surface of the microparticles; almost maximal hybridization was achieved within a few minutes. Remarkably, the efficiency increases with higher lengths till a maximal efficiency is reached with a certain length of the spacer. A longer spacer length result in a worse efficiency, probably because the capture probe interacts too much with the surface of the microcarrier. A few results raised the question whether Cy5 fluorophores are attracted to the surface, and thereby influence the hybridization of Cy5 labeled target probes. This still has to be investigated in future. An important strength of the memobead platform, compared to other suspension array platforms, is that it makes dual-color target labeling possible, which is very attractive for e.g. gene expression analysis. Multiple-color labeling might be possible with this platform, by changing the dye inside the microcarriers. Finally, a proof-of-concept has been launched that demonstrated the possibility of using the memobead platform for genotyping. Nine clinical samples were correctly genotyped for two polymorphisms of the Apolipoprotein E gene.

REFERENCES

1. Shi, M. M. Enabling large-scale pharmacogenetic studies by high-throughput mutation detection and genotyping technologies. *Clin. Chem.* **2001**, *47* (2), 164-172.
2. Hsuih, T. C.; Park, Y. N.; Zaretsky, C.; Wu, F.; Tyagi, S.; Kramer, F. R.; Sperling, R.; Zhang, D. Y. Novel, ligation-dependent PCR assay for detection of hepatitis C in serum. *J. Clin. Microbiol.* **1996**, *34* (3), 501-507.
3. Kwok, P. Y. Methods for genotyping single nucleotide polymorphisms. *Annu. Rev. Genomics Hum. Genet.* **2001**, *2*, 235-258.
4. Lyamichev, V.; Mast, A. L.; Hall, J. G.; Prudent, J. R.; Kaiser, M. W.; Takova, T.; Kwiatkowski, R. W.; Sander, T. J.; de, A. M.; Arco, D. A.; Neri, B. P.; Brow, M. A. Polymorphism identification and quantitative detection of genomic DNA by invasive cleavage of oligonucleotide probes. *Nat. Biotechnol.* **1999**, *17* (3), 292-296.
5. Gibson, N. J. The use of real-time PCR methods in DNA sequence variation analysis. *Clin. Chim. Acta* **2006**, *363* (1-2), 32-47.
6. Ma-Weiszhausz, D. D.; Warrington, J.; Tanimoto, E. Y.; Miyada, C. G. The affymetrix GeneChip platform: an overview. *Methods Enzymol.* **2006**, *410*, 3-28.
7. Oliphant, A.; Barker, D. L.; Stuelpnagel, J. R.; Chee, M. S. BeadArray technology: enabling an accurate, cost-effective approach to high-throughput genotyping. *Biotechniques* **2002**, *Suppl*, 56-1.
8. Shen, R.; Fan, J. B.; Campbell, D.; Chang, W.; Chen, J.; Doucet, D.; Yeakley, J.; Bibikova, M.; Wickham, G. E.; McBride, C.; Steemers, F.; Garcia, F.; Kermani, B. G.; Gunderson, K.; Oliphant, A. High-throughput SNP genotyping on universal bead arrays. *Mutat. Res.* **2005**, *573* (1-2), 70-82.
9. Vainrub, A.; Pettitt, B. M. Coulomb blockage of hybridization in two-dimensional DNA arrays. *Phys. Rev. E. Stat. Nonlin. Soft. Matter Phys.* **2002**, *66* (4 Pt 1), 041905.
10. Henry, M. R.; Wilkins, S. P.; Sun, J.; Kelso, D. M. Real-time measurements of DNA hybridization on microparticles with fluorescence resonance energy transfer. *Anal. Biochem.* **1999**, *276* (2), 204-214.
11. Yang, L.; Tran, D. K.; Wang, X. BADGE, Beads Array for the Detection of Gene Expression, a high-throughput diagnostic bioassay. *Genome Res.* **2001**, *11* (11), 1888-1898.
12. Ugozzoli, L. A. Multiplex assays with fluorescent microbead readout: a powerful tool for mutation detection. *Clin. Chem.* **2004**, *50* (11), 1963-1965.
13. Nolan, J. P.; Sklar, L. A. Suspension array technology: evolution of the flat-array paradigm. *Trends Biotechnol.* **2002**, *20* (1), 9-12.
14. Dunbar, S. A. Applications of Luminex xMAP technology for rapid, high-throughput multiplexed nucleic acid detection. *Clin. Chim. Acta* **2006**, *363* (1-2), 71-82.
15. Bortolin, S.; Black, M.; Modi, H.; Boszko, I.; Kobler, D.; Fieldhouse, D.; Lopes, E.; Lacroix, J. M.; Grimwood, R.; Wells, P.; Janeczko, R.; Zastawny, R. Analytical validation of the tag-it high-throughput microsphere-based universal array genotyping platform: application to the multiplex detection of a panel of thrombophilia-associated single-nucleotide polymorphisms. *Clin. Chem.* **2004**, *50* (11), 2028-2036.

16. Rao, K. V.; Stevens, P. W.; Hall, J. G.; Lyamichev, V.; Neri, B. P.; Kelso, D. M. Genotyping single nucleotide polymorphisms directly from genomic DNA by invasive cleavage reaction on microspheres. *Nucleic Acids Res.* **2003**, *31* (11), e66.
17. Iannone, M. A.; Taylor, J. D.; Chen, J.; Li, M. S.; Rivers, P.; Slentz-Kesler, K. A.; Weiner, M. P. Multiplexed single nucleotide polymorphism genotyping by oligonucleotide ligation and flow cytometry. *Cytometry* **2000**, *39* (2), 131-140.
18. Ye, F.; Li, M. S.; Taylor, J. D.; Nguyen, Q.; Colton, H. M.; Casey, W. M.; Wagner, M.; Weiner, M. P.; Chen, J. Fluorescent microsphere-based readout technology for multiplexed human single nucleotide polymorphism analysis and bacterial identification. *Hum. Mutat.* **2001**, *17* (4), 305-316.
19. Pregibon, D. C.; Toner, M.; Doyle, P. S. Multifunctional encoded particles for high-throughput biomolecule analysis. *Science* **2007**, *315* (5817), 1393-1396.
20. Wilson, R.; Cossins, A. R.; Spiller, D. G. Encoded microcarriers for high-throughput multiplexed detection. *Angew. Chem. Int. Ed Engl.* **2006**, *45* (37), 6104-6117.
21. Braeckmans, K.; De Smedt, S. C.; Leblans, M.; Pauwels, R.; Demeester, J. Encoding microcarriers: present and future technologies. *Nat. Rev. Drug Discov.* **2002**, *1* (6), 447-456.
22. Braeckmans, K.; De Smedt, S. C.; Roelant, C.; Leblans, M.; Pauwels, R.; Demeester, J. Encoding microcarriers by spatial selective photobleaching. *Nat. Mater.* **2003**, *2* (3), 169-173.
23. Derveaux, S.; Geest, B. G.; Roelant, C.; Braeckmans, K.; Demeester, J.; Smedt, S. C. Multifunctional Layer-by-Layer Coating of Digitally Encoded Microparticles. *Langmuir* **2007**.
24. Derveaux, S.; Stubbe, B. G.; Roelant, C.; Leblans, M.; De Geest, B. G.; Demeester, J.; De Smedt, S. C. Layer-by-layer coated digitally encoded microcarriers for quantification of proteins in serum and plasma. *Anal. Chem.* **2008**, *80* (1), 85-94.
25. Landegren, U.; Kaiser, R.; Sanders, J.; Hood, L. A ligase-mediated gene detection technique. *Science* **1988**, *241* (4869), 1077-1080.
26. Gerry, N. P.; Witowski, N. E.; Day, J.; Hammer, R. P.; Barany, G.; Barany, F. Universal DNA microarray method for multiplex detection of low abundance point mutations. *J. Mol. Biol.* **1999**, *292* (2), 251-262.
27. Wu, D. Y.; Wallace, R. B. The ligation amplification reaction (LAR)—amplification of specific DNA sequences using sequential rounds of template-dependent ligation. *Genomics* **1989**, *4* (4), 560-569.
28. Deng, J. Y.; Zhang, X. E.; Mang, Y.; Zhang, Z. P.; Zhou, Y. F.; Liu, Q.; Lu, H. B.; Fu, Z. J. Oligonucleotide ligation assay-based DNA chip for multiplex detection of single nucleotide polymorphism. *Biosens. Bioelectron.* **2004**, *19* (10), 1277-1283.
29. Grossman, P. D.; Bloch, W.; Brinson, E.; Chang, C. C.; Eggerding, F. A.; Fung, S.; Iovannisci, D. M.; Woo, S.; Winn-Deen, E. S. High-density multiplex detection of nucleic acid sequences: oligonucleotide ligation assay and sequence-coded separation. *Nucleic Acids Res.* **1994**, *22* (21), 4527-4534.
30. Assmann, G.; Schmitz, G.; Menzel, H. J.; Schulte, H. Apolipoprotein E polymorphism and hyperlipidemia. *Clin. Chem.* **1984**, *30* (5), 641-643.
31. Luc, G.; Bard, J. M.; Arveiler, D.; Evans, A.; Cambou, J. P.; Bingham, A.; Amouyel, P.; Schaffer, P.; Ruidavets, J. B.; Cambien, F.; . Impact of apolipoprotein E polymorphism on lipoproteins and risk of myocardial infarction. The ECTIM Study. *Arterioscler. Thromb.* **1994**, *14* (9), 1412-1419.

32. Peterson, A. W.; Heaton, R. J.; Georgiadis, R. M. The effect of surface probe density on DNA hybridization. *Nucleic Acids Res.* **2001**, *29* (24), 5163-5168.
33. Walsh, M. K.; Wang, X.; Weimer, B. C. Optimizing the immobilization of single-stranded DNA onto glass beads. *J. Biochem. Biophys. Methods* **2001**, *47* (3), 221-231.
34. Halperin, A.; Buhot, A.; Zhulina, E. B. Hybridization at a surface: the role of spacers in DNA microarrays. *Langmuir* **2006**, *22* (26), 11290-11304.
35. Day, P. J.; Flora, P. S.; Fox, J. E.; Walker, M. R. Immobilization of polynucleotides on magnetic particles. Factors influencing hybridization efficiency. *Biochem. J.* **1991**, *278* (Pt 3), 735-740.
36. Southern, E.; Mir, K.; Shchepinov, M. Molecular interactions on microarrays. *Nat. Genet.* **1999**, *21* (1 Suppl), 5-9.
37. Ishii, J. K.; Ghosh, S. S. Bead-based sandwich hybridization characteristics of oligonucleotide-alkaline phosphatase conjugates and their potential for quantitating target RNA sequences. *Bioconjug. Chem.* **1993**, *4* (1), 34-41.
38. Lockhart, D. J.; Winzeler, E. A. Genomics, gene expression and DNA arrays. *Nature* **2000**, *405* (6788), 827-836.
39. Armstrong, B.; Stewart, M.; Mazumder, A. Suspension arrays for high throughput, multiplexed single nucleotide polymorphism genotyping. *Cytometry* **2000**, *40* (2), 102-108.

CHAPTER Six

SYNERGISM BETWEEN PARTICLE- BASED MULTIPLEXING AND MICROFLUIDICS TECHNOLOGIES MAY BRING DIAGNOSTICS CLOSER TO THE PATIENT

Parts of this chapter were published in:

Derveaux S.,¹ Stubbe, B.G.,¹ Braeckmans, K.,¹ Roelant, C.,² Sato, K.,³ Demeester, J.,¹ De Smedt, S.C.¹
Analytical and Bioanalytical Chemistry **2008**, 391 (7), 2453-2467.

¹ Laboratory of General Biochemistry and Physical Pharmacy, Department of Pharmaceutics, Ghent University, 9000 Ghent, Belgium.

² Memobead Technologies NV, Rupelweg 10, 2850 Boom, Belgium.

³ Department of Applied Chemistry, School of Engineering, The University of Tokyo, 7-3-1 Hongo, Bunkyo-Ku, Tokyo 113-8656, Japan

ABSTRACT

In the field of medical diagnostics there is a growing need for inexpensive, accurate, and quick high throughput assays. On one hand, recent progress in microfluidics technologies is expected to strongly support the development of miniaturized analytical devices, which will fasten (bio)analytical assays. On the other hand, a higher throughput can be obtained by the simultaneous screening of one sample for multiple targets (multiplexing) by means of encoded particle-based assays. Multiplexing at the ‘macro’ level is nowadays common in research labs and is expected to become part of the clinical diagnostics. This chapter aims to debate on the ‘added value’ we can expect by (bio)analysis with particles in microfluidic devices. Technologies to (a) decode, (b) analyse, and (c) manipulate the particles are described. A special emphasis is on the challenges which exist to integrate currently existing detection platforms for encoded microparticles in microdevices, and on promising microtechnologies for down-scaling the detection units, in order to obtain compact miniaturized particle-based multiplexing platforms.

CHAPTER 6

SYNERGISM BETWEEN PARTICLE-BASED MULTIPLEXING AND MICROFLUIDICS TECHNOLOGIES MAY BRING DIAGNOSTICS CLOSER TO THE PATIENT

INTRODUCTION

Many automated systems have been introduced in the field of medical diagnostics to allow a more rapid and efficient collecting of data from the substantially amount of samples that hospitals daily deal with. However, such automated equipment is mostly not suitable for use in small diagnostic and research laboratories and for decentralized point-of-care testing, as they require highly qualified personnel, are often non portable and/or too expensive. Hence, there is an increasing need for (a) accurate, (b) quick, (c) miniaturized, and (d) cheap innovative tools which should bring medical diagnostics closer to the patient.

There is no doubt that the recent progress in microfluidics technologies will strongly support the development of miniaturized analytical devices ¹. Microfluidics involves the manipulation, transport, and analysis of fluids in micrometer-sized channels. A “liquid microspace” has characteristic features which differ from the properties of a “liquid bulk”: high interface-to-volume ratio, small heat capacity and, especially, short diffusion distances. The latter is a useful property in analysis, because the time a molecule needs to diffuse from point a to point b is proportional to the square of the distance between a and b ²; While it takes several hours to overcome 1 cm, it only takes tens of seconds to overcome 100 μm .

The microfluidic concept has today already evolved in promising analytical ‘lab-on-a-chip’ (LOC) tools.³ The LOC concept, or “micro total analysis systems” (μ TAS) as it is today commonly referred to was proposed in the early 1990s by Manz et al.⁴ Since that time the field has bloomed and branched off into many areas with different applications such as single molecule analysis⁵, single cell processing and analysis⁶, biological and chemical analysis⁷⁻¹⁴, point of care testing^{15,16}, clinical and forensic analysis¹⁷, molecular and medical diagnostics¹⁸⁻²¹, combinatorial chemistry²² and drug discovery²³. The fact that LOC systems are compact, which allows automation of complex tasks, makes them very attractive²⁴.

A higher throughput in (bio)analysis can be obtained (a) by parallel screening of multiple samples for one target, (b) by the simultaneous screening of one sample for multiple targets (multiplexing) or (c) by a combination of both, as recently reviewed by Situma et al.²⁵. In microfluidics, a higher throughput is currently obtained by parallel screening of a number of samples in a number of channels in one device. Sato et al.²⁶ constructed a device with branching multichannels that allow four samples to be processed simultaneously. The assay time for four samples took 50 minutes instead of 35 min for one sample in a single-channel assay. A further way to realize higher throughput analysis in microfluidic devices is by multiplexing i.e. the simultaneous detection of multiple analytes in a sample present in one channel. Kartalov et al. reported a multi-antigen microfluidic fluorescence immunoassay which measures up to 5 analytes for each of 10 samples in a 100-chamber polydimethylsiloxane (PDMS) microchip²⁷. Multiplexing at the ‘macro’ level is nowadays common in research labs and is expected to become part of the clinical diagnostics²⁸⁻³⁰. Both “planar arrays” (often called “microarrays”) and “suspension arrays” (particle-based arrays) were developed for multiplexing purposes.

Because microarrays allow (ultra) high density analysis of samples they became standard tools for gene expression analysis³¹. Multiplexing necessitates an encoding scheme for molecular identification; the code allows knowing which capture probe is bound at that particular position on the array and therefore also which analyte is analyzed. Whereas planar arrays strictly rely on spatially positional encoding, particle-based arrays have used a great number of encoding schemes that can be classified as optical, graphical, electronic or physical^{32,33}. Particle-based arrays benefit from (a) “near-solution” kinetics -which means that the kinetics between a molecule bound to the surface of a particle and a free molecule equals those between two free molecules-, (b) lower instrument related costs, (c) higher sample throughput and (d) good quality control by batch synthesis^{34,35}. When compared with microarrays, particle-based arrays offer a more flexible choice of the “probe-set”; the detection of extra targets only implies the addition of extra microparticles to the sample while in case of microarray-assaying a new microarray has to be made. Particle-based arrays are especially most favored over microarrays when rather a modest instead of a very high number of targets has to

be simultaneously analyzed. This feature may explain the recent exponential increase of particle-based applications at the ‘macro’ level²⁸.

Currently, multiplexing at the microlevel is mainly done by combining flat surface microarrays with microchannels. Delehanty and Ligler³⁶ used non-contact microarray printing to immobilize biotinylated capture antibodies at discrete locations on a avidin-coated microscope slide and processed the samples with a six channel flow module. Assays were completed in 15 minutes. The group of Delamarche combined concepts of micromosaic immunoassays and microfluidic networks to detect C-reactive protein (CRP) and other cardiac markers^{37,38}. By using 20 μm by 10 μm sized channels (5 mm in length), CRP was detected in 10 minutes in only one microliter of human plasma down to concentrations of 30 ng/ml. So far only few examples have been reported on multiplexing by particles in microfluidic devices³⁹. One of the problems is that the implementation of the detection systems, currently used to analyze particles in macro-assays, into microfluidic devices is not straightforward.

This chapter aims to debate on the ‘added value’ we can expect by (bio)analysis with particles in microfluidic devices. Technologies to (a) decode, (b) analyze and (c) manipulate the particles are described. Also, an interdisciplinary effort is made to overview possibilities for the integration of different processes like decoding and sorting of encoded particles.

STRATEGIES TO DECODE MICROPARTICLES

For an overview of the particle encoding technologies and the strategies to decode particles, we refer to Chapter 1. Additional information can be found in some excellent reviews on this matter^{32,33,40,41}.

MULTIFUNCTIONALITY OF MICROPARTICLES IN MICROFLUIDIC DEVICES

Especially attractive and powerful is that particles in microfluidic based assays may have different functionalities, as outlined below.

Particles offer a huge analytical surface.

Clearly, when compared with flat supports, three dimensional particles offer a huge surface which should improve the (bio) chemical reaction rates. Already one decade ago, Zammatteo et al. demonstrated faster nucleic acid hybridization kinetics when DNA-probes were coated on the surface of 4.5 μm sized particles instead of on the surface of the wells of microtiterplates⁴². Because the microparticles continuously move in the surrounding fluid (a very dynamic process), the reactions at their surface follow “near solution” kinetics. (Spherical) microparticles also have a high surface-to-volume ratio, which enables reactions to be performed in smaller volumes without confessing to a smaller reaction surface. This again leads to a smaller diffusion distance and a shorter analysis time. Interestingly, even in microfluidic devices, hybridization kinetics are faster if the probes are coupled to the surface of particles instead of the walls of the microchannels, as recently shown by Kim et al.⁴³. The authors showed the analysis of 2 μl volumes of samples on the order of a few minutes with flow rates of some hundreds of nanoliters per second. Not only hybridization reactions, but also protein-protein reactions take advantage of the size effect of the liquid microspace. Sato et al. demonstrated that the reaction time between antibodies and antigens coupled to the surface of 45- μm polystyrene particles in a microfluidic device is 1/90 of the time needed in a conventional microtiterplate⁴⁴. The overall analysis time was shortened from 24 hours to less than 1 hour and troublesome operations could be substantially limited. Worth mentioning is that new technologies are in progress which offer high flexibility for surface coating of microparticles which will further broaden their molecular applications^{34,45}.

Particles allow mixing.

Another advantage is that particles allow mixing, which is important for (bio) chemical reactions. Because of the dimensions, the Reynolds number of fluid flows in microfluidic devices is extremely small (usually less than 1). This means that the flow profile is laminar and that molecular transport only occurs by diffusion, which is relatively time-consuming despite the rather small dimensions involved in the assay. The lack of turbulence makes mixing in microdevices a very challenging issue. Liu et al. have shown that oscillating the sample within a microchip accelerates the

hybridization of nucleic acids to their probes spotted on the bottom of the channel ⁴⁶. As much as 5 times signal improvement was achieved with sample oscillation after 15 minutes of hybridization. Similar conclusions on hybridization kinetics using conventional microarrays were made by Pappaert et al.; they showed that a shear-driven flow reduces the analysis time (from 16 hours down to 30 minutes) ⁴⁷. The effect of sample oscillation could be improved even further by using microparticles which were continuously moved around in the sample to cause a local turbulent flow. This has been demonstrated by Seong et al. ⁴⁸ who studied how enzymes, immobilized on microparticles, convert their substrates. Herrmann et al. recently described a microfluidic ELISA (enzyme-linked immunosorbent assay) reaction at the surface of microparticles, using about 10^6 paramagnetic particles of 1 μm in diameter, trapped into a reaction chamber with dimensions of 6 mm x 2 mm x 50 μm and showed that mixing by applying an external magnetic field enhances the reaction speed ⁴⁹.

Particles allow sorting.

This is an important feature as particles allow the (a) enrichment of molecules of interest from complex samples, (b) separation of cells, viral particles and bacteria from a large population,...⁵⁰ Technical aspects related to sorting of samples with particles in microfluidics will be considered in Chapter 4.

Particles are very practical.

Particles are also of interest from a practical point of view. E.g. it is much easier to 'handle' (detect, trap, transport) microparticles than single molecules in microfluidic systems. Also, modifying the surface of microparticles is an easier process than modifying the walls of a microchannel in a chip. The surface of microparticles can be easily modified off-chip. Adding extra probes to an existing microfluidic based assay can simply be done by adding microparticles carrying the probes; No new device has to be produced. By adding more or less microparticles it is also straightforward to change the total capture surface (related to the number of probe molecules) in the assay; note that the total capture surface of a flat array (in a microwell or microarray) is constant. This can result in higher signals on particles than on flat arrays, for instance for enzyme/substrate reactions ⁴².

(Encoded) particles allow multiplexing.

This is highly important in situations where the amount of sample is very limited like in e.g. the analysis of blood from newborns, tumour tissue from biopsies... Additionally, multiplexing allows a more efficient and thereby less expensive use of reagents, and because the different targets are

screened simultaneously, they experience equal conditions in each step of the assay procedure. The integration of microparticles in microdevices for multiplexing goals is still in its early stage and only few publications demonstrated this synergism^{39,51,52}. Technical challenges related to this integration process will be overviewed in a separated chapter.

PARTICLE TRAPPING AND SORTING IN MICROFLUIDICS

Propulsion of fluids in microdevices.

Microfluidics involves the transport, manipulation and analysis of fluids or substances in fluids in micrometer-sized channels. Flow in microfluidics can be generated (a) mechanically (by pressure), (b) electrokinetically (electroosmotic flow; EOF), (c) by capillary forces or (d) by centrifugal forces. The type of propulsion force used is highly dependent on the application, the requested flow rate and the material composition of the the microchannel.

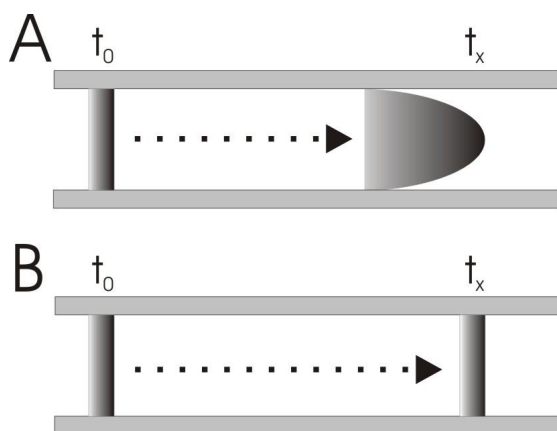


Figure 1: A pressure driven flow profile at time 0 and at time x after applying pressure. The profile is typically parabolic (higher velocities in the centre of the channel). B electrokinetically driven flow profile stays typically pluglike in the time (equal velocities in the centre as at the border of the channel)

In Figure 1, a typical pressure driven (e.g. caused by external syringe pumps) and electrokinetically driven flow profile is shown. The flow profile is parabolic (higher flow velocities in the centre than at the borders of the channel) and pluglike (equal velocities in the centre and at the borders of the channel), respectively. A parabolic flow profile can be attractive for the sorting of particles as will be further on described. On the other hand, an EOF is preferred for microchip

electrophoresis and electrochromatography, because the pluglike flow profile makes a more accurate separation possible^{53,54}. However, to allow EOF the surface of the microchannels has to be charged which requires appropriate materials to fabricate the microchannels. Also, EOF requires a specific buffer solution which should be compatible with the (bio)chemical assays.

Propulsion by capillary forces, driven by local heating of a fluid and due to the high heat-exchange rate in a microchannel, is still in an early stage of development and might not be compatible with (bio)chemical assaying in microfluidics as the high temperature can have a negative effect on the assay.

Centrifugal fluidic platforms (called lab-on-a-disc) were recently reviewed by Madou et al.⁵⁵ Due to the rotation speed it is possible to have identical flow rates, to load identical volumes, and to have identical incubation times in parallel assay capillaries. Therefore, they have great potential for parallel screening⁵⁶.

Manipulation of particles in microdevices.

To perform (bio)chemical reactions on a set of particles in microfluidic devices and to take full advantage of their multifunctionality (mixing, sorting, multiplexing,...), they usually have to be trapped into a constrained volume inside the chip, while samples and reagents are being flushed through the device. Sometimes more 'selective' methods are needed which aim to isolate and manipulate individual particles. For example, an excellent review on the manipulation of single cells in microfluidic devices has recently been published by Toner and Irimia⁵⁷; Some of the methods described herein are applicable to microparticles as well. However, as certain microparticles have unique properties complementary techniques to separate and sort microparticles in microchannels exist as well.

Mechanical trapping

The most straightforward method to trap microparticles is by the use of a mechanical barrier. "Mechanical trapping" is only based on the size of the particles. The simplest design is a continuous flow-through microchannel that contains a dam structure (Figure 2A) or an array of pillars transversal to the direction of the channel, and with gaps in-between the pillars that are smaller than the diameter of the particles (Figure 2B)⁴⁴. By means of mechanical barriers differently sized particles can be separated, however a single particle cannot 'selectively' be trapped and separated⁵⁸. Another inherent problem to mechanical trapping is clogging, especially in narrow channels. As Figure 2 C1

and Figure 2 C2 show, to avoid clogging of 5.5 μm sized polystyrene beads, Andersson et al. made use of a square filter-chamber (side length is 100 μm) filled with pillars (instead of using pillars in a channel; pillars are 3 μm wide with a spacing of 2 μm) surrounded by a waste chamber⁵⁹. Mechanical trapping of microparticles in a microdevice without clogging is also possible by microcontact printing⁶⁰, but this makes the system comparable with a microarray and thus less flexible. For the analysis of new targets, a new (microcontact printed) device has to be made.

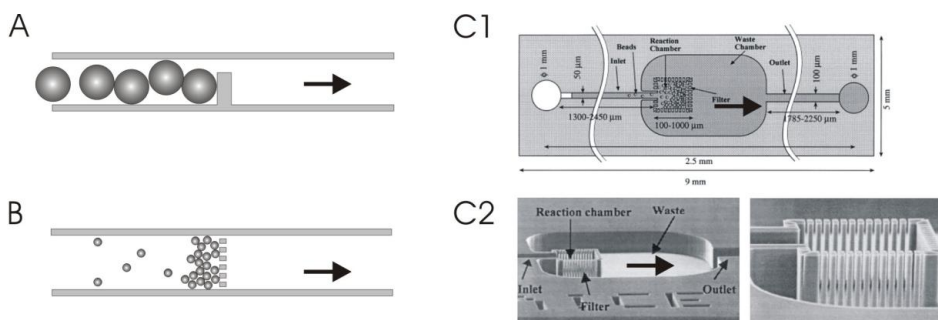


Figure 2: Schematics of a microchannel that contains a dam structure (A), an array of pillars transversal to the direction of the channel (B), and a filter-chamber (C1). The arrows show the direction of the flow. SEM images of the microchip with filter-chamber as proposed by Andersson et al. (C2). The pillars are 3 μm wide and 50 μm high with spacing of 2 μm . (Part C with permission from ref⁵⁹).

Magnetic trapping

Magnetic microparticles can also be immobilized and trapped in microdevices by means of magnetic forces exerted by an external rare earth magnet^{49,61}. The relatively large size of such an external magnet may, however, complicate a precise handling of the microparticles. This issue has recently been solved by using microfabricated 3D magnetic devices positioned in a continuous flow-through microfluidic chamber (10 mm x 5 mm x 0.1 mm)⁶². Magnetic particles between 1 and 5 μm in diameter were trapped at flow rates on the order of 10-100 $\mu\text{l}/\text{min}$. Another original concept is the manipulation of groups of magnetic particles, described by Rida and Gijs⁶³. The local rotational motion of the particles in a microfluidic flow, generated by an external local alternating magnetic field, enhances the interaction between the particles and the liquid: 95% mixing efficiency was achieved over a mixing length of 400 μm at flow rates on the order of 5 mm/s. A challenge remains the accurate manipulation (and separation) of individual particles by magnetic forces. Note that the presence of magnetic material in/on the microparticles is sometimes a limitation because it often renders them opaque.

Dielectrophoretic trapping

Electrically polarizable microparticles can be manipulated by dielectrophoresis (DEP) ⁶⁴. When such microparticles are subjected to an alternating electric field, a dipole moment is induced in the particles. In a non-uniform electrical field the polarized particles experience a dielectrophoretic force which may move them to regions of high or low electrical field. The motion depends on the particle polarizability compared to the suspending medium. The magnitude and direction of the dielectrophoretic force on a particle depends on its dielectric properties too, so that a heterogeneous mixture of microparticles in a continuous flow can be spatially separated to produce a more homogeneous population in an appropriate electrical field.

The separation of microparticles by DEP in a microdevice (DEP migration) has been demonstrated by several research groups. Kentsch et al. developed a particle-based assay for the detection of viruses in serum ⁶⁵. Kralj et al. simulated the flow behaviour of spherical particles in a DEP based device and verified experimentally the model for DEP sorting of differently sized particles ⁶⁶. The separation efficiency can be improved by combining DEP with other physical forces (DEP retention); Microparticles mechanically driven through a microdevice by pressure-based flow fields can be separated by a dielectrophoretic force perpendicular to the flow, because the particles acquire different velocities, due to the parabolic flow profile, depending on their dielectric characteristics. This is an example of what is called field-flow fractionation (FFF). In FFF particles move in a flow and become separated by an external force, perpendicular to the flow. Particles with different properties attain different positions relative to the chamber wall, due to a number of possible forces: diffusive, hydrodynamic, gravitational (sedimentational), electrophoretic, dielectric and other forces or a combination thereof ^{67,68}.

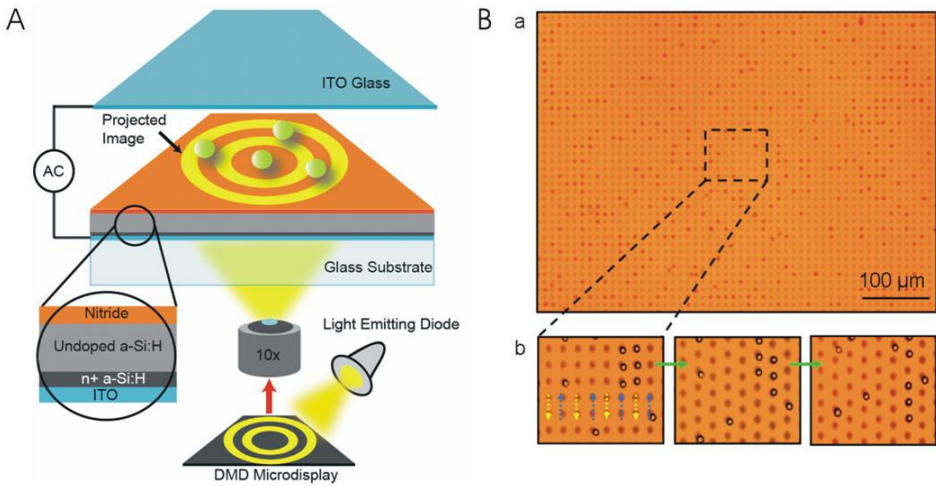


Figure 3: A Schematic overview of the microdevice used in optoelectronic tweezers (OET). Liquid that contains microscopic particles is sandwiched between the top indium tin oxide (ITO) glass and the bottom photosensitive surface consisting of ITO-coated glass covered with additional layers. The top and bottom surfaces are biased with an a.c. electric signal. A LED creates optical images on the digital micromirror display (DMD) which are then focused onto the photosensitive surface resulting in a non-uniform electric field for DEP manipulation. B Massively parallel manipulation of single particles by OET. (a) 15,000 particle traps are created across a 1.3mm x 1.0mm area. The 4.5- μm sized PS particles experiencing negative DEP forces are trapped in the darker circular areas. Single particle resolution is possible because each trap has a diameter of 4.5 μm . (b) Three snapshots from the video show parallel transportation of single particles in part of the manipulation area. The trapped particles in two adjacent columns move in opposite directions, as indicated by the blue and yellow arrows. (With permission from ref ⁶⁹).

DEP forces can be used to manipulate and trap individual microparticles as well. Indeed, by microelectrodes it is relatively easy to generate an electric field in a specific area of a microchip (the ‘particle trap’) with physical dimensions close to the size of the microparticles. Such ‘energy traps’ can hold particles against volumetric fluid flow rates of about 10 to 50 $\mu\text{l}/\text{min}$ by forces in the sub-piconewton range ^{70,71}. This technique is generally limited to trapping particles larger than approximately 1 μm because Brownian motion makes it difficult to trap smaller ones with sufficient accuracy, although some reports did describe the separation of submicron particles ⁷². For the trapping of multiple cells in parallel with single cell resolution, Taff and Voldman developed a DEP trap array in which multiple cells can be sorted individually ⁷³. This type of device can be used for particle sorting too, and recently the same research group has developed an array, possessing equal numbers of rows and columns, which needs only $2n$ electrodes to control n traps (which significantly simplified fabrication) ⁷¹. Another attractive approach that does not require patterned electrodes was demonstrated by Chiou et al. who developed a light-induced DEP trap; As Figure 3 shows, a light image was converted in an electrical field creating local DEP forces ⁶⁹. Each trap could be individually manipulated by programming the projected light images. The authors demonstrated

trapping of 4.5 μm sized polystyrene microparticles by parallel manipulation of 15 000 traps on a 1.3 mm x 1.0 mm area.

Optical trapping

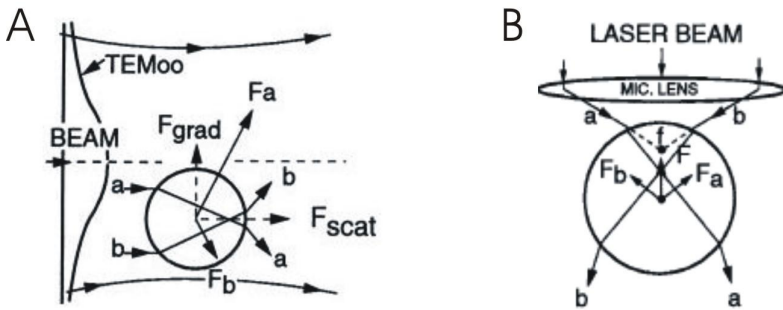


Figure 4: Illustration of forces that originate from radiation pressure A Consider a high index particle which is displaced from the TEM₀₀ beam axis of a mildly focused Gaussian light beam. A typical pair of rays "a" and "b" striking the sphere symmetrically about its center is shown. Because most of the rays refract through the particle (resulting in a change in momentum of the light), rays "a" and "b" result in forces F_a and F_b in the direction of the momentum change with $F_a > F_b$, because the intensity of ray "a" is higher than that of ray "b". Adding all such symmetrical pairs of rays striking the sphere, the resultant net force can be resolved into two components, the scattering force component (F_{scat}) pointing in the direction of the incident light, and a gradient component (F_{grad}) arising from the gradient in light intensity and pointing transversely toward the high intensity region of the beam. B Illustration of the ray diagram of a particle trapped in an optical trap (tweezers trap). The focus of the laser (f) is above the center of the particle, creating an upward gradient force, balanced by a downward scattering force (not shown), resulting in a stable laser trap. (With permission from ref ⁷⁴).

A fourth way to trap particles without 'physical contact' is optical trapping which is based on the response of a 'dielectric' microparticle to light. If a particle reflects or refracts incident laser light (with a 'Gaussian intensity profile'), it will result in a change in the momentum of the light (Figure 4A). Conservation of momentum requires that the particle must undergo an equal and opposite momentum change. The manipulation of neutral microparticles by a single laser beam that is strongly focused through a high NA objective is based on the same forces of radiation pressure, as depicted in Figure 4B. In this way the position of a single particle can be easily and accurately controlled in three dimensions, whereas in the case of DEP forces the manipulation of the particles is limited by the fixed configuration of the electrodes in the chip. The use of the so called 'optical tweezers' has been demonstrated by the group of Ashkin for the manipulation of individual (biological and polymeric) particles without optical damage ^{74,75}. Single beam trapping can nowadays also be done by using optical fibres as well ⁷⁶.

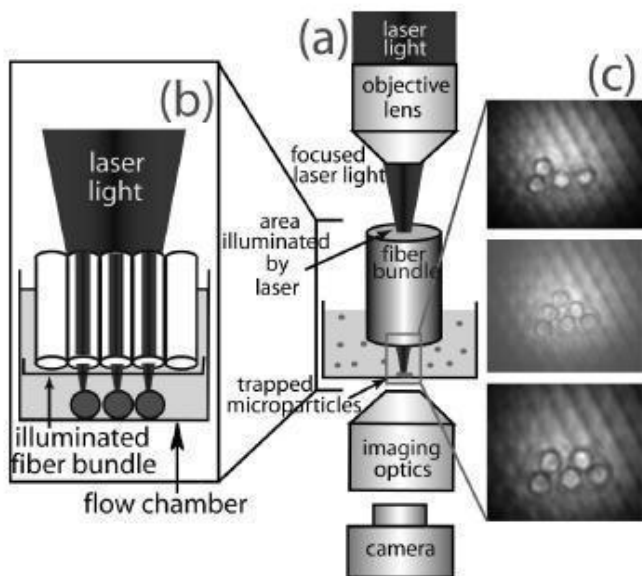


Figure 5: (a) Composition of an imaging fiber-based optical tweezer array system. (b) Detailed view on the region of the optical tweezer array system. Laser light illuminates a specific number of optical fibers in the array, depending on the magnification of the objective lens. All photons are continuously internally reflected on the inner walls of each fiber so that light travels down the length of the fiber. The lens elements (glass microparticles) at the end of each illuminated fiber focus the light into optical traps. Microparticles flowing into these regions become trapped by these fibers by approximately 12 mW of power (flow rate = 3 $\mu\text{m/s}$). (c) Consecutive images of trapped 4.5 μm sized silica microparticles. (With permission from ref ⁷⁷).

To trap multiple particles in parallel, efforts have been made to simultaneously generate multiple beams. However, only tens to hundreds of particles could be trapped at once ⁷⁸. A new approach to optically trap (tens of) thousands of microparticles in a single array was recently introduced by the group of Walt. The etched fibres of an optical fibre bundle are loaded at the end with glass microparticles, which act as spherical lenses. The light that is introduced via the fibre is focused by each lens, thereby creating an array of highly focused points of light ^{77,79} (Figure 5). A dense array ($\sim 5 \times 10^4$ traps/ mm^2 using fibre bundles with 3 μm diameter cores) can be made in this way, from which the number of optical traps is determined by the number of fibres in the optical fibre bundle. The authors demonstrated trapping of 4.5 μm sized silica particles from a particle solution with a flow rate of 3 $\mu\text{m/s}$ and calculated that each particle was trapped with approximately 12 mW of power.

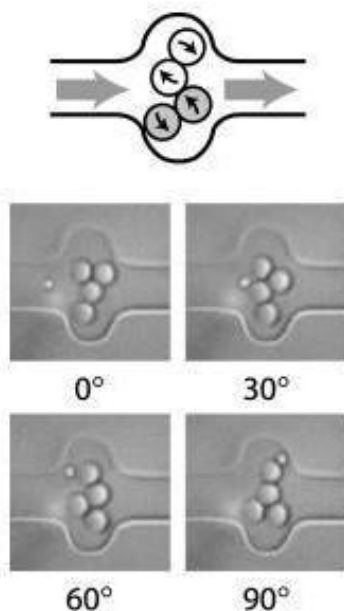


Figure 6: Two groups (“lobes”) of 3 μm sized particles (two particles per group) are rotated in opposite directions by means of optical trapping (the top pair rotates clockwise, the bottom counterclockwise). Those functional structures are able to generate a net fluid movement from left to right. A net flow is achieved by repeated and rapid rotations and the direction of the flow can be reversed by changing the rotation direction of the lobes. Frames are separated by two cycles to show movement of a 1.5- μm colloidal silica tracer particle. (With permission from ref ⁸⁰).

An attractive application of optical trapping in microdevices has been reported by Terray et al.; By optical trapping they have succeeded in arranging groups of 3- μm silica microspheres into functional structures which could subsequently be activated to generate microfluidic valving and pumping with flow rates of about 1 nl/hour ⁸⁰ (Figure 6). MacDonald et al. used a three-dimensional optical lattice to deflect selectively microparticles in a flow of mixed particles in a microdevice, while other particles are not hindered and pass straight through. The strength of the interaction between the particles and the lattice depends on their optical polarizability. A high sorting efficiency was demonstrated, even for throughputs of 25 particles per second ⁸¹.

To obtain a more precise (single particle) trapping, DEP and optical tweezing have been combined by Arai et al. They describe a device in which DEP and laser trapping forces are used to selectively isolate one single microbe from of a huge population in a microdevice in less than 20 s ⁸². Laser trapping was used to trap the microbe of interest, while DEP forces were applied to exclude other objects around the target microbe. Reichle et al. combined DEP and optical tweezing (OT) for receptor-ligand interactions on single cells in microdevices ⁸³. Ligands were coupled to particles of 4.1

μm in diameter which were brought in contact by OT with the cell (receptors). The latter one was held in a DEP cage.

INTEGRATION OF DECODING AND DETECTION PLATFORMS

Despite the popularity of the conventional flow (cyto)meters for multiplexing, combining them with microfluidic chips is, unfortunately, not straightforward; after carrying out the (bio)chemical reactions in the chip (the recipient), the particles have to be transferred to the flow cytometer (which is also the case when an optical fibre platform would be used) which is not desirable. Also, the currently available flow cytometers are relatively expensive, cumbersome (difficult to handle because size and weight) and need trained personnel.

(Fluorescent) microscope reading platforms, which allow both the (fluorescence) analysis of the (bio)chemical reaction at the particle's surface as well as the decoding by simply placing the particle containing microfluidic device under a microscope are of high interest. Nevertheless, for that purpose some requirements need to be fulfilled. First, the part of the microfluidic device where decoding and detection of the particles occurs should be optically transparent and compatible with the microscope optics. Besides thin glass also other materials like poly(dimethylsiloxane) (PDMS) are used to this end⁸⁴⁻⁸⁶. Secondly, the movement of the particles must be negligible during image acquisition in the case of graphically encoded particles to avoid blurring of the code. This can be accomplished by the trapping techniques described above. If the microparticles are located closely to each other, parallel detection of multiple particles should be possible. The number of particles detected simultaneously will depend on the trapping system, the dimensions of the detection chamber, the field-of-view and the size of the particles. Thirdly, suitable dimensions should be selected for the particle detection chamber since the encoded particles have to be arranged in a monolayer. For example, Yuen et al. developed a microdevice in which glass microbarcodes can be arranged next to each other by means of centrifugal forces⁸⁷. The device consists of a central 1 mm high reservoir, surrounded by a 35 μm high sorting region (less than twice the height of the 20 μm x 20 μm x 100 μm microbarcodes). The outer side of the sorting region was connected to a network of sixty 20 μm wide microchannels (equal to the width of the microbarcodes). After loading a suspension of the microbarcodes in the central reservoir, a monolayer of microbarcodes was formed in the sorting region by spinning the device. The microchannels stopped the microbarcodes from passing through, but acted as a drain for the liquid. The group of Ducree arranged particles in a

monolayer within a disk-based detection chamber, which allowed parallel read-out of multiplexed particle-based immunoassays^{39,88}.

As mentioned above, apart from microscope reading systems, other types of currently available reading instruments are not easily compatible with microfluidic devices. Microtechnology research is currently going on to integrate electronics, optics, and detectors in microfluidic devices. The next section overviews recent advances in this field.

Micro flow (cyto)meter.

Advances in flow (cyto)metric analysis of cells and particles in microfluidic devices have recently been described^{89,90}. Meanwhile the first commercial microfabricated flow (cyto)meter has become commercially available (2100 Bioanalyzer, Agilent Technologies). Similar to conventional flow (cyto)meters, micro flow meters require precise fabrication to obtain optimal fluid flows in which particles are hydrodynamically focused into a single-file stream. The cost and complexity of fabricating fluidic components, traditionally made of glass, can be reduced by using inexpensive polymers like PDMS or SU-8^{91,92}. Although sheath liquid-based hydrodynamic focusing serves as a standard technology in both conventional and micro flow (cyto)meters, it requires a large volume of sheath liquid to process a very small amount of sample (up to 1L for 1mL of sample) preventing further reduction in size and volume of the whole system. It also needs continuous pumping of sheath liquid at high flow rates to generate a thin sample stream. Alternatively, ambient air can be used⁹³.

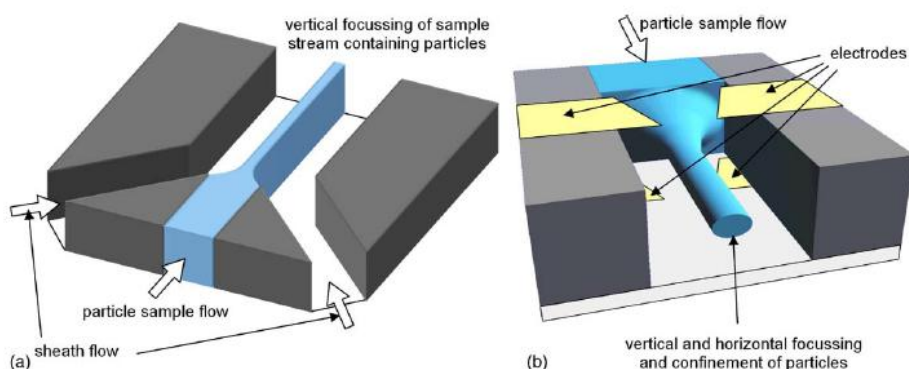


Figure 7: (a) Illustration of the origin of 1-D hydrodynamic focusing. The input particle stream is confined on both sides by sheath flow resulting in a focusing of the particle stream. (b) Illustration of 2-D focusing of particles in an input sample stream by means of dielectrophoresis. 100 nm thin microelectrodes on the top and bottom of the channel push the particles into the centre of the microchannel. The electrodes do not influence the fluid flow. (With permission from ref⁹⁴).

Another attractive approach is to use two-dimensional (2D) focusing of microparticles in a microdevice. This is illustrated in Figure 7 where Holmes et al. obtained a cylindrically focused particle sample flow (in a device of 40 μm high and 250 μm wide) by means of dielectrophoresis (generated by 100 nm thin microelectrodes on the top and bottom of the channel)⁹⁴. Latex particles with a diameter of 6 μm were detected at a throughput of up to 250 particles per second. 2D hydrodynamic focusing in a pressure driven flow was reported by Simonnet et al.^{95,96}. They demonstrated a high-throughput microfluidic device which could analyze as many as 17 000 particles/s (particle size of 1.9 μm) and had fluorescence detection accuracy comparable with that of commercial flow cytometers. Finally focussing can also be obtained electrokinetically⁹⁷. Already in 1999 Fu et al. demonstrated the basic principle of a microfabricated fluorescence-activated cell sorter, which could sort fluorescent microparticles at a throughput of approximately 10 particles per second⁹⁸. Sorting was obtained via electrokinetic flow switching. The same sorting technique was later on used by Dittrich et al., where sorting was preceded by reaction and detection on the same chip⁸⁴. Meanwhile, other flow-switching techniques were introduced: hydrodynamic and valve switching^{99,100}. For more information on this, we refer the interested reader to an excellent recent review regarding μFACS systems written by Huh et al.⁸⁹.

Light-emitting diodes and detectors.

In the previous chapter it was explained that high throughput screening of encoded microcarriers by means of the existing optical reading instruments is possible 'on a chip', while the optical components, such as the light source, sensors, lenses and waveguides, remain 'off the chip'. In meanwhile, researchers have taken on-chip high-throughput screening systems of encoded microcarriers one step further by integrating optics on the chip. The group of deMello reported thin-film polymer (polyfluorene-based) light-emitting diodes (LEDs) and thin-film organic photodiodes as integrated excitation sources and detectors, respectively^{101,102}. Since the LED is a very small, low-power, inexpensive device, it can be integrated into microfluidics as a disposable light source. Recently, the same group made progress in the fabrication of disposable high quality monolithically integrated optical filters¹⁰³. Chabynic et al. reported the integration of an optical fiber and a fluorescence detector based on a microavalanche photodiode (μAPD) into a microfluidic device fabricated in PDMS¹⁰⁴. No transfer optics were necessary, because the pixel size of the μAPD matched the dimensions of the channels and the μAPD was incorporated in close proximity to the

microchannel. However, in this system there was a lot of light loss because focusing of the LED light was not possible on the optical fiber (100 μm diameter) that coupled light into the microdevice, resulting in ineffective illumination and insensitive analyses. This can be circumvented, as reported by Miyaki et al., by placing the light-emitting face of the LED close to the microchannel by incorporation into the chip fabricated through in situ polymerisation: the detection sensitivity was comparable to that of laser induced fluorescence⁸⁶. Seo and Lee have reported work on a disposable integrated device with self-aligned planar microlenses for bioanalytical systems, having LEDs as excitation sources and photodiodes as detectors¹⁰⁵. The lenses enable an increased detection sensitivity and a reduced time for optical alignments.

Optofluidics.

In the previous paragraph, the integration of solid state optics in microfluidic devices was described, in order to make the device more compact. Meanwhile, a new field of optics has been explored, which is called 'optofluidics'. This refers to materials which are fabricated through the integration of optical components and fluids on the same chip, resulting in optical instruments that are fabricated with fluids. Lenses with a perfect curvature (a perfect spherical meniscus) can be made for instance from fluid-only devices at much lower cost than solid state optical-quality lenses. Recently, a novel microfluidic based lensless imaging technique, termed optofluidic microscopy (OFM) has been reported (Figure 8)^{106,107}. The feasibility of the method was demonstrated by imaging of *C. elegans*. The acquired OFM images are comparable to that obtained with a conventional microscope (40 \times objective lens). The measured resolution limit of the OFM was 490 ± 40 nm. A high throughput imaging rate of approximately 40 worms/min was achieved, corresponding to a sample transport rate of 300 $\mu\text{m}/\text{second}$. Considering encoded particles of around 10 μm , a maximal velocity of 30 particles/sec can be achieved. As about 45% of the acquired images were rejected due to sample rotation and aggregation, the effective detection velocity will be much lower. Especially for graphical encoded particles sample rotation may cause a mistake in read-out of the code (e.g. by altering the diffraction pattern). In order to prevent the misinterpretation of the code Pregibon et al. added orientation indicators to its graphical encoded fluorescently dyed particles⁵². For encoded carriers having a magnetic memory, OFM in combination with an external magnetic field could be used⁴⁵. During imaging with the OFM those particles can be oriented for their code to be visible by applying a weak magnetic field.

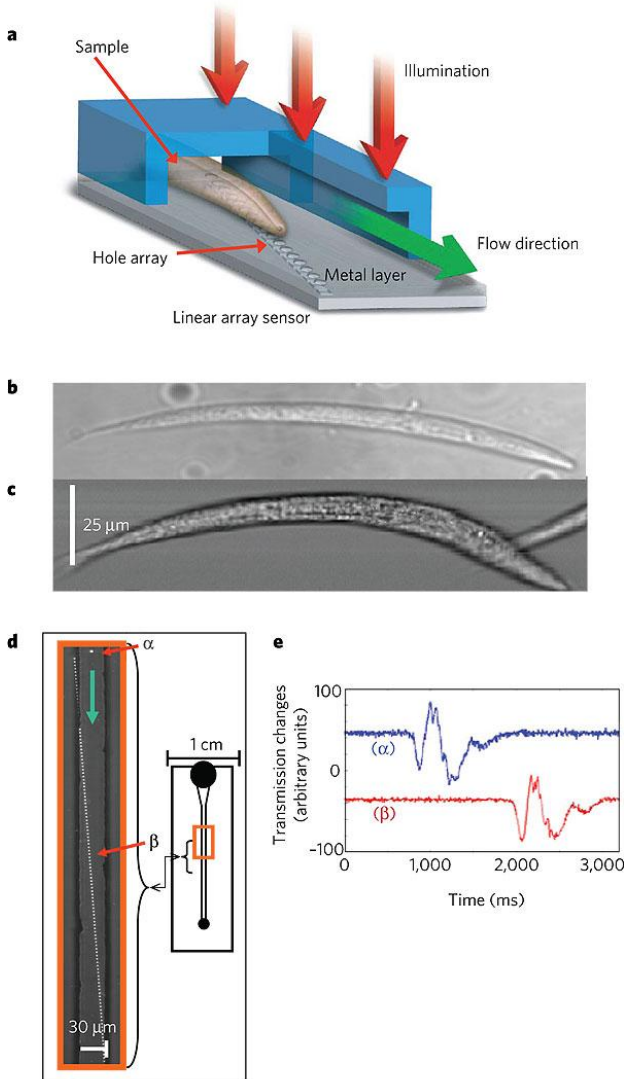


Figure 8: Illustration of the optofluidic microscope (OFM) integrated in a microdevice. The microfluidic channel is 15 μm tall and 30 μm wide. The channel is bonded onto a metal layer with an etched nano-aperture array (length = 600 μm , diameter apertures = 600 nm, spacing = 5 μm) (a) The device is uniformly illuminated from the top. The target sample flows through the channel, and the transmission through each hole is recorded on a linear array sensor (the device can be fabricated directly onto a CCD array). The composition of the transmission traces creates a transmission image of the target sample. (b) A conventional microscope image of *C. elegans* is comparable with (c) an optofluidic microscope image of *C. elegans*. The OFM has a measured resolution limit of 490 ± 40 nm. (d) By staggering the holes along the length of the channel, the separation between holes can be made equal to the pixel size of the underlying sensor array and enable the unique mapping of each hole to a pixel. The lateral displacement of the holes across the channel can be made arbitrarily small and it defines the resolution of the microscope. (e) The transmission trace through two representative holes, α and β , on the microscope as the sample flows across them. (With permission from ref ¹⁰⁷).

Optical imaging fibers.

Multiple articles describe the implementation of optical imaging fibres into microfluidics^{86,104}. However, the implementation of optical fibre arrays is still under development. The group of Walt recently developed the first microfluidic platform equipped with an optical imaging fiber microarray capable to detect DNA at the attomolar level. The use of a microfluidic platform enabled faster DNA hybridisations, lower sample volumes and a 100-fold more sensitive detection when compared with a static platform (where the fiber is submerged in the target DNA sample and hybridization occurred by diffusion only): the minimal detectable concentration with the microfluidic platform was equal to 10 aM after 15 minutes of hybridization of a 50 μ l target DNA sample at flow rates of 1 μ l/min, compared with 1 pM detection with the static platform after 30 minutes of hybridization of a 200 μ l target DNA sample¹⁰⁸. As is the case for the microscope reading platforms, future developments in order to incorporate multiplexed microparticle arrays, optics, fluidic channels, and a detection unit, are necessary before a portable system becomes reality.

CONCLUSIONS AND FUTURE PERSPECTIVES

This review focused on miniaturised multiplexing using encoded microparticles. The combination of microfluidic technologies with encoded microparticle-arrays is a very promising lab-on-a-chip tool, due to the remarkable characteristics of both technologies which complete each other. A special emphasis is on the challenges which exist to integrate currently existing detection platforms for encoded microparticles in microdevices. Nowadays the flow-cytometer is a very popular detection platform for medium-throughput particle-based ‘macroscopic’ multiplexing assays. When comparing the opportunities of conventional decoding instruments for miniaturized multiplexing, it seems that the microscope reading platforms have a clear advantage over the other platforms because the microparticles can remain on the chip for decoding, as long as the microdevice is optically transparent. Recent research shows that optical fibres may be usable ‘on-chip’ too. However, therefore the fiber (carrying the encoded particles) will have to be inserted in a microchip in a sealed way without liquid leakage.

Nowadays, developments are going on in the field of microtechnologies in order to down-scale the decoding unit to the microlevel, which circumvents the use of conventional instruments for miniaturized multiplexing. Considerable cost savings can potentially be realized by integrating optics, electronics, and detection instruments on-chip, in close proximity to the microchannels carrying the multiplexed microparticle-arrays. Although this field is still in its infancy, it will probably result in new fundamental concepts for the decoding of miniaturized multiplexed microparticle assays with the same throughput as the existing conventional decoding instruments, which will finally replace the latter ones. Promising examples are the first generation of micro-flow cytometers, integrated light-emitting diodes and detectors, and so on.

Which type of detection system will become popular for multiplexing in microfluidics devices, will not only depend on decoding system-associated parameters, like portability, costs, and ease of use, but also on, for instance, the level of multiplexing that can be achieved. The latter one depends on the encoding way of the microparticles and is mainly defined by the application goal of the microparticle-array (genotyping, protein analysis, gene expression analysis...). Advances in encoding technologies of microcarriers are expected to result in new multiplexing platforms and will therefore certainly influence the future choice of detection/decoding system.

Finally, the goal of those integrated lab-on-a-chip tools is point-of-care assessment. To this purpose, the real challenge will come from the coupling of the decoding modules under investigation in this study in an appropriate way on one chip to other advanced modules for sub-tasks, such as blood processing, extraction of DNA, RNA or proteins, and so on. In order to bring diagnostics closer to the patient, future requirements will also involve progress in non-hardware tools, like data acquisition, data management... Research in each of these fields is full of promise, and within the next decade, the first prototypes of multiplexed particle-based LOC tools can probably be expected, assuming that new nano-engineering technologies are rapidly accepted.

REFERENCES

1. Whitesides, G. M. The origins and the future of microfluidics. *Nature* **2006**, *442* (7101), 368-373.
2. Sato, K.; Hibara, A.; Tokeshi, M.; Hisamoto, H.; Kitamori, T. Integration of chemical and biochemical analysis systems into a glass microchip. *Anal. Sci.* **2003**, *19* (1), 15-22.
3. Figeys, D.; Pinto, D. Lab-on-a-chip: a revolution in biological and medical sciences. *Anal. Chem.* **2000**, *72* (9), 330A-335A.
4. Manz, A.; Graber, N.; Widmer, H. M. Miniaturized Total Chemical-Analysis Systems - A Novel Concept for Chemical Sensing. *Sensors and Actuators B-Chemical* **1990**, *1* (1-6), 244-248.
5. Craighead, H. Future lab-on-a-chip technologies for interrogating individual molecules. *Nature* **2006**, *442* (7101), 387-393.
6. Gao, J.; Yin, X. F.; Fang, Z. L. Integration of single cell injection, cell lysis, separation and detection of intracellular constituents on a microfluidic chip. *Lab Chip* **2004**, *4* (1), 47-52.
7. Beebe, D. J.; Mensing, G. A.; Walker, G. M. Physics and applications of microfluidics in biology. *Annu. Rev. Biomed. Eng* **2002**, *4*, 261-286.
8. Chovan, T.; Guttman, A. Microfabricated devices in biotechnology and biochemical processing. *Trends Biotechnol.* **2002**, *20* (3), 116-122.
9. Jakeway, S. C.; de Mello, A. J.; Russell, E. L. Miniaturized total analysis systems for biological analysis. *Fresenius. J. Anal. Chem.* **2000**, *366* (6-7), 525-539.
10. deMello, A. J. Control and detection of chemical reactions in microfluidic systems. *Nature* **2006**, *442* (7101), 394-402.
11. Janasek, D.; Franzke, J.; Manz, A. Scaling and the design of miniaturized chemical-analysis systems. *Nature* **2006**, *442* (7101), 374-380.
12. Bange, A.; Halsall, H. B.; Heineman, W. R. Microfluidic immunosensor systems. *Biosens. Bioelectron.* **2005**, *20* (12), 2488-2503.
13. Hansen, C.; Quake, S. R. Microfluidics in structural biology: smaller, faster em leader better. *Curr. Opin. Struct. Biol.* **2003**, *13* (5), 538-544.
14. Lion, N.; Reymond, F.; Girault, H. H.; Rossier, J. S. Why the move to microfluidics for protein analysis? *Curr. Opin. Biotechnol.* **2004**, *15* (1), 31-37.
15. Tudos, A. J.; Besselink, G. J.; Schasfoort, R. B. Trends in miniaturized total analysis systems for point-of-care testing in clinical chemistry. *Lab Chip*. **2001**, *1* (2), 83-95.
16. Holland, C. A.; Kiechle, F. L. Point-of-care molecular diagnostic systems--past, present and future. *Curr. Opin. Microbiol.* **2005**, *8* (5), 504-509.
17. Verpoorte, E. Microfluidic chips for clinical and forensic analysis. *Electrophoresis* **2002**, *23* (5), 677-712.
18. Huang, Y.; Mather, E. L.; Bell, J. L.; Madou, M. MEMS-based sample preparation for molecular diagnostics. *Anal. Bioanal. Chem.* **2002**, *372* (1), 49-65.

19. Vo-Dinh, T.; Cullum, B. Biosensors and biochips: advances in biological and medical diagnostics. *Fresenius. J. Anal. Chem.* **2000**, *366* (6-7), 540-551.
20. Dupuy, A. M.; Lehmann, S.; Cristol, J. P. Protein biochip systems for the clinical laboratory. *Clin. Chem. Lab Med.* **2005**, *43* (12), 1291-1302.
21. Walt, D. R. Chemistry. Miniature analytical methods for medical diagnostics. *Science* **2005**, *308* (5719), 217-219.
22. Garcia-Egido, E.; Spikmans, V.; Wong, S. Y.; Warrington, B. H. Synthesis and analysis of combinatorial libraries performed in an automated micro reactor system. *Lab Chip* **2003**, *3* (2), 73-76.
23. Dittrich, P. S.; Manz, A. Lab-on-a-chip: microfluidics in drug discovery. *Nature Reviews Drug Discovery* **2006**, *5* (3), 210-218.
24. Haeberle, S.; Zengerle, R. Microfluidic platforms for lab-on-a-chip applications. *Lab Chip* **2007**, *7* (9), 1094-1110.
25. Situma, C.; Hashimoto, M.; Soper, S. A. Merging microfluidics with microarray-based bioassays. *Biomol. Eng* **2006**, *23* (5), 213-231.
26. Sato, K.; Yamanaka, M.; Takahashi, H.; Tokeshi, M.; Kimura, H.; Kitamori, T. Microchip-based immunoassay system with branching multichannels for simultaneous determination of interferon-gamma. *Electrophoresis* **2002**, *23* (5), 734-739.
27. Kartalov, E. P.; Zhong, J. F.; Scherer, A.; Quake, S. R.; Taylor, C. R.; Anderson, W. F. High-throughput multi-antigen microfluidic fluorescence immunoassays. *Biotechniques* **2006**, *40* (1), 85-90.
28. Elshal, M. F.; McCoy, J. P. Multiplex bead array assays: performance evaluation and comparison of sensitivity to ELISA. *Methods* **2006**, *38* (4), 317-323.
29. Kersten, B.; Wanker, E. E.; Hoheisel, J. D.; Angenendt, P. Multiplex approaches in protein microarray technology. *Expert. Rev. Proteomics.* **2005**, *2* (4), 499-510.
30. Ling, M. M.; Ricks, C.; Lea, P. Multiplexing molecular diagnostics and immunoassays using emerging microarray technologies. *Expert. Rev. Mol. Diagn.* **2007**, *7* (1), 87-98.
31. Lockhart, D. J.; Winzler, E. A. Genomics, gene expression and DNA arrays. *Nature* **2000**, *405* (6788), 827-836.
32. Braeckmans, K.; De Smedt, S. C.; Leblans, M.; Pauwels, R.; Demeester, J. Encoding microcarriers: present and future technologies. *Nat. Rev. Drug Discov.* **2002**, *1* (6), 447-456.
33. Yingyongnarongkul, B. E.; How, S. E.; az-Mochon, J. J.; Muzerelle, M.; Bradley, M. Parallel and multiplexed bead-based assays and encoding strategies. *Comb. Chem. High Throughput. Screen.* **2003**, *6* (7), 577-587.
34. Nolan, J. P.; Sklar, L. A. Suspension array technology: evolution of the flat-array paradigm. *Trends Biotechnol.* **2002**, *20* (1), 9-12.
35. Wilson, R.; Cossins, A. R.; Spiller, D. G. Encoded microcarriers for high-throughput multiplexed detection. *Angew. Chem. Int. Ed Engl.* **2006**, *45* (37), 6104-6117.
36. Delehanty, J. B.; Ligler, F. S. A microarray immunoassay for simultaneous detection of proteins and bacteria. *Anal. Chem.* **2002**, *74* (21), 5681-5687.
37. Bernard, A.; Michel, B.; Delamarque, E. Micromosaic immunoassays. *Anal. Chem.* **2001**, *73* (1), 8-12.

38. Wolf, M.; Juncker, D.; Michel, B.; Hunziker, P.; Delamarque, E. Simultaneous detection of C-reactive protein and other cardiac markers in human plasma using micromosaic immunoassays and self-regulating microfluidic networks. *Biosens. Bioelectron.* **2004**, *19* (10), 1193-1202.
39. Riegger, L.; Grumann, M.; Nann, T.; Riegler, J.; Ehlert, O.; Bessler, W.; Mittenbuehler, K.; Urban, G.; Pastewka, L.; Brenner, T.; Zengerle, R.; Ducree, J. Read-out concepts for multiplexed bead-based fluorescence immunoassays on centrifugal microfluidic platforms. *Sensors and Actuators A-Physical* **2006**, *126* (2), 455-462.
40. Venkatasubbarao, S. Microarrays--status and prospects. *Trends Biotechnol.* **2004**, *22* (12), 630-637.
41. Wilson, R.; Cossins, A. R.; Spiller, D. G. Encoded microcarriers for high-throughput multiplexed detection. *Angew. Chem. Int. Ed Engl.* **2006**, *45* (37), 6104-6117.
42. Zamatteo, N.; Alexandre, I.; Ernest, I.; Le, L.; Brancart, F.; Remacle, J. Comparison between microwell and bead supports for the detection of human cytomegalovirus amplicons by sandwich hybridization. *Anal. Biochem.* **1997**, *253* (2), 180-189.
43. Kim, J.; Heo, J.; Crooks, R. M. Hybridization of DNA to Bead-Immobilized Probes Confined within a Microfluidic Channel. *Langmuir* **2006**, *22* (24), 10130-10134.
44. Sato, K.; Tokeshi, M.; Otake, T.; Kimura, H.; Ooi, T.; Nakao, M.; Kitamori, T. Integration of an immunosorbent assay system: analysis of secretory human immunoglobulin A on polystyrene beads in a microchip. *Anal. Chem.* **2000**, *72* (6), 1144-1147.
45. Derveaux, S.; Geest, B. G.; Roelant, C.; Braeckmans, K.; Demeester, J.; Smedt, S. C. Multifunctional Layer-by-Layer Coating of Digitally Encoded Microparticles. *Langmuir* **2007**, *23* (20), 10272-10279.
46. Liu, Y.; Rauch, C. B. DNA probe attachment on plastic surfaces and microfluidic hybridization array channel devices with sample oscillation. *Anal. Biochem.* **2003**, *317* (1), 76-84.
47. Pappaert, K.; Vanderhoeven, J.; Van, H. P.; Dutta, B.; Cliecq, D.; Baron, G. V.; Desmet, G. Enhancement of DNA micro-array analysis using a shear-driven micro-channel flow system. *J. Chromatogr. A* **2003**, *1014* (1-2), 1-9.
48. Seong, G. H.; Crooks, R. M. Efficient mixing and reactions within microfluidic channels using microbead-supported catalysts. *Journal of the American Chemical Society* **2002**, *124* (45), 13360-13361.
49. Herrmann, M.; Veres, T.; Tabrizian, M. Enzymatically-generated fluorescent detection in micro-channels with internal magnetic mixing for the development of parallel microfluidic ELISA. *Lab Chip* **2006**, *6* (4), 555-560.
50. Horak, D.; Babic, M.; Mackova, H.; Benes, M. J. Preparation and properties of magnetic nano- and microsized particles for biological and environmental separations. *J. Sep. Sci.* **2007**, *30* (11), 1751-1772.
51. Klostranec, J. M.; Xiang, Q.; Farcas, G. A.; Lee, J. A.; Rhee, A.; Lafferty, E. I.; Perrault, S. D.; Kain, K. C.; Chan, W. C. Convergence of quantum dot barcodes with microfluidics and signal processing for multiplexed high-throughput infectious disease diagnostics. *Nano Lett.* **2007**, *7* (9), 2812-2818.
52. Pregibon, D. C.; Toner, M.; Doyle, P. S. Multifunctional encoded particles for high-throughput biomolecule analysis. *Science* **2007**, *315* (5817), 1393-1396.

53. Szekely, L.; Guttman, A. New advances in microchip fabrication for electrochromatography. *Electrophoresis* **2005**, *26* (24), 4590-4604.
54. Wang, W.; Zhou, F.; Zhao, L.; Zhang, J. R.; Zhu, J. J. Measurement of electroosmotic flow in capillary and microchip electrophoresis. *J. Chromatogr. A* **2007**, *1170* (1-2), 1-8.
55. Madou, M.; Zoval, J.; Jia, G.; Kido, H.; Kim, J.; Kim, N. Lab on a CD. *Annu. Rev. Biomed. Eng* **2006**, *8*, 601-628.
56. Lai, S.; Wang, S.; Luo, J.; Lee, L. J.; Yang, S. T.; Madou, M. J. Design of a compact disk-like microfluidic platform for enzyme-linked immunosorbent assay. *Anal. Chem.* **2004**, *76* (7), 1832-1837.
57. Toner, M.; Irimia, D. Blood-on-a-chip. *Annual Review of Biomedical Engineering* **2005**, *7*, 77-103.
58. Huang, L. R.; Cox, E. C.; Austin, R. H.; Sturm, J. C. Continuous particle separation through deterministic lateral displacement. *Science* **2004**, *304* (5673), 987-990.
59. Andersson, H.; van der, W. W.; Stemme, G. Micromachined filter-chamber array with passive valves for biochemical assays on beads. *Electrophoresis* **2001**, *22* (2), 249-257.
60. Andersson, H.; Jonsson, C.; Moberg, C.; Stemme, G. Patterned self-assembled beads in silicon channels. *Electrophoresis* **2001**, *22* (18), 3876-3882.
61. Fan, Z. H.; Mangru, S.; Granzow, R.; Heaney, P.; Ho, W.; Dong, Q.; Kumar, R. Dynamic DNA hybridization on a chip using paramagnetic beads. *Anal. Chem.* **1999**, *71* (21), 4851-4859.
62. Ramadan, Q.; Samper, V.; Poenar, D. P.; Yu, C. An integrated microfluidic platform for magnetic microbeads separation and confinement. *Biosens. Bioelectron.* **2006**, *21* (9), 1693-1702.
63. Rida, A.; Gijs, M. A. Manipulation of self-assembled structures of magnetic beads for microfluidic mixing and assaying. *Anal. Chem.* **2004**, *76* (21), 6239-6246.
64. Pohl, H. A. Dielectrophoresis. *Cambridge University Press* **1978**.
65. Kentsch, J.; Durr, M.; Schnelle, T.; Gradl, G.; Muller, T.; Jager, M.; Normann, A.; Stelzle, M. Microdevices for separation, accumulation, and analysis of biological micro- and nanoparticles. *IEE Proc. Nanobiotechnol.* **2003**, *150* (2), 82-89.
66. Kralj, J. G.; Lis, M. T.; Schmidt, M. A.; Jensen, K. F. Continuous dielectrophoretic size-based particle sorting. *Anal. Chem.* **2006**, *78* (14), 5019-5025.
67. Wang, X. B.; Vykoukal, J.; Becker, F. F.; Gascoyne, P. R. Separation of polystyrene microbeads using dielectrophoretic/gravitational field-flow-fractionation. *Biophys. J.* **1998**, *74* (5), 2689-2701.
68. Pethig, R.; Markx, G. H. Applications of dielectrophoresis in biotechnology. *Trends Biotechnol.* **1997**, *15* (10), 426-432.
69. Chiou, P. Y.; Ohta, A. T.; Wu, M. C. Massively parallel manipulation of single cells and microparticles using optical images. *Nature* **2005**, *436* (7049), 370-372.
70. Voldman, J.; Braff, R. A.; Toner, M.; Gray, M. L.; Schmidt, M. A. Holding forces of single-particle dielectrophoretic traps. *Biophys. J.* **2001**, *80* (1), 531-541.
71. Taff, B. M.; Voldman, J. A scalable addressable positive-dielectrophoretic cell-sorting array. *Anal. Chem.* **2005**, *77* (24), 7976-7983.

-
72. Morgan, H.; Hughes, M. P.; Green, N. G. Separation of submicron bioparticles by dielectrophoresis. *Biophys. J.* **1999**, *77* (1), 516-525.
 73. Voldman, J.; Gray, M. L.; Toner, M.; Schmidt, M. A. A microfabrication-based dynamic array cytometer. *Anal. Chem.* **2002**, *74* (16), 3984-3990.
 74. Ashkin, A. Optical trapping and manipulation of neutral particles using lasers. *Proc. Natl. Acad. Sci. U. S. A* **1997**, *94* (10), 4853-4860.
 75. Ashkin, A.; Dziedzic, J. M. Optical trapping and manipulation of viruses and bacteria. *Science* **1987**, *235* (4795), 1517-1520.
 76. Taguchi, K.; Atsuta, K.; Nakata, T.; Ikeda, M. Single laser beam fiber optic trap. *Optical and Quantum Electronics* **2001**, *33* (1), 99-106.
 77. Tam, J. M.; Biran, I.; Walt, D. R. An imaging fiber-based optical tweezer array for microparticle array assembly. *Applied Physics Letters* **2004**, *84* (21), 4289-4291.
 78. Daria, V. R.; Rodrigo, P. J.; Gluckstad, J. Dynamic formation of optically trapped microstructure arrays for biosensor applications. *Biosens. Bioelectron.* **2004**, *19* (11), 1439-1444.
 79. Tam, J. M.; Biran, I.; Walt, D. R. Parallel microparticle manipulation using an imaging fiber-bundle-based optical tweezer array and a digital micromirror device. *Applied Physics Letters* **2006**, *89* (19).
 80. Terray, A.; Oakey, J.; Marr, D. W. Microfluidic control using colloidal devices. *Science* **2002**, *296* (5574), 1841-1844.
 81. MacDonald, M. P.; Spalding, G. C.; Dholakia, K. Microfluidic sorting in an optical lattice. *Nature* **2003**, *426* (6965), 421-424.
 82. Arai, F.; Ichikawa, A.; Ogawa, M.; Fukuda, T.; Horio, K.; Itoigawa, K. High-speed separation system of randomly suspended single living cells by laser trap and dielectrophoresis. *Electrophoresis* **2001**, *22* (2), 283-288.
 83. Reichle, C.; Sparbier, K.; Muller, T.; Schnelle, T.; Walden, P.; Fuhr, G. Combined laser tweezers and dielectric field cage for the analysis of receptor-ligand interactions on single cells. *Electrophoresis* **2001**, *22* (2), 272-282.
 84. Dittrich, P. S.; Schuille, P. An integrated microfluidic system for reaction, high-sensitivity detection, and sorting of fluorescent cells and particles. *Analytical Chemistry* **2003**, *75* (21), 5767-5774.
 85. Gambin, Y.; Legrand, O.; Quake, S. R. Microfabricated rubber microscope using soft solid immersion lenses. *Applied Physics Letters* **2006**, *88* (17).
 86. Miyaki, K.; Guo, Y. L.; Shimosaka, T.; Nakagama, T.; Nakajima, H.; Uchiyama, K. Fabrication of an integrated PDMS microchip incorporating an LED-induced fluorescence device. *Analytical and Bioanalytical Chemistry* **2005**, *382* (3), 810-816.
 87. Yuen, P. K.; Despa, M.; Li, C. C.; Dejneka, M. J. Microbarcode sorting device. *Lab Chip* **2003**, *3* (3), 198-201.
 88. Grumann, M.; Dobmeier, M.; Schippers, P.; Brenner, T.; Kuhn, C.; Fritsche, M.; Zengerle, R.; Ducree, J. Aggregation of bead-monolayers in flat microfluidic chambers - simulation by the model of porous media. *Lab Chip* **2004**, *4* (3), 209-213.

89. Huh, D.; Gu, W.; Kamotani, Y.; Grotberg, J. B.; Takayama, S. Microfluidics for flow cytometric analysis of cells and particles. *Physiol Meas.* **2005**, *26* (3), R73-R98.
90. Holmes, D.; She, J. K.; Roach, P. L.; Morgan, H. Bead-based immunoassays using a micro-chip flow cytometer. *Lab Chip* **2007**, *7* (8), 1048-1056.
91. McDonald, J. C.; Duffy, D. C.; Anderson, J. R.; Chiu, D. T.; Wu, H.; Schueller, O. J.; Whitesides, G. M. Fabrication of microfluidic systems in poly(dimethylsiloxane). *Electrophoresis* **2000**, *21* (1), 27-40.
92. Wang, Z.; El-Ali, J.; Englund, M.; Gotsaed, T.; Perch-Nielsen, I. R.; Mogensen, K. B.; Snakenborg, D.; Kutter, J. P.; Wolff, A. Measurements of scattered light on a microchip flow cytometer with integrated polymer based optical elements. *Lab Chip* **2004**, *4* (4), 372-377.
93. Huh, D.; Tkaczyk, A. H.; Bahng, J. H.; Chang, Y.; Wei, H. H.; Grotberg, J. B.; Kim, C. J.; Kurabayashi, K.; Takayama, S. Reversible switching of high-speed air-liquid two-phase flows using electrowetting-assisted flow-pattern change. *J. Am. Chem. Soc.* **2003**, *125* (48), 14678-14679.
94. Holmes, D.; Morgan, H.; Green, N. G. High throughput particle analysis: Combining dielectrophoretic particle focussing with confocal optical detection. *Biosensors & Bioelectronics* **2006**, *21* (8), 1621-1630.
95. Simonnet, C.; Groisman, A. Two-dimensional hydrodynamic focusing in a simple microfluidic device. *Applied Physics Letters* **2005**, *87* (11).
96. Simonnet, C.; Groisman, A. High-throughput and high-resolution flow cytometry in molded microfluidic devices. *Analytical Chemistry* **2006**, *78* (16), 5653-5663.
97. McClain, M. A.; Culbertson, C. T.; Jacobson, S. C.; Ramsey, J. M. Flow cytometry of *Escherichia coli* on microfluidic devices. *Anal. Chem.* **2001**, *73* (21), 5334-5338.
98. Fu, A. Y.; Spence, C.; Scherer, A.; Arnold, F. H.; Quake, S. R. A microfabricated fluorescence-activated cell sorter. *Nature Biotechnology* **1999**, *17* (11), 1109-1111.
99. Kruger, J.; Singh, K.; O'Neill, A.; Jackson, C.; Morrison, A.; O'Brien, P. Development of a microfluidic device for fluorescence activated cell sorting. *Journal of Micromechanics and Microengineering* **2002**, *12* (4), 486-494.
100. Wolff, A.; Perch-Nielsen, I. R.; Larsen, U. D.; Friis, P.; Goranovic, G.; Poulsen, C. R.; Kutter, J. P.; Telleman, P. Integrating advanced functionality in a microfabricated high-throughput fluorescent-activated cell sorter. *Lab on A Chip* **2003**, *3* (1), 22-27.
101. Hofmann, O.; Miller, P.; Sullivan, P.; Jones, T. S.; deMello, J. C.; Bradley, D. D. C.; deMello, A. J. Thin-film organic photodiodes as integrated detectors for microscale chemiluminescence assays. *Sensors and Actuators B-Chemical* **2005**, *106* (2), 878-884.
102. Edel, J. B.; Beard, N. P.; Hofmann, O.; deMello, J. C.; Bradley, D. D.; deMello, A. J. Thin-film polymer light emitting diodes as integrated excitation sources for microscale capillary electrophoresis. *Lab Chip* **2004**, *4* (2), 136-140.
103. Hofmann, O.; Wang, X.; Cornwell, A.; Beecher, S.; Raja, A.; Bradley, D. D.; deMello, A. J.; deMello, J. C. Monolithically integrated dye-doped PDMS long-pass filters for disposable on-chip fluorescence detection. *Lab Chip* **2006**, *6* (8), 981-987.
104. Chabinyk, M. L.; Chiu, D. T.; McDonald, J. C.; Stroock, A. D.; Christian, J. F.; Karger, A. M.; Whitesides, G. M. An integrated fluorescence detection system in poly(dimethylsiloxane) for microfluidic applications. *Analytical Chemistry* **2001**, *73* (18), 4491-4498.

-
105. Seo, J.; Lee, L. P. Disposable integrated microfluidics with self-aligned planar microlenses. *Sensors and Actuators B-Chemical* **2004**, *99* (2-3), 615-622.
 106. Heng, X.; Erickson, D.; Baugh, L. R.; Yaqoob, Z.; Sternberg, P. W.; Psaltis, D.; Yang, C. Optofluidic microscopy--a method for implementing a high resolution optical microscope on a chip. *Lab Chip*. **2006**, *6* (10), 1274-1276.
 107. Psaltis, D.; Quake, S. R.; Yang, C. Developing optofluidic technology through the fusion of microfluidics and optics. *Nature* **2006**, *442* (7101), 381-386.
 108. Bowden, M.; Song, L. N.; Walt, D. R. Development of a microfluidic platform with an optical imaging microarray capable of attomolar target DNA detection. *Analytical Chemistry* **2005**, *77* (17), 5583-5588.

C H A P T E R Seven

INTEGRATION OF LAYER-BY-LAYER COATED DIGITALLY ENCODED MICROCARRIERS IN MICROFLUIDIC DEVICES

ABSTRACT

Affinity assays that occur at the surface of microcarriers can be made more sensitively by using signal amplification methods to increase the signal-to-noise ratio, or by amplifying the reaction between probes and target molecules. This chapter challenges the integration of LbL coated memobeads in microfluidic channels, to enhance the contact between target molecules and probes attached to the surface of microcarriers. The memobeads were immobilized in the microchip by means of a dam structure. It is shown that affinity reaction times between proteins are remarkably reduced, up to almost 10 times, compared to reaction on microcarriers loaded in a micro-centrifuge tube. The integration did not increase the amount of non-specific binding, and decoding of the memobeads was also possible in the microchip, although other immobilization strategies, such as a DEP cage, might work better for the memobead platform.

CHAPTER 7

INTEGRATION OF MICROCARRIERS IN MICROFLUIDIC DEVICES

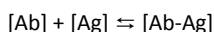
INTRODUCTION

As described earlier in this thesis a very large proportion of multiplexing technologies involve affinity reaction between capture probes that are immobilized on a solid support and free targets (such as solid phase antibody-antigen interactions, DNA hybridization reaction, and receptor-ligand interactions). These affinity assays involve probe-target interactions within a reaction volume close to the solution/solid phase interface, and display therefore characteristics that differ from probe-target affinity reactions that occur in solution. Affinity reactions between immobilized probes and free target molecules at the macro-level, e.g. at the bottom of a micro-wellplate or at the wall of a micro-centrifuge tube, are strongly diffusion-limited, because interactions occur within a distance that is less than 100 Å and probably closer to 10 Å, meaning that diffusion is needed to move reactants from the total fluid volume to the true interfacial reaction volume ¹. As a result, the time required to reach equilibrium for such solid-phase affinity reactions is greater than for solution-phase interactions, and it increases in proportion to the ratio of the volume occupied by the liquid to that occupied by the reactive interface (probe coated surface). The equilibrium time in a micro-wellplate can be enhanced by the introduction of vortex agitation, the use of a porous matrix, or the use of microcarriers as the solid-phase. Because microcarriers increase the total reaction surface, it takes less time to reach equilibrium compared with reactions at the bottom of for instance a micro-wellplate ². As described in the introduction of this thesis, this is one of the advantages of suspension arrays compared to planar microarrays. The aim of this chapter is to investigate whether the

integration of our microcarriers in a microchannel of a microfluidic chip results in more efficient interactions between the capture probe coupled microcarriers and the free target molecules in the sample. By introducing the microcarriers in a microchannel, and flushing the sample solution through the microchannel, the sample indeed intensively contacts the (surface of the) microcarriers, and affinity reactions might reach equilibrium faster, due to a decreased diffusion distance. As the diffusion time is proportional to the square of the diffusion distance, this integration should result in a drastically decreased reaction time³.

As a proof-of-concept, we investigate the binding between mouse IgGs that are coupled to our microcarriers, and free goat anti-mouse IgG (H+L) antibodies (targets). Because each step in a protein quantification assay, as demonstrated in Chapter 3 and 4 of this thesis, is at the simplest level based on such affinity interaction between two proteins (capture probe/target of interest, target of interest/detection antibody,..), the result of this experiment is valid for each separate step. This means that if the equilibrium time is shortened due to this integration, it is valid for every step during the formation of the sandwich construct if all steps would be performed in a microchannel, which means that the total assay time would shorten equally. Although only protein interactions are investigated in our study, the results will also yield for other types of biomolecular assays that are diffusion-dependent (e.g. DNA hybridization reactions, receptor-ligand...) ⁴.

The proof-of-concept of our study is basically an interaction between an antibody and an antigen, which resides on some fundamental principles. The first one is the specific and high-affinity 'key-lock' principle between the variable parts of the antibody ('Fab-domains') and specific parts of the antigen (which are called 'epitopes'). The interaction is always based on several non-covalent weak physical bindings, such as hydrogen bonds, electrostatic interactions, hydrophobic interactions, and Vanderwaals interactions. Secondly, the interaction between the Fab domain and the epitope is based on thermodynamic rules, and characterized by a certain strength, that is called the 'affinity'. It is described as the affinity constant, K_A , which is a measure of the amount of antibody-antigen complexes at equilibrium conditions. Because of the non-covalent nature of the interactions, it can be concluded that they are reversible. To study the kinetics of such reactions, one can consider the next equilibrium equation:



with [Ab] : concentration antibody,
[Ag]: concentration antigen,
[Ab-Ag]: concentration antibody-antigen construct

The forward reaction resembles the formation of the antibody-antigen construct (Ab-Ag), while the opposite unbinding reaction resembles the dissociation of the complex into its original components, antibody (Ab) and antigen (Ag). At equilibrium, as many amounts of antigen and antibody react to antibody-antigen complexes, as complexes dissociate (*dynamic equilibrium*).

The time at which equilibrium is set, can be determined by measuring the formation of the antibody-antigen complexes. Because the free goat anti-mouse IgG (H+L) antibody is conjugated with AF647® in our experiments, the formation of the antibody-antigen construct at the surface of the microcarriers can be indirectly followed by the appearance of red fluorescence. The rate for binding is proportional to the concentration of antigens and antibodies. Therefore low antigen concentrations take the longest to equilibrate, and as a result equilibrium has to be tested with low antigen concentrations. We have used four different antigen concentrations, and compared the binding event between microcarriers that were incubated in a micro-centrifuge tube, and microcarriers that were integrated in a microchannel. The binding event was measured as a function of the time after the addition of the antigen solution. The number of complexes increases as a function of the time till a plateau is reached (Y_{\max}) at which as many amounts of antigen and antibody react to antibody-antigen complexes, as complexes dissociate (*dynamic equilibrium*). Because this value depend on the concentration of antigen used in the experiment, it will be different for the four concentrations under investigation. The binding event can then be fitted with the next hyperbolic equation:

$$Y = \frac{Y_{\max} \cdot X}{X + T_{50\%}}$$

- With X = time point after addition of antigen solution
 Y = fluorescent signal (proportional to the formation of Ab-Ag construct)
 Y_{\max} = maximum signal at dynamic equilibrium
 $T_{50\%}$ = the time at which half of the amount of antibodies are occupied with antigen

The $T_{50\%}$ value has been used in our experiments, to compare experiments performed at the micro- and macro-level, and to compare rates of binding at one level, when adding different antigen concentrations.

MATERIALS & METHODS

Materials.

Non-magnetic fluorescent carboxylated microcarriers (CFP-40052-100, $\phi = 39 \mu\text{m}$) were purchased from Spherotech (Libertyville, Illinois, USA). Poly (allylamine hydrochloride) [PAH; 28,322-3], sodium poly (styrene sulfonate) [PSS, MW $\sim 70\,000$; 24,305-1] and poly (acrylic acid) [PAA, MW $\sim 45\,000$; 18,128-5] were obtained from Sigma Aldrich (Steinheim, Germany). The polymers were dissolved into 0.5 M sodium chloride (31434, Sigma Aldrich, Seelze, Germany). Bovine serum albumine (BSA, A-7906) and 2-[N-Morpholino]ethanesulfonic acid (MES, M-8259) were purchased from Sigma (Bornem, Belgium), PBS Dulbecco's (14190-094) from Gibco and Tween-20 (655204) from Calbiochem. EDC (1-ethyl-3-(3-dimethyl aminopropyl) carbodiimide HCl, 22980) was obtained from Perbio Science (Erembodegem, Belgium); desiccated and stored at -20°C . Sulfo-NHS (N-hydroxysulfosuccinimide sodium salt, 106627-54-7) was purchased from Sigma Aldrich (Steinheim, Germany); desiccated and stored at 4°C . Purified mouse anti-human TNF α (551220) was purchased from BD Pharmingen (Erembodegem, Belgium). AF 647[®] goat anti-muis IgG (H+L) was purchased from Molecular Probes (Eugene, Oregon, USA). The microchips and its accessoires were a gift from professor Kitamori (Microchemistry Group, Kanagawa Academy of Science and Technology, Kanagawa, Japan).

Layer-by-Layer coating of the microcarriers.

The Layer-by-Layer modification of the microcarriers is described in Chapter 2.

Encoding of the microcarriers.

The encoding of the microcarriers is described in Chapter 2.

Coupling of capture antibodies to the LbL coated microcarriers.

The coupling procedure is described in Chapter 3.

Microchip fabrication.

Figure 1 shows a top view and cross section of the used microchip. It has been designed with a dam structure necessary to pack a definite amount of the microcarriers in the microchip. The free opening at the dam structure was $20\ \mu\text{m}$, which allows the reagents to pass through the dam, but obstructed the microcarriers. The dimension of the channel ($60\ \mu\text{m}$ by $60\ \mu\text{m}$) was kept at less than 2 times the diameter of one microcarrier ($40\ \mu\text{m}$), allowing an optimal packaging of a single row of microcarriers. The details of the microchip fabrication were described elsewhere⁵. The chip was composed of three quartz glass plates ($30\ \text{mm} \times 70\ \text{mm}$), the cover, middle, and bottom plates with thicknesses of $1\ \text{mm}$, $100\ \mu\text{m}$, and $170\ \mu\text{m}$, respectively. The thickness of the bottom glass was taken as low as possible to allow microscopic analysis of the binding events. Two access holes (inlet and outlet) of $0.5\ \text{mm}$ diameter were mechanically drilled into the cover glass. The cover, middle, and bottom plate were attached to each other without any adhesive in an oven at $1150\ ^\circ\text{C}$.

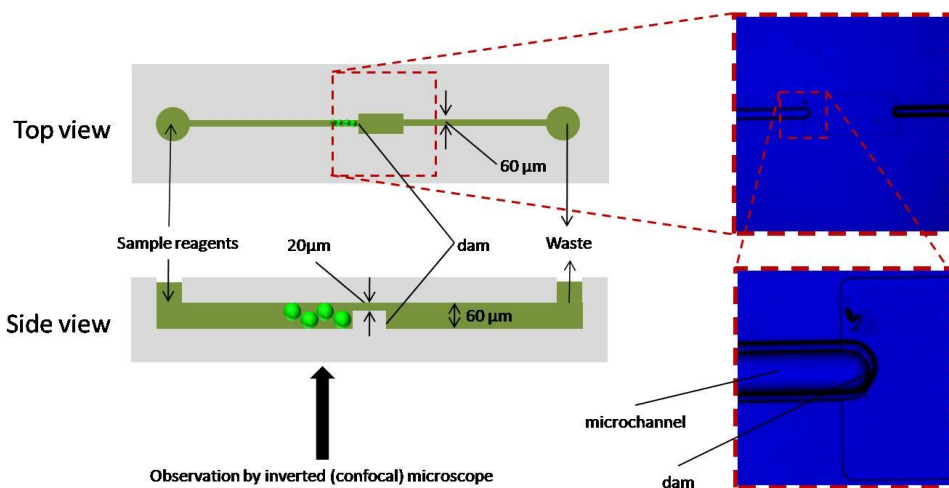


Figure 1: Left: microchip design - top view and side view. Right: magnification of the dam region. Four of those microchannels were fabricated on one microchip. Microchip made by the group of Kitamori (School of Engineering, University of Tokyo, Japan).

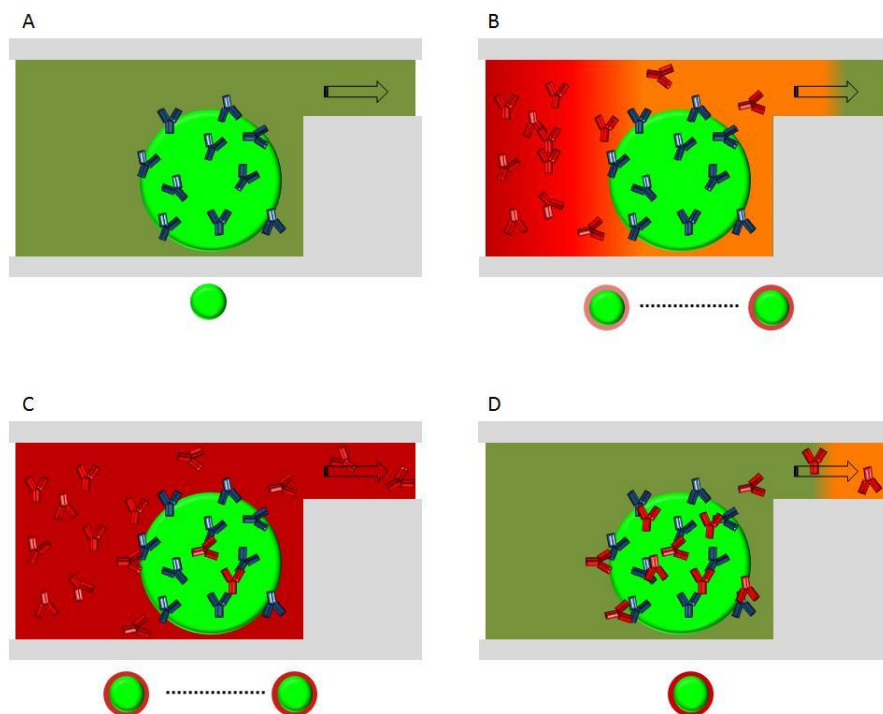
Analytical procedures in the microchip (micro-level).

Figure 2: Assay principle. A/ Mouse IgG coupled microcarriers are loaded in the microchip. B-D/ A solution of AF647[®] labeled goat anti-mouse IgG (H+L) is flushed through the microchip so that it intensively contacts the microcarriers. The appearance of red fluorescence is measured with a confocal microscope via the bottom of the microchip in real-time. The red fluorescence gradually increases as a function of the incubation time.

Schematic illustrations of our microcarrier-bed system are shown in Figure 2. LbL coated microcarriers were pre-coated with mouse IgG capture antibodies, and approximately 25 of them were then injected into one microchannel (Figure 2A) by means of a 100 μ l Hamilton syringe, which was connected to the inlet of the microchip via a fused silica capillary and a stainless steel connector. The excess of microcarriers was withdrawn by flushing assay buffer through the channel in the opposite direction. After the microcarrier loading process, the microcarrier-containing syringe was removed from the system, the chip was connected to a micropump (see next paragraph). Subsequently, assay buffer, and a sample containing a certain concentration of red fluorescent (AF647[®]) conjugated goat anti-mouse IgG (H+L) antibodies (Figure 2B) were introduced into the microcarrier packed microchannel at 100 nl per second, successively. The affinity reaction between the antibodies at the surface of the microcarriers, was monitored in real-time by measuring the

appearance of red fluorescence at the surface (Figure 2 B-D). Therefore red fluorescent images were taken every 2 seconds. After the measurements, the microcarriers were removed from the microchip by a reverse flow of assay buffer and the microchannel was washed with 0.1 M NaOH solution. In that way, the microchip could be used repeatedly.

Apparatus.

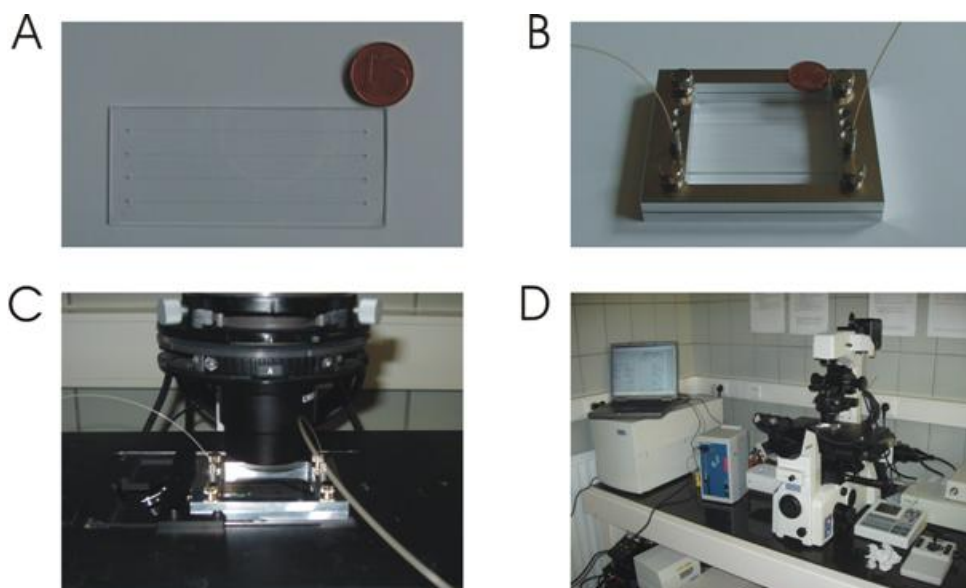


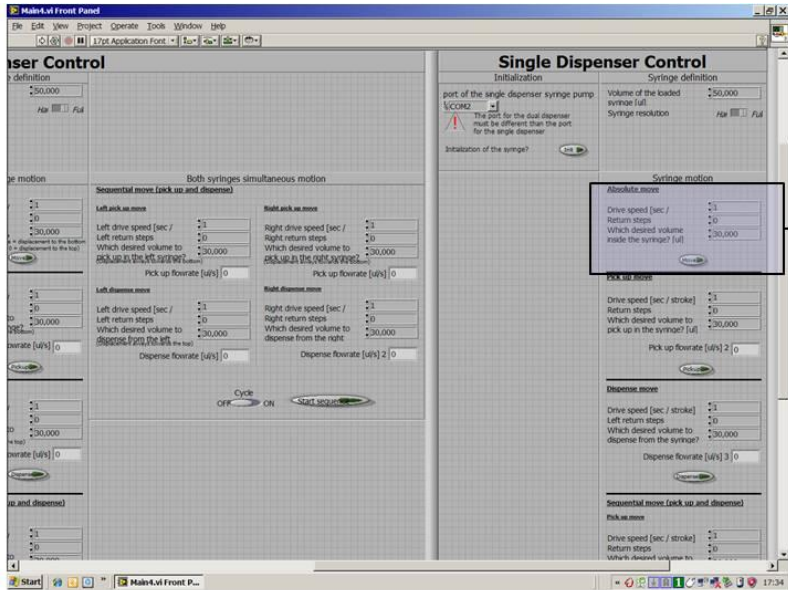
Figure 3: Overview of the microchip installation. A/ One microchip consist of four equal microchannels with dam structure, B/ Microchip mounted in a stainless steel holder. One microchannel is connected with outside via stainless steel connectors and capillary tubing, C/ Holder with microchip mounted on the XY-table of the microscope: observation via bottom, and D/ Microchip is connected with the micropump via capillary tubing. The liquid flow is controlled with Labview software.

To determine the appearance of red fluorescence at the surface of the microcarriers in the microchip in real-time, the microchip was fixed in a stainless steel holder (microchip was sandwiched between two plate holders) that was placed on top of the XY-table of a confocal microscope before the microcarriers and reagents were introduced (Nikon EZC1 confocal microscope) (Figure 3 A till C).

The liquid flow during the assay was controlled with a microsyringe pump (Microlab 500B, Hamilton) and Hamilton gastight syringes with untreated fused silica capillary tubing and capillary column connectors (GL Science, Tokyo, Japan). The fused silica capillary for reagent introduction was

connected at one side to the microsyringe pump, and at the outer side to the inlet hole of the microchip. The outlet capillary was connected to a waste reservoir (Figure 1). Before the assay, the inner walls of the capillaries and the microchannel were blocked with assay buffer (BSA = blocking reagent) for a few minutes. A change of supplied reagents could be achieved simply by changing syringes in the pump. The micropump was automatically controlled via RS-232 connection with Labview-software installed on a notebook (Figure 3D). The software was developed by the group of prof. Renaud (Ecole Polytechnique Fédérale de Lausanne, Lausanne, Switzerland) and in-house adapted to our application. Figure 4 shows the interface of the software and the block diagram behind it. Parameters that can be adjusted are the volume of the syringe, the motion of the syringe, and the driver speed.

A



B

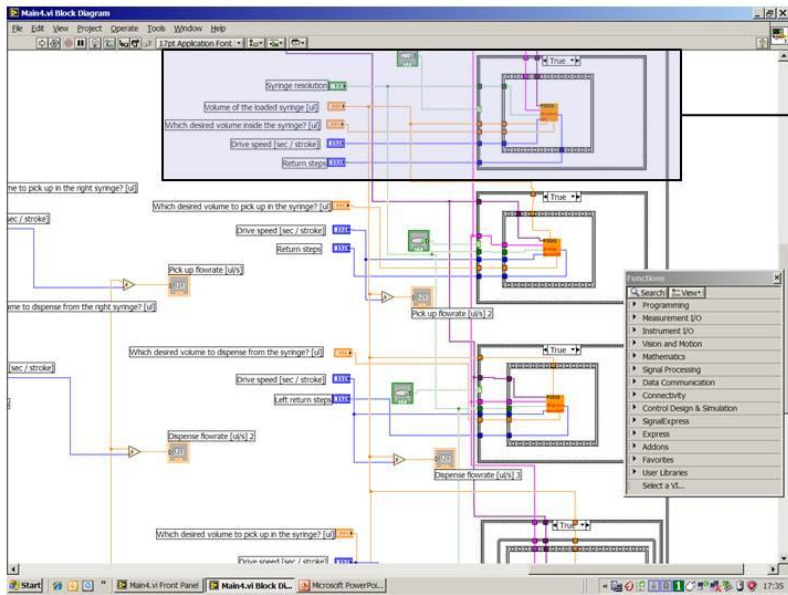


Figure 4: Control of Liquid flow. A/ User interface, B/ Block diagram behind it.

Analytical procedures in the micro-centrifuge tube (macro-level).

The micro-level experiments were compared with similar test performed on microcarriers loaded in 500 μl sized micro-centrifuge tubes. In order to be able to measure the fluorescence as a function of the time in the latter ones, several tubes were loaded with equal amounts of microcarriers (approximately 25 microcarriers), subjected to an equal volume of the target solution of AF647[®] fluorescently labeled goat anti-mouse IgG (H+L) antibodies (100 μl), and allowed to incubate on a Rotamax 120 rotator (Heidolph, Duitsland) at 250 rpm for different times. After incubation, excess of not bound AF647[®] fluorescently labeled goat anti-mouse IgG (H+L) was immediately removed by washing that tube for three times with 400 μl assay buffer. The tube was then stored at 4°C till all tubes were gathered. Finally, all tubes were analyzed at the end of the experiment, and therefore the red fluorescence was not measured in real-time.

Confocal microscopy imaging of the microcarriers.

The microcarriers were observed using a Nikon C1si confocal laser scanning module attached to a motorized Nikon TE2000-E inverted microscope (Nikon Benelux, Brussels, Belgium). Images were captured with a Nikon Plan Apochromat 10x objective lens (NA of 0.45) using the 488 nm line from an Ar-ion laser for the excitation of the dye loaded in the microcarriers, and the 647 nm line from a diode laser for the excitation of AF647[®]. To determine the average red fluorescence of one microcarrier (due to coupled AF647[®] labeled antibodies) a region of interest (ROI) was drawn around the microcarrier and the red fluorescence within the ROI was measured using the Matlab 7.1 version equipped with home-made imaging processing software. The average red fluorescence of each microcarrier was defined as the average of the fluorescence of all pixels within the ROI.

For the orientation of memobeads, a weak external magnetic field was applied with the same orientation as the magnetic field applied during the encoding process (relative to the direction of the laser light). In the presence of this weak magnetic field, the 'remanent' nanoparticles tend to align with the magnetic field, so they will turn the microcarriers (at which surface they are fixed) into a position that the code can be read (the code is present in a plane perpendicular to the direction of the laser. For the decoding process, images were captured with a 60x water immersion objective lens.

RESULTS AND DISCUSSION

Interaction of biomolecules at the micro-level.

Figure 5 shows the red mean fluorescence intensity of approximately 25 microcarriers loaded in the microchannel as a function of the time after loading a certain concentrated solution of red fluorescently labeled target molecules (A: 40 $\mu\text{g/ml}$, B: 4 $\mu\text{g/ml}$, C: 400 ng/ml , and D: 40 ng/ml) at a flow velocity of 100 nl/s . Note that the fluorescence of only one microcarrier is followed as a function of the time. The automatic microcarrier detection algorithm that was used so far, was not able to detect single microcarriers in one image, because the microcarriers made contact with each other when they were arrayed in the channel. Therefore, we had to manually determine a single microcarrier. As expected, the fluorescence intensity follows a hyperbolic profile, with a strong increase in fluorescence at the first moments (due to the fact that more and more target molecules have interacted with the microcarriers) till a plateau phase is reached where equilibrium occurs.

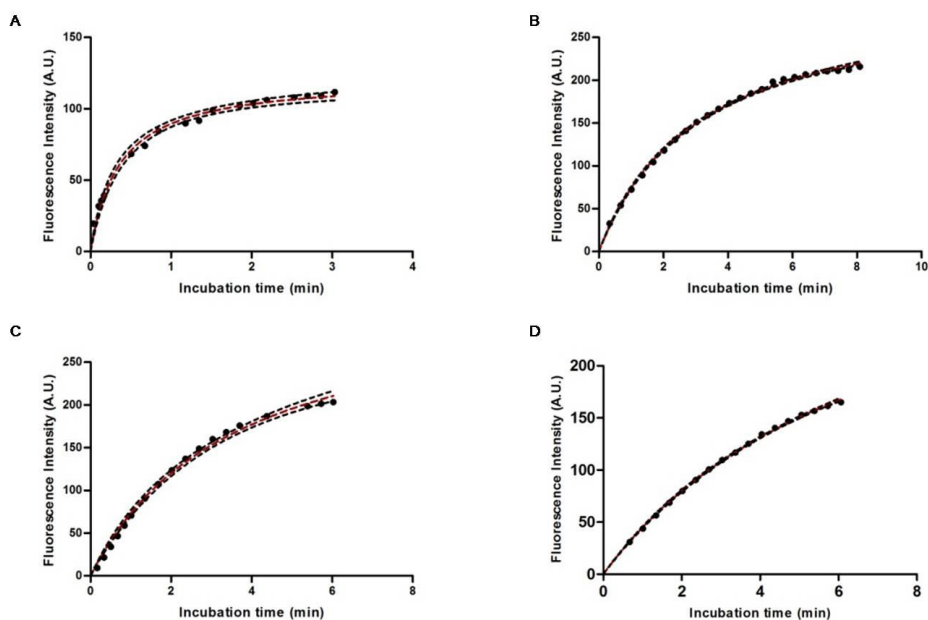


Figure 5: Kinetics of labeling of trapped goat anti-mouse IgG (H+L) with mouse IgG conjugated microcarriers loaded in a microchip at input goat anti-mouse IgG (H+L) concentrations of 40 $\mu\text{g/ml}$, 4 $\mu\text{g/ml}$, 400 ng/ml , and 40 ng/ml (respectively A, B, C, and D). Development of the relative fluorescence signal intensity at the surface of the microcarriers over time. Different settings of the microscope were used for each curve, so they cannot be compared as such. Dotted lines represent the 95% confidence intervals of the fitting procedure. Note that each data point represent the same microcarrier at another point of time (the fluorescence is not averaged).

It can be visually observed that the equilibrium is reached faster with the most concentrated solutions, which corresponds with theoretical expectations. In order to make the comparison more clearly, and because the four graphs in Figure 5 are obtained with different microscope settings, Figure 6 shows the normalized datapoints and fittings. Normalization was done against the Y_{\max} value that was obtained from the fitting procedure in Figure 5. This was possible, because the error on this parameter is acceptable (the standard error on Y_{\max} was less than 5% for each of the concentrations), as can be seen from the 95% confidence intervals that are shown in Figure 5 (dotted lines). Clearly, the higher the concentration of goat anti-mouse IgG antibody in the sample, the faster the plateau phase, and thus equilibrium is reached.

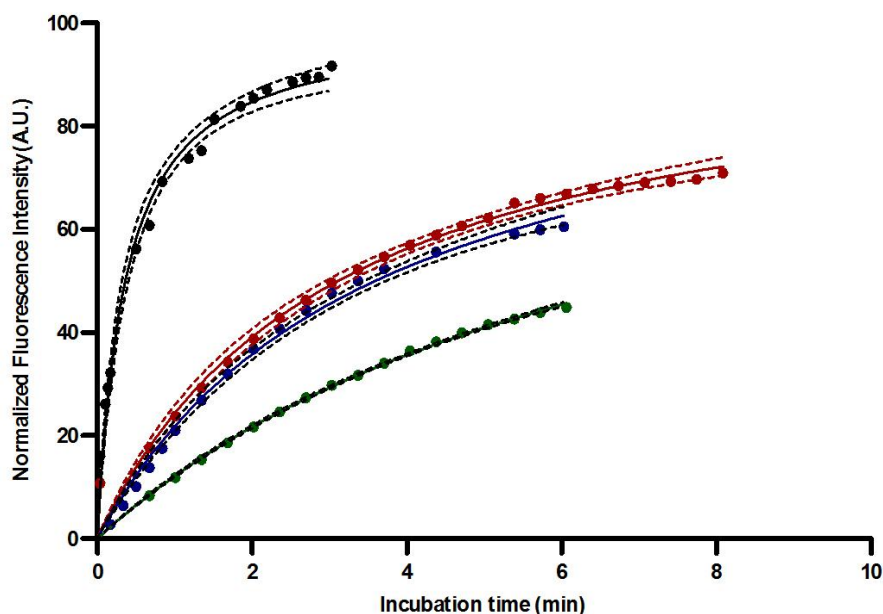


Figure 6: Kinetics of labeling of trapped goat anti-mouse IgG (H+L) with mouse IgG conjugated microcarriers loaded in a microchip at input goat anti-mouse IgG (H+L) concentrations of 40 $\mu\text{g/ml}$, 4 $\mu\text{g/ml}$, 400 ng/ml , and 40 ng/ml (respectively black, red, blue, and green line). Development of the fluorescence intensity at the surface of the microcarriers over time. The fluorescence signals were normalized to the maximum signal for each curve (as obtained from the fitting procedure). This is possible because of the narrow confidence intervals on these values.

Table 1 contains the $T_{90\%}$ and $T_{50\%}$ values of each fitting process, which are the times at which 90%, respectively 50% of the maximal signal is reached, showing that the binding event occurs faster at

high target concentrations. It takes only some tens of minutes for low goat anti-mouse IgG antibody concentrations to reach equilibrium. Remarkably, we didn't observe almost any difference in reaction kinetics between 4000 and 400 ng/ml solutions, for which the reason is still unclear.

Table 1: Summary of the hyperbolic fitting procedure at the micro-level.

Concentration (ng/ml)	Y_{max} (A.E.)	SE (A.E.)	SE (%)	$T_{90\%}$ (min)	$T_{50\%}$ (min)
40 000	100.029	1.962	1.962	3.249	0.362
4000	99.960	3.109	3,110	28.084	3.108
400	100.002	3.934	3,934	32.322	3.592
40	100.000	2.268	2.268	64.971	7.219

Interaction of biomolecules at the macro-level.

Figure 7 shows the red mean fluorescence intensity of approximately 25 microcarriers, that are loaded in a micro-centrifuge tube, as a function of the time after incubation with 100 μ l of a certain concentrated solution of red fluorescently labeled target molecules (A: 40 μ g/ml, B: 4 μ g/ml, C: 0.4 μ g/ml, and D: 40 ng/ml). As expected, the fluorescence appears at the surface following a hyperbolic profile, with a strong increase in fluorescence at the first moments (due to the fact that more and more target molecules have interacted with the microcarriers) till a plateau phase is reached where equilibrium occurs. Regarding the effect of the target concentration, the same effect is observed as on the micro-level: low concentration take the longest to equilibrate. Equilibrium, however, is reached at a much later point of time, compared to the micro-level. The graphs were again normalized to the Y_{max} value that was obtained from the hyperbolic fitting procedure. This was possible, because the error on this parameter was again acceptable (the standard error on Y_{max} was less than 10% for each of the concentrations), as can be seen from the 95% confidence intervals that are shown in Figure 7 (dotted lines). The result of the normalization is shown in Figure 8.

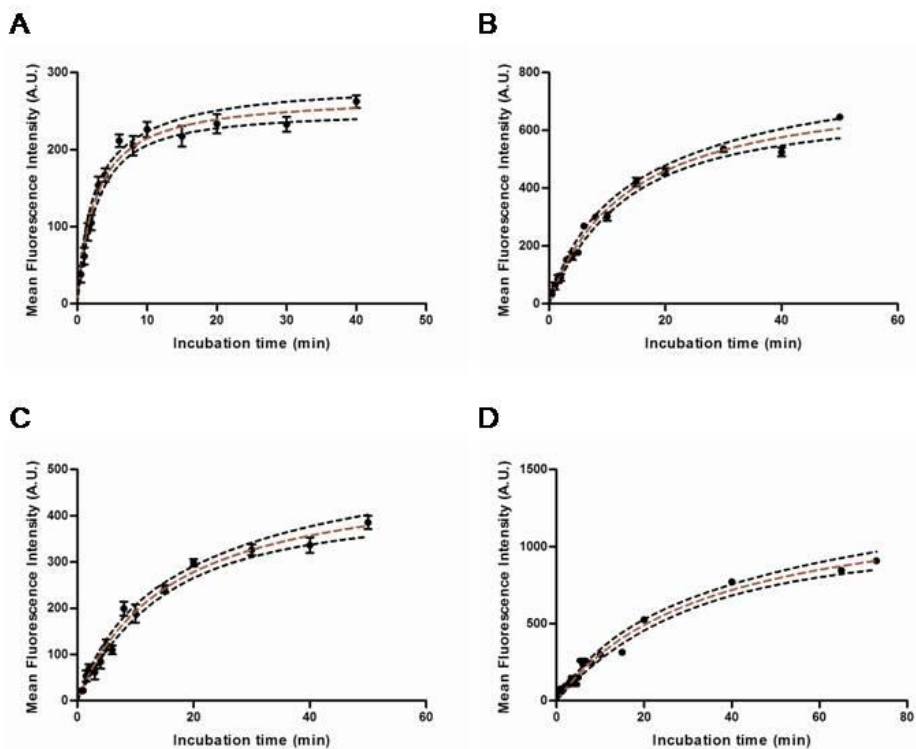


Figure 7: Kinetics of labeling of trapped goat anti-mouse IgG (H+L) with mouse IgG conjugated microcarriers loaded in a microcentrifuge tube at input goat anti-mouse IgG (H+L) concentrations of 40 $\mu\text{g/ml}$, 4 $\mu\text{g/ml}$, 0.4 $\mu\text{g/ml}$, and 40 ng/ml (respectively A, B, C, and D). The incubation was performed in a volume of 100 μl . Development of the relative fluorescence signal intensity at the surface of the microcarriers over time. Different settings of the microscope were used for each curve, so they cannot be compared as such. Note that each data point represents the averaged fluorescence of 10-15 microcarriers and that another group of microparticles is used at each data point (because separate tubes were used, see materials & methods).

As expected, the higher the concentration of goat anti-mouse IgG antibody, the faster the plateau phase, and thus equilibrium is reached. Table 2 contains the $T_{90\%}$ (close to equilibrium) and $T_{50\%}$ values of each fitting process, showing that it takes a long time for low goat anti-mouse IgG antibody concentrations to reach equilibrium, with values up to some hours. Remarkably, we did not observe almost any difference in reaction kinetics between 4000 and 400 ng/ml solutions, as was the case at the micro-level.

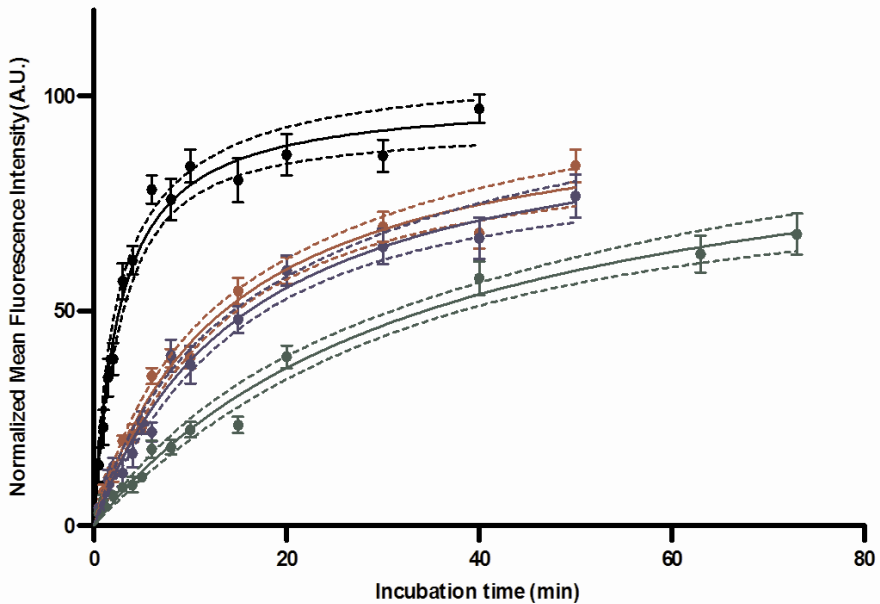


Figure 8: Kinetics of labeling of trapped goat anti-mouse IgG (H+L) with mouse IgG conjugated microcarriers loaded in a microcentrifuge tube at input goat anti-mouse IgG (H+L) concentrations of 40 µg/ml, 4 µg/ml, 0.4 µg/ml, and 40 ng/ml (respectively black, red, blue, and green line). The incubation was performed in a volume of 100 µl. Development of the fluorescence intensity at the surface of the microcarriers over time (the fluorescence of 10-15 microcarriers is averaged at each data point). The fluorescence signals were normalized to the maximum signal for each curve (as obtained from the fitting procedure). This is possible because of the narrow confidence intervals on these values.

Table 2: Summary of the hyperbolic fitting procedure at the macro-level.

Concentration (ng/ml)	Y_{max} (A.E.)	SE (A.E.)	SE (%)	$T_{90\%}$ (min)	$T_{50\%}$ (min)
40 000	99.999	3.085	3,085	23.528	2.61
4000	100	4.480	4.480	121.680	13.52
400	99.201	5.354	5.397	155.047	15.851
40	100.916	6.775	6.713	288.411	34.981

The reaction time required for the probe-target reaction was remarkably cut in the microcarrier-bed microchip-based assay system, which can be seen in Figure 9 where the $T_{50\%}$ values are compared between the macro- and micro-level. It can be concluded that the total assay time for the detection of proteins could be considerably reduced, when performing those assays in microchips, when taking into account that the gain in speed is valid for every step in such a microcarrier-based protein detection assay. Besides protein-protein interactions, enzymatic substrate conversion reactions occur also faster in microchips⁶. It would therefore be of interest to apply the Tyramide Signal Amplification assay, as demonstrated in Chapter 4, in a microchip.

Note that a flow velocity of 100 nl per second has been used in the microchip experiments, which is low enough to guarantee almost no reaction limitation: it is obvious that the higher the velocity, the less time target molecules have to diffuse to the surface of a microcarrier. On the other hand, if the velocity is too low, the transport of free target molecules can be limited⁷. So far, however, we were not yet able to investigate the effect of the flow velocity.

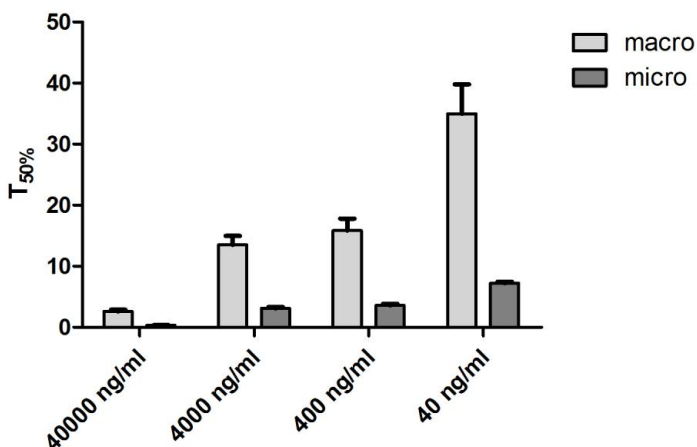


Figure 9: Comparison of the $T_{50\%}$ values at the macro-level and at the micro-level for four different target concentrations.

Specificity of the microchip bead-assay.

The introduction of microcarriers into a microchannel seemed to improve the interaction between bound probe and free target molecules, because the diffusion distance is decreased by flushing the target sample stream through the surface of the microcarriers. However, there exists a

chance that, besides this enhanced specific binding, the non-specific interaction of target molecules with the surface of the microcarriers is also increased.

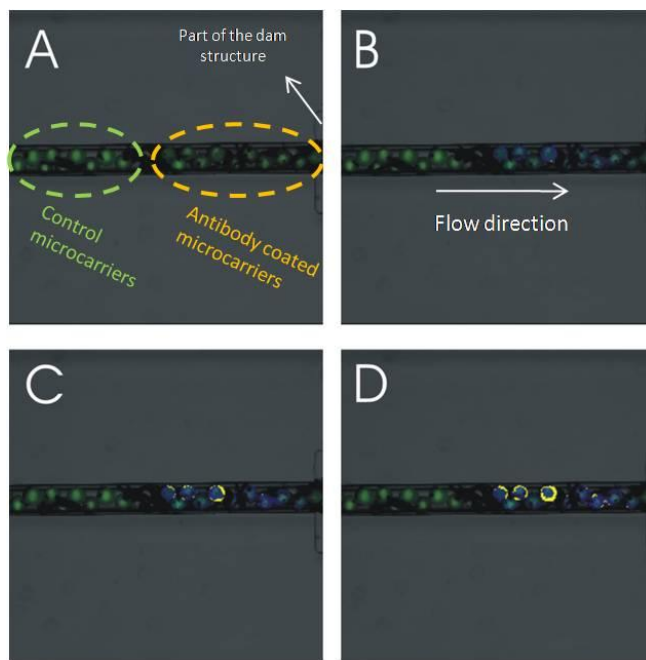


Figure 10: Specificity test of the microchip bead-assay. Two different types of microcarriers were separately loaded into the microchip (first mouse IgG coated microcarriers and then control microcarriers without any antibody). Red and green merged fluorescent images after loading the microcarriers (A), and at different time points after flushing AF647 goat anti-mouse IgG (H+) antibodies (40 ng/ml) through the microchannel (3, 5, and 7 minutes for respectively B, C, and D). Note that the colors are artificial, because fluorescence is measured with a confocal scanning beam; hence the green color represents the green fluorescence inside the microcarriers, while the blue color represents the red fluorescence at the surface of the microcarriers (yellow areas: overbleached red fluorescence).

To test whether the microcarrier platform retains its specificity after introduction of the microcarriers into the microchannel, antibody coated and control (no antibody coated) microcarriers were separately loaded into the same microchannel, and subsequently the target solution was flushed through the microchannel, so that it first contacts the control microcarriers, and thereafter the specific microcarriers. The red fluorescence on both type of microcarriers was again measured as a function of the time of interaction. Figure 10 shows an image of the microchannel immediately after loading (time 0, panel A), and 3 images taken at four different time points after adding a 40 ng/ml solution of AF647® fluorescently labeled goat anti-mouse IgG (H+L) at 100 nl/s (3, 5, and 7 minutes, respectively panels B, C, and D). Note that the blue color is an artificial color and represents

the red fluorescence, while yellow areas represent over-bleached regions. It can already be visually observed that the control microcarriers behave differently from the other ones. Although only 4 different time points between 0 and 7 minutes are depicted in Figure 10, in reality a fluorescent scan was taken every 2 seconds. Figure 11 shows a more detailed analysis of the red fluorescence on top of the microcarriers shown in Figure 10, and clearly demonstrates that the control microcarriers do not exhibit any red fluorescence besides some background fluorescence, and this value seems to be independent of the time of interaction. This proves that the specificity of the bead-platform is retained after integration with microchip technology.

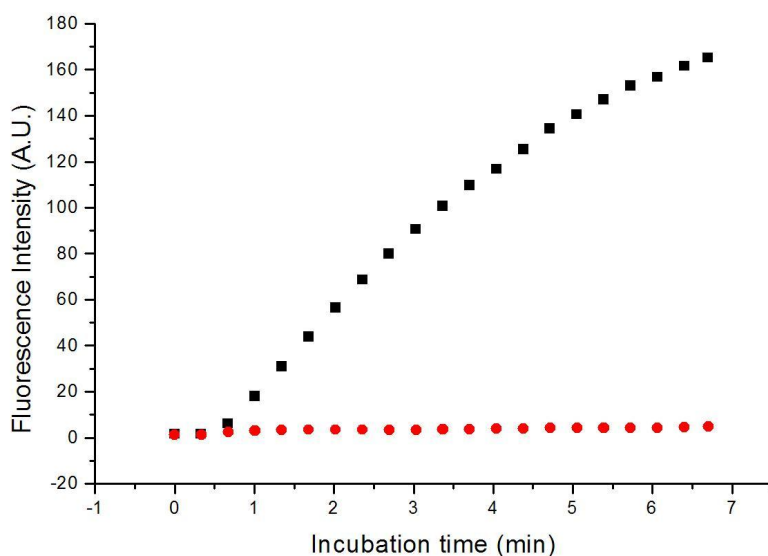


Figure 11: The red fluorescence at the surface of control microcarriers (red data points) and mouse IgG coated microcarriers (black data points) as a function of the incubation time with a solution of AF647[®] labeled goat anti-mouse IgG (H+L) antibodies (40 ng/ml).

Decoding of memobeads in microchip.

So far it has been shown that the integration of the LbL coated microcarriers in microchips remarkably cuts the reaction time, and does not affect the specificity as far as investigated. In order to be able to perform multiplex analysis by means of LbL coated memobeads integrated in microchips, this microchip format must not affect the decoding process at all. There are reasons why the decoding process might be impeded. This micro-format could influence, for instance, the

mobility of the memobeads, and their orientation during the decoding process due to increased surface interactions. In the previous chapters, we have demonstrated that those LbL coated memobeads could be turned into their appropriate read-out position at the time of decoding when decoding was done at the bottom of a well plate. In a narrow microchannel, however, such as the one with a diameter of only 60 micrometer that is used in these experiments, the situation is completely different, because a) the memobeads can interact with the wall of the channel at each side (not only via the bottom), b) the memobeads are arrayed in the channel, meaning that they make contact with each other which was almost never the case in a well-plate, where they behave almost always separately and c) besides memobeads the channel is also filled with some debris during the experiment, which adhered to the wall of the channel and even to the surface of the memobeads. Debris is inherent to the layout of our microchip: disadvantageous to the dam structure is that it works as a kind of filter, and not only prevents memobeads to go further through the channel, but also blocks dust and other small particles, which was also observed by others⁸. This filter-effect is even increased when loading memobeads in the channel. For all those reasons, the integration of the memobeads into the microchannel diminishes their freedom, which might influence their read-out.

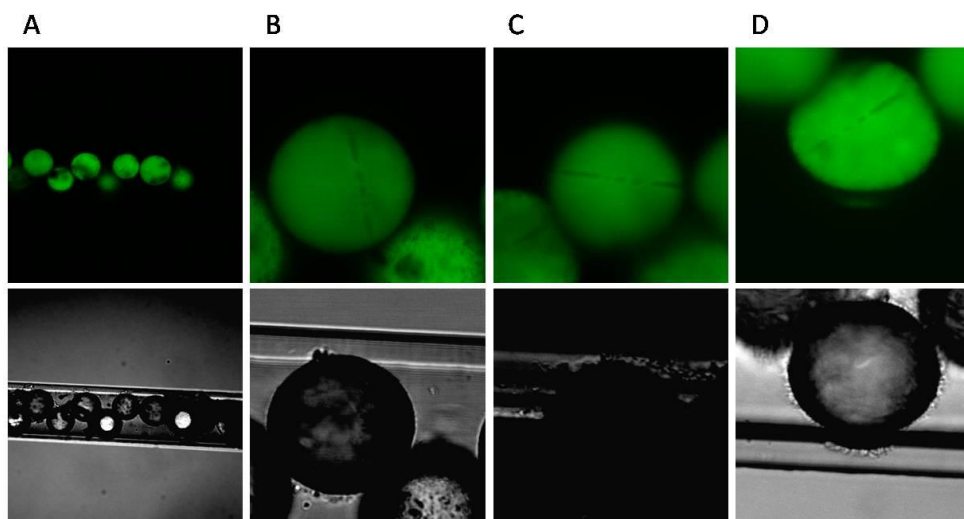


Figure 12: Decoding of memobeads loaded into the microchannel. The microcarriers turned into the appropriate position by means of magnetic forces due to the proximity of an external magnet. Confocal green fluorescent images (top row) and transmission images (bottom row). A/ overview of loaded memobeads before applying magnetic forces, and B/ Detailed magnification of some of the loaded memobeads.

Encoded memobeads were loaded into the microchannel, and they were tried to be oriented into the appropriate read-out position by means of an external magnet. Figure 12A shows the memobeads immediately after the loading step. Only one bead can be decoded (third one from right), because by chance, its code is present in a plane perpendicular to the direction of the laser light. The other panels in Figure 12 (B, C, and D) show a magnification of some of the loaded memobeads after applying an external magnetic force, proving the possibility of orienting the memobeads. Although almost all memobeads could be decoded, we have to admit that when memobeads were surrounded with debris, it was sometimes not possible to position them in the appropriate way. An example of such debris is shown in Figure 12 D, at the upper left part of the encoded microcarrier. As mentioned in chapter 6, other methods are available for keeping microcarriers in a confined area. Abandoning the dam structure and using one of the other methods could solve this problem.

Capturing memobeads in microchips.

One other way to keep microcarriers in a microchip at a certain position is by using dielectrophoresis (DEP) forces⁹. As explained in Chapter 6, when polarizable microparticles are subjected to an alternating electric field, they experience a DEP force in a non-uniform electrical field, which may move them to regions of high or low electrical field. The motion depends on the particle polarizability, compared to the surrounded medium. The magnitude and direction of the DEP force depends on the microcarrier dielectric properties. When using several electrodes at a time, DEP forces can be used to manipulate and trap individual microcarriers in a microchip, as explained in Chapter 6. It is relatively easy to generate an electric field in a specific area of a microchip with physical dimensions close to the size of the microcarriers by using microelectrodes. This so-called ‘microcarrier trap’ can hold particles against volumetric fluid flow rates of about 10 to 50 $\mu\text{l}/\text{min}$ by forces in the sub-piconewton range¹⁰⁻¹³. An advantage of such a trap is that the channel size might be taken large enough to prevent clogging of debris material, because the microcarriers are fixed at one position without any physical contact. We therefore tested whether the LbL coated microcarriers could be caught in such a trap.

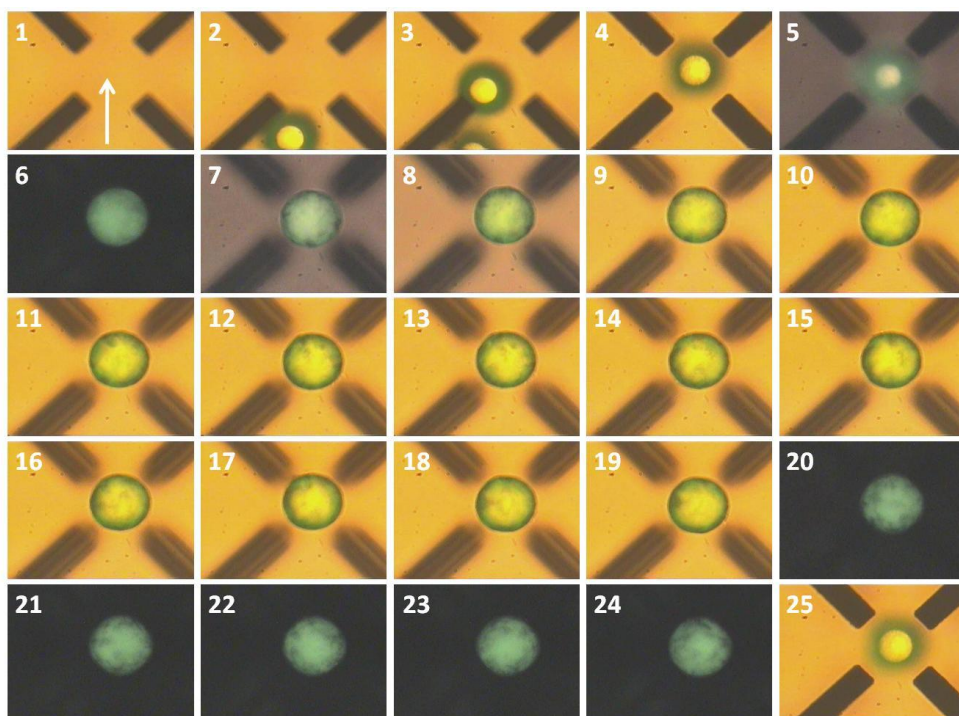


Figure 13: Proof-of-principle of a DEP-trap inside a microchip. The DEP-trap consist of four pairs of micro-electrodes that are integrated in the capillary walls: four in the top plate, and four in the bottom plate. 1: View on the four microcarrier in the DEP-trap inside the chip. 2-4: Transmission images of the catching process of a 40 μm sized microcarrier in the DEP-trap inside the chip. Only one carrier is trapped at a time, the other ones are repelled, as can be seen in 2 and 3. The microcarrier is suspended in a liquid that flows from the bottom to the top of the image (arrow shows flow direction), and is caught centrally between the electrodes. Note that only a small part of the microchip is shown. 5-7: Green fluorescent and transmission superimposed images, taken at three different heights, focused at the electrodes (5), the central plane of the microcarrier (6), and the surface of the microcarrier (7) Images 8-24: A randomly moving external magnetic field is applied, which rotates very easy the microcarrier around its axis, while it is caught via the DEP forces in the trap. Note that the liquid was continuously flowing while trapping the microcarrier (Experiment performed at Evotec Technologies - www.evotec-technologies.com, recently acquired by PerkinElmer).

Figure 13 shows a (no encoded) LbL coated microcarrier, that is suspended in a continuously liquid flow, and captured at a certain moment in a DEP trap by means of DEP forces. The microcarrier is hold in the trap, while liquid flows through the microchannel. At a certain moment, while still trapping the microparticle, an external magnetic field is randomly applied, which rotates the microparticle in the trap. Although the microparticle was not encoded at that time, this example clearly demonstrates the possibility of decoding memobeads in a microchip by using DEP and magnetic forces at the same time.

CONCLUSION

The previous experiments show evidence that the reaction time of a suspension array can be remarkably reduced by the integration of the suspension array technology with microfluidics. Another advantage is that sample and reagent volumes can be incredibly reduced. Note that in our experiments samples were continuously flushed through the microchannel at 100 nl per second, but that we didn't investigate yet other parameters, such as the influence of the flow rate, the difference between a continuous and start-stop sample flow, one-way versus reciprocal flow, etc. Changing one of those parameters might even shorten the reaction time, as was also observed by other groups^{7,14}. Although only protein interactions were shown in this study, one can expect the same result when performing DNA hybridization, because the latter one is diffusion-dependent too. A faster DNA hybridization reaction on microparticles that were loaded in microchannels, instead of in micro-centrifuge tubes, was already observed by other people⁴.

Concerning the applicability of the LbL coated memobeads, it is shown that the integration in microchips is acceptable as long as the magnetic positioning is possible. Although the decoding of memobeads in a microchannel has been proven, we have to admit that other factors like the presence of dust and/or other material, can negatively influence this process, and it is expected that it will become more difficult when assaying complex samples, as plasma or blood. To circumvent this issue, in future other methods have to be tested to hold microcarriers at a specific location in a microchip while flushing sample and reagent stream through it, such as for instance the use of dielectrophoresis as demonstrated in this study. An advantage of DEP immobilization is indeed its (almost) independency to the size of the channel. When using channels that are wide enough, it should be possible to assay more complex samples, without any issues related the decoding process. Interestingly, as mentioned in Chapter 6, hundreds till thousands of DEP traps can be combined in one microchannel, due to the development of microelectrodes, making this an attractive approach for microparticle-based multiplex analysis, in which several microparticles have to be trapped at a time.

REFERENCES

1. Butler, J. E. Solid supports in enzyme-linked immunosorbent assay and other solid-phase immunoassays. *Methods* **2000**, *22* (1), 4-23.
2. Zammattéo, N.; Alexandre, I.; Ernest, I.; Le, L.; Brancart, F.; Remacle, J. Comparison between microwell and bead supports for the detection of human cytomegalovirus amplicons by sandwich hybridization. *Anal. Biochem.* **1997**, *253* (2), 180-189.
3. Sato, K.; Hibara, A.; Tokeshi, M.; Hisamoto, H.; Kitamori, T. Integration of chemical and biochemical analysis systems into a glass microchip. *Anal. Sci.* **2003**, *19* (1), 15-22.
4. Kohara, Y.; Noda, H.; Okano, K.; Kambara, H. DNA hybridization using "bead-array": probe-attached beads arrayed in a capillary in a predetermined order. *Nucleic Acids Res. Suppl* **2001**, (1), 83-84.
5. Sato, K.; Tokeshi, M.; Odake, T.; Kimura, H.; Ooi, T.; Nakao, M.; Kitamori, T. Integration of an immunosorbent assay system: analysis of secretory human immunoglobulin A on polystyrene beads in a microchip. *Anal. Chem.* **2000**, *72* (6), 1144-1147.
6. Tanaka, Y.; Slyadnev, M. N.; Sato, K.; Tokeshi, M.; Kim, H. B.; Kitamori, T. Acceleration of an enzymatic reaction in a microchip. *Anal. Sci.* **2001**, *17* (7), 809-810.
7. Zimmermann, M.; Delamarque, E.; Wolf, M.; Hunziker, P. Modeling and optimization of high-sensitivity, low-volume microfluidic-based surface immunoassays. *Biomed. Microdevices.* **2005**, *7* (2), 99-110.
8. Andersson, H.; van der, W. W.; Stemme, G. Micromachined filter-chamber array with passive valves for biochemical assays on beads. *Electrophoresis* **2001**, *22* (2), 249-257.
9. Pohl, H. A. Dielectrophoresis. *Cambridge University Press* **1978**.
10. Chiou, P. Y.; Ohta, A. T.; Wu, M. C. Massively parallel manipulation of single cells and microparticles using optical images. *Nature* **2005**, *436* (7049), 370-372.
11. Taff, B. M.; Voldman, J. A scalable addressable positive-dielectrophoretic cell-sorting array. *Anal. Chem.* **2005**, *77* (24), 7976-7983.
12. Voldman, J.; Braff, R. A.; Toner, M.; Gray, M. L.; Schmidt, M. A. Holding forces of single-particle dielectrophoretic traps. *Biophys. J.* **2001**, *80* (1), 531-541.
13. Voldman, J.; Gray, M. L.; Toner, M.; Schmidt, M. A. A microfabrication-based dynamic array cytometer. *Anal. Chem.* **2002**, *74* (16), 3984-3990.
14. Kohara, Y. Hybridization reaction kinetics of DNA probes on beads arrayed in a capillary enhanced by turbulent flow. *Anal. Chem.* **2003**, *75* (13), 3079-3085.

Summary & General Conclusions

Summary & General Conclusions

SUMMARY

The sequencing of the human genome resulted in the exponential discovery of diagnostic and prognostic biomarkers that provide a deeper insight into the molecular biology of diseases. It moved healthcare to a more efficient level in which a disease is not only recognized by its phenotype, but also understood at the molecular level. For a lot of diseases it is proven that the combination of multiple biomarkers together indicates a particular state of that disease. Multiplex assay technologies are of great interest to diagnose such diseases, because they can detect multiple biomarkers simultaneously in one sample, and have a lot of advantages compared to the traditional monoplex assays that only measure one biomarker at a time. They benefit e.g. from much less sample volume that is needed to analyze all biomarkers, a more efficient use of reagents, and less hands-on time.

Meanwhile several multiplex technologies have been proposed, from which the main important are the planar microarray and the suspension array platforms, as summarized in **Chapter 1**. Suspension arrays enjoy higher reaction kinetics, and flexibility regarding the attachment of new probes, and are therefore preferred to planar microarrays when it comes to low- or medium throughput multiplexing. Because suspension arrays consist of mobile microparticles on which surface probes are attached that recognize specific targets, an encoding system has to be introduced in order to identify the multiple targets that have reacted with the microparticles. To this aim, several strategies have been developed, from which the spatial selective photobleaching technology that has been proposed by our group, is one. The primary aim of this thesis was to check whether this type of encoded polystyrene microparticles, that are also called memobeads, could be applied to multiplexed detection of proteins or DNA molecules.

Because this encoding technology needs ferromagnetic microparticles, first of all polystyrene microparticles have been used that were made magnetic by polymerization of monostyrene in the presence of ferromagnetic nanoparticles on the surface of core polystyrene microparticles. Such microparticles, however, exhibited aggregates of magnetic nanoparticles at their surface, which

caused shadowing areas in the inner part of the microparticles upon excitation with fluorescent light, and as a result accurate decoding was impossible. An even worse effect was that capture probes couldn't be coupled homogeneously, due to the presence of these magnetic nanoparticles at the (outside of) the surface. Therefore, in **Chapter 2**, we have used an alternative strategy for the preparation of magnetic microparticles. The surface of negatively charged non-magnetic carboxylated polystyrene microparticles was modified by means of the Layer-by-Layer technology, which is based on the sequential adsorption of positively and negatively charged polymers and/or nanoparticles on the surface of charged microparticles. This technology was applied as well to incorporate ferromagnetic chromium dioxide nanoparticles on the surface of the microparticles, as to provide them at the same time with functional carboxylic acid groups. We showed that the LbL coating allows (a) an optimal (optical) read out of the codes, (b) a perfect orientation within pixel accuracy ($0.7 \mu\text{m}/\text{pixel}$) of the microparticles (leading to a correct decoding), and (c) an optimal coupling of capture probes to the surface. Importantly, the LbL coatings remained stable at the surface of the microparticles after a storage period during some months, and the microparticles could be freeze-dried, and even autoclaved, which is important when the microparticles have to be applied in a research or diagnostic kit, or when they have to be used as cell-carriers, respectively.

We showed in **Chapter 3** that the LbL coated digitally encoded microparticles allowed the quantitative and sensitive detection of proteins, like TNF- α , P24 and FSH, not only in buffer but also in complex media, such as serum and plasma. The LbL coatings remained stable at the surface of the microparticles when they were incubated in serum or plasma, and we didn't observe any non-specific binding of serum/plasma molecules to the capture antibody loaded LbL layers. Importantly, we observed that (a) the digital code of the microparticles could be still accurately decoded and (b) the red fluorescence at their surface could be quantified even when the microparticles remained in "whole blood". These properties make the LbL coated digitally encoded microparticles investigated in this study ideally suited for the simultaneous (multiplexing) assaying of proteins in "whole" blood instead of in serum or plasma. We showed that using a lower number of LbL coated microparticles in the protein assay even profoundly improves the sensitivity of the assay, an interesting feature when one wants to make use of the microparticles for assaying in microchips which only allow using a rather low number of microparticles.

Besides the sensitive detection of proteins, we showed in **Chapter 5** that the LbL coated digitally encoded microparticles act also as good candidates for the quantitative detection of DNA molecules. The length of the spacer molecule, by which the capture probes are attached to the surface of the microparticles, plays an important role in the hybridization of targets probes thereto. Although we expected a higher hybridization efficiency with higher spacer lengths (and thus with a greater flexibility of the capture probe), there was, remarkably, an optimal spacer length. Greater

spacer lengths, probably resulted in too much freedom of the capture probe, so that it starts to interact with the surface of the microparticles by multiple positions in its sequence. We observed that the hybridization occurred very fast on the surface of the microparticles; almost maximal hybridization was achieved within a few minutes. A few results raised the question whether the Cy5 fluorophores are attracted to the surface, by which they could influence the efficiency of hybridization of Cy5 labeled targets. This is, however, still unclear, and has to be investigated in future. Some nucleic acid tests (NATs) on suspension arrays, such as e.g. gene expression analysis and the detection of single nucleotide polymorphisms, would benefit from making use of multiple colours, for the differential labeling of a control sample vs. the sample of interest, or for the differential labeling of all alleles of one gene, respectively. An important strength of our multiplex platform, compared to other suspension array platforms, is its possibility for multi-colour labeling. We have clearly proven that dual-colour target labeling - with Cy5 and TexasRed fluorophores - is possible with the LbL coated microparticles under investigation in our study, and suggested that multi-colour labeling might be possible with this platform, by using another fluorophore to stain the microparticles, which (optimal) excitation wavelength is located in the UV- or far red spectrum. We finally demonstrated the use of the LbL coated digitally encoded microparticles as genotyping platform, by combining it with the oligo ligation assay for the simultaneous detection of two single nucleotide polymorphisms in the Apolipoprotein E gene. Nine different genotypes were correctly identified, as compared to microarray analysis, and sequencing.

There are in general two ways to improve the sensitivity of affinity assays. If no PCR-like target amplification method exists, as is the case in the detection of proteins, the use of signal amplification methods could improve the sensitivity. One condition has to be fulfilled therefore, which is that the signals of the (negative) control samples are not amplified as much as those of the positive ones (that have reacted). This will result in a higher signal-to-noise ratio, and the gain in sensitivity will depend on the amount of amplification that is reached. In **Chapter 4** we demonstrate this principle by using the tyramide signal amplification (TSA) method, which is based on the enzymatic conversion by horse radish peroxidase (HRP) of inactive tyramide-residues to active residues, that are able to bind to electronrich groups of protein in the neighbourhood. Signal amplification is very challenging on multiplexed suspension arrays, because the microparticles are mobile and false positive results may arise due to cross-reaction of the amplified signal with not reacted microparticles. Therefore, in order to know unambiguously which microparticle (and thus which target) has dealt with the amplified signal, the signal should be 'attached' to that microparticle. We expected TSA to be suitable in multiplex microparticle-based platforms, because a) several proteins that consist electronrich groups are present at the surface of the microparticles (antibodies, bovine serum albumin, etc.), b) HRP can be easily linked to the capture

antibody/antigen/detection antibody sandwich construct that is formed at the surface of the microparticles, and c) the active tyramide molecules are very instable. This means that they become again inactive when they do not bind immediately to electronrich groups, which diminishes their chance for binding to other microparticles in the neighbourhood.

In fact, the combination of microparticles and TSA has already been shown once in literature. It was, however, only applied to a duplex assay, and it was never demonstrated to which extent this labelling procedure was more sensitive than the conventional method that is used on suspension arrays (and which is based on fluorescently labelled streptavidin that binds to biotinylated detection antibodies). We showed evidence that TSA method is indeed attractive for the fast and simultaneous detection of (multiple) targets in a sample, as well with our memobeads, as with the commercially available *xMAP*[®] microparticles. Compared to currently used detection methods, TSA significantly amplifies the fluorescence signals on the microparticles (up to 100 times) resulting in (much) higher signal-to-noise ratios. We show that TSA on microparticles is applicable in real (serum) samples - sub-pg detection of P24 was possible – and that it worked perfect in a multiplex (quadruplex) format.

Another way to improve the sensitivity of affinity assays within a certain assay time, is by enhancing the affinity reaction between the probes and target molecules. This study challenged the integration of LbL coated memobeads in microfluidic channels in **Chapter 7**. (Bio)molecular affinity reactions are often diffusion limited, and occur therefore much faster in a micro-environment, where diffusion distances are much smaller compared to those in conventional microtiter plates. This is a useful property in bioanalysis, because the time a molecule needs to diffuse from point a to point b is proportional to the square of the distance between a and b. While it takes several hours to overcome 1 cm, it only takes tens of seconds to overcome 100 μm . A “liquid microspace” has also other characteristic features which differ from the properties of a “liquid bulk”: high interface-to-volume ratio, and small heat capacity. For those reasons, we suggested that the integration of memobeads into microchannels could enhance the interaction between free target molecules and the probes that are attached to the surface of the memobeads. As a proof-of-concept, memobeads to which mouse antibodies were attached, were immobilized in a microchannel by means of a dam structure, and a solution of red fluorescent goat anti-mouse IgGs was then flushed through the channel. The affinity reaction between mouse IgG and goat anti-mouse IgG was followed by the appearance of red fluorescence at the surface of the memobeads, and the reaction was compared with that on memobeads that were loaded in a micro-centrifuge tube. We showed that rate of the protein affinity interactions was remarkably enhanced in the microchannel (up to almost 10 times compared to the rate measured on the microparticles that were loaded in the micro-centrifuge tube). The integration in the microchannel did not increase the amount of non-specific binding, and the decoding of the memobeads was also possible in the microchip, which means that the

combination of our memobead platform and microfluidics technologies might result in a fast and sensitive detection of multiple proteins. We proposed, however, that other immobilization strategies might work better for the memobead platform, because the dam structure that was used in these experiments worked also as a kind of filter, that accumulated debris (such as dust). We expected that this effect will be enhanced when measuring in more complex samples, and tested therefore whether the memobeads could be immobilized in a microchip by using a dielectrophoresis (DEP) cage, from which the main advantages are that no physical contact occurs with the memobeads, and that they can be immobilized in much broader channels than when using a dam structure. Although we didn't investigate yet the immobilization of an encoded memobead, we saw that the LbL coated microparticles could be caught in such a cage, and they could be rotated easily by applying an external magnetic field, superimposed on the DEP field. Therefore, decoding of memobeads would be possible in this way too.

The combination of microfluidic technologies with encoded microparticle-arrays is a very promising lab-on-a-chip tool, due to the remarkable characteristics of both technologies which complete each other. **Chapter 6** aimed to debate on the 'added value' we can expect by (bio)analysis with particles in microfluidic devices. We overview technologies that are able to decode, analyse, and manipulate microparticles in microfluidic chips, with a special emphasis on the challenges which exist to integrate currently existing detection platforms for encoded microparticles in microdevices, and on promising microtechnologies for down-scaling the detection units, in order to obtain compact miniaturized particle-based multiplexing platforms. Although our focus was on the integration of multiplexed suspension array technology with microfluidics technology, the goal of those integrated lab-on-a-chip tools is point-of-care assessment. To this purpose, the real challenge will probably come from the coupling of the decoding modules under investigation in this chapter in an appropriate way on one chip to other advanced modules for sub-tasks, such as blood processing, extraction of DNA, RNA or proteins, and so on. In order to bring diagnostics closer to the patient, future requirements will also involve progress in non-hardware tools, like data acquisition, data management... Research in each of these fields is full of promise, and within the next decade, the first prototypes of multiplexed particle-based LOC tools can probably be expected, assuming that new micro- and nano-engineering technologies are rapidly accepted.

GENERAL CONCLUSIONS

In conclusion the primary aim of this study was to proof the possibility of using memobeads for multiplexed protein and DNA detection. After optimizing the surface characteristics of the memobeads by modification with the use of the LbL technology, we succeeded in sensitive multiplex protein measurements in complex samples, such as serum, and plasma, and showed that genotyping and multi-color target labeling might be possible with this memobead platform. We also succeeded in making our platform more sensitive by combining it with the tyramide signal amplification method, and by integrating it in microfluidic channels, and suggested that this is possible with other suspension array platforms too. Finally, we believe that the 'added value' by (bio)analysis with suspension arrays in microfluidic devices, will result in future in lab-on-a-chip tools for point-of-care assessment.

Samenvatting & Algemene Besluiten

Samenvatting & Algemene Besluiten

SAMENVATTING

Het sequencen van het menselijk genoom bracht een exponentiële toename in ontdekking van diagnostische en prognostische biomerkers met zich mee, die een dieper inzicht geven in de moleculaire biologie achter ziekten. Het heeft ertoe geleid dat gezondheidszorg momenteel efficiënter wordt toegepast, omdat ziekten niet enkel herkend worden enkel op basis van hun fenotype, maar ook moleculair gekarakteriseerd worden. Bepaalde stadia van vele ziektes worden gekenmerkt door een combinatie van meerdere biomerkers. Multiplex technologieën spelen een belangrijke rol in de diagnose van deze ziektes, omdat ze in staat zijn om meerdere biomerkers tegelijkertijd te analyseren in slechts één staal, en omdat ze veel andere voordelen hebben ten opzichte van de klassieke monoplex technologieën, die slechts één biomarker per keer kunnen meten. Ze hebben bijvoorbeeld veel minder staal nodig om alle merkers te analyseren, verbruiken veel minder reagentia en vragen veel minder werk om uit te voeren.

Er zijn ondertussen reeds verschillende multiplex technologieën voorgesteld, waarvan de vlakke substraat “microarrays” en de “platforms” op basis van micropartikels de belangrijkste zijn, zoals samengevat in **Hoofdstuk 1**. Indien een lage tot middelmatige hoeveelheid doelmoleculen tegelijkertijd moet worden getest, zijn platforms op basis van micropartikels te verkiezen boven de vlakke substraat microarrays, omdat ze o.a. een snellere reactiekinetiek vertonen en flexibeler zijn wat betreft de toevoeging van nieuwe “probes” aan een bestaande set van probes. Aangezien deze platforms bestaan uit een set van mobiele micropartikels, op wier oppervlak verschillende probes worden gebonden die elk specifieke doelmoleculen kunnen herkennen en binden, moeten de micropartikels gecodeerd worden om de verschillende doelmoleculen te identificeren die gereageerd hebben met de probes. Verscheidene strategieën werden reeds ontwikkeld om micropartikels te coderen, waartoe de ruimtelijke selectieve fotoblekingstechnologie behoort, die door onze onderzoeksgroep werd ontwikkeld. Het hoofddoel van deze onderzoeksscriptie is na te gaan in hoeverre dit type van gecodeerde polystyreen micropartikels, ook memobeads genaamd, kan worden toegepast voor de simultane detectie van diverse eiwitten of diverse DNA moleculen.

Aangezien deze coderingstechnologie gebruik maakt van ferromagnetische micropartikels, werden in eerste instantie magnetische polystyreen micropartikels gebruikt, die aangemaakt werden door polymerisatie van monostyreen, op het oppervlak van vooraf aangemaakte polystyreen micropartikels, in aanwezigheid van ferromagnetische nanopartikels. Aan het oppervlak van de micropartikels werden er bij dit proces echter aggregaten gevormd van die magnetische nanopartikels, die schaduwvlekken veroorzaakten in het binnenste van de micropartikels, wanneer deze belicht werden. Accurate decoding was om die reden onmogelijk. Nefaster was dat probes niet homogeen konden gekoppeld worden aan het oppervlak van deze micropartikels, omwille van de aanwezigheid van die magnetische nanopartikels. Om deze problemen te vermijden, hebben we in **Hoofdstuk 2** een alternatieve methode aangewend om magnetische micropartikels aan te maken. Het oppervlak van negatief geladen niet-magnetische gecarboxyleerde polystyreen micropartikels werd gemodificeerd door middel van de "Layer-by-Layer" (LbL) technologie, die gebaseerd is op de laagsgewijze adsorptie van positief en negatief geladen polymeren en/of nanopartikels aan het oppervlak van geladen micropartikels. Ferromagnetische chroomdioxide nanopartikels werden op die manier ingebouwd in het oppervlak van de micropartikels. Tegelijkertijd werden de micropartikels voorzien van functionele carboxyl-groepen. We hebben aangetoond dat de LbL modificatie (a) zowel een optimale optische uitlezing van de code, als (b) een perfecte oriëntatie toelaat (met accuraatheid tot op het niveau van een pixel - 0.7 $\mu\text{m}/\text{pixel}$) van de micropartikels, eigenschappen die resulteren in een correcte decoding. Daarenboven maakt de LbL modificatie een optimale koppeling van probes mogelijk aan het oppervlak van de micropartikels. De LbL lagen blijven stabiel vastgehecht aan het oppervlak van de micropartikels, zelfs na een bewaarperiode van enkele maanden, en de LbL gemodificeerde micropartikels kunnen gevriesdroogd en zelfs geautoclaveerd worden, wat belangrijk is, indien ze respectievelijk worden aangewend in kits voor onderzoek of diagnostiek, of worden gebruikt als drager voor celculturen.

We hebben in **Hoofdstuk 3** aangetoond dat de LbL gemodificeerde micropartikels op een kwantitatieve en gevoelige wijze eiwitten, zoals bijvoorbeeld TNF- α , P24 en FSH, kunnen detecteren, niet enkel in een buffer, maar ook in meer complexe stalen, zoals serum en plasma. De LbL lagen bleven stabiel gehecht aan het oppervlak van de micropartikels, wanneer deze in serum of plasma werden geïncubeerd, en er werd geen specifieke adsorptie opgemerkt van serum- en plasmafactoren aan de LbL lagen. Zowel een accurate uitlezing van deze memobeads, als het kwantificeren van de rode fluorescentie aan hun oppervlak, was zelfs nog mogelijk wanneer ze aanwezig waren in een bloedstaal. Dit maakt de toepassing van memobeads voor de simultane detectie van meerdere eiwitten in volledig bloed mogelijk, in plaats van in serum of plasma. We hebben aangetoond dat de gevoeligheid voor de detectie van eiwitten van zo'n test op basis van micropartikels drastisch kan verhoogd worden door minder micropartikels te gebruiken in de test. Dit

kan een interessante eigenschap zijn, wanneer deze testen zouden aangewend worden om eiwitten te detecteren in “microfluidic chips”, die immers enkel een beperkt aantal micropartikels toelaten.

Behalve de gevoelige detectie van eiwitten met deze LbL gemodificeerde en digitaal gecodeerde micropartikels, hebben we eveneens aangetoond in **Hoofdstuk 5** dat ze kunnen worden gebruikt voor de kwantitatieve detectie van DNA moleculen. De lengte van de “spacer” molecule, via dewelke de oligonucleotide probes gebonden worden aan het oppervlak van de micropartikels, speelt een belangrijke rol in de efficiëntie van de hybridisatie tussen doelmoleculen en deze oligonucleotide probes. Hoewel we verwacht hadden dat de efficiëntie van deze hybridisatie zou verhogen bij gebruik van langere spacers (dat immers gepaard gaat met een grotere flexibiliteit van de probe), merkten we echter een optimale lengte op. Langere spacers gaven waarschijnlijk te veel flexibiliteit aan de probe, zodat deze contact kon maken met het oppervlak van de micropartikels via meerdere plaatsen in zijn sequentie. We merkten eveneens op dat de hybridisatie aan het oppervlak van de micropartikels zeer snel verliep; een maximale hybridisatie werd al bereikt na ongeveer een paar minuten. Enkele resultaten suggereerden een mogelijke interactie van de Cy5 moleculen met het oppervlak van de micropartikels, wat een invloed zou kunnen hebben op de efficiëntie van de hybridisatie van Cy5 geconjugeerde doelmoleculen. Dit moet echter nog dieper worden onderzocht, vooraleer er verder uitspraak over te doen. Het gebruik van meerdere kleuren voor het merken van de doelmoleculen zou een voordeel kunnen zijn voor sommige nucleïnezuurtesten die uitgevoerd worden op platforms op basis van gecodeerde micropartikels. Hierbij denken we bijvoorbeeld aan een differentiële kleuring van het controle staal en het te testen staal bij genexpressie analyse, of een afzonderlijke kleur voor de verschillende allelen van eenzelfde gen bij de detectie van polymorfismen. De mogelijkheid om meerdere kleuren aan te wenden voor het merken van doelmoleculen, is een sterkte van het multiplex platform dat is voorgesteld in deze studie, in vergelijking met andere platforms op basis van gecodeerde micropartikels. We hebben duidelijk aangetoond dat gebruik van twee kleuren (Cy5 en TexasRed) mogelijk is op de LbL gemodificeerde micropartikels, en we hebben gesuggereerd dat zelfs meer kleuren zouden kunnen worden aangewend, indien de kleurstof waarmee de micropartikels zelf gekleurd worden, vervangen wordt door een kleurstof die fluoresceert bij belichting met UV- of ver rood licht. We hebben dit DNA luik tenslotte beëindigd door de simultane genotypering aan te tonen van de 2 polymorfismen van het Apolipoproteïne E gen met behulp van memobeads, door gebruik te maken van de oligonucleotide ligatie test. Negen verschillende genotypes werden correct geïdentificeerd, dit werd aangetoond door vergelijking met microarray analyses en sequencen.

Er kunnen in het algemeen twee wegen worden gevolgd om de gevoeligheid van affiniteitstesten te verhogen. Indien er geen PCR-achtige techniek voorhanden is om doelmoleculen te vermenigvuldigen, hetgeen o.a. het geval is voor de detectie van eiwitten, kunnen methoden

worden aangewend die het signaal vergroten, dat resulteert uit de reactie tussen een probe en een doelmolecule. Het signaal van de (negatieve) controle stalen mag dan evenwel niet even sterk vergroten, als dat van de positieve (gereageerde) stalen. Enkel dan zal de verhoging in signaal immers resulteren in een hogere signaal/ruis verhouding. De toename in gevoeligheid is afhankelijk van de mate waarmee het signaal vergroot kan worden. Dit principe hebben we in **Hoofdstuk 4** gedemonstreerd op het multiplex platform dat is voorgesteld in deze studie door gebruik te maken van de tyramide signaal amplificatie (TSA) methode. TSA is gebaseerd op de enzymatische conversie van inactieve tyramide residuen, door middel van horseradish peroxidase (HRP), tot actieve residuen welke in staat zijn te reageren met electronenrijke groepen van eiwitten in de omgeving van de conversie. Signaalamplificatie is zeer uitdagend bij alle platforms op basis van gecodeerde micropartikels, omdat deze micropartikels mobiel zijn, en vals positieve resultaten makkelijk kunnen ontstaan door binding van signaalmoleculen aan het oppervlak van niet-gereageerde micropartikels. Met andere woorden, om een ondubbelzinnig antwoord te krijgen op de vraag welke micropartikels geleid hebben tot het signaal (en dus welke doelmoleculen gereageerd hebben met de probes), moet dit signaal fysisch gekoppeld worden aan enkel en alleen de desbetreffende micropartikels. We verwachtten dat de TSA methode toegepast zou kunnen worden op alle multiplex platforms op basis van gecodeerde micropartikels, omdat a) allerlei eiwitten (antilichamen, BSA moleculen, etc.) aanwezig zijn op het oppervlak van de micropartikels die alle electronenrijke groepen bevatten, b) HRP vrij makkelijk kan worden gekoppeld aan het probe/doelmolecule sandwich construct dat gevormd wordt aan het oppervlak van de micropartikels, en c) de actieve tyramide residuen zich in een zeer onstabiele toestand bevinden. Dit laatste betekent dat ze, ofwel onmiddellijk moeten reageren met electronenrijke groepen, ofwel opnieuw overgaan in hun inactieve vorm, waarin ze onmogelijk nog kunnen reageren. Dit vermindert met andere woorden de kans dat ze nog kunnen binden op andere micropartikels in de omgeving.

De toepassing van de TSA methode op micropartikels in een duplex test werd reeds eenmaal beschreven in de literatuur, maar tot nu toe werd er nog nooit aangetoond in hoeverre deze methode gevoeliger werkt dan de methode die conventioneel gebruikt wordt bij multiplex platforms op basis van gecodeerde micropartikels (welke gebruik maakt van fluorescent streptavidine dat bindt met gebiotinylerde detectie antilichamen). We hebben aangetoond in hoofdstuk 4 dat deze TSA methode een zeer attractieve methode is om snel en simultaan diverse eiwitten te detecteren, zowel met de memobeads, als met de commercieel beschikbare *xMAP*[®] micropartikels. De TSA methode vergroot het fluorescente signaal dat resulteert uit de reactie tussen probes en doelmoleculen significant (tot 100 keer ten opzichte van de huidige methode), met veel grotere signaal/ruis verhoudingen tot gevolg. We hebben aangetoond dat deze methode bruikbaar is in serum – sub-pg detectie van P24 was mogelijk – en perfect werkt in een multiplex (quadruplex) formaat.

Een tweede manier om de gevoeligheid van affiniteitstesten te verhogen binnen een bepaalde reactietijd, is door het contact tussen de probes en doelmoleculen efficiënter te maken. We hebben daartoe in deze studie in **Hoofdstuk 7** de integratie van de LbL gemodificeerde micropartikels in “microfluidic chips” onderzocht. Affiniteitsreacties tussen (bio)moleculen zijn zeer vaak diffusie gelimiteerd, en zullen om die reden sneller plaatsvinden in een microruimte, waarin de diffusie afstanden veel korter zijn vergeleken met deze in conventionele microtiter platen. Dit is een belangrijke eigenschap aangezien de tijd die een molecule nodig heeft om van plaats a naar plaats b te diffunderen, proportioneel is met het kwadraat van de afstand tussen a en b. Hoewel het enkele uren duurt om een afstand van 1 cm te overbruggen, duurt het ongeveer 10 seconden om 100 μm te overbruggen. Een microruimte heeft daarenboven nog andere karakteristieke eigenschappen waardoor het verschilt van een macro-omgeving: een grote oppervlak/volume ratio en een lage warmtecapaciteit. De integratie van LbL gemodificeerde micropartikels in microkanalen zou om die redenen kunnen leiden tot een versnelde interactie tussen de vrije doelmoleculen en de probes, gebonden aan het oppervlak van de micropartikels. Als proof-of-concept hiervoor werden LbL gemodificeerde micropartikels, op wiens oppervlak muis antilichamen werden gekoppeld, geïmmobiliseerd in een microkanaal door middel van een soort damstructuur, en vervolgens werd een oplossing van rode fluorescente geit anti-muis IgGs doorheen het microkanaal gestuurd. De affiniteitsreactie tussen de beide antilichamen was visueel waarneembaar door het ontstaan van rode fluorescentie aan het oppervlak van de micropartikels; de reactiesnelheid werd vergeleken met die aan het oppervlak van LbL gemodificeerde micropartikels in een microcentrifuge tube (macro-ruimte). We hebben aangetoond dat deze reactie veel sneller verliep in het microkanaal (tot zelfs 10 maal sneller vergeleken met de microcentrifuge tube). Er werd niet meer specifieke binding waargenomen op de micropartikels nadat ze in het microkanaal geïntegreerd werden, en decoding van geïntegreerde memobeads was eveneens mogelijk, wat betekent dat de combinatie van memobeads en microchips zou kunnen leiden tot een snelle en gevoelige test voor de simultane detectie van diverse eiwitten. Aangezien de damstructuur een soort van filtereffect teweeg bracht, waarbij niet alleen micropartikels maar ook stof en dergelijke accumuleerden, en omdat we verwachten dat dit effect nog meer zou worden benadrukt bij metingen in complexe stalen, hebben we voorgesteld om in de toekomst andere methoden aan te wenden voor het immobiliseren van micropartikels in microchips. We hebben dit aangetoond door de LbL gemodificeerde micropartikels te immobiliseren in een microkanaal door middel van dielectroforese, dat gekenmerkt wordt door het feit dat er geen enkel fysisch contact is met de micropartikels, en dat het kan toegepast worden in veel bredere microkanalen, dan bij gebruik van een damstructuur. Hoewel we nog geen test hebben uitgevoerd met gecodeerde memobeads, hebben we wel aangetoond dat een LbL gemodificeerd micropartikel precies kan gevangen worden op een bepaalde locatie in een

microkanaal door middel van dielectroforese-krachten, en dat het micropartikel makkelijk ter plaatste geroteerd kan worden door een extern magneetveld aan te leggen bovenop het dielectroforese veld. Dit betekent dat decodering van de memobeads mogelijk moet zijn op deze manier.

De combinatie van “microfluidica” technologieën met multiplex platforms op basis van micropartikels, is een veelbelovende zogenaamde “lab-on-a-chip” (LOC) toepassing, dankzij de opmerkelijke en elkaar aanvullende eigenschappen van beide technologieën. We hebben in **Hoofdstuk 6** getracht een debat te openen over de ‘toegevoegde waarde’ die we mogen verwachten als we dit soort (bio)analyses zouden uitvoeren in microfluidica systemen. We hebben de technologieën bekeken die gebruikt kunnen worden om micropartikels te decoderen, te analyseren en te manipuleren in microfluidica systemen, met een speciale focus op a) de uitdagingen waarvoor we momenteel staan, om de huidige detectie platformen voor gecodeerde micropartikels te integreren in deze microfluidica systemen, en op b) veelbelovende microtechnologieën die aangewend kunnen worden om de huidige detectie units compacter te maken, om op die manier geminiaturiseerde multiplex platforms op basis van micropartikels te verkrijgen. Hoewel de focus in dit hoofdstuk vooral lag op de integratie van beide technologieën, zullen deze geïntegreerde LOC analysesystemen uiteindelijk worden toegepast om ter plaatse snel diagnoses uit te voeren, in plaats van in laboratoria. De echte uitdaging zal daarom waarschijnlijk liggen in de koppeling van de geïntegreerde decodering modules, die we beschreven in hoofdstuk 6, aan andere geavanceerde modules. Hierbij denken we aan modules die instaan voor andere taken, zoals voor de verwerking/voorbereiding van (bloed)stalen, voor de extractie van DNA, RNA of eiwitten, enz. Om de diagnostiek in te toekomst letterlijk dichterbij de patiënt te brengen, zullen er ook niet-hardware gerelateerde zaken verder moeten ontwikkeld worden, zoals data acquisitie, data management, enz. Het onderzoek in elk van deze velden is zeer belovend, en er wordt verwacht dat de eerste prototypes van multiplex LOC systemen op basis van micropartikels in het volgende decennium gelanceerd zullen worden, onder voorbehoud dat nieuwe micro- en nano-technologieën snel aanvaard worden.

ALGEMENE BESLUITEN

Deze doctoraatsstudie had tot hoofddoel de mogelijkheid na te gaan in hoeverre memobeads kunnen worden gebruikt voor de simultane detectie van meerdere eiwitten of DNA moleculen. Nadat we de oppervlakte-eigenschappen van de memobeads door middel van de LbL technologie geoptimaliseerd hadden, hebben we zowel gevoelige simultane eiwit metingen in complexe stalen, zoals serum en plasma, als genotypering en het merken van meerdere doelmoleculen met verschillende kleuren, aangetoond met dit memobead platform. We zijn er eveneens in geslaagd om het platform gevoeliger te maken door toepassing van de tyramide signaal amplificatie methode, en door integratie van het platform in microkanalen, en hebben gesuggereerd dat beide ook kunnen worden toegepast op andere multiplex platforms op basis van gecodeerde micropartikels. We zijn ervan overtuigd dat de ‘toegevoegde waarde’ die gecreëerd wordt door (bio)analyses op gecodeerde micropartikels uit te voeren in microkanalen, uiteindelijk zal resulteren in LOC instrumenten die kunnen worden toegepast voor “point-of-care” diagnoses.

Curriculum Vitae

Personalia

Stefaan Derveaux
 Kazernestraat 10
 9200 Dendermonde
 tel.: 0472/52.43.21
 email privé: derveaux.verwaeren@telenet.be; email werk : stefaan.derveaux@ugent.be

Geboren op 10 januari 1979 te Dendermonde.
 Nationaliteit: Belg.
 Gehuwd op 13 november 2004 met Lien Verwaeren (Kabinetshoofd Cultuur, Middenstand & Milieu bij gedeputeerde Jozef Dauwe, provincie Oost-Vlaanderen).
 Vader van Stan (*10/05/2008).

Opleiding

Bio-ingenieur in de Cel- en Genbiotechnologie	
Universiteit Gent	okt. 1997 – jul. 2003
Latijn-Wiskunde	
Heilig-Maagdcollege Dendermonde	sep. 1991 – jun. 1997

Cursussen

Managementscursus 'Fundamental Skills in Technology Transfer'	
Universiteit Gent/Vlerick Leuven Gent Management School	sep. 2006 – jul. 2007

Professionele ervaring

Doctoraatstudent Laboratorium voor Algemene Biochemie en Fysische Farmacie, Universiteit Gent	
	aug. 2003 – heden
Wetenschappelijk medewerker Memobead Technologies NV	
Spin-off Universiteit Gent & Tibotec Boom	aug. 2003 – aug. 2006

Assessments

Assessment center for innovation advisor

De Witte & Morel/Hudson
Gent

okt. 2007

Buitenlandse verblijven

Design, ontwikkeling en purificatie van amino- en fluorofoor geconjugeerde oligonucleotiden + multiplexhybridisatie technieken

Biocity, Organic Chemistry Department, Prof. Honnberg,
Universiteit van Turku
Finland

3-24 juni 2004

Design en ontwikkeling van microfluidic systemen voor manipulatie van en diagnostische testen met gecodeerde microsferen

Laboratory of Microtechnologies, Prof. Philippe Renaud
Ecole Polytechnique Fédérale de Lausanne
Zwitserland

17-21 juli 2007

Publicaties

1. Internationale tijdschriften in science citation index

Derveaux S, De Geest BG, Roelant C, Braeckmans K, Demeester J, De Smedt SC. Multifunctional layer-by-layer coating of digitally encoded microparticles. *Langmuir*. 2007 Sep 25;23(20):10272-9.

Fayazpour F., Lucas B., Huyghebaert N., Braeckmans K., **Derveaux S.**, Stubbe B.G., Remon J.P., Demeester J., Vervaeke C., De Smedt S.C. Digitally encoded drug tablets to combat counterfeiting. *Advanced Materials* 2007; 19 (22), 3854-3858.

Derveaux S, Stubbe BG, Roelant C, Leblans M, De Geest BG, Demeester J, De Smedt SC. Layer-by-layer coated digitally encoded microcarriers for quantification of proteins in serum and plasma. *Analytical Chemistry*. 2008 Jan 1;80(1):85-94.

Highlighted in Journal of Proteome Research 2008; 7 (2),479.

Derveaux S, Stubbe BG, Braeckmans K, Roelant C, Sato K, Demeester J, De Smedt SC. Synergism between particle-based multiplexing and microfluidics technologies may bring diagnostics closer to the patient. *Analytical & Bioanalytical Chemistry*. 2008 Aug;391(7):2453-67.

Stubbe B.G., Gevaert K., **Derveaux S.**, Braeckmans K., De Geest B.G., Goethals M., Vandekerckhove J., Demeester J., De Smedt S.C. Evaluation of encoded layer-by-layer coated microparticles as protease sensors. *Advanced Functional Materials* 2008 Jun; 18 (11): 1624-1631.

Fayazpour F., Lucas B., Huyghebaert N., Braeckmans K., **Derveaux S.**, Vandenbroucke R., Remon J.P., Demeester J., Vervaeke C., De Smedt S.C. Evaluation of digitally encoded layer-by-layer coated microparticles as cell carriers. *Advanced Functional Materials* 2008, accepted for publication.

2. Abstracts van congresmededelingen of postervoorstellingen

Derveaux S., Roelant C., De Smedt S.C. and Demeester J. (2005). Optimisation of surface characteristics of encoded microspheres and their use as capture agents in a multiplexing whole blood assay. Biofarmaciedag, Gent, België, 20 mei 2005. - *poster*

De Smedt S.C., Derveaux S. (2005). Digitally Readable, Barcoded Microspheres: Their Use in Medical Diagnostics, Genomics, Drug Discovery, Cellular Assays and Sorting of Biomolecules. Nanotech 2005, Montreux, Zwitserland, 15-17 november 2005. - *poster / voordracht*

Derveaux S., De Geest B.G., Demeester J. and De Smedt S.C. (2006). Multifunctional Layer-by-Layer coating allows the positioning of optical encoded microcarriers. Nanotech 2006, Montreux, Zwitserland, 14-16 november 2006. - *poster / voordracht*

Derveaux S., De Geest B.G., Braeckmans K., Stubbe B.G., Roelant C., Leblans M., Demeester J. and De Smedt, S.C. (2007). Layer-by-Layer coated digitally encoded microcarriers allow sensitive quantification of proteins in serum and plasma. POC Diagnostics 2007, Washington DC, USA, 13-17 augustus 2007. - *poster*

Derveaux S., De Geest B.G., Braeckmans K., Stubbe B.G., Roelant C., Leblans M., Demeester J. and De Smedt, S.C. (2007). Layer-by-Layer coated digitally encoded microcarriers allow sensitive quantification of proteins in serum and plasma. Nanotech 2007, Montreux, Zwitserland, 14-16 november 2007. - *voordracht*

Derveaux S. (2007). Encoded microcarriers for medical diagnostics. Material Challenges for Biomedical Applications, Gent, België, 27 november 2007. - *poster*

Derveaux S., Roelant C., Leblans M., Braeckmans K., Stubbe B.G., De Geest B.G., Demeester J. and De Smedt S.C. (2008). Layer-by-Layer coated digitally encoded microcarriers allow sensitive quantification of proteins in serum and plasma. Zing Microfluidics 2008, Cancun, Mexico, 21-24 februari 2008. - *voordracht*

Derveaux S., Demeester J. and De Smedt S.C. (2008). Digitally encoded memobeads : a universal tool for multiplexed molecular diagnostics and cell based assays. Follow the Beads, BVAC, Antwerpen België, 25 april 2008. - *voordracht*

3. Passieve deelname aan congressen

MicroTAS 2007, Parijs, Frankrijk, 7-11 oktober 2007.

Advances in qPCR, Stockholm, 17-18 september 2008.

Benelux qPCR 2008 Symposium, Gent, 6 oktober 2008.

4. Deelname aan congressen als medewerker van Memobead Technologies NV

Derveaux S., Roelant C. (2006). Applications on Memobead technology. Bio2006, Chicago, USA, 9-12 april 2006. - *poster*

Derveaux S., Roelant C. (2006). Applications on Memobead technology. Knowledge-for-growth 2006, Gent, België, 16 juni 2006. - *poster*

Derveaux S., Roelant C. (2006). Applications on Memobead technology. NVVI Annual Congress – Lunteren, Nederland, 23-24 Maart 2006. - *poster*

5. Patenten

WO/2008/034275, EP20060019661. Coating for microcarriers. De Smedt Stefaan, Derveaux Stefaan, Demeester Joseph, De Geest Bruno, Biocartis SA. Publication date: 26 maart 2008.

6. Thesis

Invloed van bacteriën op de invasie van colonkankercellen.
Thesis in het kader van de opleiding Bio-ingenieur Cel- en Genbiotechnologie
Laboratorium voor Experimentele Cancerologie (Prof. Marc Mareel) 2003
Universitair Ziekenhuis Gent

7. Thesissen begeleid door Stefaan Derveaux

- The use of encoded microspheres in diagnostics: basic biochemical experiments on the surface. Agata Olszak. **2004**. Promotor: Prof. Stefaan De Smedt, Geneesmiddelenleer, Universiteit Gent.
- Optimalisatie van digital gecodeerde microscopische draggers voor multi-parameteranalyse in de medische diagnostiek. Pieter Colman. **2005**. Promotor: Prof. Jo Demeester, Geneesmiddelenleer, Universiteit Gent.
- Het gebruik van digital gecodeerde microsferen in multiplex diagnostische toepassingen: optimalisatie van cytokine binding assays. Wannes Ryckebosch. **2006**. Promotor: Dr. Apr. Filip Dumont, Vesalius, Departement Gezondheidszorg, Hogeschool Gent.
- Digitaal geencodeerde beads voor multi-parameter analyse in de medische diagnostiek: optimalisatie van de oppervlakte eigenschappen. Kristof Behey. **2007**. Promotor: Prof. Stefaan De Smedt, Geneesmiddelenleer, Universiteit Gent.
- Karakterisatie van de stabiliteit van Layer-by-Layer gecoate microsferen. Sara Lee Meesschaert. **2007**. Promotor: Prof. Stefaan De Smedt, Geneesmiddelenleer, Universiteit Gent.
- Integratie van beads in microcapillairen en toepassing van enzymatische labeling op beads: tijdswinst voor multi-parameteranalyses. Lindsey Cappaert. **2008**. Promotor: Dr. D Bruneel, Departement Industrieel Ingenieur, Katholieke Hogeschool St.-Lieven.

